The near-minimum time control of a robot arm.

Ozaslan, Kemal.

NAVAL POSTGRADUATE SCHOOL
Monterey, California

THESIS

THE NEAR-MINIMUM TIME CONTROL
OF A ROBOT ARM

by

Kemal Ozaslan

December 1986

Thesis Advisor George J. Thaler

Approved for public release; distribution is unlimited.

SECURITY CLASSIFICATION OF THIS PAGE

REPORT DOCUMENTATION PAGE

1a REPORT SECURITY CLASSIFICATION UNCLASSIFIED	1b RESTRICTIVE MARKINGS
2a SECURITY CLASSIFICATION AUTHORITY	3 DISTRIBUTION / AVAILABILITY OF REPORT Approved for public release; distribution unlimited.
2b DECLASSIFICATION / DOWNGRADING SCHEDULE	
4 PERFORMING ORGANIZATION REPORT NUMBER(S)	5 MONITORING ORGANIZATION REPORT NUMBER(S)
6a NAME OF PERFORMING ORGANIZATION Naval Postgraduate School 6b OFFICE SYMBOL (If applicable) 62	7a NAME OF MONITORING ORGANIZATION Naval Postgraduate School
6c ADDRESS (City, State, and ZIP Code) Monterey, California 93943-5000	7b ADDRESS (City, State, and ZIP Code) Monterey, California 93943-5000
8a NAME OF FUNDING / SPONSORING ORGANIZATION 8b OFFICE SYMBOL (If applicable)	9 PROCUREMENT INSTRUMENT IDENTIFICATION NUMBER
8c ADDRESS (City, State, and ZIP Code)	10 SOURCE OF FUNDING NUMBERS PROGRAM ELEMENT NO / PROJECT NO / TASK NO / WORK UNIT ACCESSION NO

11 TITLE (Include Security Classification)

THE NEAR-MINIMUM TIME CONTROL OF A ROBOT ARM

12 PERSONAL AUTHOR(S)

Ozaslan, Kemal

13a TYPE OF REPORT	13b TIME COVERED	14 DATE OF REPORT (Year, Month, Day)	15 PAGE COUNT
Master's Thesis	FROM _____ TO _____	1986 December	186

16 SUPPLEMENTARY NOTATION

17 COSATI CODES			18 SUBJECT TERMS (Continue on reverse if necessary and identify by block number)
FIELD	GROUP	SUB-GROUP	Computer adaptive model Curve following velocity loop servo Robot manipulator

19 ABSTRACT (Continue on reverse if necessary and identify by block number)

The feasibility of controlling a robot manipulator in minimum time with an adaptive computer simulation model is investigated. Updating of model parameters; position, velocity and motor gain constant are accomplished from motor position only thereby eliminating the requirement for a tachometer. The interactive nonlinear dynamics of the system such as Coupling inertia, Centripetal forces, Actuator dynamics and Gravity effects are also investigated. A two link robot manipulator is chosen as the simulation model.

20 DISTRIBUTION / AVAILABILITY OF ABSTRACT ☒ UNCLASSIFIED/UNLIMITED ☐ SAME AS RPT ☐ OTIC USERS	21 ABSTRACT SECURITY CLASSIFICATION UNCLASSIFIED
22a NAME OF RESPONSIBLE INDIVIDUAL George J. Thaler	22b TELEPHONE (Include Area Code) / 22c OFFICE SYMBOL 62Tr

DD FORM 1473, 84 MAR 83 APR edition may be used until exhausted
All other editions are obsolete

SECURITY CLASSIFICATION OF THIS PAGE

Approved for public release; distribution is unlimited.

The Near-Minimum Time Control of A Robot Arm

by

Kemal Ozaslan
Lieutenant JG, Turkish Navy
B.S., Turkish Naval Academy, 1980

Submitted in partial fulfillment of the
requirements for the degree of

MASTER OF SCIENCE IN ELECTRICAL ENGINEERING

from the

NAVAL POSTGRADUATE SCHOOL
December 1986

ABSTRACT

The feasibility of controlling a robot manipulator in minimum time with an adaptive computer simulation model is investigated. Updating of model parameters; position, velocity and motor gain constant are accomplished from motor position only thereby eliminating the requirement for a tachometer. The interactive nonlinear dynamics of the system such as Coupling inertia, Centripetal forces, Actuator dynamics and Gravity effects are also investigated. A two link robot manipulator is chosen as the simulation model.

TABLE OF CONTENTS

LIST OF TABLES

LIST OF FIGURES

I. INTRODUCTION

In motion execution of a robot arm, one basic problem is to design a control system. This problem is complicated because the dynamic motion of a manipulator is strongly influenced by mechanical design and physical properties of the manipulator, as well as environmental effects. Coupling inertia, joint friction, coriolis forces, centripetal forces, actuator dynamics and gravity effects are considered among these factors. These factors produce an interactive nonlinear dynamic system. Under these circumstances a robust and flexible control system is needed.

The curve following scheme is used in all high performance disk files as part of the read/write head positioning servo. It has been shown [Ref. 1] that the entire loop can be modelled in a computer or microprocessor and the model can be used to drive a motor. Algorithms were developed to adapt the computer model for small parameter discrepancies and to update the states in the computer. In the robot arm there will be large parameter variations in mass and moment of inertia due to loading and the nonlinear dynamics of the manipulator.

The purpose of this thesis is to investigate the possibility of using the Curve Following Velocity Loop Servo to obtain near minimum time positioning of a robot manipulator. In this study, a two link robot manipulator with two degrees of freedom is chosen as the simulation model. The same control scheme is used to drive both motors.

Figure 1.1 is a simplified block diagram of the control scheme to be investigated. The second order model is a simple approximation of the actuator. A Velocity feedback loop is used in the adaptive model only. The "Adaptive Algorithm" uses Actuator position output to calculate the Actuator velocity, and updates the second order model gain constant, position and velocity at certain time intervals. Therefore the requirement for a tachometer is eliminated. The "Curve" approximates the deceleration curve of an ideal motor. It is chosen as a parabola. The "Environment" represents Gravitational torques, Centripetal forces, Coriolis forces and Inertia loading. The "Actuator" includes the servo motor and load. Both the second order model and the actuator are driven by the same velocity error input.

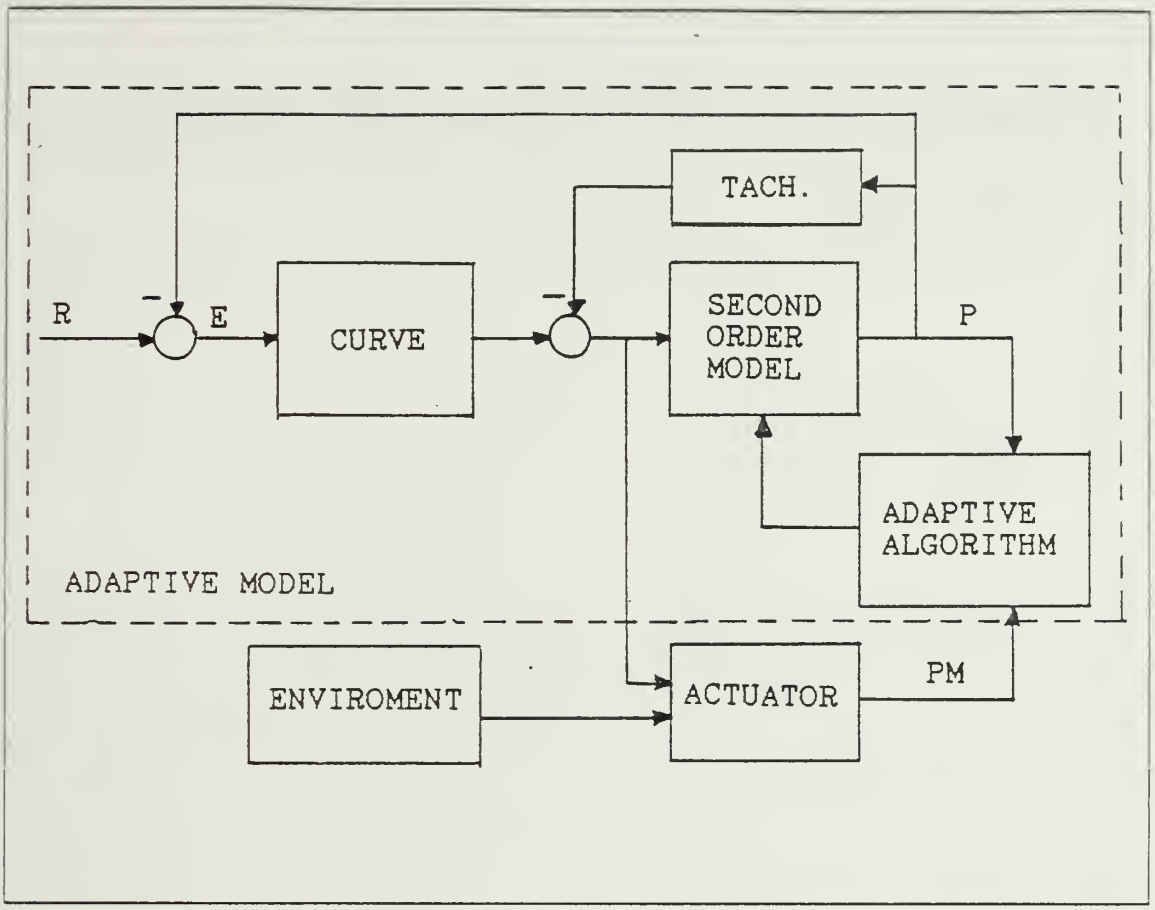

Figure 1.1 Simplified Block Diagram of the System.

Development of the computer simulation model is presented in Chapter II. Chapter III discusses the modelling of the robot arm. The computer adaptive model is developed in Chapter IV. Simulation studies are planned in Chapter V. Simulations under different conditions for a Voltage Source Drive System are studied in Chapter VI. Chapter VII discusses the development of a Current Source Drive System and presents simulation studies under different conditions. Conclusions and further study areas are presented in Chapter VIII. DSL simulation programs and derivation of mathematical model for robot arm are given in Appendixes A – F.

II. DEVELOPMENT OF THE COMPUTER SIMULATION MODEL

A. INTRODUCTION

It can be shown [Ref. 2] that the equivalent transfer function of the servo motor is

$$\frac{\theta(s)}{V(s)} = \frac{1/K_V}{S\left(S\frac{JR}{K_V K_t}+1\right)\left(S\frac{L}{R}+1\right)} \qquad \text{(eqn 2.1)}$$

where parameters θ, V, K_V, K_t, J, R, and L are defined in Chapter VII. The arm of a robot is a large inertia, and when this is added to the motor inertia the mechanical pole of the motor becomes smaller. Since R/L is normally a large number, the electrical pole of the motor may be neglected and the transfer function of the robot arm and motor becomes approximately

$$\frac{\theta(s)}{V(s)} \simeq \frac{K_m}{s^2} \qquad \text{(eqn 2.2)}$$

Figure 2.1 shows the second order model with a curve following velocity loop. The Curve used is the deceleration curve for the idealized motor. Bang-Bang control is chosen to drive the system with full power. [Ref. 3]

For a given step position command, the error signal (E) will produce a velocity command input. This signal saturates the amplifier and drives the system into full acceleration. When the commanded velocity signal ($\dot{X}$) becomes equal to the velocity feedback signal ($K\dot{P}$) the system changes into curve following mode and follows the curve until the desired position is reached.

B. OBTAINING THE CURVE AND MODEL PARAMETERS

Selection of the curve must be done in such a way that the system will be able to follow the curve under different loading conditions. Since a parabolic curve approximates the deceleration curve of an ideal motor, it was chosen as the curve to be followed.

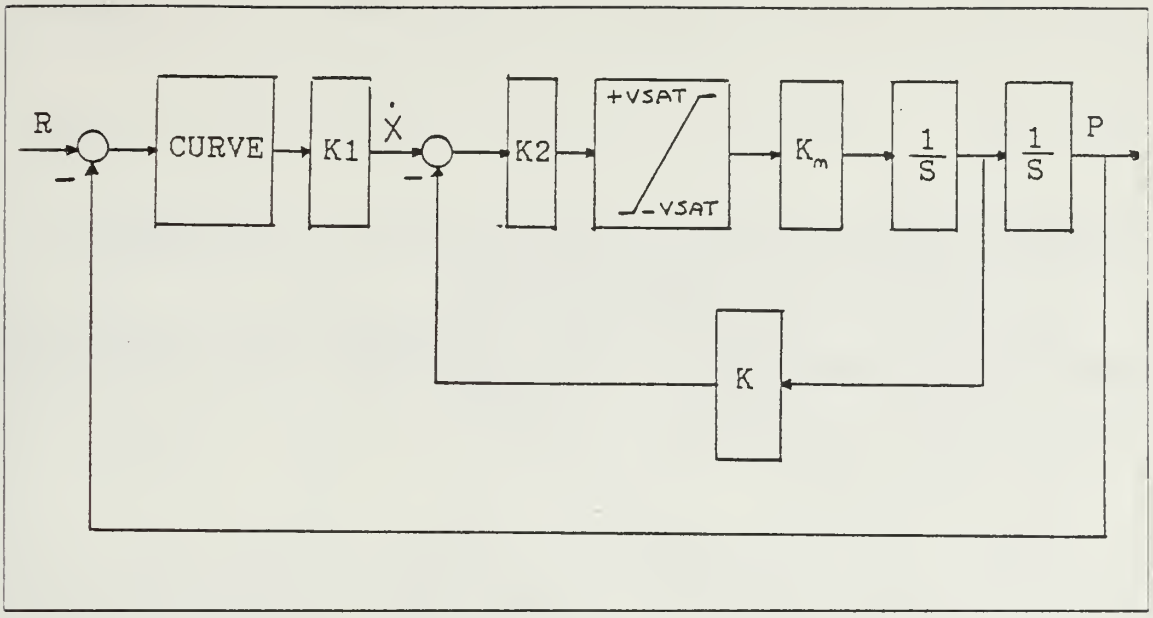

Figure 2.1 Block Diagram of the Model.

In the robot arm, simulation studies show that the curve must be shaped due to the mechanical design of the arm, actuator parameters and gravity effects. Therefore the gain constant (K1) is used to reshape the curve. In our case K1 was set to a value of 0.6. It has been shown [Ref. 1] that the equation of the curve was derived from the idealized motor equations as follows:

$$\ddot{C} = K_m \, Vsat \qquad \text{(eqn 2.3)}$$

$$\dot{C} = \int \ddot{C} \, dt = K_m \, Vsat \, t + \dot{C}(0), (C(0)=0) \qquad \text{(eqn 2.4)}$$

$$C = \int \dot{C} \, dt = 1/2(K_m \, Vsat \, t^2) + C(0) \qquad \text{(eqn 2.5)}$$

When we solve Equation 2.4 for t and substitude into Equation 2.5,

$$C = \frac{\dot{C}^2}{2 \, K_m \, Vsat} \qquad \text{(eqn 2.6)}$$

For deceleration from initial conditions with the input R = 0,

$$C = -E \qquad \text{(eqn 2.7)}$$

$$\dot{C} = -\dot{E} \qquad \text{(eqn 2.8)}$$

finally when we substitude Equation 2.7 and 2.8 into Equation 2.6 we come up with:

- $\dot{X} = \sqrt{2K_m Vsat}\,\sqrt{E}$ = commanded velocity

The second order model gain constant (K_m) is determined by the actuator parameters and the effective inertia seen by the actuator. The values of K_m were given below (to be derived in Chapter IV.

- K_{m1} = 0.17 rad/volt
- K_{m2} = 4.0 rad/volt

The saturation limits of the amplifiers are determined by available servo motor parameters, mechanical design of the arm, working conditions and curve constant (K1). In this study, the same servo motor is used for both actuators, whether or not gravity loading exists. The values of Vsat are:

- Vsat1 = 150 volts, Vsat2 = 50 volts (gravity-free environment)
- Vsat1 = 300 volts, Vsat2 = 150 volts (with gravity loading)

The gain parameter (K2) of the saturation amplifier is chosen to saturate the amplifier for small signals so that it acts as a switch to drive the system with full forward and reverse drive signals in the curve following mode. Therefore K2 was set to the value of 10,000 to guarantee the saturation of the amplifier.

The gain of the velocity feedback channel (K) has been given [Ref. 1] K = K1. In hardware realization of the system the value of K can be adjusted to compare the commanded velocity signal and the velocity feedback signal. For our purpose simulation studies show the best curve following is achieved for K = 1.

C. SIMULATION STUDIES OF THE MODEL

The model was simulated using DSL/VS. The DSL simulation program is listed in Appendix A. Vsat and K_m were set to 150 volts, 4.0 rad/volt respectively for these studies. Figure 2.2 shows phase plane trajectories (Angular velocity $\dot{P}$ versus angular position P) for a step position command of 1 radian. The figure shows that the model angular velocity increases with constant acceleration until the curve is reached. Then the voltage applied to the model reverses and the model velocity follows the curve until the desired angular position is reached. The step response of the model is shown in Figure 2.3.

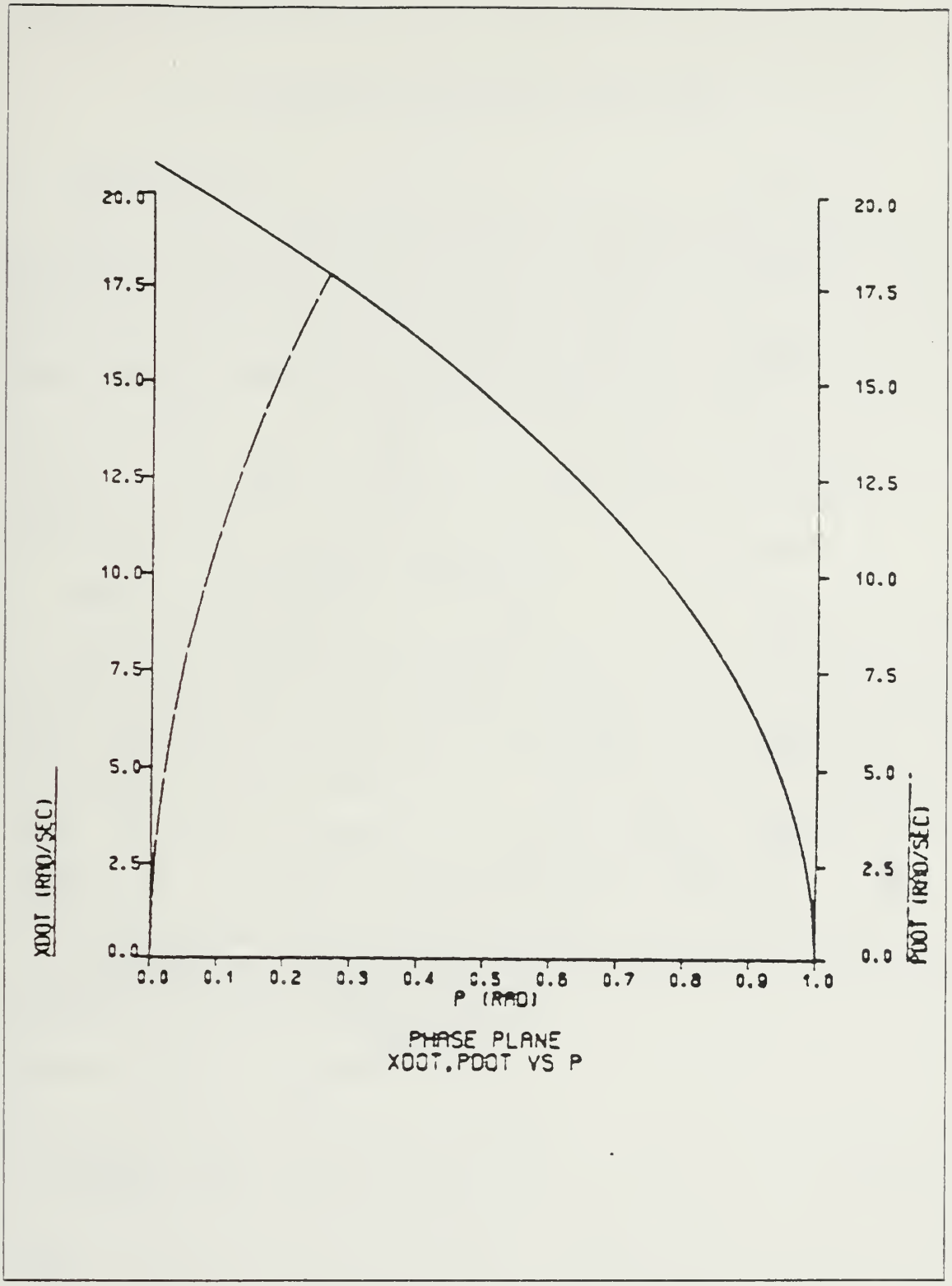

Figure 2.2 Phase Plane trajectories of the Model.

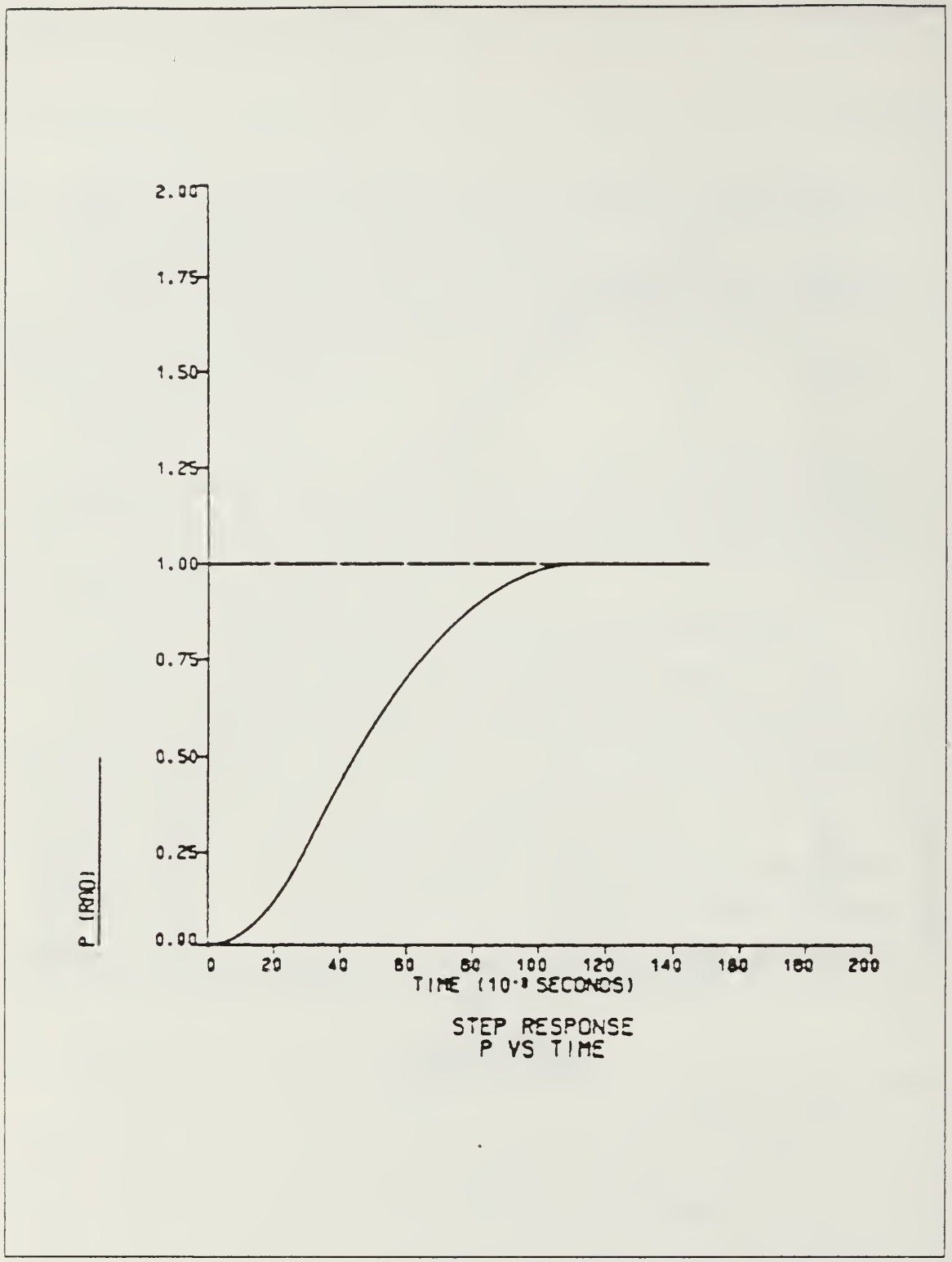

Figure 2.3 Step Response of the Model.

III. MODELLING THE ROBOT ARM

A. INTRODUCTION

In this chapter, a mathematical model of a two-degrees-of-freedom planar robot arm is developed using lagrangian mechanics. The dynamics equations relate torques and forces to positions, velocities and accelerations. We need dynamics equations to get the equations of motion of the manipulator. We need to know the relationship between torque and acceleration at a joint, and the relationship between torque at one joint and acceleration at other joints. We also need to know effects of the gravity torques and velocity dependent torques. Velocity dependent torques are typically small compared to other system torques. They are important when the manipulator is moving at high speed.

B. MODEL DEVELOPMENT

The two-degrees-of-freedom planar robot arm considered is illustrated in Figure 3.1. The motion of the robot arm is constrained to the xy plane. Both joints are rotary joints. There are two links, connecting the two joints and a terminal grasping device at JOINT2 with or without load. It is assumed that the links are massless and two equivalent masses are lumped at the end of LINK1 and LINK2. The lengths of LINK1 and LINK2 are denoted d_1, d_2 and two masses are denoted m_1, m_2 respectively. T_1, T_2 represents the external driving torques to the joints.

C. DERIVATION OF EQUATION OF MOTION

The lagrangian L is defined as the difference between the kinetic energy K and the potential energy V of the system. $L = K - V$

Equation 3.1 defines the Lagrange's Equation

$$\frac{d}{dt}\left(\frac{\partial L}{\partial \dot{q}_i}\right) - \frac{\partial L}{\partial q_i} = F_i \quad i = 1,\ldots,n \qquad \text{(eqn 3.1)}$$

where

q_i = generalized coordinates

$\dot{q}_i$ = corresponding velocity

F_i = the corresponding force or torque

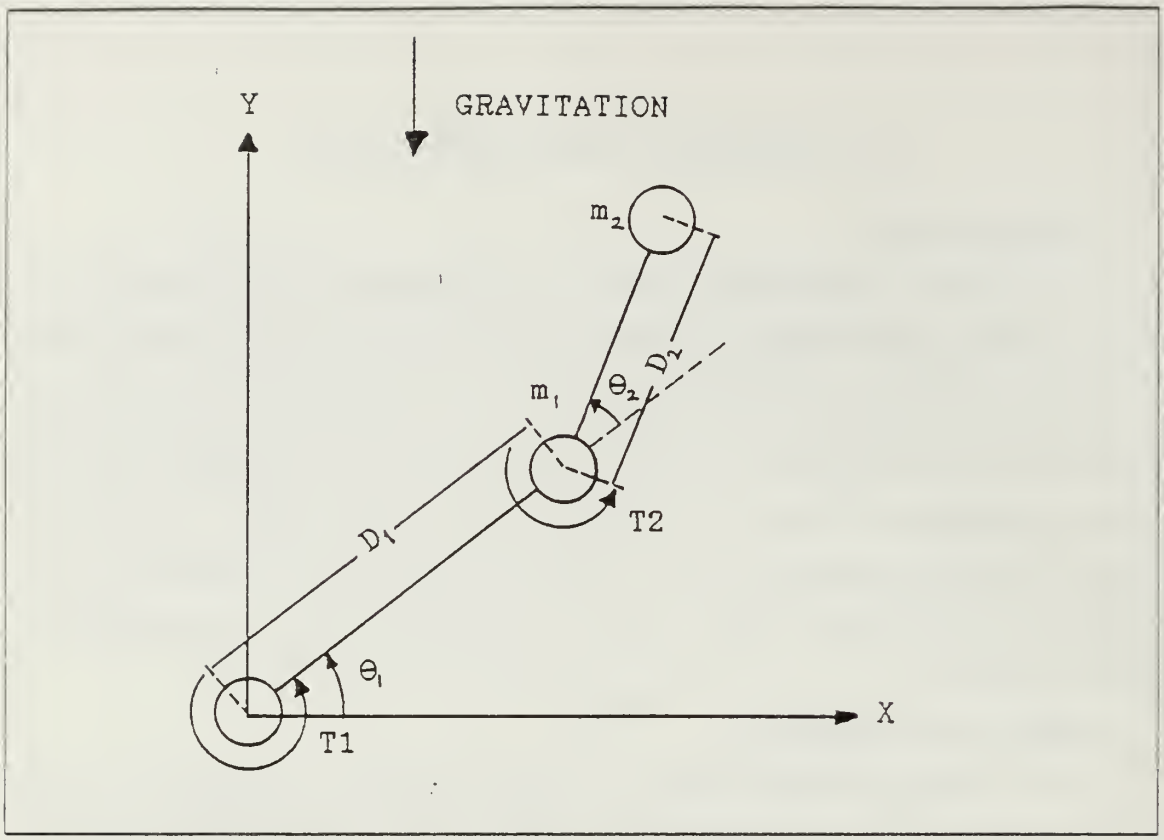

Figure 3.1 Point Mass Representation of a Two-Degrees-Of-Freedom planar Robot Arm.

L = Langrangian of the system

n = number of degrees of freedom

To apply equation 3.1 to the robot arm, the rotation angles θ_1 and θ_2 are chosen as the generalized coordinates. The generalized forces F_1, F_2 would be the total torques about the axis of rotation of θ_1 and θ_2 The detailed derivation is presented in Appendix B. The following pair of second-order nonlinear differential equations has been derived and will be used as the basic mathematical model for this thesis.

$$(D_{11}+J_{m1})\ddot{\theta}_1 = T_1 - (D_{12}\ddot{\theta}_2 + D_{122}\dot{\theta}_2^2 + D_{112}\dot{\theta}_1\dot{\theta}_2 + D_{121}\dot{\theta}_1\dot{\theta}_2 + G_1) \quad \text{(eqn 3.2)}$$

$$(D_{22} + J_{m2})\ddot{\theta}_2 = T_2 - (D_{12}\ddot{\theta}_1 + D_{211}\dot{\theta}_1^2 + G_2) \quad \text{(eqn 3.3)}$$

where

$$D_{11} = (m_1+m_2)d_1^2 + m_2d_2^2 + 2m_2d_1d_2\cos\theta_2$$
$$D_{12} = m_2d_2^2 + m_2d_1d_2\cos\theta_2$$
$$D_{22} = m_2d_2^2$$
$$D_{122} = -m_2d_1d_2\sin\theta_2$$
$$D_{112} = -m_2d_1d_2\sin\theta_2 = D_{121}$$
$$D_{211} = m_2d_1d_2\sin\theta_2$$
$$G_1 = [(m_1+m_2)d_1\cos\theta_1 + m_2d_2\cos(\theta_1+\theta_2)]g$$
$$G_2 = m_2d_2\cos(\theta_1+\theta_2)g$$

J_{m1} = motor inertia for Joint 1 motor

J_{m2} = motor inertia for Joint 2 motor

m_1 = 0.248 oz in/sec^2

m_2 = 0.041 oz in/sec^2

m_2 = 0.082 oz/in/sec^2 (with load)

d_1 = 15 inches

d_2 = 10 inches

g = 386.4 in/sec^2

Let us rewrite Equations 3.2 and 3.3 in the form

$$T_1 = (D_{11} + J_{m1})\ddot{\theta}_1 + D_{12}\ddot{\theta}_2 + D_{112}\dot{\theta}_1\dot{\theta}_2 + D_{121}\dot{\theta}_1\dot{\theta}_2 + D_{122}\dot{\theta}_2^2 + G_1 \qquad \text{(eqn 3.4)}$$

$$T_2 = (D_{22} + J_{m2})\ddot{\theta}_2 + D_{12}\ddot{\theta}_1 + D_{211}\dot{\theta}_1^2 + G_2 \qquad \text{(eqn 3.5)}$$

In these equations $(D_{11}+J_{m1})$ and $(D_{22}+J_{m2})$ are known as the effective inertia at joints 1 and 2. Accelerations at these joints cause torques and are referred to as inertial torques. D_{12} is known as the coupling enertia between JOINT1 and JOINT2. $D_{12}\ddot{\theta}_2$ is the reaction torque acting on JOINT1 induced by the angular acceleration of JOINT2; $D_{12}\ddot{\theta}_1$ is the reaction torque acting on JOINT2 induced by

angular acceleration of JOINT1. $D_{122}\dot{\theta}_2^2$ is the centripetal force acting on JOINT1 generated by the angular velocity of JOINT2; $D_{211}\dot{\theta}_1^2$ is the centripetal force acting on JOINT2 due to angular velocity at JOINT1. $D_{112}\dot{\theta}_1\dot{\theta}_2 + D_{121}\dot{\theta}_1\dot{\theta}_2$ is the coriolis force acting on JOINT1 generated by the angular velocities of both JOINT1 and JOINT2. G_1 and G_2 represent the gravity forces on JOINT1 and JOINT2 respectively. [Ref. 4]

IV. THE COMPUTER ADAPTIVE MODEL

A. INTRODUCTION

The second order model of Chapter II is to be used to drive, open loop, the servo motor of one joint of the robot arm. The servo motor has to follow a predetermined curve until a desired position is reached. To accomplish this, the second order model states and gain constant have to be adapted in such a way, that the model mimics the position and velocity and has a gain constant equivalent to that of the actual servo motor. In this chapter we will first discuss the selection of servo motors for testing of the adaptive systems and will then obtain the algorithm to update the second order model position, velocity and gain constant. The calculation of the initial value of the model gain constant (K_m) is also given in this Chapter.

B. SELECTION OF THE SERVO MOTORS

A permanent magnet motor drive currently used in industrial robots was selected to test the adaptive system. Parametric data for the motor are listed in Table 1.[Ref. 5]

TABLE 1
PARAMETRIC DATA FOR JOINT SERVO MOTORS

Torque Constant K_t	14.4	oz-in/amp
Total Inertia J_m	0.033	oz-in-sec^2/rad
Damping Coefficient B_m	0.04297	oz-in-sec/rad
Back emf Const. K_v	0.1012	volts-sec/rad
Armature Inductance L	100	μ-henries
Ave. Terminal Resistance R	0.91	ohms

The same motor drive is used for both JOINT1 and JOINT2 with a different power supply. To calculate the transfer functions of the servo motors, we need to know the effective joint inertias:

- $J_{EFF1} = D_{11} + J_{m1}$

- $J_{EFF2} = D_{22} + J_{m2}$

Where D_{11}, D_{22}, J_{m1}, J_{m2} are given in Chapter II. When we substitute parameters, we come up with:

- $J_{EFF1} = 81.425$ oz.in.s^2 (for $\theta_2 = 0°$)
- $J_{EFF2} = 4.14$ oz.in.s^2

Substituting effective inertias calculated above and parameters given in Table 1 into Equation 2.1, gives us the transfer functions of the servo motors.

$$G1(s) = \frac{9.88}{S(S/9100+1)(S/0.019+1)} \quad \text{radians/volts} \qquad \text{(eqn 4.1)}$$

$$G2(s) = \frac{9.88}{S(S/9100+1)(S/0.39+1)} \quad \text{radians/volts} \qquad \text{(eqn 4.2)}$$

The Open Loop Bode plots for the servo motors are shown in Figures 4.1 and 4.2. From the Open Loop Bode plots it can be observed that the - 40dB/decade slope crosses the 0.0 dB axis at $\omega_1 = 0.412$ rad/sec and $\omega_2 = 2.0$ rad/sec for JOINT1 and JOINT2 servo motors respectively. When we use the ω_1 and ω_2 frequencies as the gain crossover frequencies of the second-order ideal motors, we come up with:

- $K_{m1} = 0.17$ rad/volt
- $K_{m2} = 4.0$ rad/volt

Thus the gain constants K_{m1} and K_{m2} of the second-order models were set initially to these calculated values to determine the curve derived in Chapter II. Open Loop Bode diagrams of the K_m/s^2 ideal motors are given in Figures 4.3 and 4.4.

C. OBTAINING THE ADAPTIVE ALGORITHM

Figure 4.5 shows block diagram of the adaptive system for a joint servo drive. The same adaptive scheme is used to drive both servo motors separately. In this diagram T_L refers to the sum of disturbance torques such as Centripetal Torques, Centrifugal Torques, Reaction Torques and Gravitational Torques. The saturation amplifier output signal is common input to both the second-order model and servo motor. Output of the servo motor is measured and fed into the Adaptive Algorithm block. Our next step will be to calculate an estimate of the servo motor gain parameter (K_m) and the velocity of the servo motor. In these calculations, two criteria must be taken into consideration:

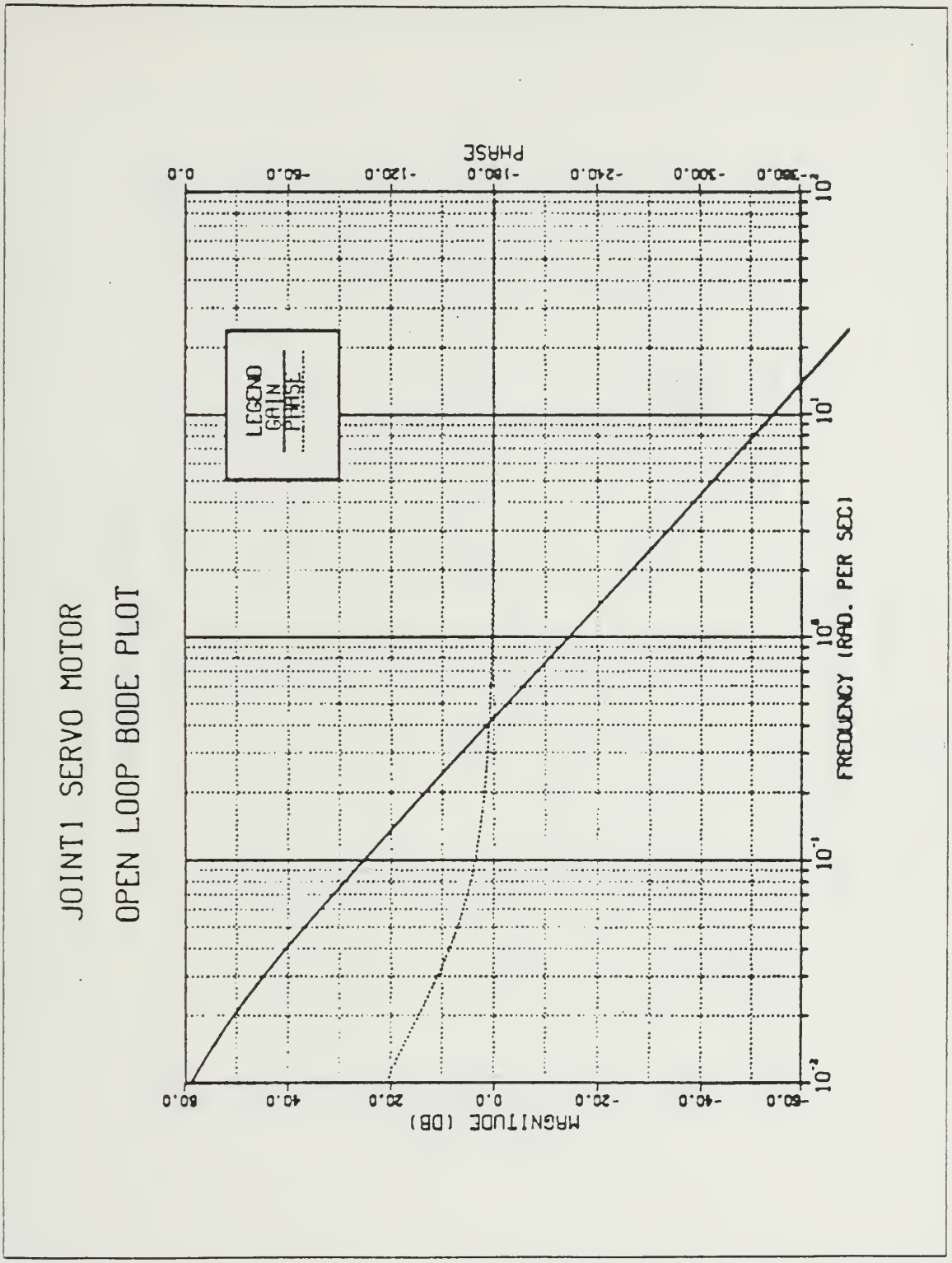

Figure 4.1 Open Loop Bode Plot of the JOINT1 Servo Motor.

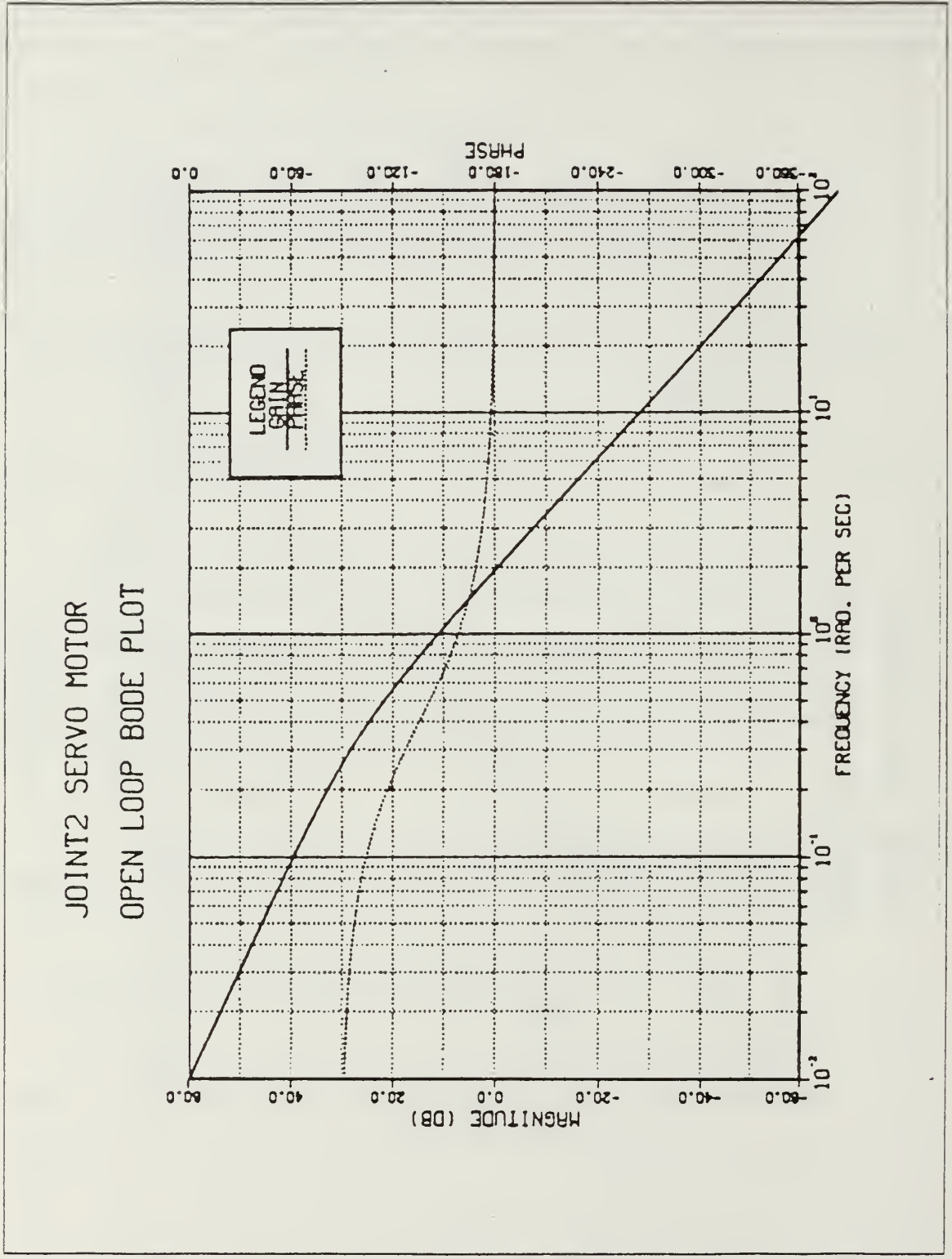

Figure 4.2 Open Loop Bode Plot of the JOINT2 Servo Motor.

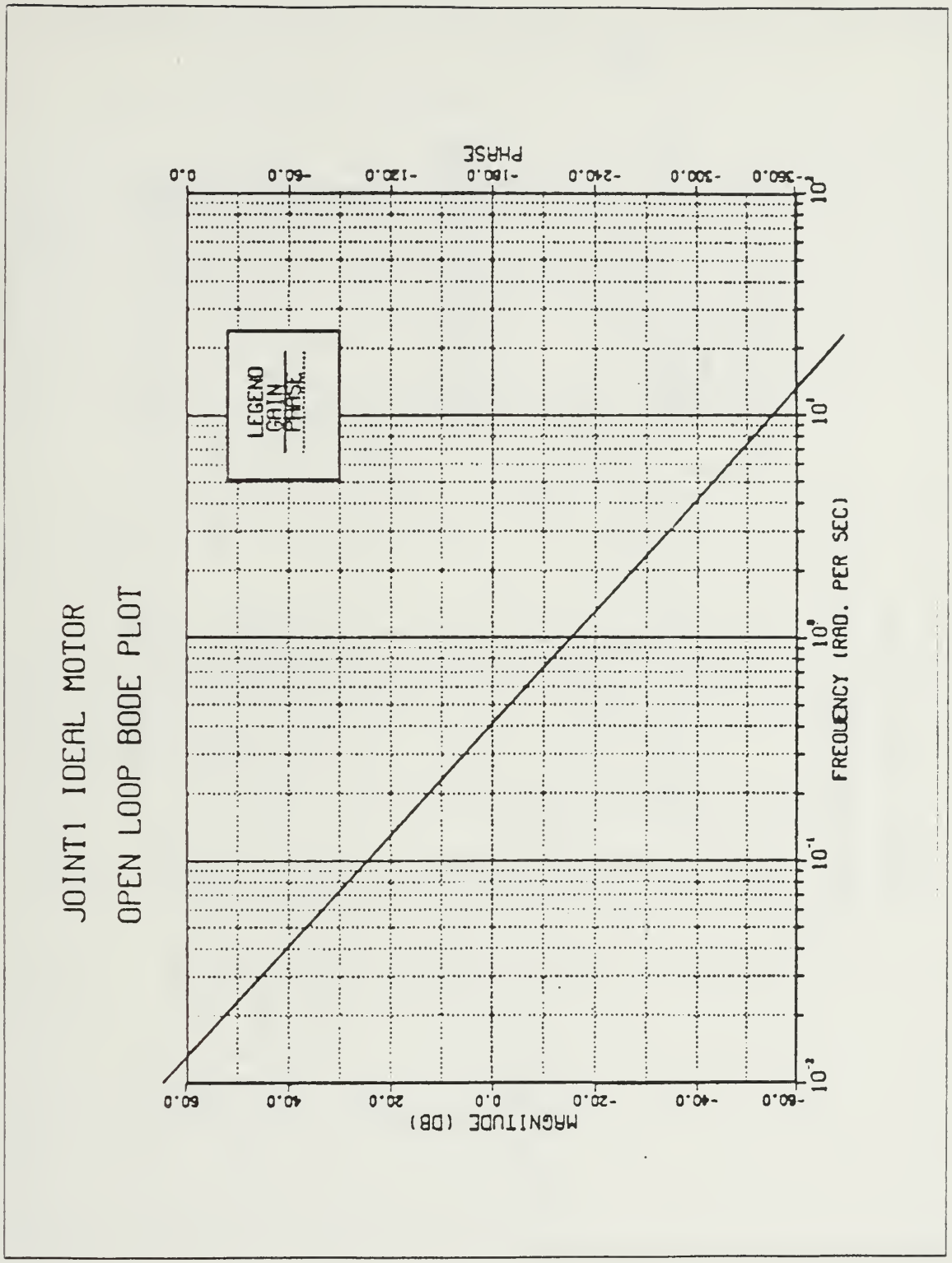

Figure 4.3 Open Loop Bode Plot of the K_{m1}/s^2 Motor.

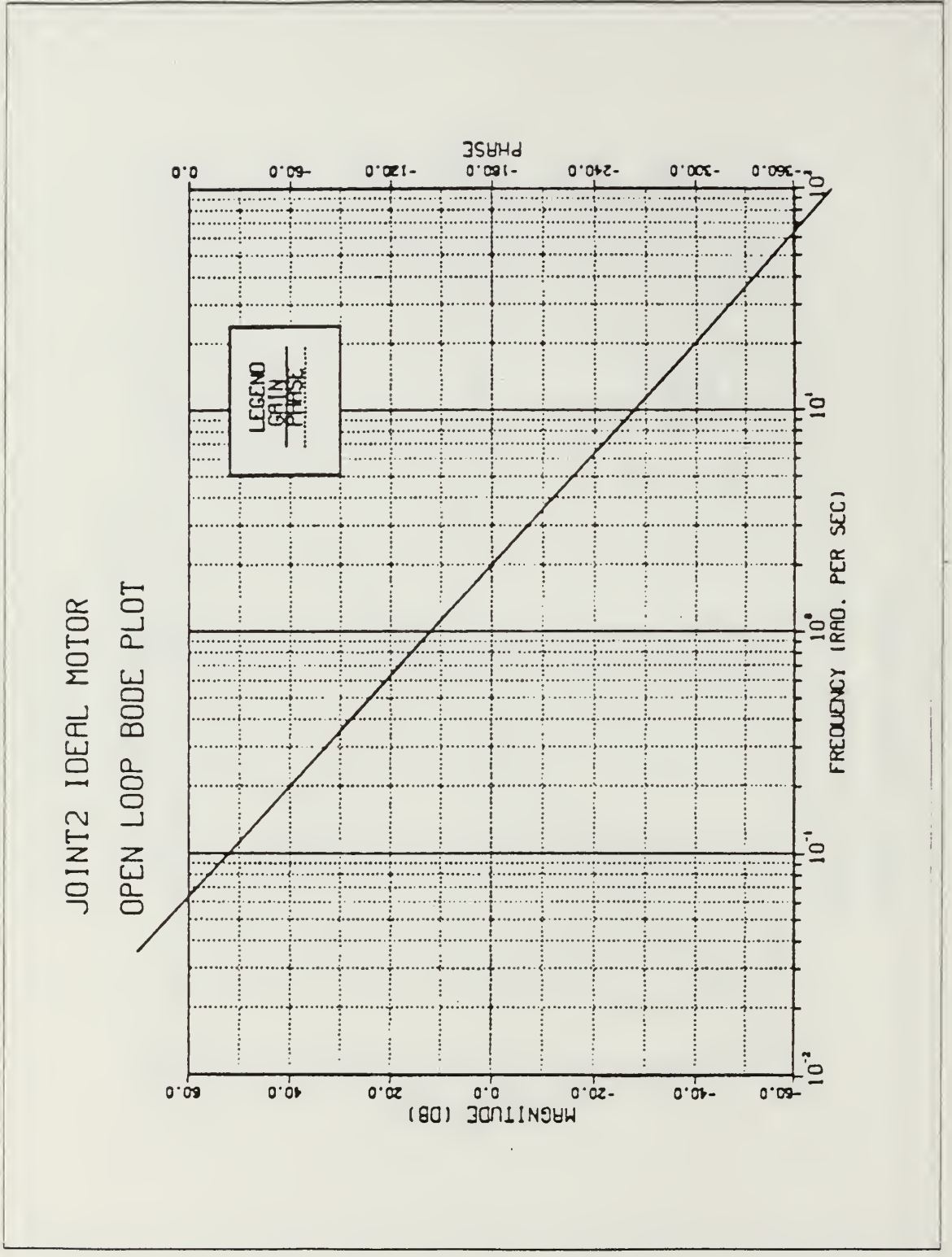

Figure 4.4 Open Loop Bode Plot of the K_{m2}/s^2 Motor.

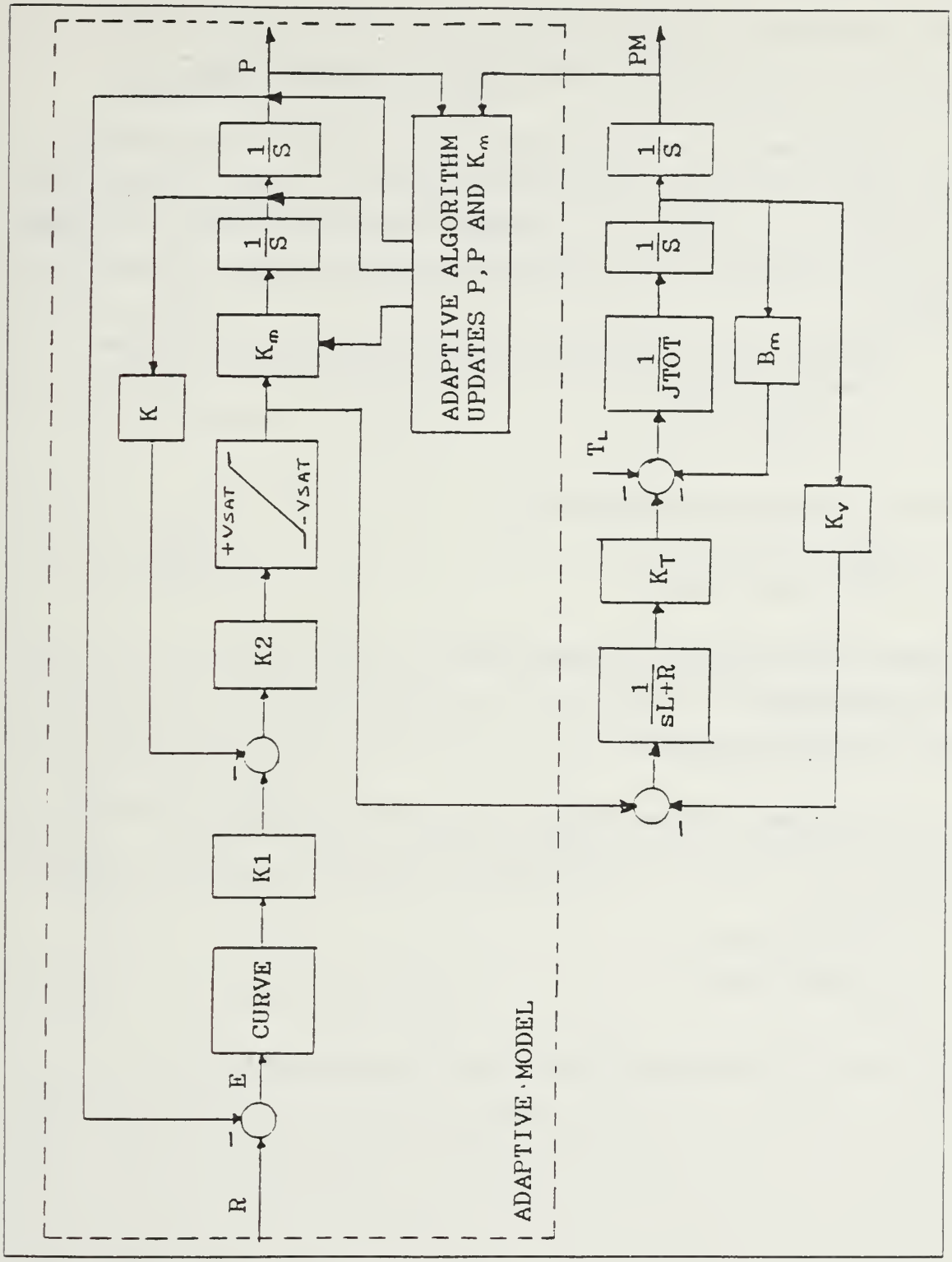

Figure 4.5 Block Diagram of the Adaptive Joint Drive System.

V. PLANNING THE SIMULATION STUDIES

A set of sample motions was selected to serve as a basis for simulation studies of the system. The sample motions were designed to remove as many of the nonlinearities as possible and to investigate the system behavior for possible overloading conditions. The set of sample motions used are depicted in Figures 5.1, 5.2 and 5.3.

Simulation studies were done for two different drive systems. These were:

- Voltage Source Drive
- Current Source Drive

Each drive system was tested separately for:

- Gravity-Free Environment
- With Gravity Loading

Position Command inputs to the system were:

- Step Input
- Time Varying Input

In this thesis, a free work space is assumed for the robot arm. To find the minimum time response for a given step position command, a step input was applied to the servo motors:

- At the same time
- At different times

All simulation studies are planned for both loaded and unloaded robot arms.

- The calculations must be accurate enough to allow the second-order model states to approximate the trajectory of the servo motor.
- The calculations must be kept simple to update the second-order model states and gain constant in minimum time.

There are several means of doing these calculations. For our purpose, the method described in [Ref. 1] best satisfies the criterion given above. It can be shown [Ref. 1] that; when we solve Equation 2.5 for K_m,

$$K_m = \frac{2P}{Vsat\ t^2} \qquad \text{(eqn 4.3)}$$

For discrete time intervals and letting P = PM,

$$K_m = \frac{2PM}{Vsat(NT)^2} \qquad \text{(eqn 4.4)}$$

Where T is the sampling period and N is the number of sampling intervals. Equation 4.4 is valid only for constant acceleration of the servo motor. Therefore the value of K_m is updated during the full acceleration of the servo motor, then remains unchanged for the curve following portion.

The estimation of the angular velocity of the servo motor has been given [Ref. 1]

$$\dot{PM}(N) = 2[PM(N) - PM(N-1)]/T - \dot{PM}(N-1) \qquad \text{(eqn 4.5)}$$

$$\dot{PM}(N-1) = [PM(N) - PM(N-2)]/2T \qquad \text{(eqn 4.6)}$$

Equation 4.5 requires the storage of the last sample position of the servo motor [PM(N − 1)] and the last estimated angular velocity [$\dot{PM}(N-1)$]. The stored value of $\dot{PM}(N-1)$ can be recalculated after 2 samples of position are taken. If the second-order model switches from full acceleration to curve following between samples of position, Equation 4.5 is not self-correcting until two position samples can be taken after switching. To take care of the deficiency, the switching time is detected and the present value of the second-order model velocity is stored as $\dot{PM}(N-1)$ to be used in the next calculation.

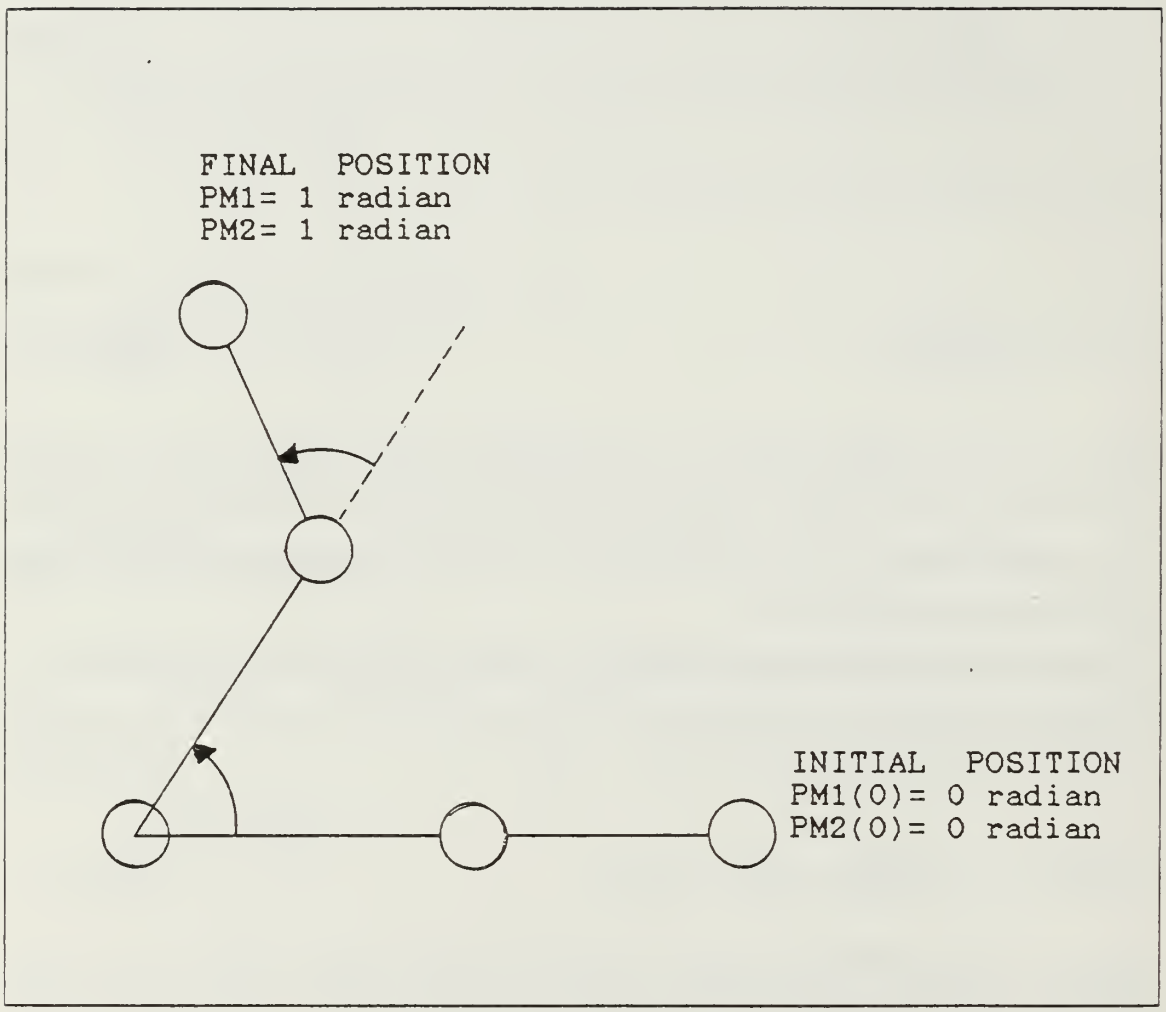

Figure 5.1 Sample Move #1.

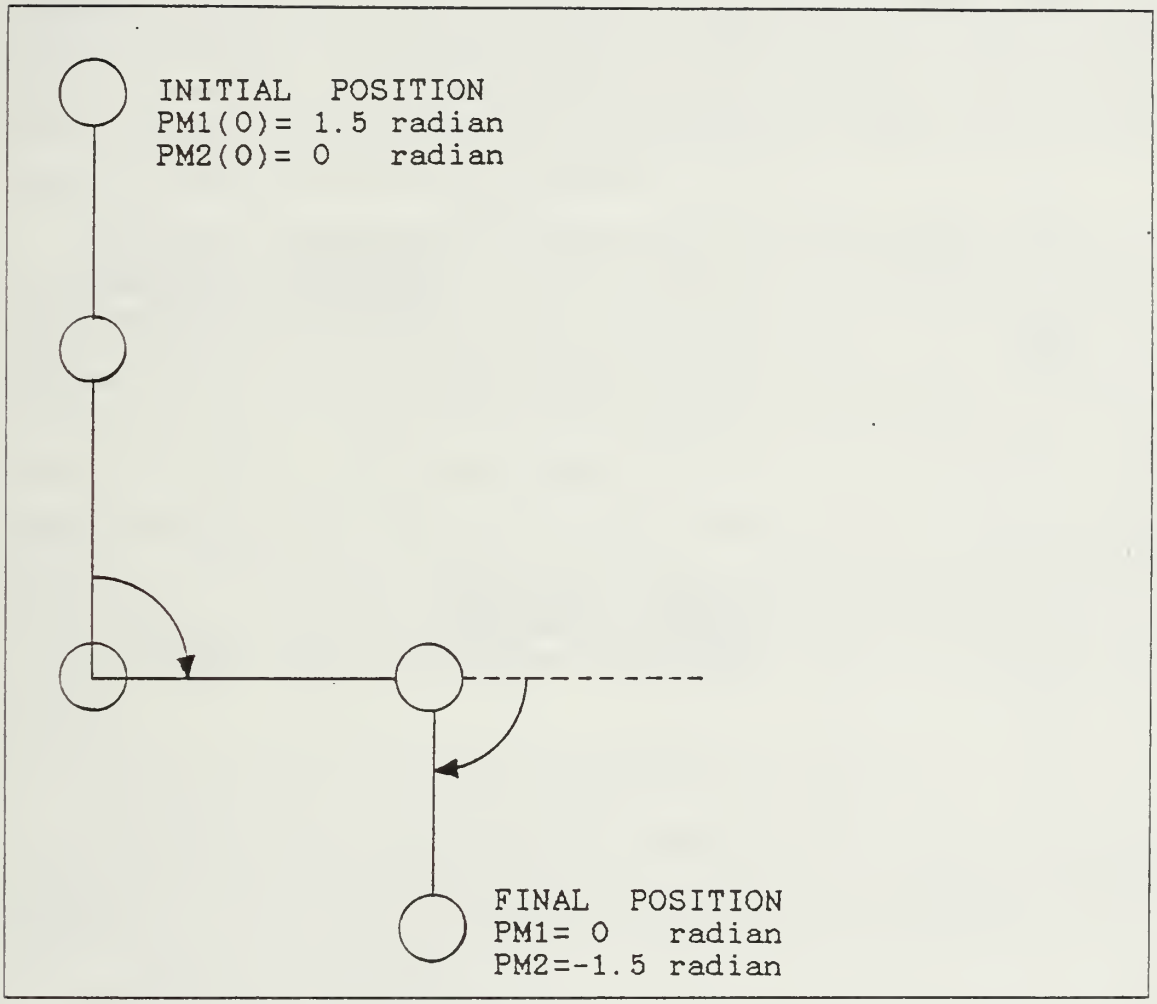

Figure 5.2 Sample Move #2.

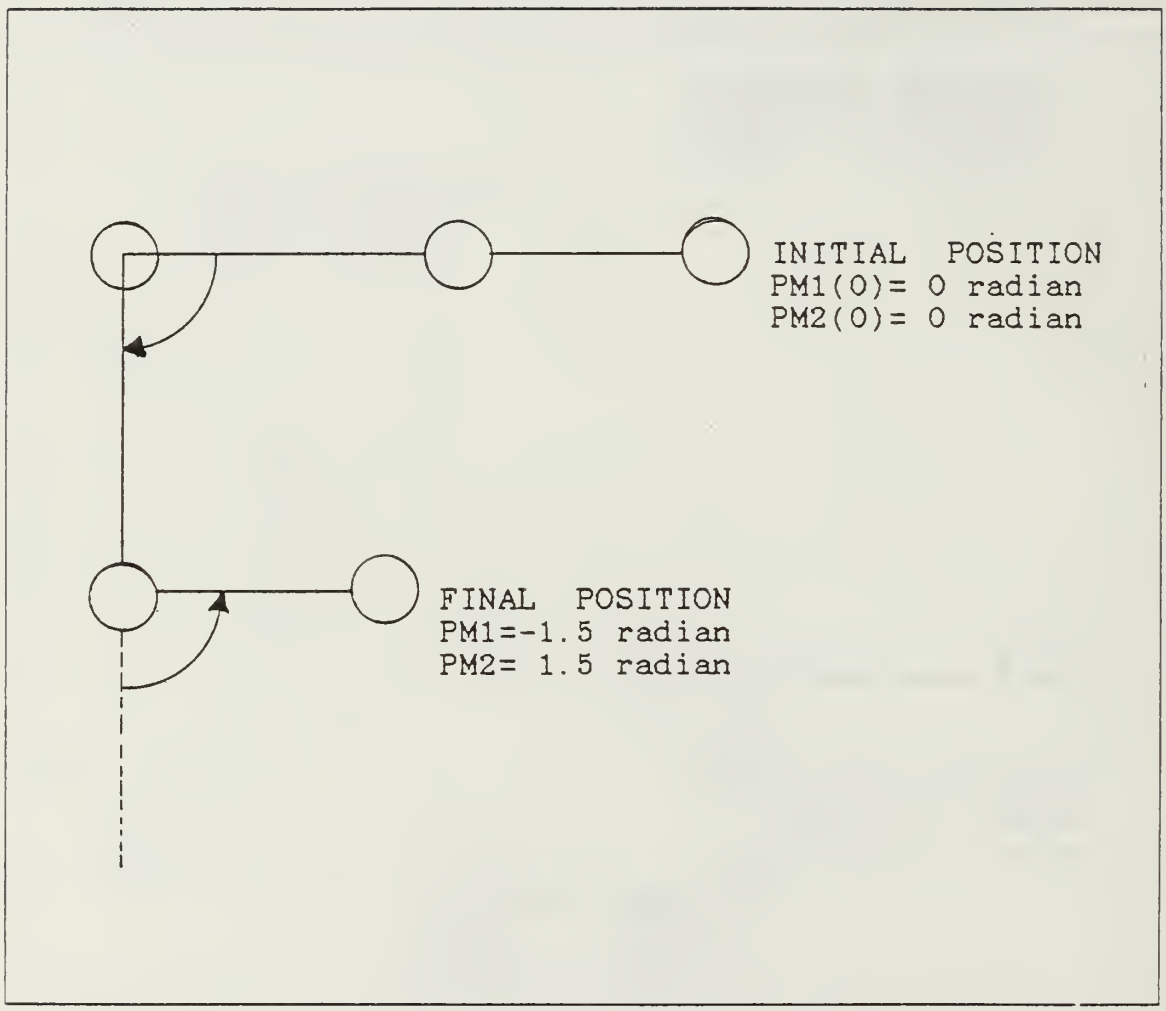

Figure 5.3 Sample Move #3.

VI. THE VOLTAGE SOURCE DRIVE SYSTEM

A. INTRODUCTION

The computer adaptive system with voltage source drive was developed in Chapter IV. Figure 4.5 illustrates the block diagram of the adaptive system with voltage source drive. The DSL/VS simulation program used in the testing of the adaptive system with Voltage Source Drive, is listed in Appendix C. Both adaptive models with servo motors are simulated at the same time in the program to assure realistic interaction between joint servo motors.

A sample region was added to obtain the servo motor angular positions at discrete time intervals PM(N). The DELS parameter of the DSL VS simulation program allows the simulation to enter the sample region every $T = 0.25$ milliseconds. The adaptive algorithm, also included in the sample region, calculates the estimates of servo motor angular velocity ($\dot{PM}$) and the second-order model gain parameter (K_m) from the sample of the servo motor angular position. At every sampling time, the second-order model states P, $\dot{P}$ are reset with the values of the servo motor position and velocity PM, $\dot{PM}$ and the model gain parameter K_m is updated during the full acceleration part. Fixed step integration was used in the simulation to support easy hardware implementation. The integration interval was chosen to be 1/5 the sampling period.

B. SIMULATION STUDIES OF THE ADAPTIVE SYSTEM

Appendix C and D list the DSL/VS simulation programs used in testing the adaptive system. The simulation program for the gravity-free environment is included in Appendix C. The simulation program in Appendix D includes gravitational torques.

1. Gravity-free Environment

The adaptive system without gravitational torques is tested for both step position command and time varying position command inputs. Note that on all phase plane plots the velocity of the second-order model and the velocity of the servo motor are both plotted as ordinates. In general these curves fall on top of each other. Move #1 and Move #2 are used in this part of the simulation studies. The following results are observed:

a. Step Position Command Input Used

Figures 6.1 and 6.2 are the phase plane plot and step response curves for the unloaded arm. In the phase plane plot, the second-order angular velocity $\dot{P}$ and the servo motor angular velocity $\dot{PM}$ are plotted versus servo motor angular position PM. Although $\dot{PM}$ cannot be observed in the actual system, it is available in the simulation and is used to check the validity of the algorithm.

Figure 6.1 shows that the second-order model and servo motor have good curve following characteristics for both joints. The step response curves of Figure 6.2 show the models and servo motors tracking together. Steady state accuracy of the order of 10E-4 is observed. The loaded arm was simulated in Figures 6.3 and 6.4 In these figures, effects of the reaction torques can be observed. At the beginning of the move, upward motion of the LINK2 creates an interaction torque on JOINT1 servo motor. Therefore it takes time to overcome the reaction torque and LINK1 starts accelerating. To avoid this unwanted situation, the position command for JOINT2 servo motor is delayed 150 millisecond at the beginning of the move. This is shown in Figures 6.5 - 6.8.

The effects of the delayed input for phase plane trajectories can be observed in Figures 6.5 and 6.7. When JOINT2 servo motor starts accelerating, the reaction torque causes JOINT1 servo motor to decelerate for a while. Meanwhile, curve following seems lost but after a while the adaptive system tracks and follows the curve until the desired position is reached. Faster over-all response was obtained with this strategy also.

Simulation studies for Move #2 are shown in Figures 6.9 - 6.16. Figures 6.9 and 6.11 are good illustrations to point out the importance of the reaction torques between joints. Interactive torques gain more importance when servo motors operate in opposite directions. In these figures it can be observed, acceleration of the JOINT2 servo motor helps JOINT1 servo motor to speed up quickly. When JOINT2 servo motor reaches the curve and starts deceleration, the interaction torque created by JOINT2 servo motor opposes JOINT1 servo motor acceleration. Maximum angular velocity of 3.7 rad/sec and 13.4 rad/sec are observed for motors 1 and 2 respectively. Step response curves of Move #2 are shown in Figures 6.10 and 6.12.

The adaptive system was also simulated for a different input sequence, ie JOINT2 servo motor position command delayed at 0.15 second. The effects of the delayed input can be observed in phase plane plots of Figures 6.13 and 6.15.

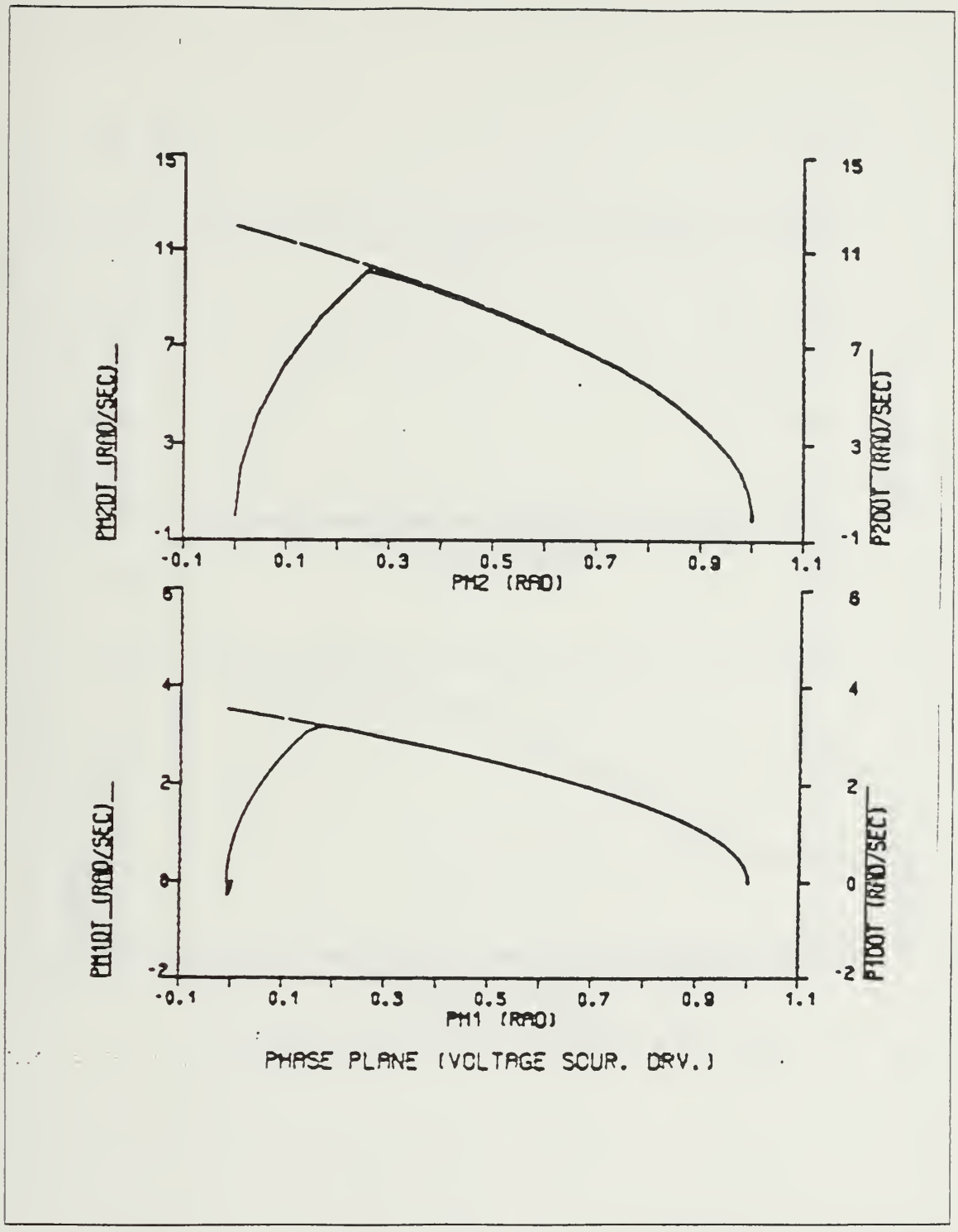

Figure 6.1 Phase Plane Trajectory For Move #1 (No Gravity).

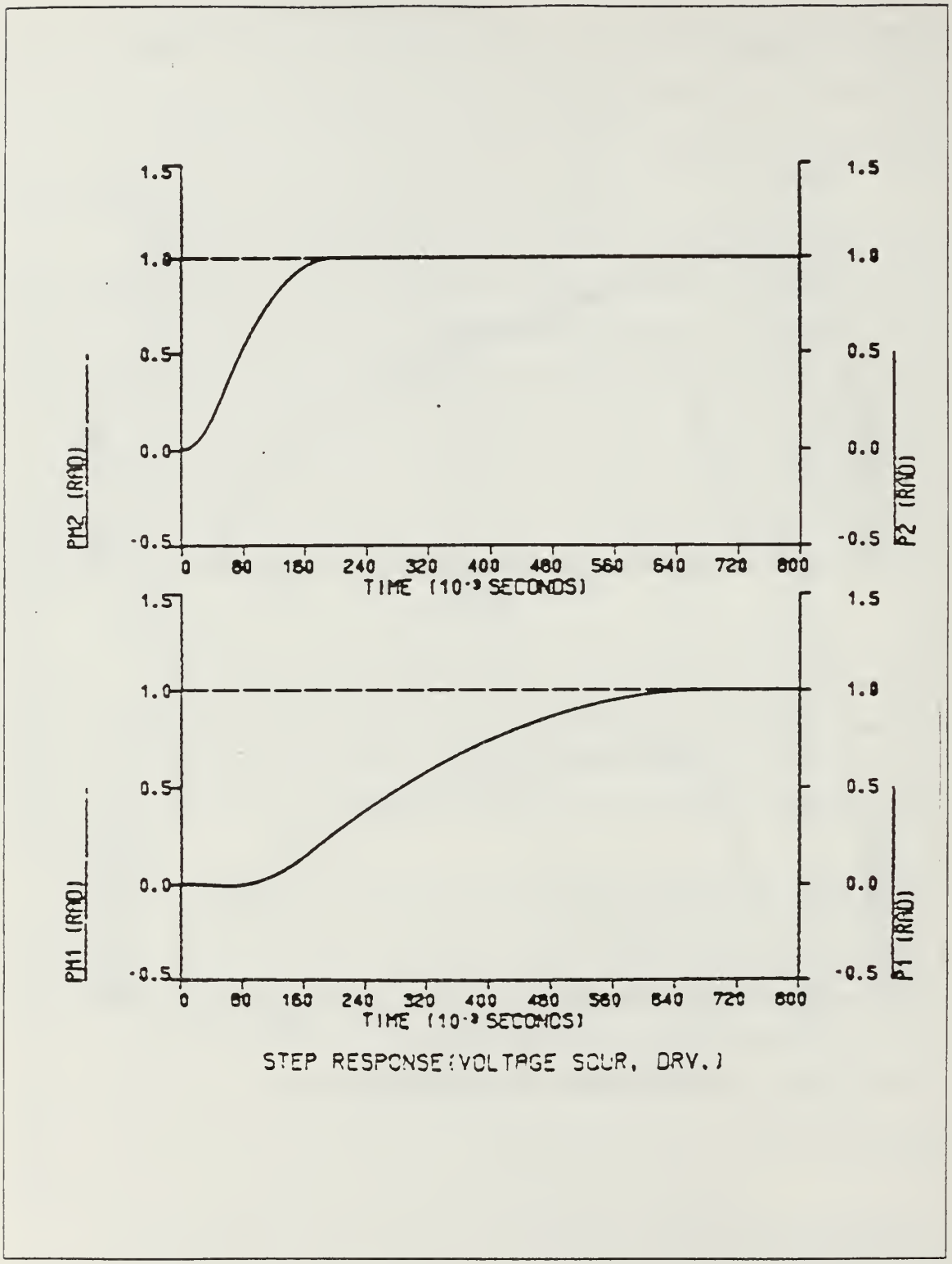

Figure 6.2 Step Response For Move #1 (No Gravity).

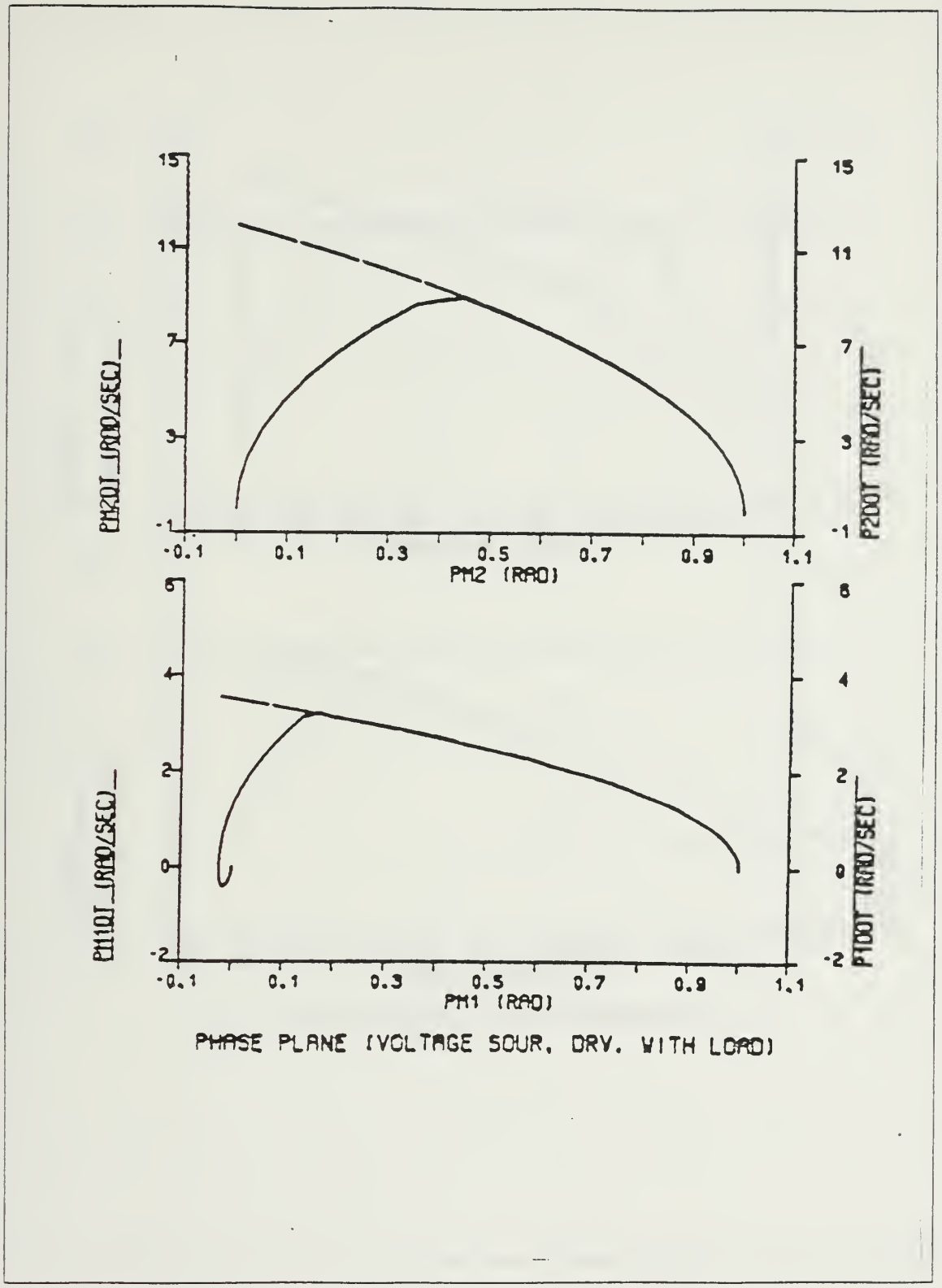

Figure 6.3 Phase Plane Trajectory For Move #1 (No Gravity).

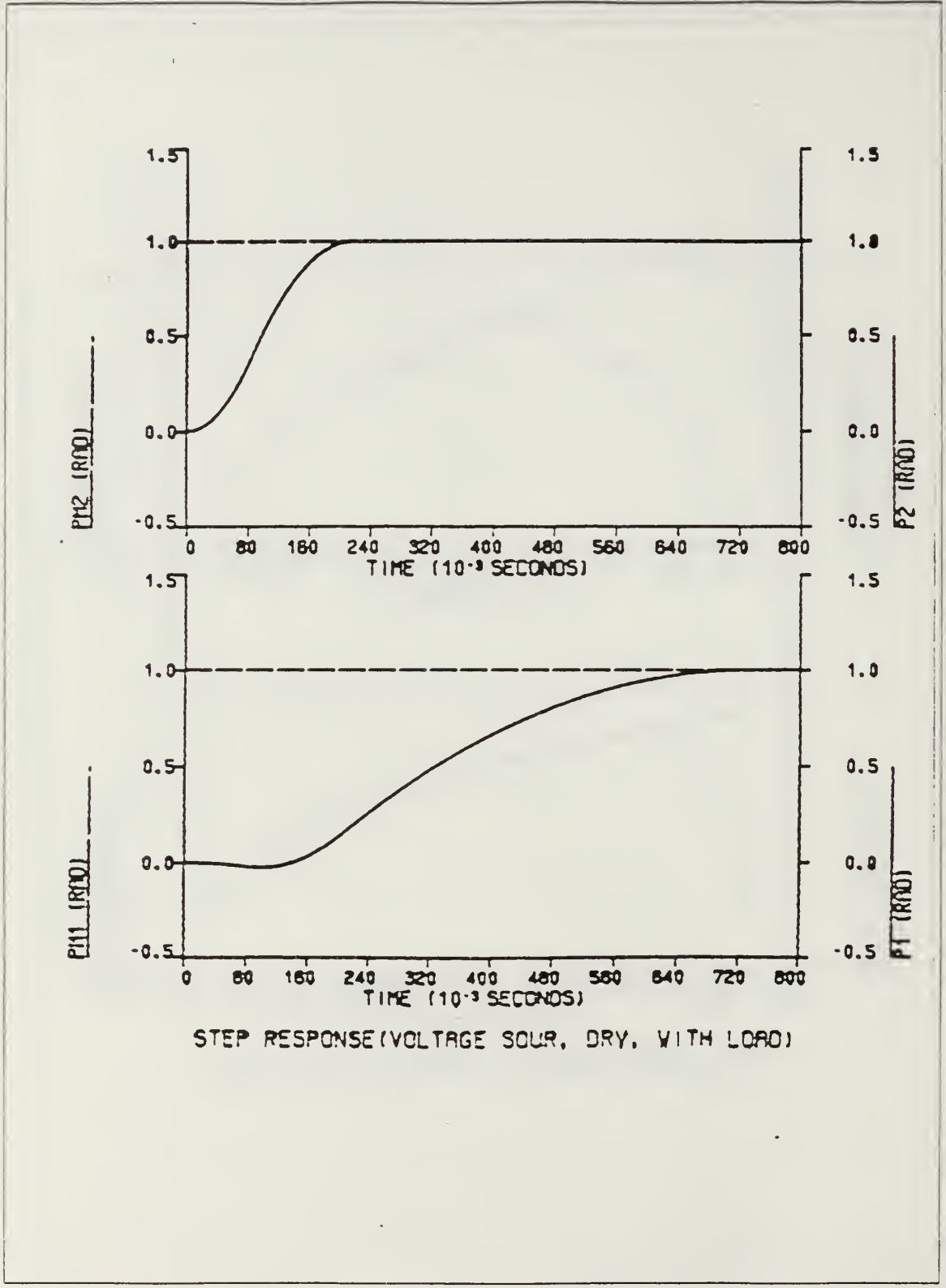

Figure 6.4 Step Response For Move #1 (No Gravity).

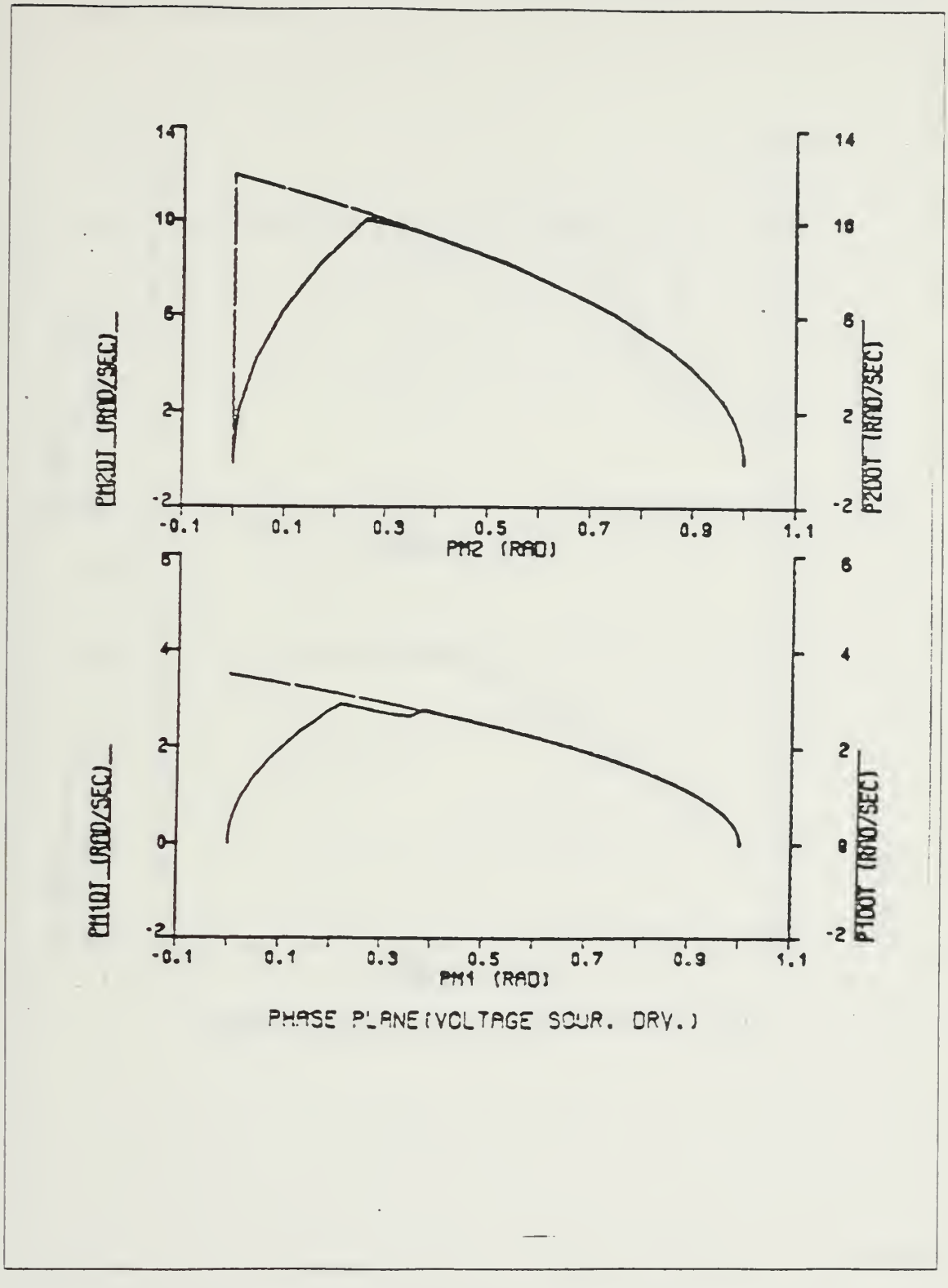

Figure 6.5 Phase Plane Trajectory For Move #1 (No Gravity)
JOINT2 Servo Motor Input Delayed 0.15 sec.

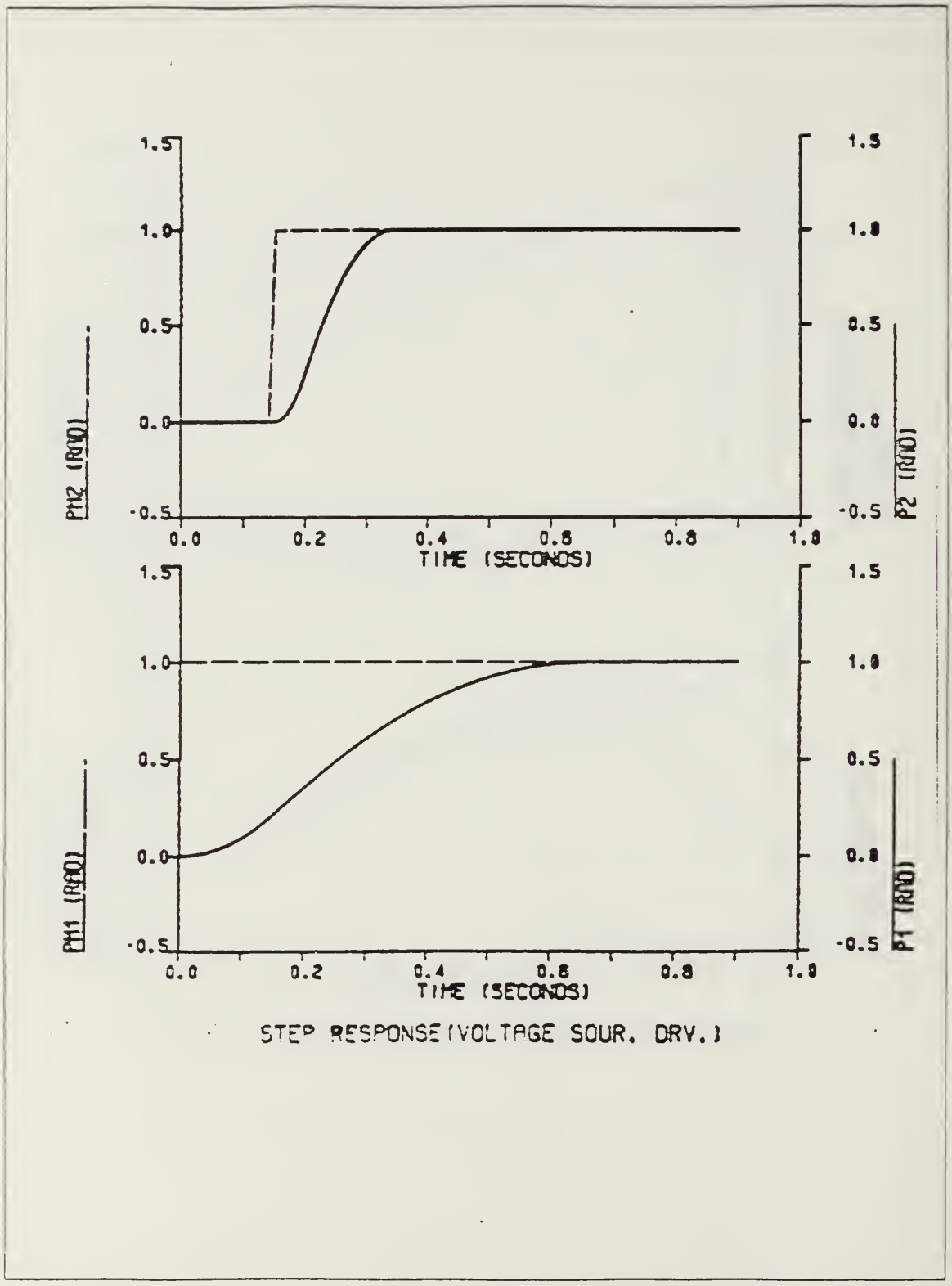

Figure 6.6 Step Response For Move #1 (No Gravity)
JOINT2 Servo Motor Input Delayed 0.15 sec.

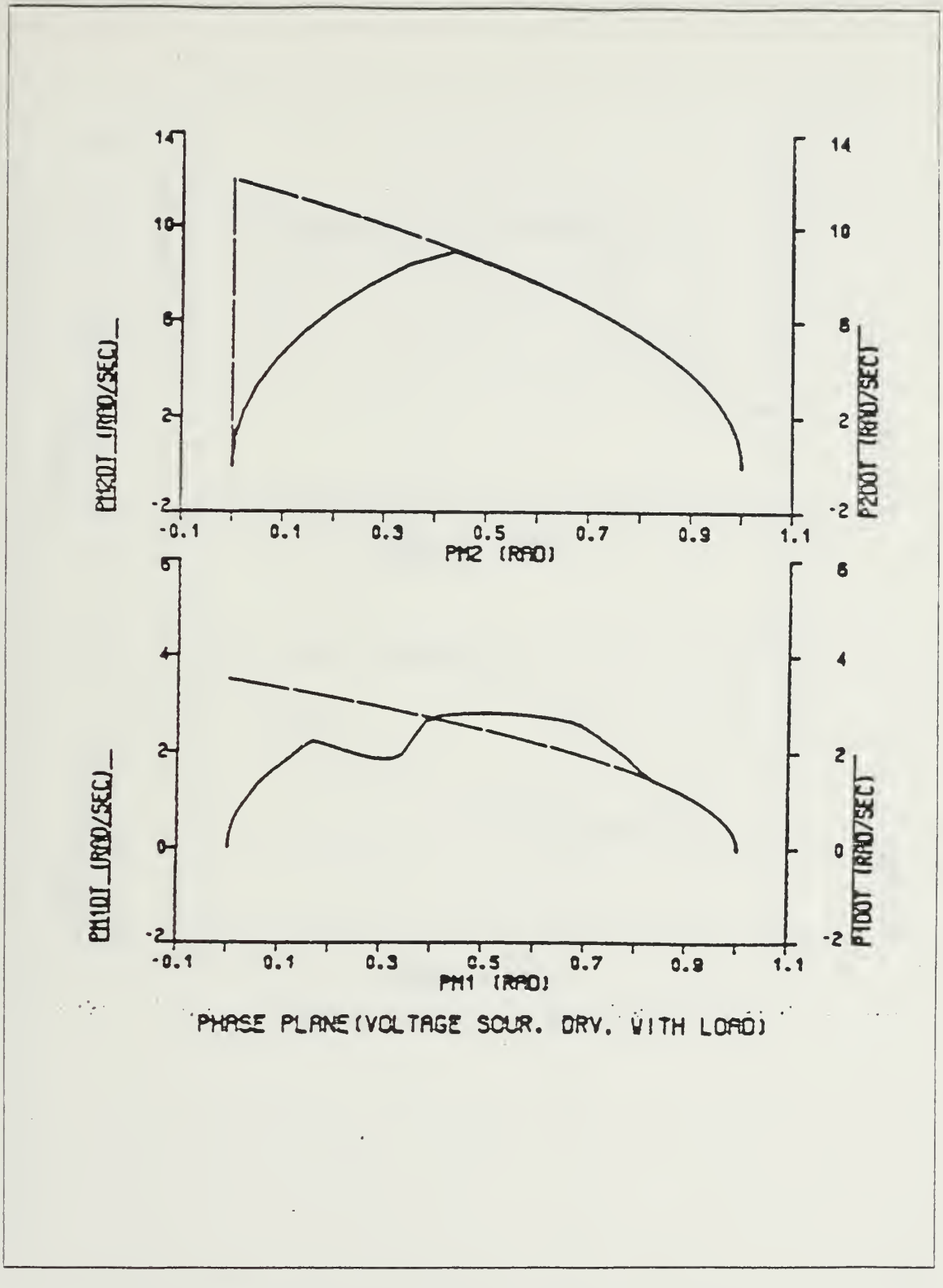

Figure 6.7 Phase Plane Trajectory For Move #1 (No Gravity)
JOINT2 Servo Motor Input Delayed 0.15 sec.

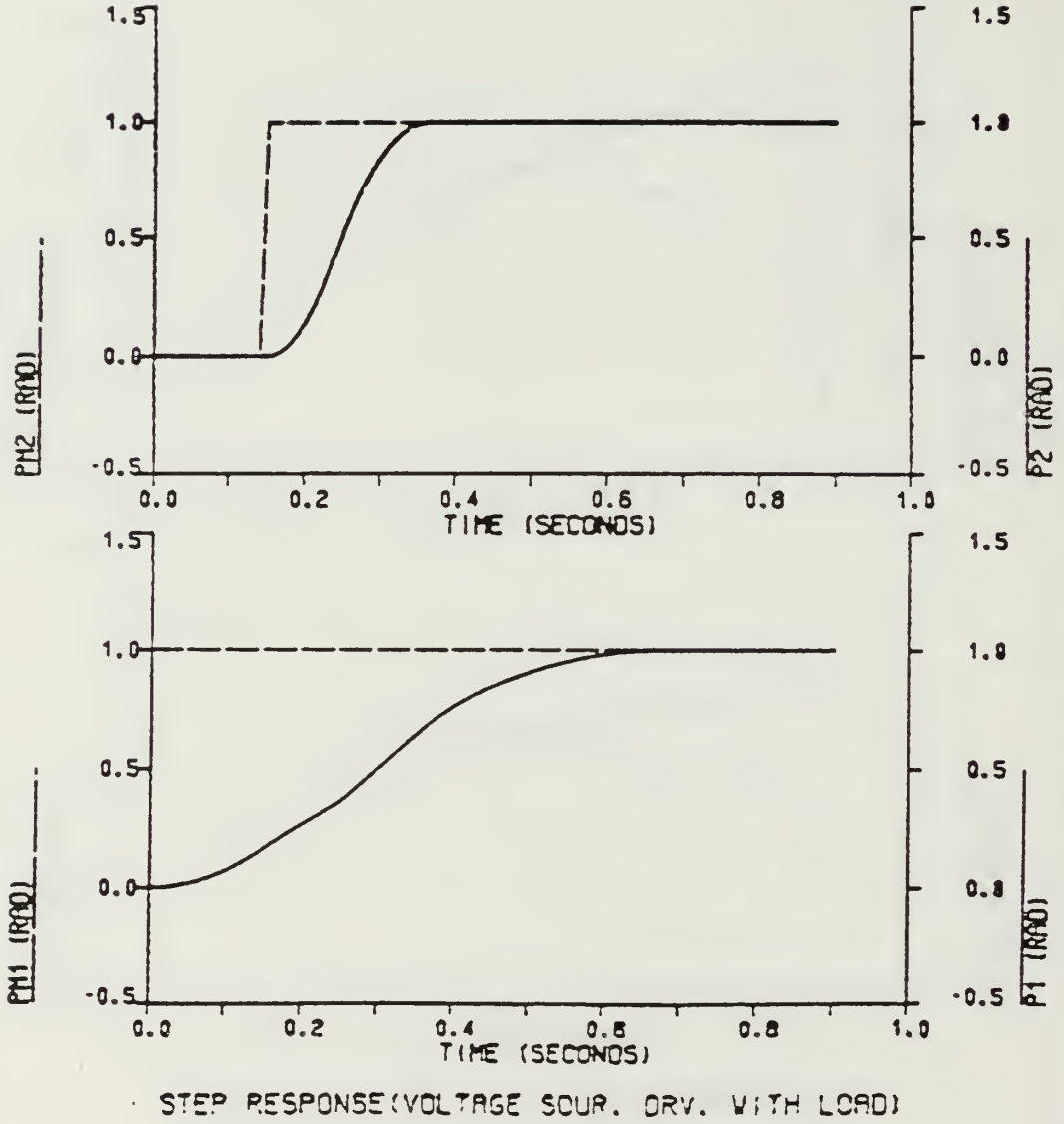

Figure 6.8 Step Response For Move #1 (No Gravity)
JOINT2 Servo Motor Input Delayed 0.15 sec.

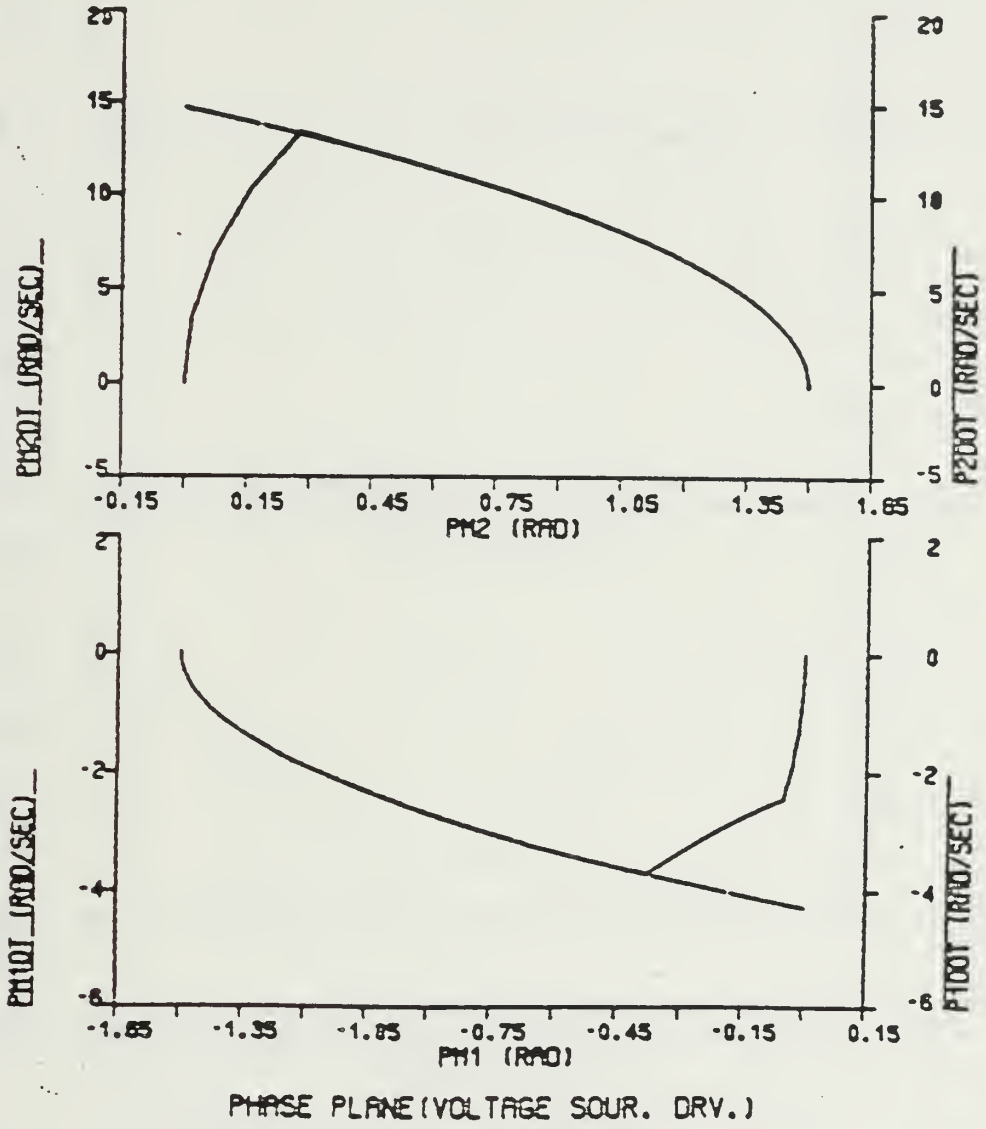

Figure 6.9 Phase Plane Trajectory For Move #2 (No Gravity).

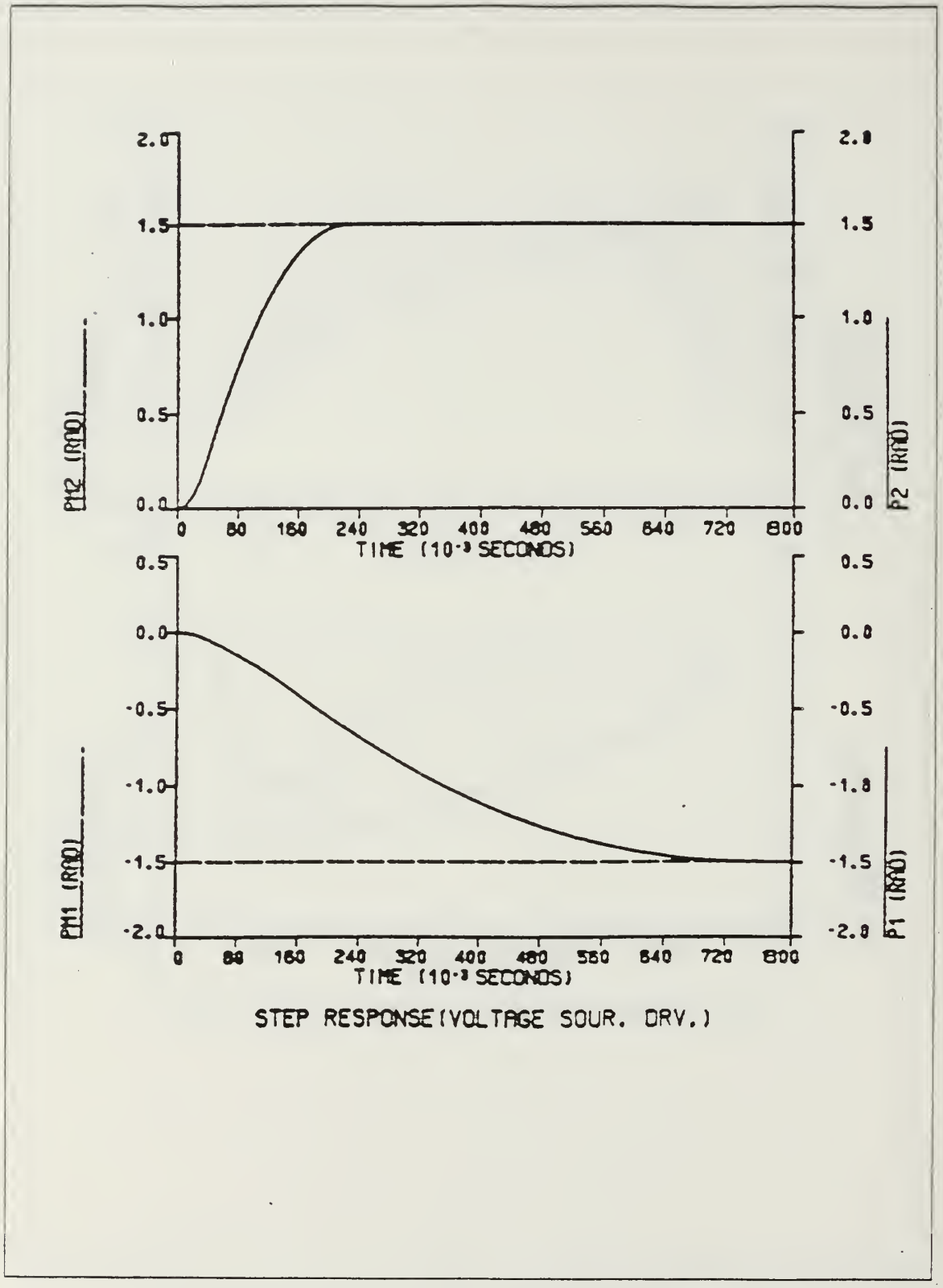

Figure 6.10 Step Response For Move #2 (No Gravity).

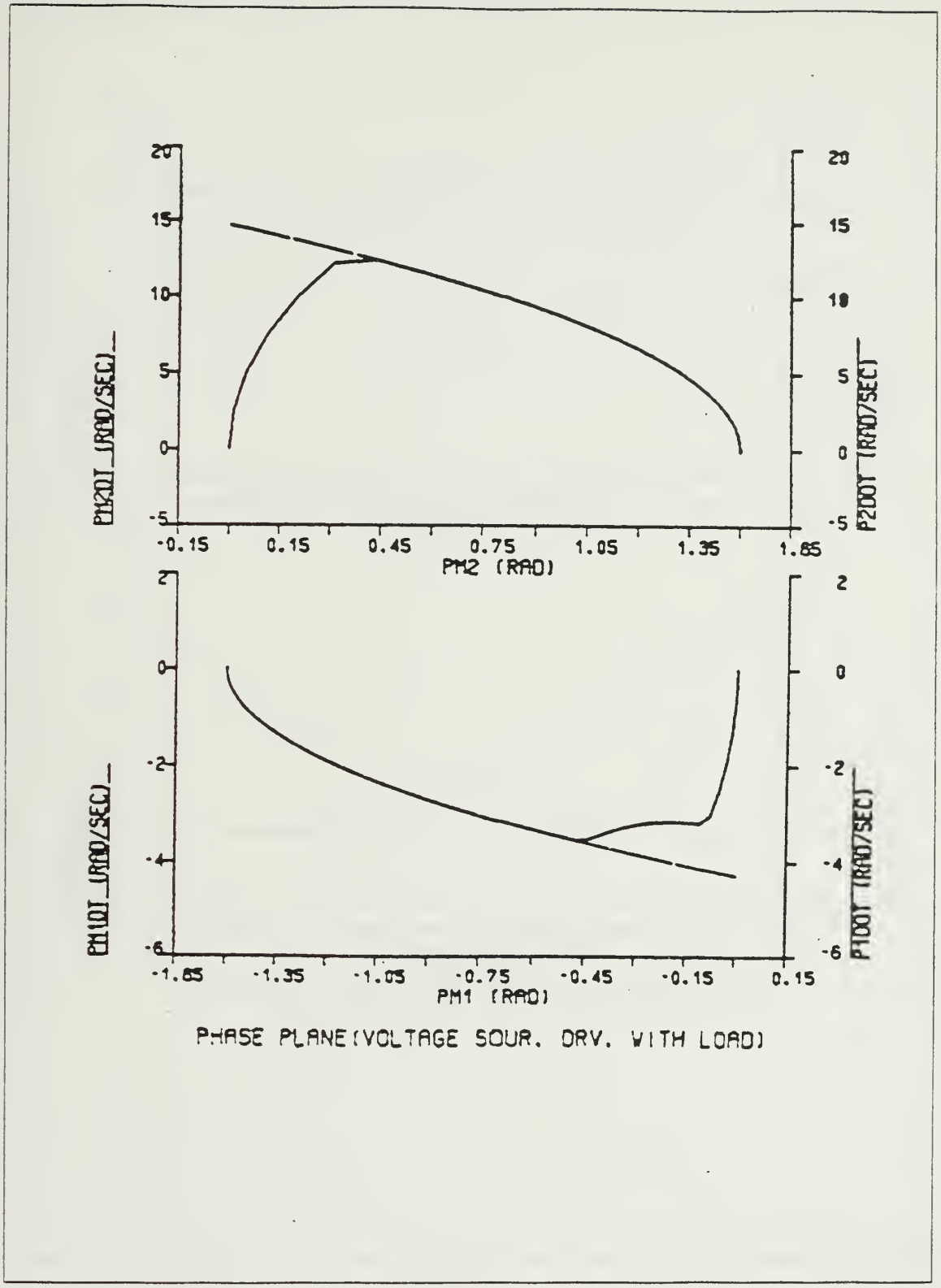

Figure 6.11 Phase Plane Trajectory For Move #2 (No Gravity).

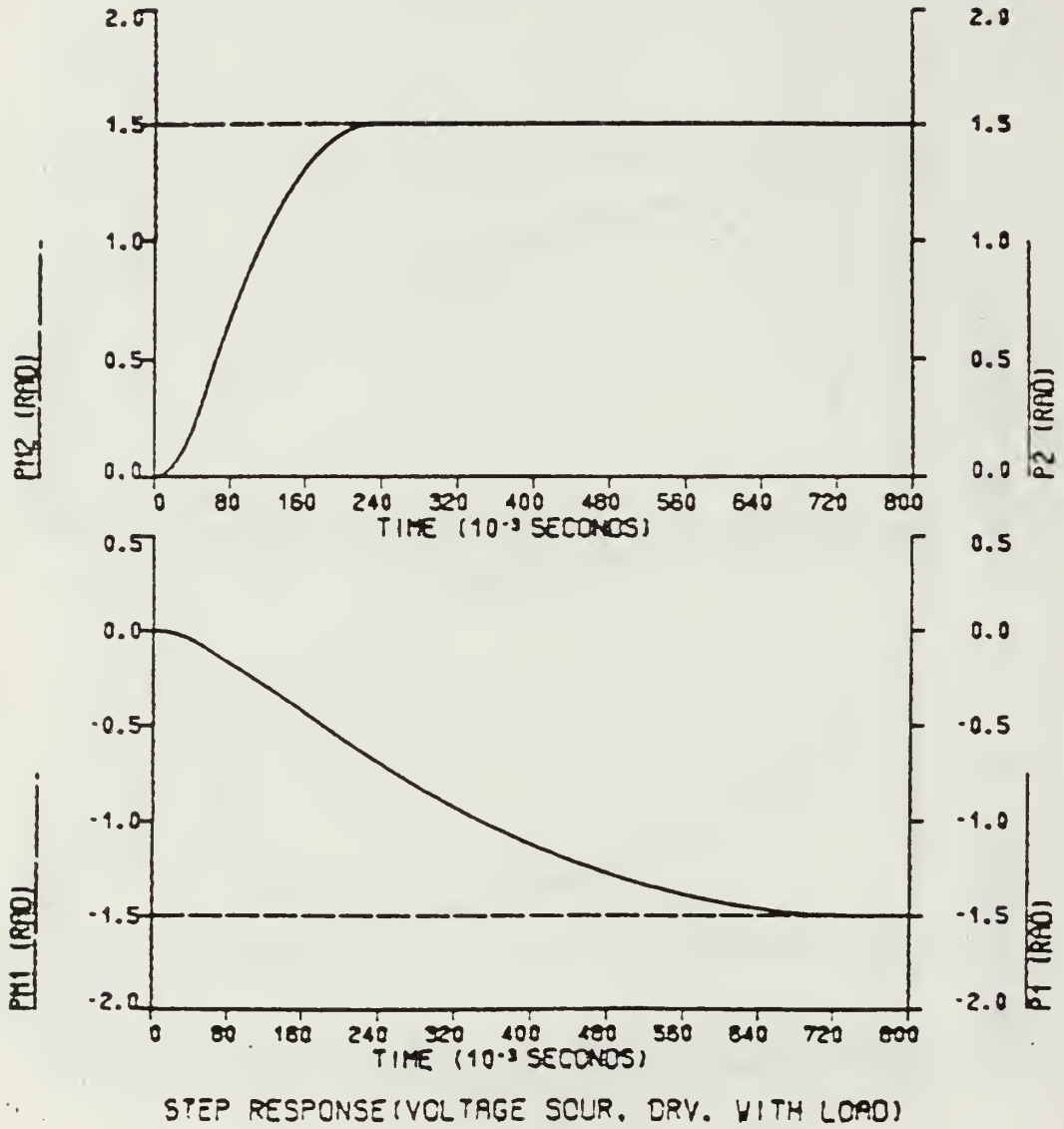

Figure 6.12 Step Response For Move #2 (No Gravity).

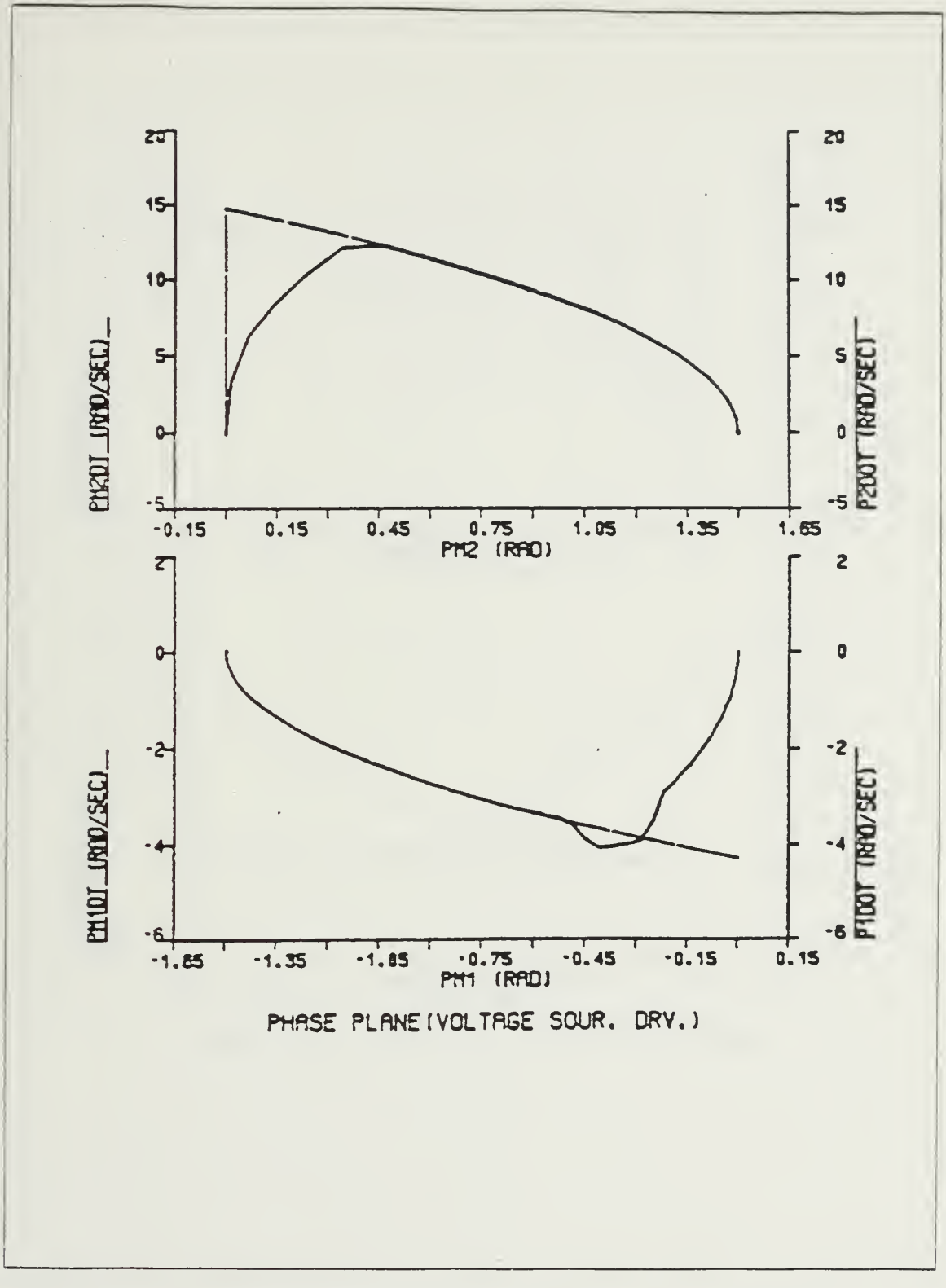

Figure 6.13 Phase Plane Trajectory For Move #2 (No Gravity)
JOINT2 Servo Motor Input Delayed 0.15 sec.

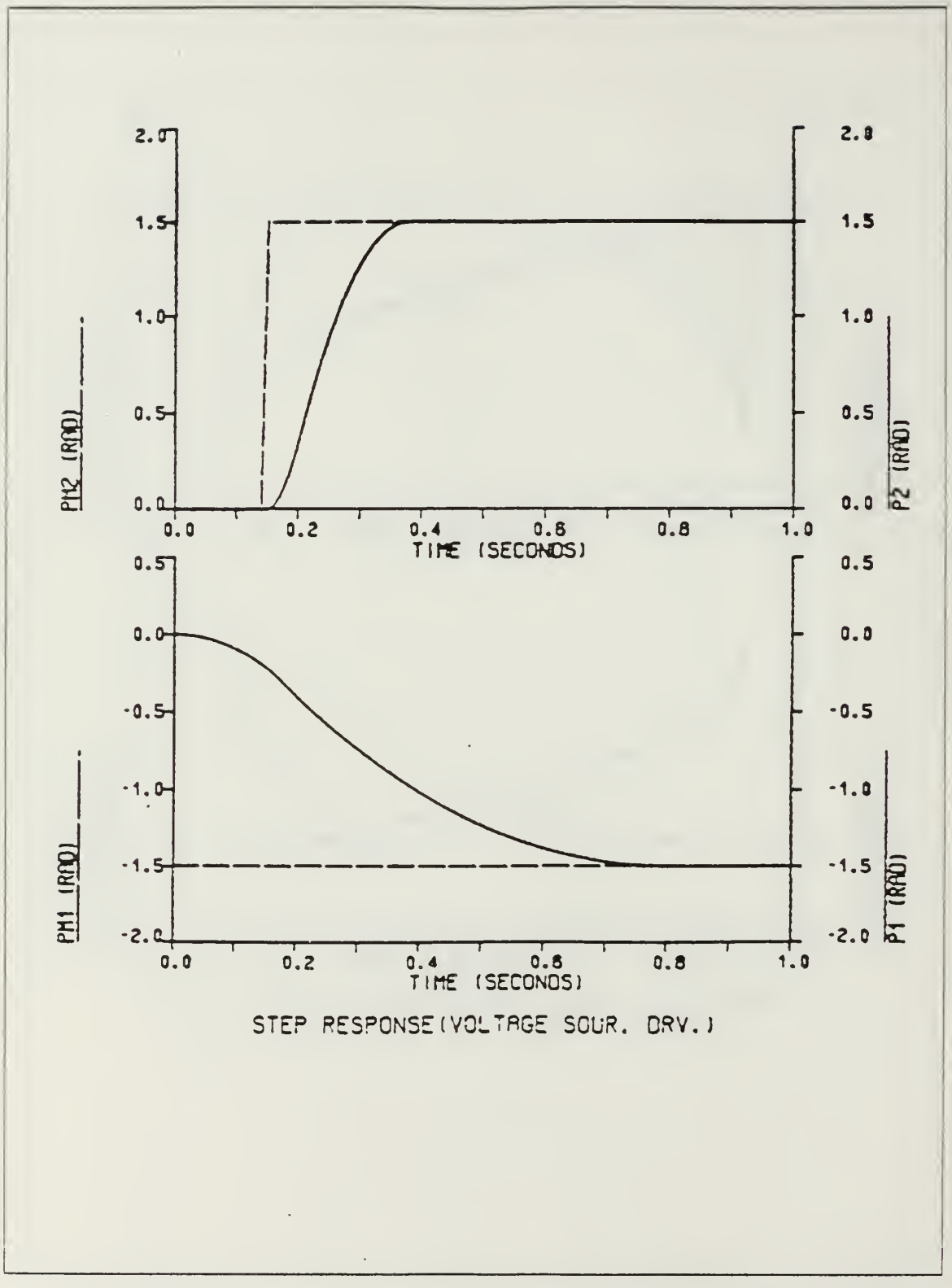

Figure 6.14 Step Response For Move #2 (No Gravity)
JOINT2 Servo Motor Input Delayed 0.15 sec.

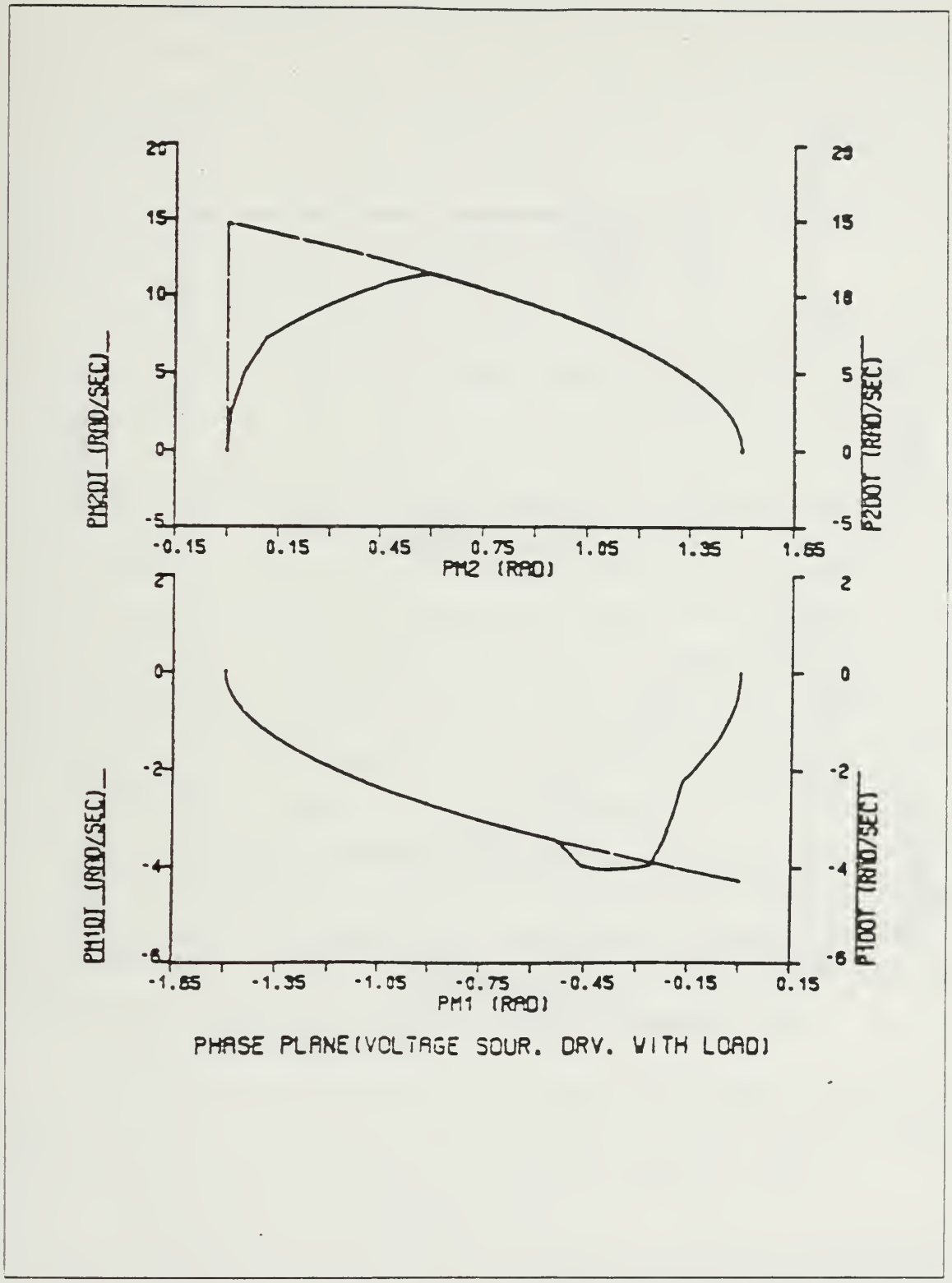

Figure 6.15 Phase Plane Trajectory For Move #2 (No Gravity)
JOINT2 Servo Motor Input Delayed 0.15 sec.

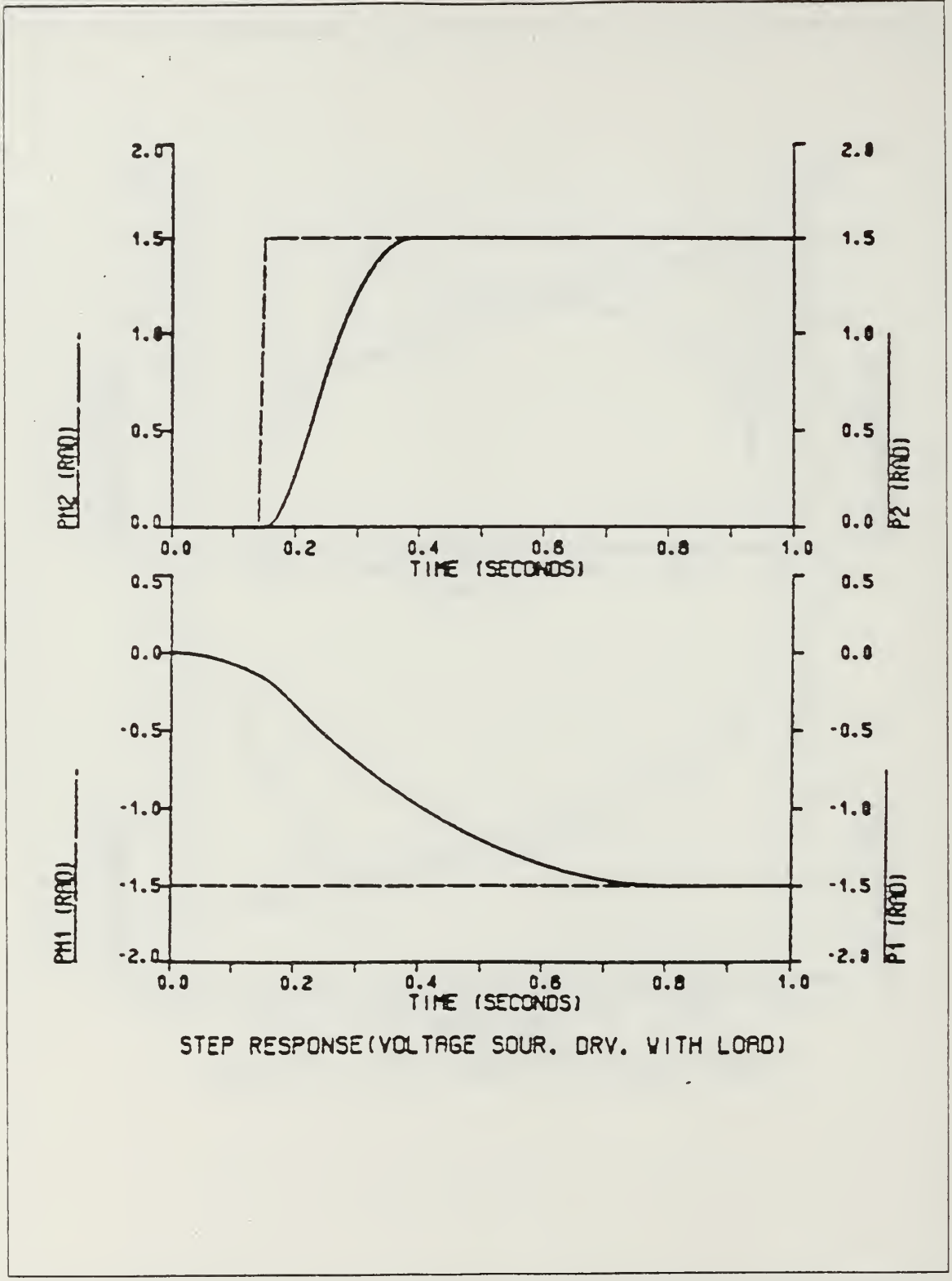

Figure 6.16 Step Response For Move #2 (No Gravity)
JOINT2 Servo Motor Input Delayed 0.15 sec.

At the beginning of Move #2 JOINT1 servo motor moves slower while the other servo motor stands still. After JOINT2 servo motor starts accelerating, appreciable speed-up can be observed in the first servo motor phase plane trajectory. This speed-up results in passing over the curve a little. After a while the system tracks the curve and follows it until the position is reached. Step response curves in Figures 6.14 and 6.16 show 40 milliseconds slower response time in comparison to the simulation results obtained when simultaneous inputs are applied.

b. Time Varying Position Command Input Used

To simulate the adaptive system under time varying command, a ramp input with tangent of 1 rad/sec and sinusoidal input are used. Simulation results are shown in Figures 6.17 - 6.28. Phase plane trajectories for ramp input are shown in Figures 6.17 and 6.20. Good curve following is observed in the figures. JOINT2 servo motor velocity builds up and becomes closer to steady-state velocity in a short time interval. JOINT1 servo motor velocity can't build up as fast as the second servo motor because of large inertial and interaction torques. Therefore JOINT1 servo motor follows the ramp input with larger errors. Figures 6.19 and 6.22 show position error for servo motors. Phase plane trajectories for sinusoidal input are shown in Figures 6.23 and 6.26. Good curve following is seen in these figures. JOINT2 servo motor follows the given input command easily with small errors but JOINT1 servo motor lags behind the sine input curve because of the reasons mentioned above in the case of a ramp input. Position error between commanded position input and actual servo motor position output is given in Figures 6.25 and 6.28.

Simulation studies show that the magnitude of the position error depends on the sinusoidal position command input magnitude and frequency. The smaller the frequency, the smaller the position error that is obtained. For a fixed frequency, the smaller magnitude of input gives a smaller position error.

2. **Gravitational Torques Included**

The adaptive system was simulated under gravitational torques. Moves #1, #2 and #3 were used to test the system for the existence of excess interactive torques. Both step input and time varying input were used in the simulation studies.

a. Step Position Command Input is Used

Figures 6.29 - 6.32 are the phase plane plots and step response curves for simultaneously applied step position input commands. Phase plane trajectories show that JOINT1 servo motor develops negative velocity (in the opposite direction of the

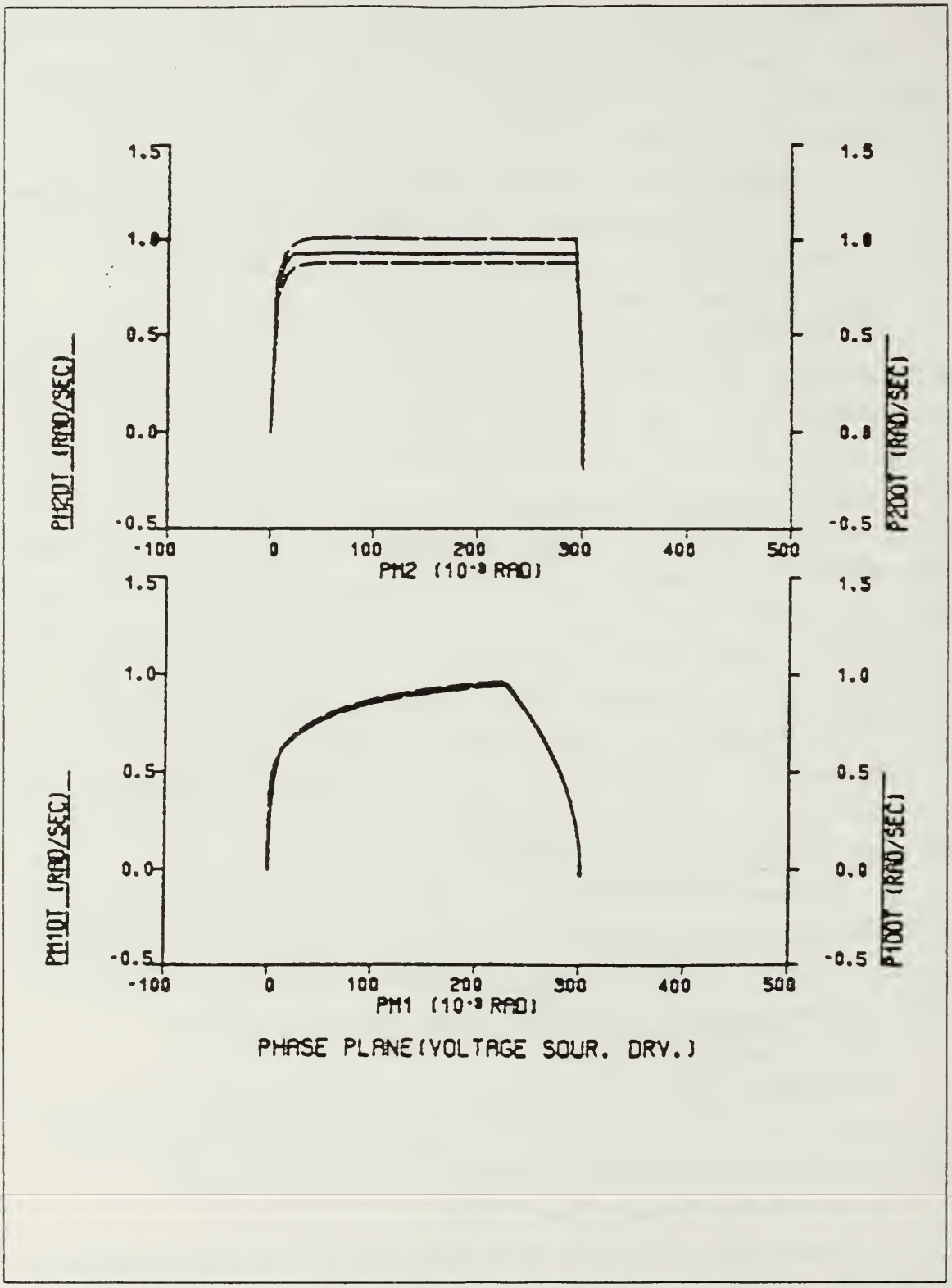

Figure 6.17 Phase Plane Trajectory For Ramp Input (No Gravity).

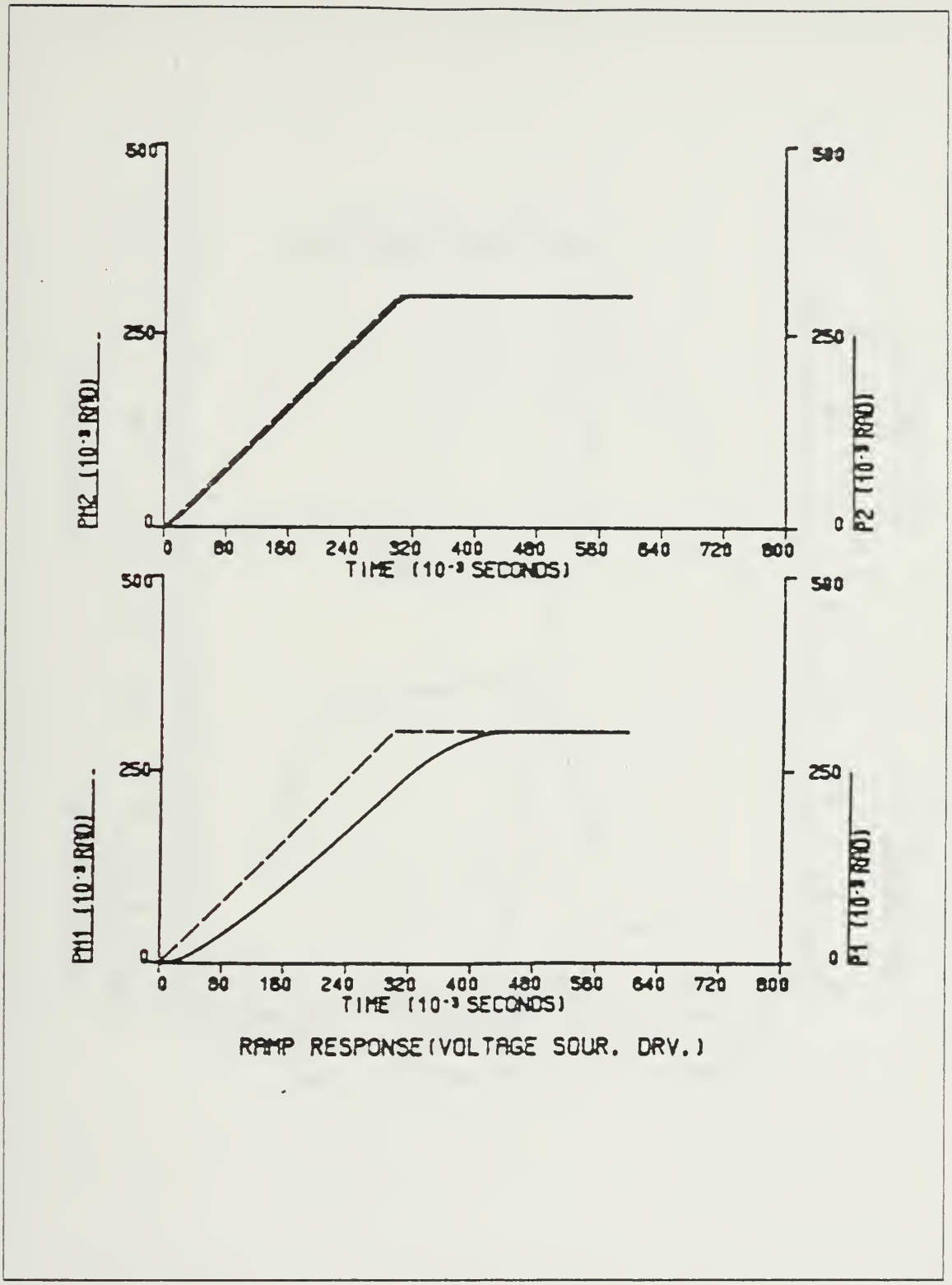

Figure 6.18 Ramp Response (No Gravity).

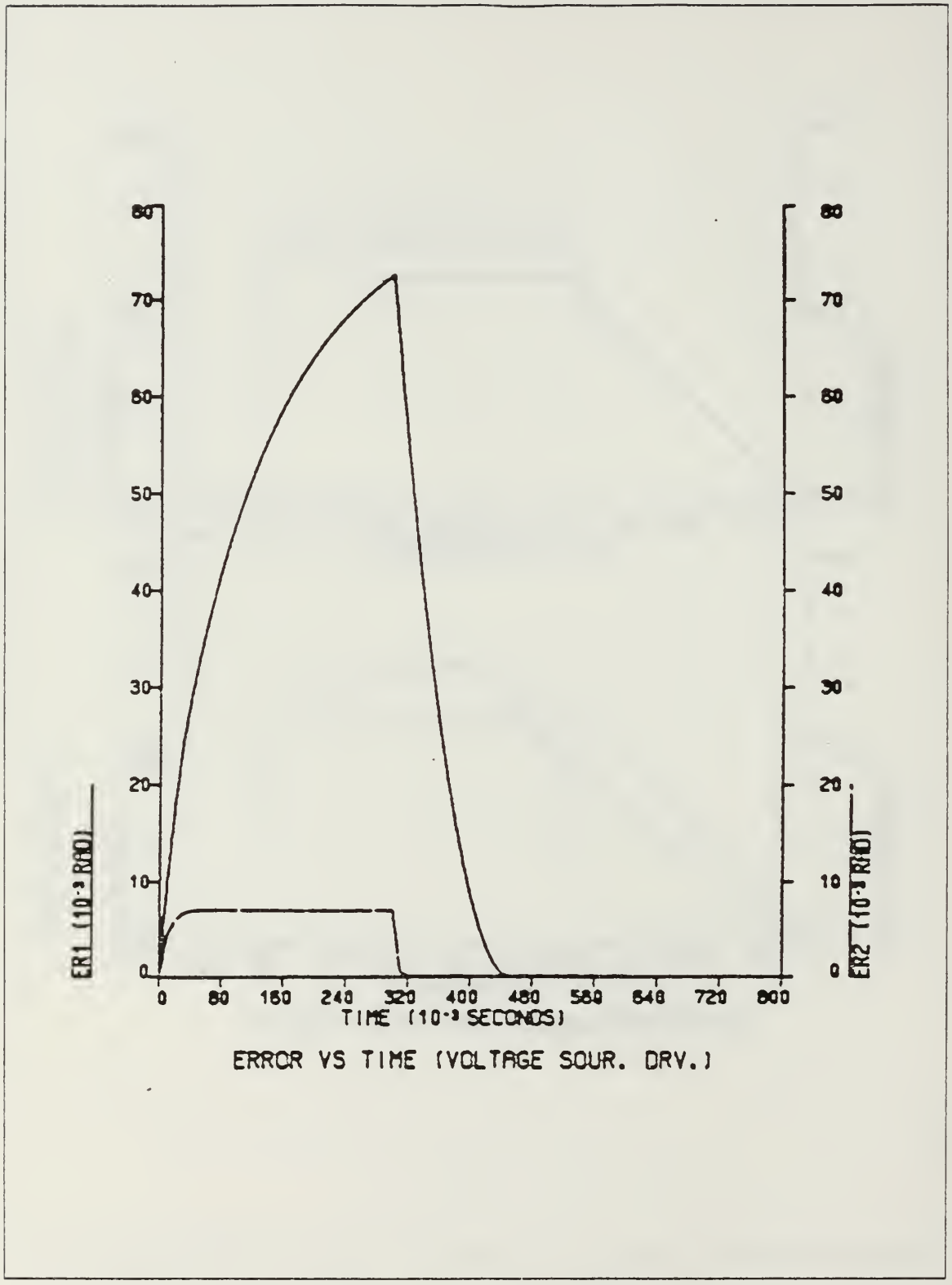

Figure 6.19 Error Between Commanded and Actual Position (No Gravity).

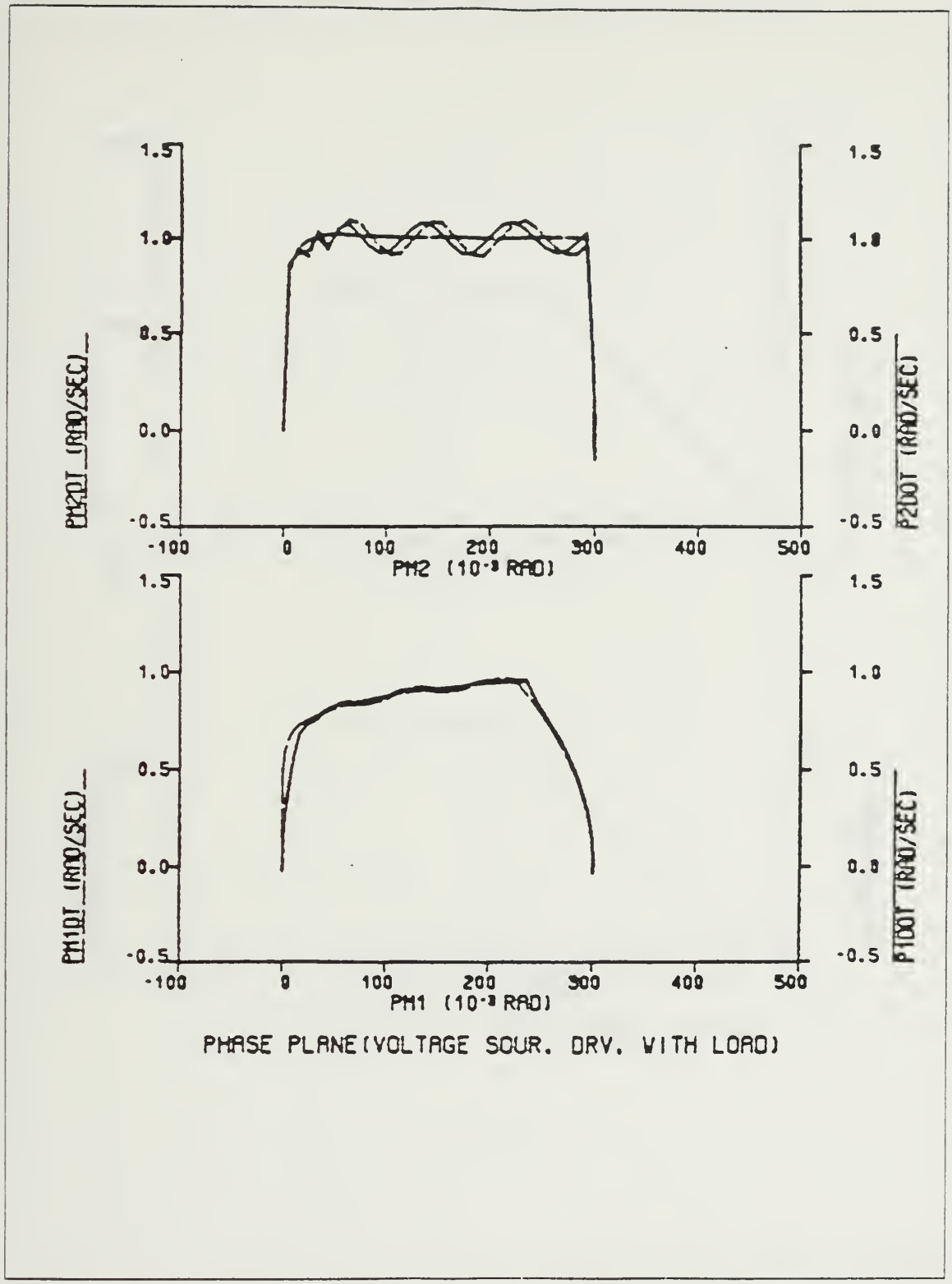

Figure 6.20 Phase Plane Trajectory For Ramp Input (No Gravity - Loaded Arm).

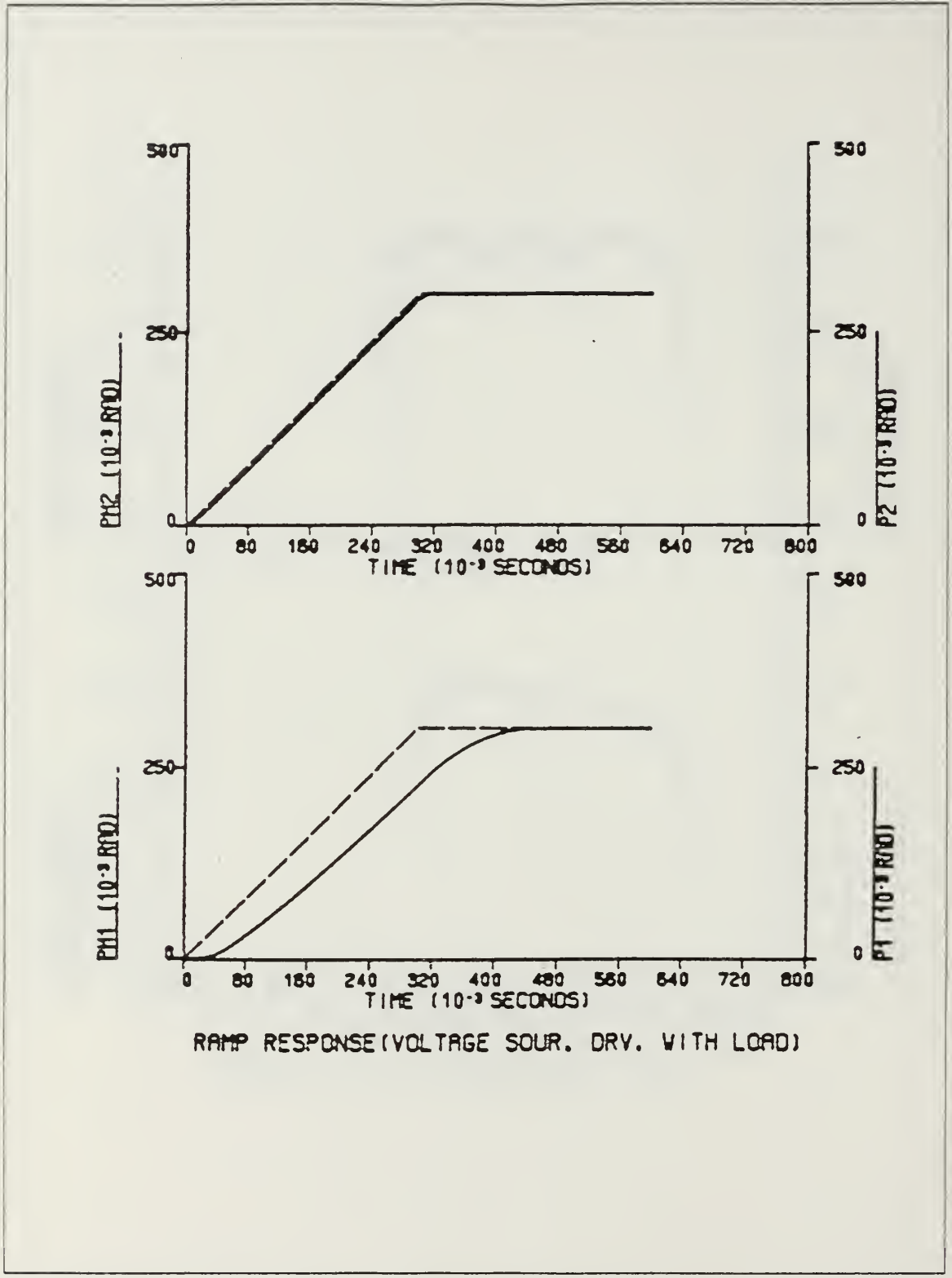

Figure 6.21 Ramp Response (No Gravity - Loaded Arm).

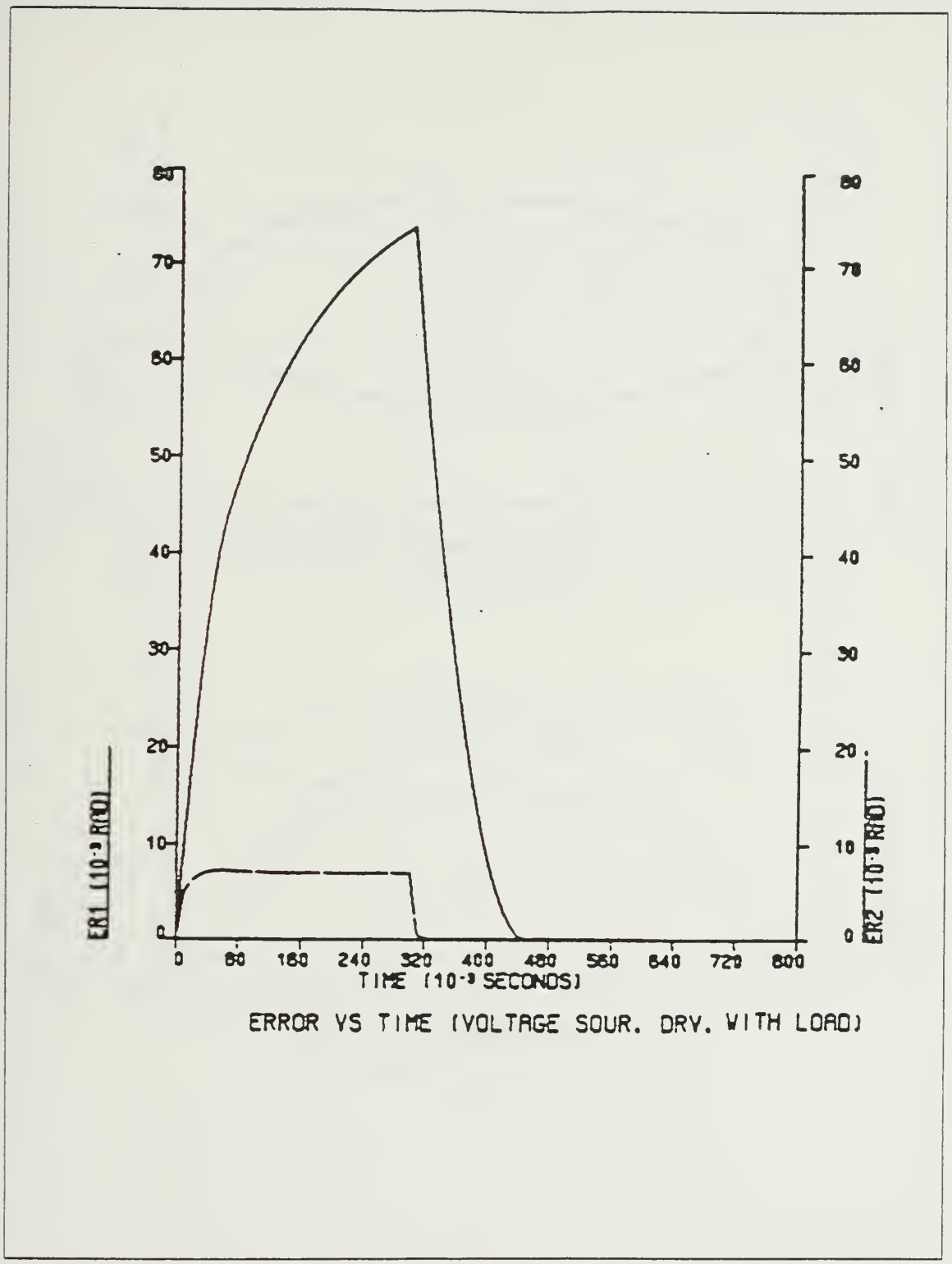

Figure 6.22 Error Between Commanded and Actual Position (No Gravity - Loaded Arm).

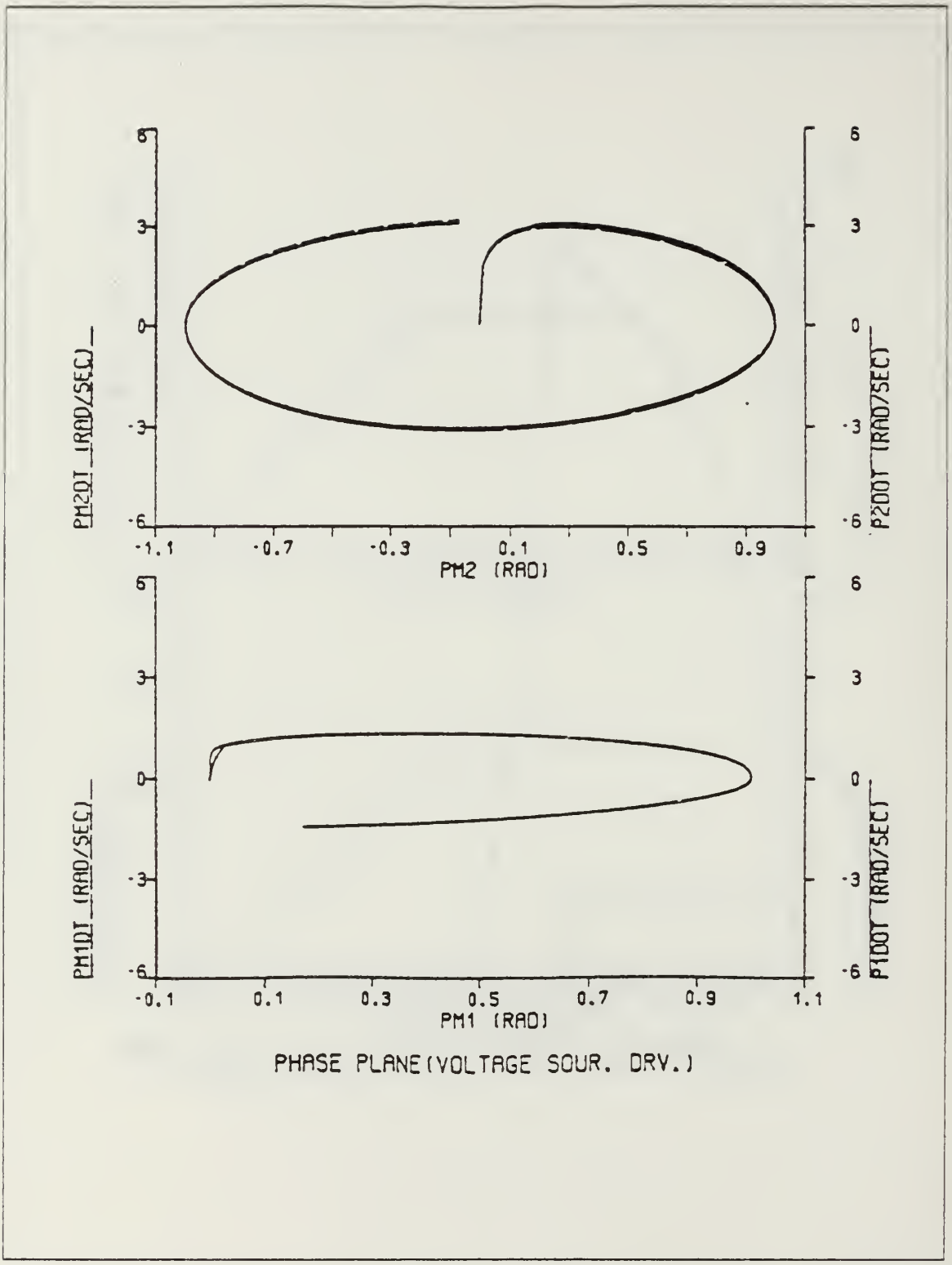

Figure 6.23 Phase Plane Trajectory For Sinusoidal Input (No Gravity).

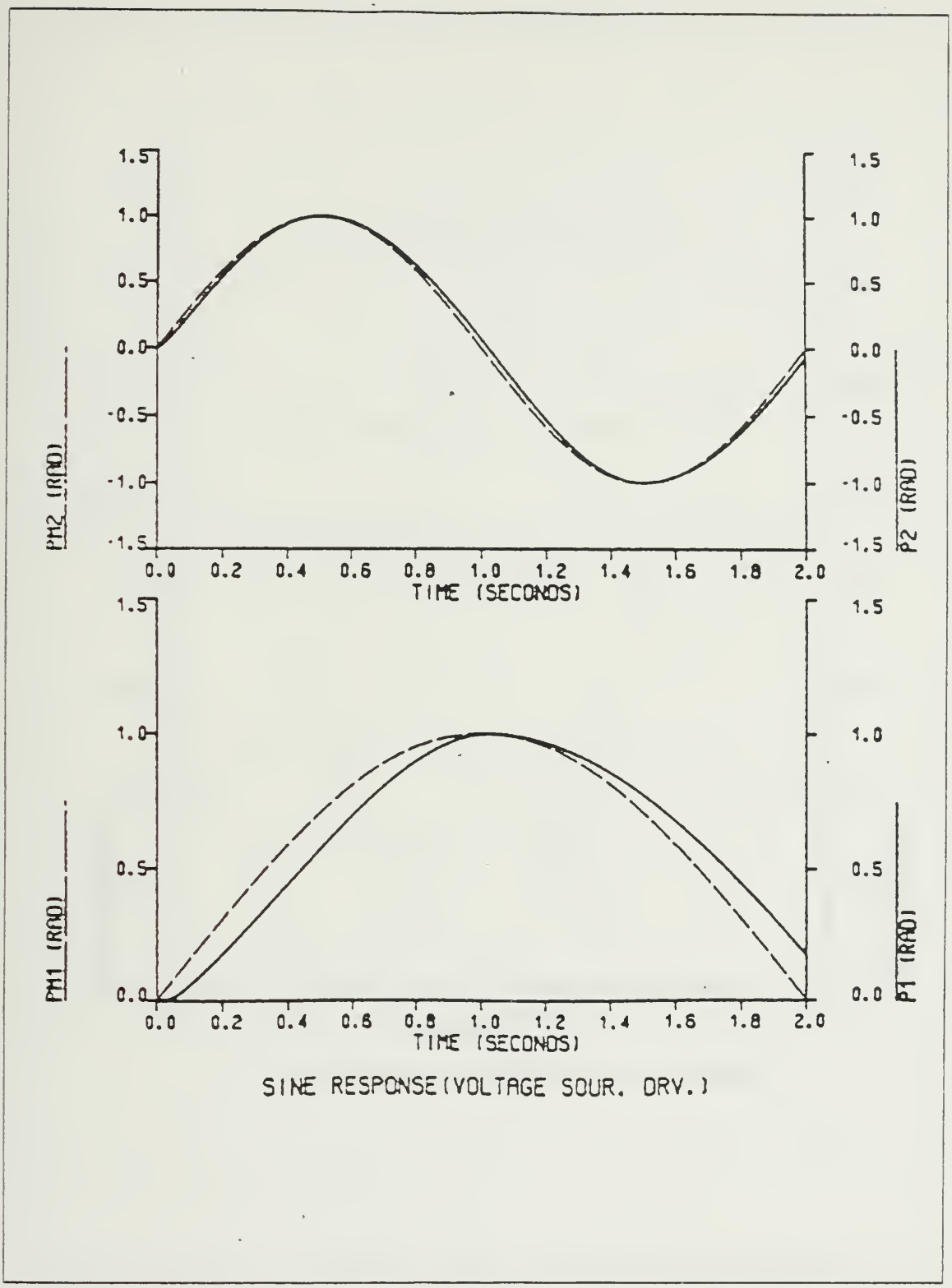

Figure 6.24 Sine Response (No Gravity).

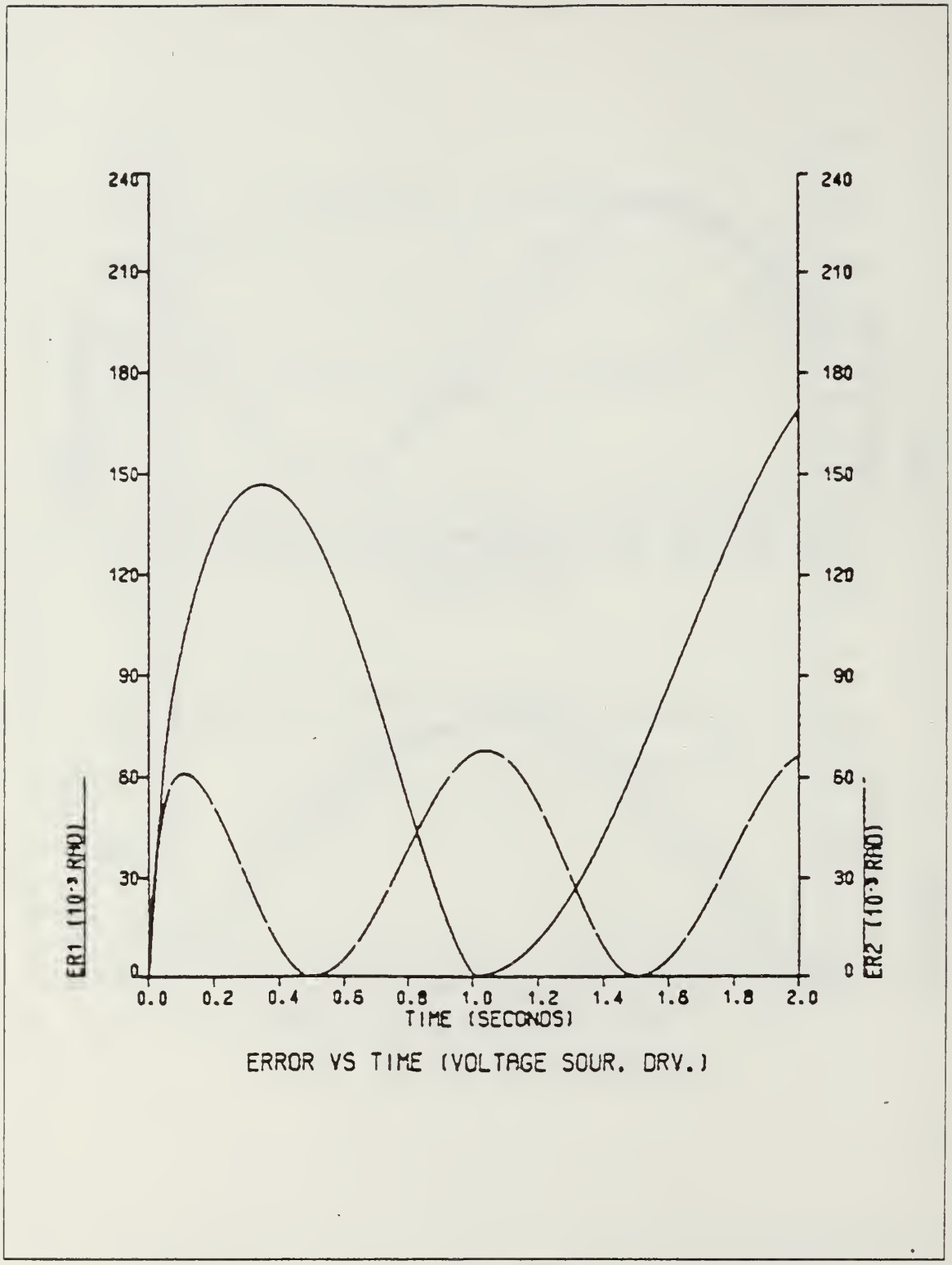

Figure 6.25 Error Between Commanded and Actual Position (No Gravity).

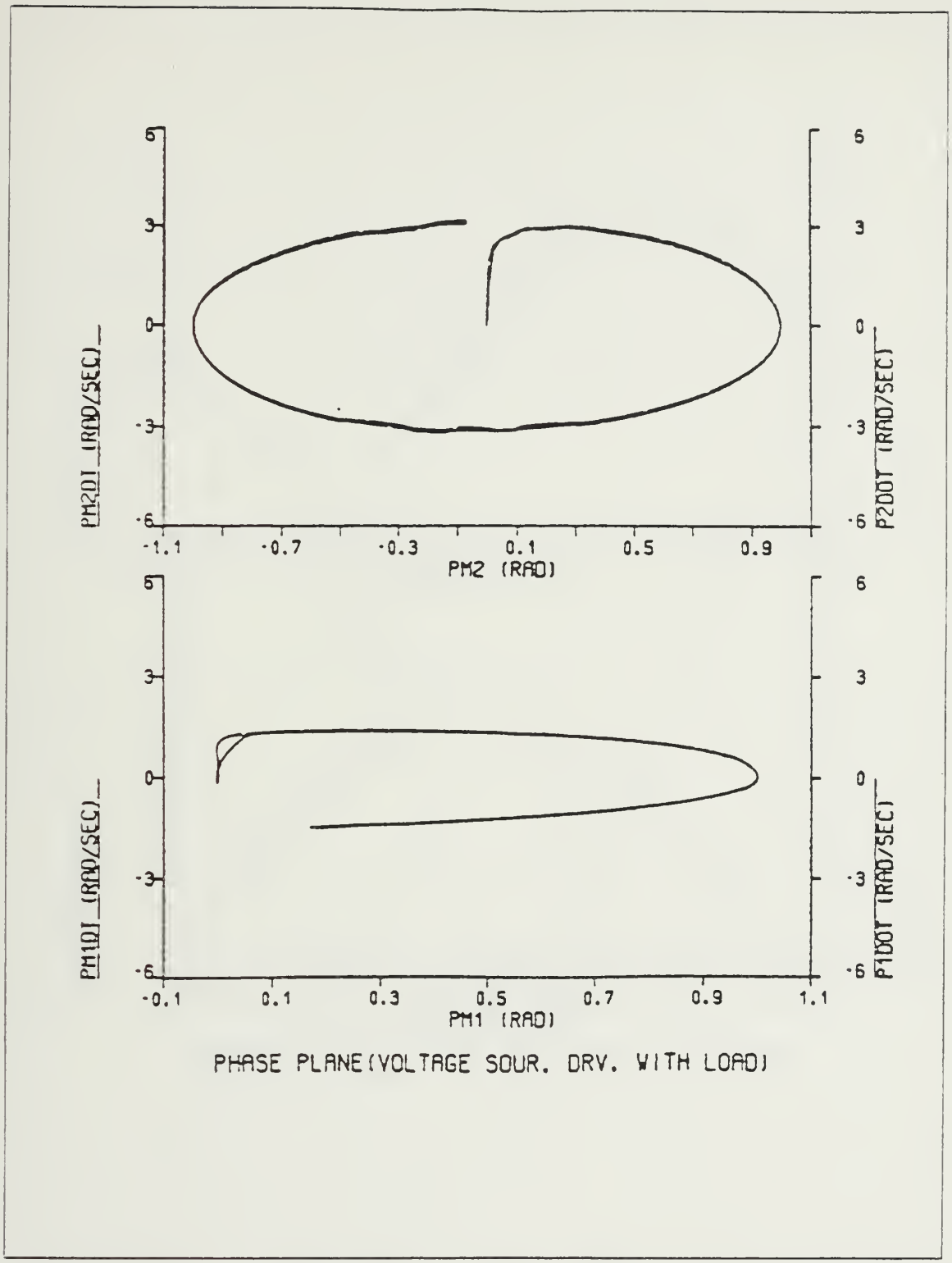

Figure 6.26 Phase Plane Trajectory For Sinusoidal Input (No Gravity - Loaded Arm).

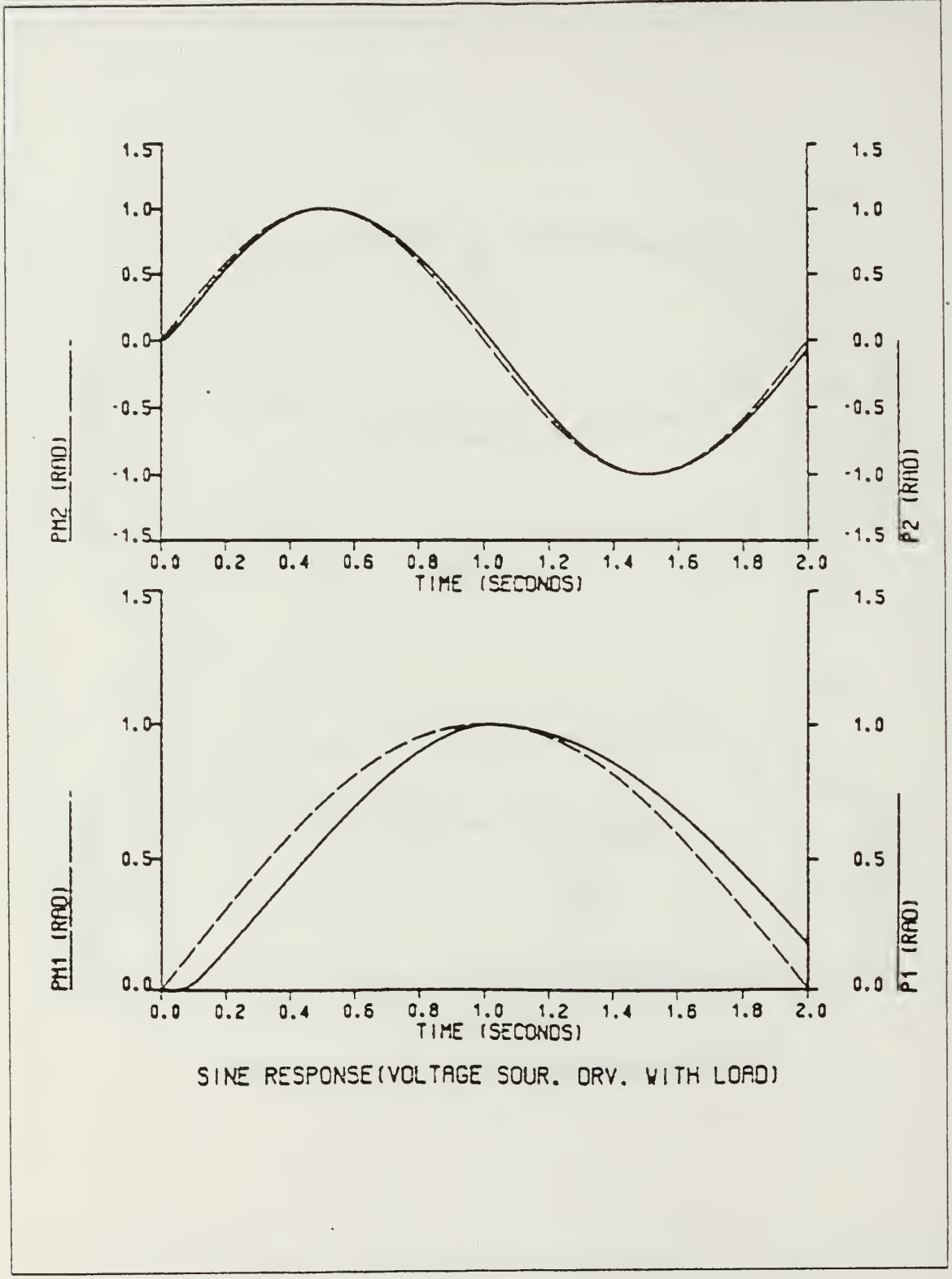

Figure 6.27 Sine Response (No Gravity - Loaded Arm).

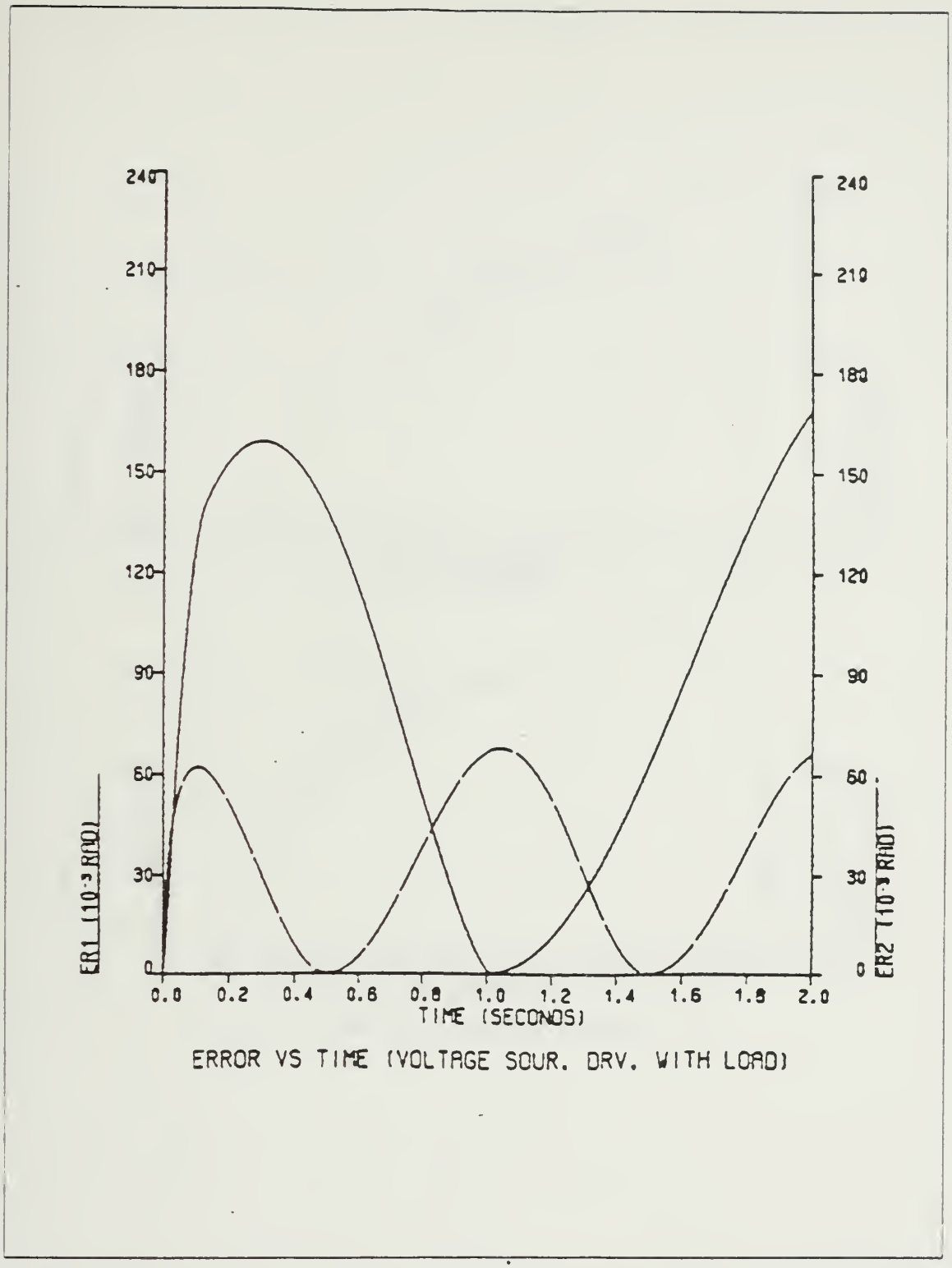

Figure 6.28 Error Between Commanded and Actual Position (No Gravity - Loaded Arm).

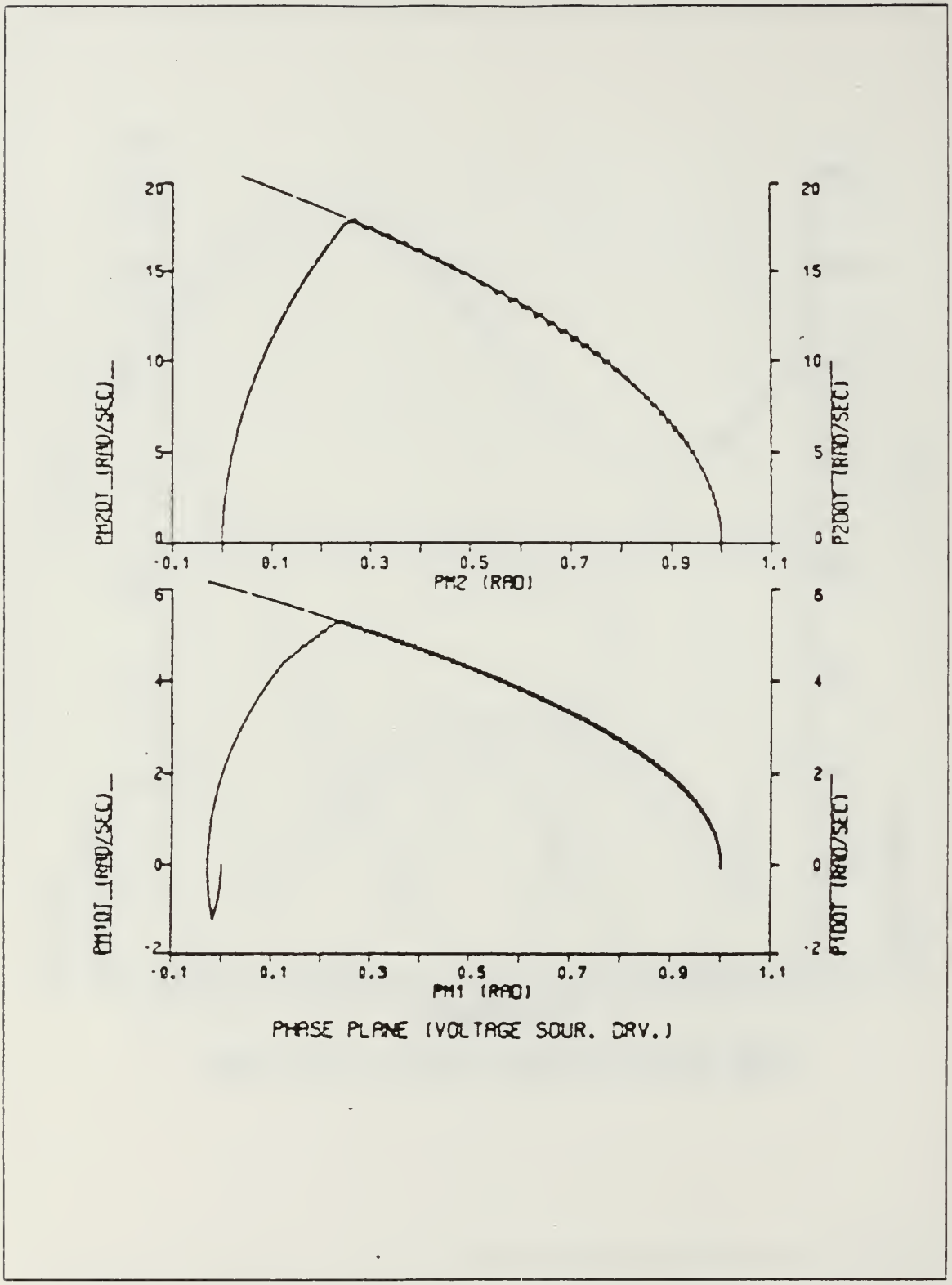

Figure 6.29 Phase Plane Trajectory For Move #1 (With Gravity).

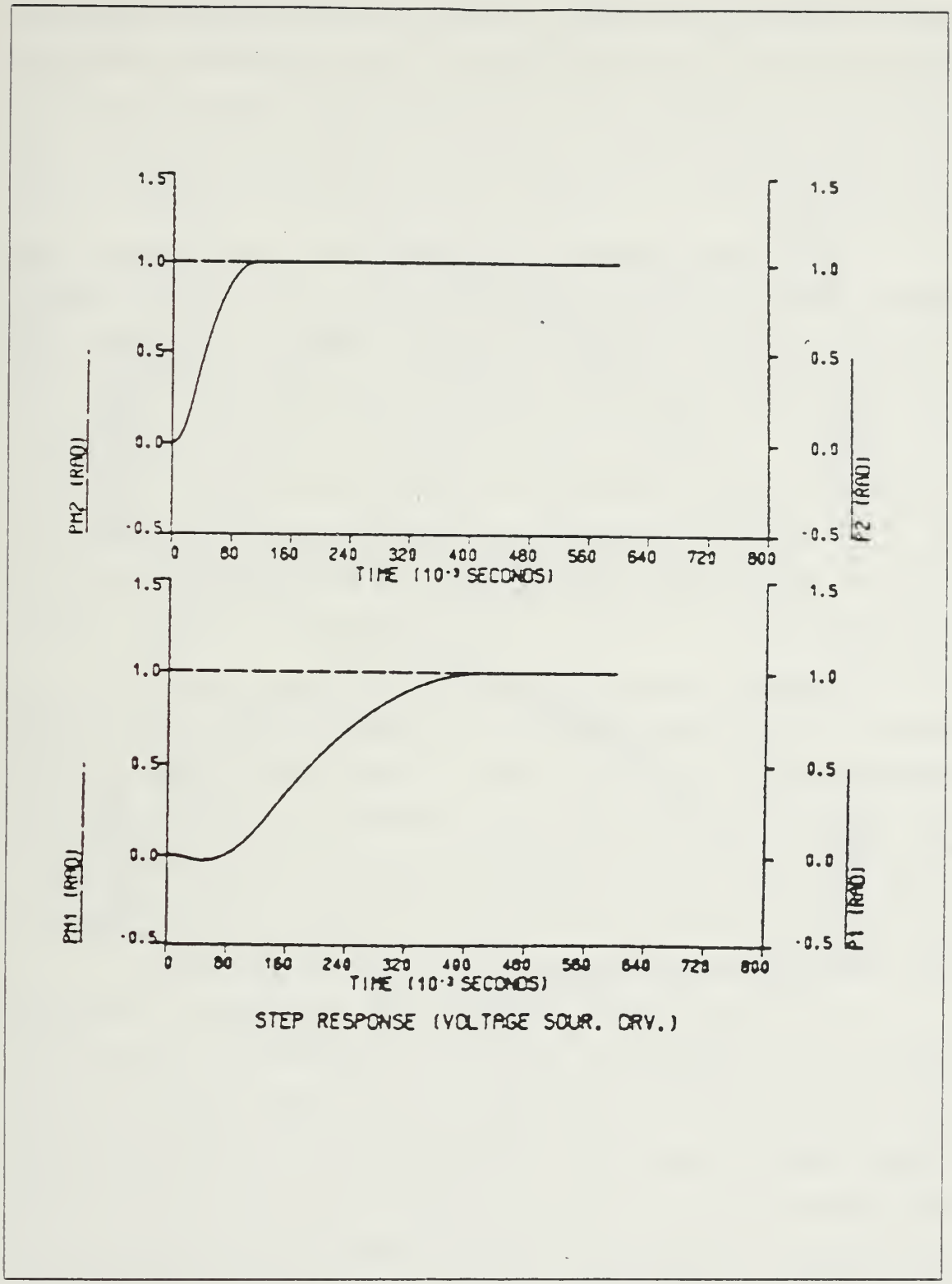

Figure 6.30 Step Response For Move #1 (With Gravity).

move) at the beginning of the motion. This negative velocity is caused by gravitational torques and interactive torques in the system. It can be observed that gravitational torques are at the maximum value when servo motors start moving. After JOINT1 servo motor torque overcomes the disturbance torques, the servo motor starts accelerating in the direction of the move, catches and follows the curve until the final position is reached.

In the case of a loaded arm, a larger magnitude of negative velocity is seen because of greater gravitational torques. Step response curves are shown in Figures 6.30 and 6.32. It can be observed that the negative velocity at the beginning of the move resulted in JOINT1 servo motor moving in the wrong direction initially. One might think that the situation at the beginning of the move may bring problems in some applications. To avoid this situation, JOINT2 servo motor position command was delayed 0.1 second at the beginning. Simulation results are shown in Figures 6.33 - 6.36. Phase plane trajectories show that the negative velocity at the beginning of the move is lost. A zig-zag shape in JOINT1 servo motor phase trajectory is seen due to reaction torque produced by JOINT2 servo motor. The same overall time response was obtained.

Simulation studies with Move #2 are shown in Figures 6.37 - 6.40. It can be seen that both second-order model and servo motor have good curve following capabilities and they are on top of each other. Maximum velocities of 6.6 rad/secand 22 rad/sec are seen for servo motors 1 and 2 respectively. In this sample move, the reaction torques increase the servo motor acceleration until the curve is reached. After that, reaction torques oppose the servo motor deceleration along the curve. As a result, acceleration time of the move is shorter than deceleration time. Step response curves are shown in Figures 6.38 and 6.40.

Move #3 was used for extensive testing of the system. Phase plane trajectories are shown in Figures 6.41 and 6.43. It can be seen at the beginning of the move, when servo motors start accelerating, the reaction torque produced by JOINT2 servo motor keeps JOINT1 servo motor from accelerating, even causing it to move in the opposite direction to the motion. This situation is clearer in the step response curves of Figures 6.42 and 6.44. To avoid the unwanted effects of the reaction torques at the beginning of the motion, step position command input to the second servo motor was delayed 100 milliseconds. Simulation results are shown in Figures 6.45 - 6.48. For the unloaded arm, a different input sequence worked out well. From the phase plane plot (Figure 6.45) good curve following can be seen.

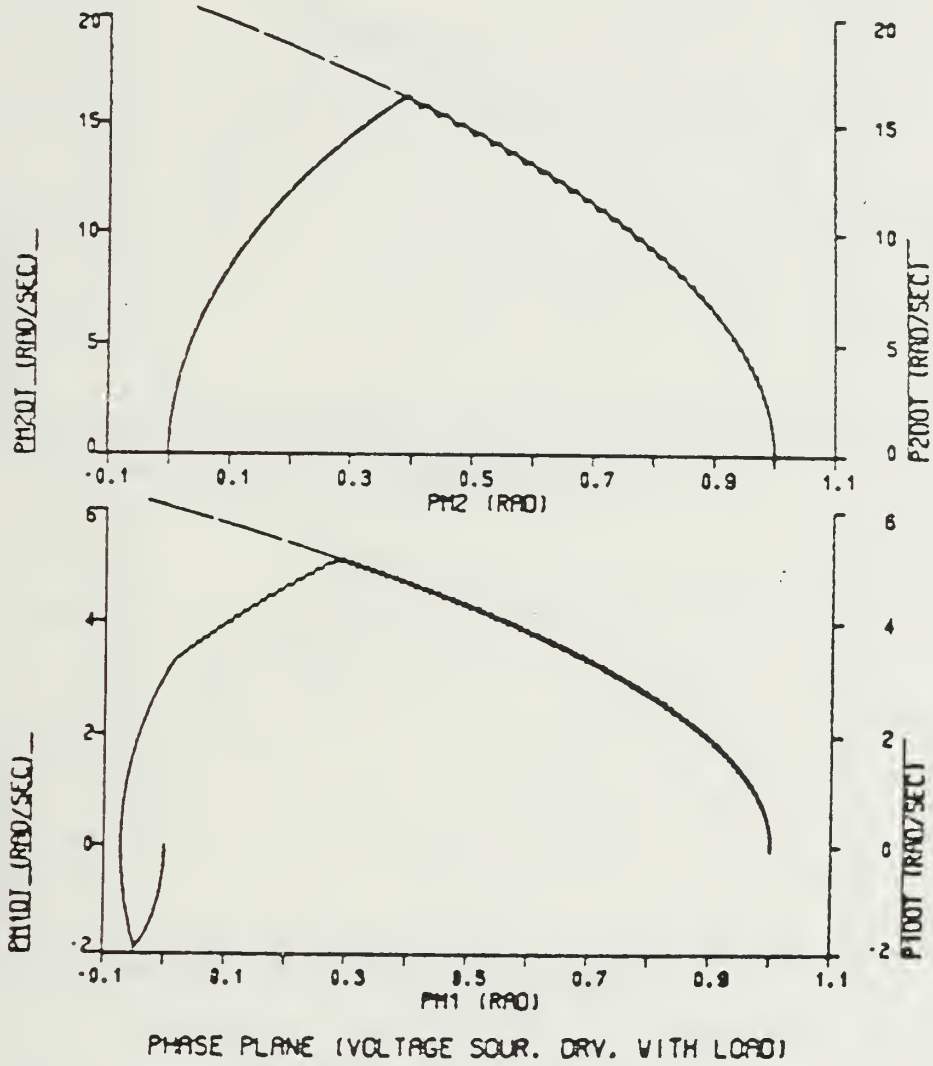

Figure 6.31 Phase Plane Trajectory For Move #1 (With Gravity).

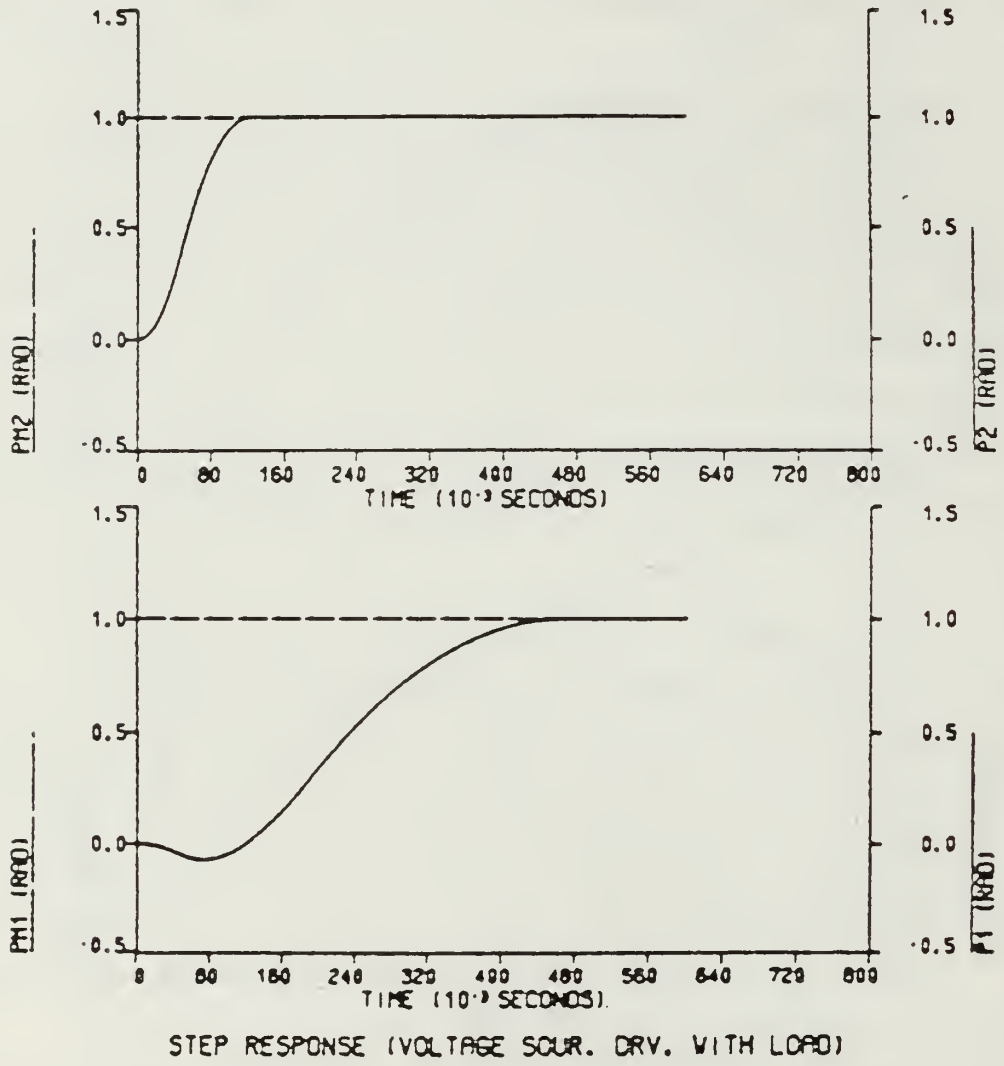

Figure 6.32 Step Response For Move #1 (With Gravity).

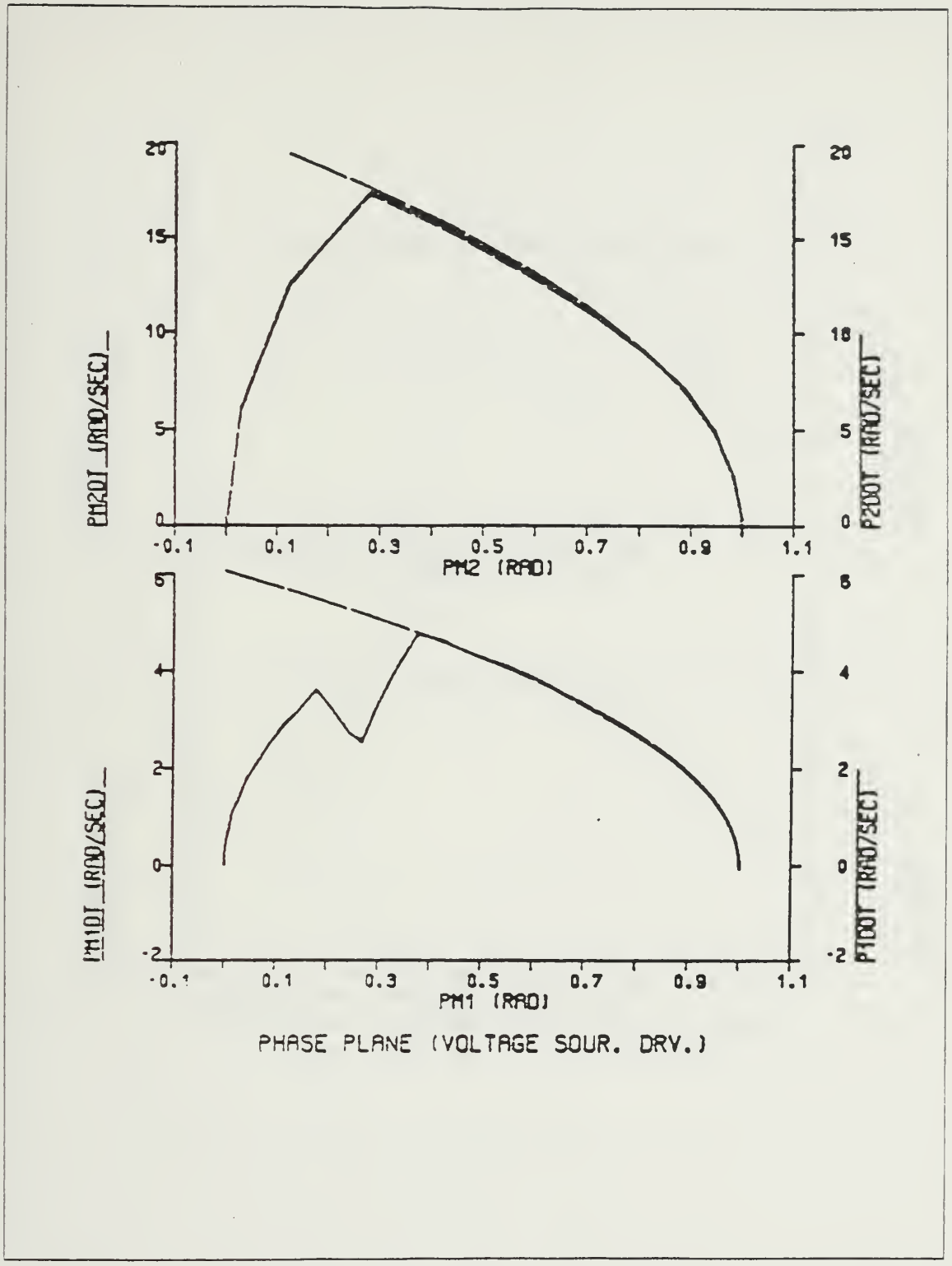

Figure 6.33 Phase Plane Trajectory For Move #1 (With Gravity)
JOINT2 Servo Motor Input Delayed 0.10 sec.

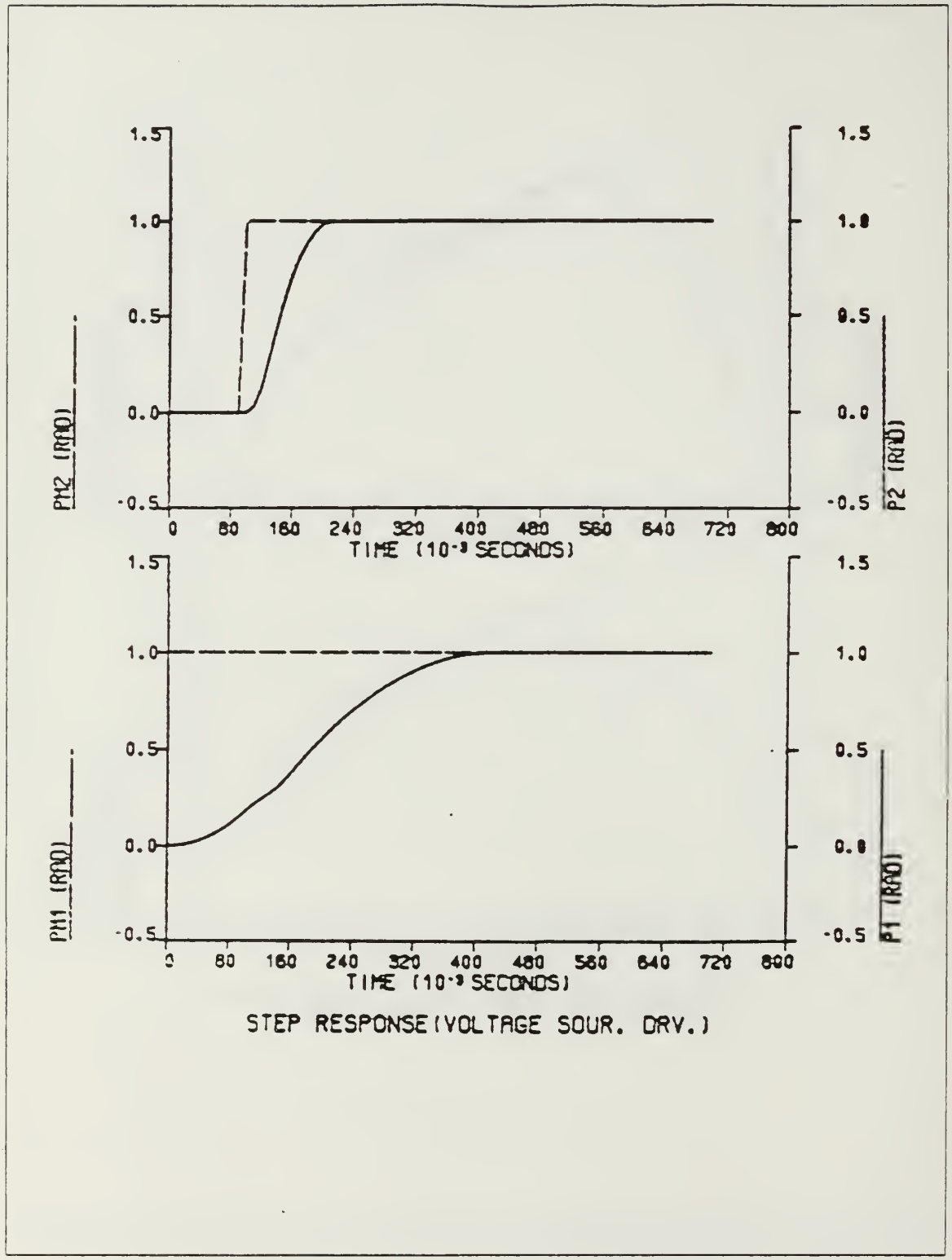

Figure 6.34 Step Response For Move #1 (With Gravity)
JOINT2 Servo Motor Input Delayed 0.10 sec.

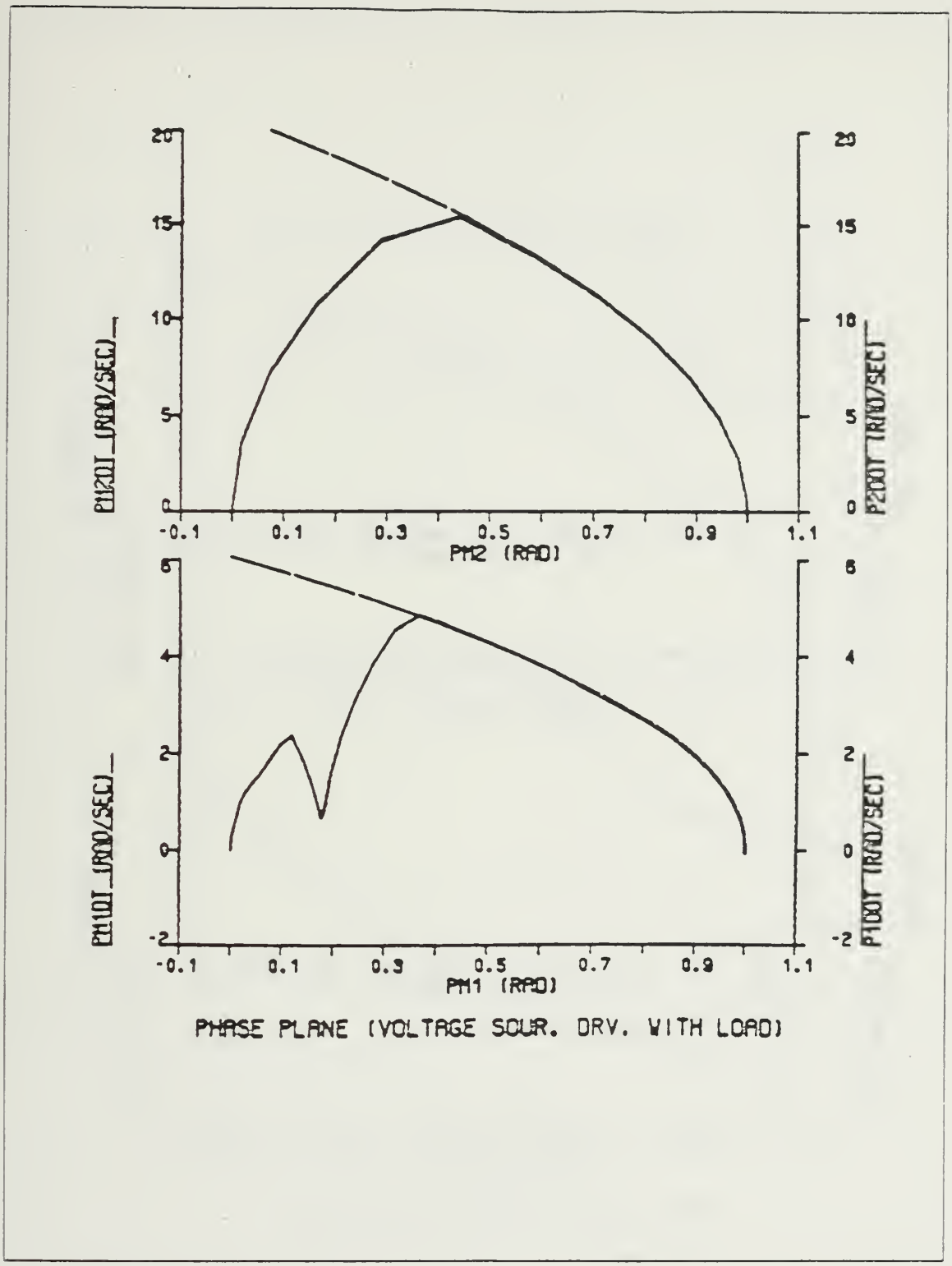

Figure 6.35 Phase Plane Trajectory For Move #1 (With Gravity)
JOINT2 Servo Motor Input Delayed 0.10 sec.

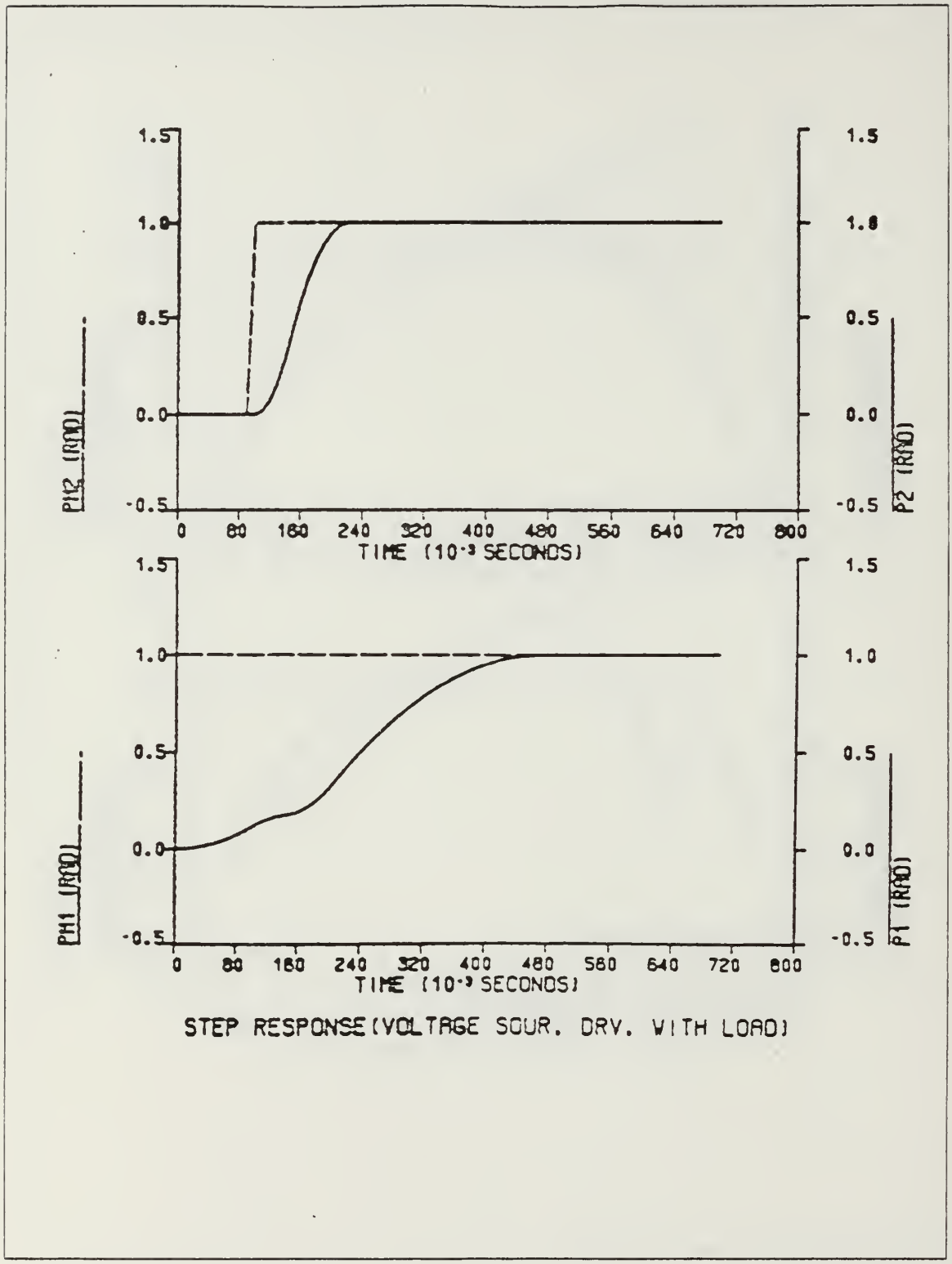

Figure 6.36 Step Response For Move #1 (With Gravity)
JOINT2 Servo Motor Input Delayed 0.10 sec.

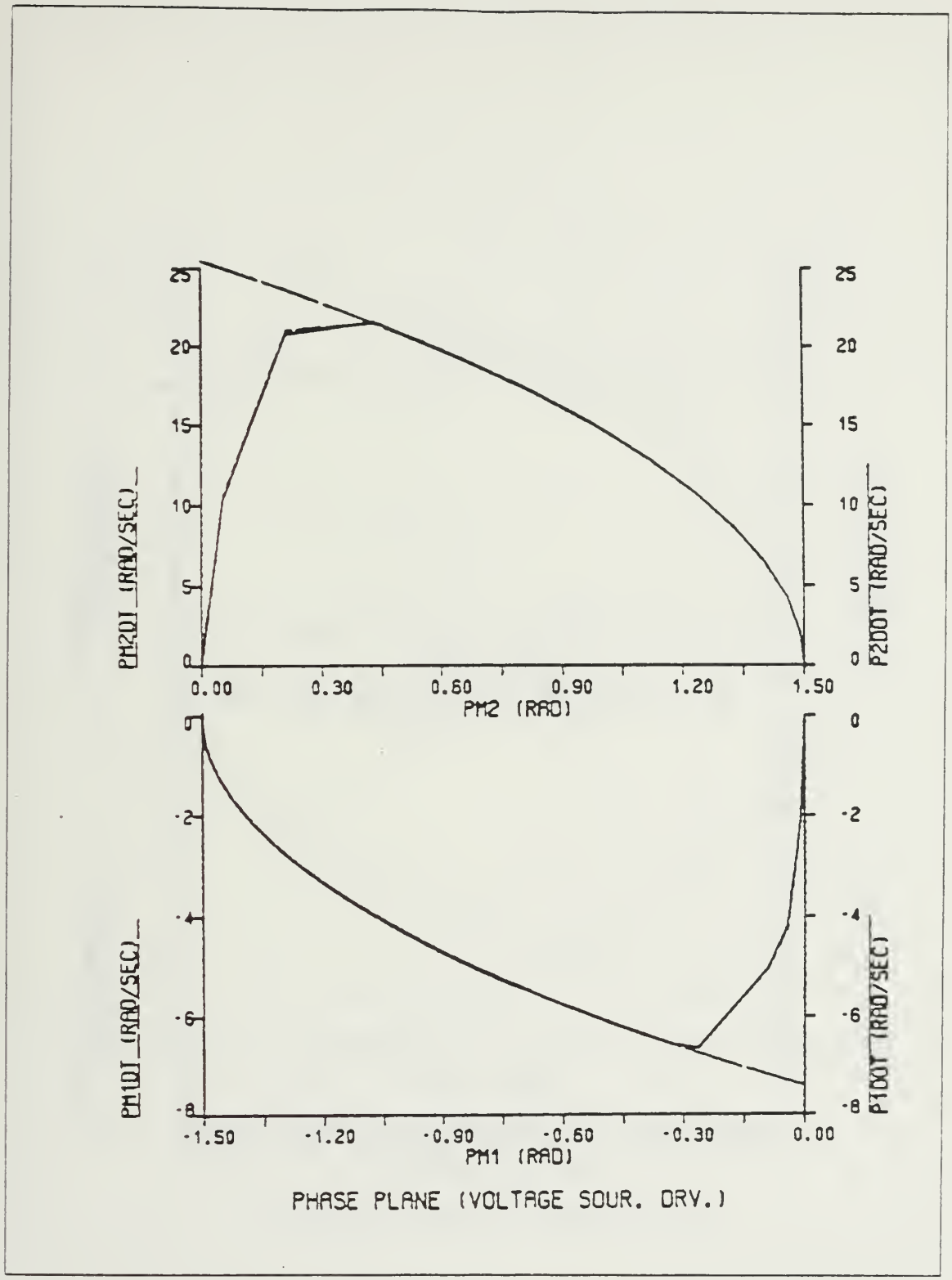

Figure 6.37 Phase Plane Trajectory For Move #2 (With Gravity).

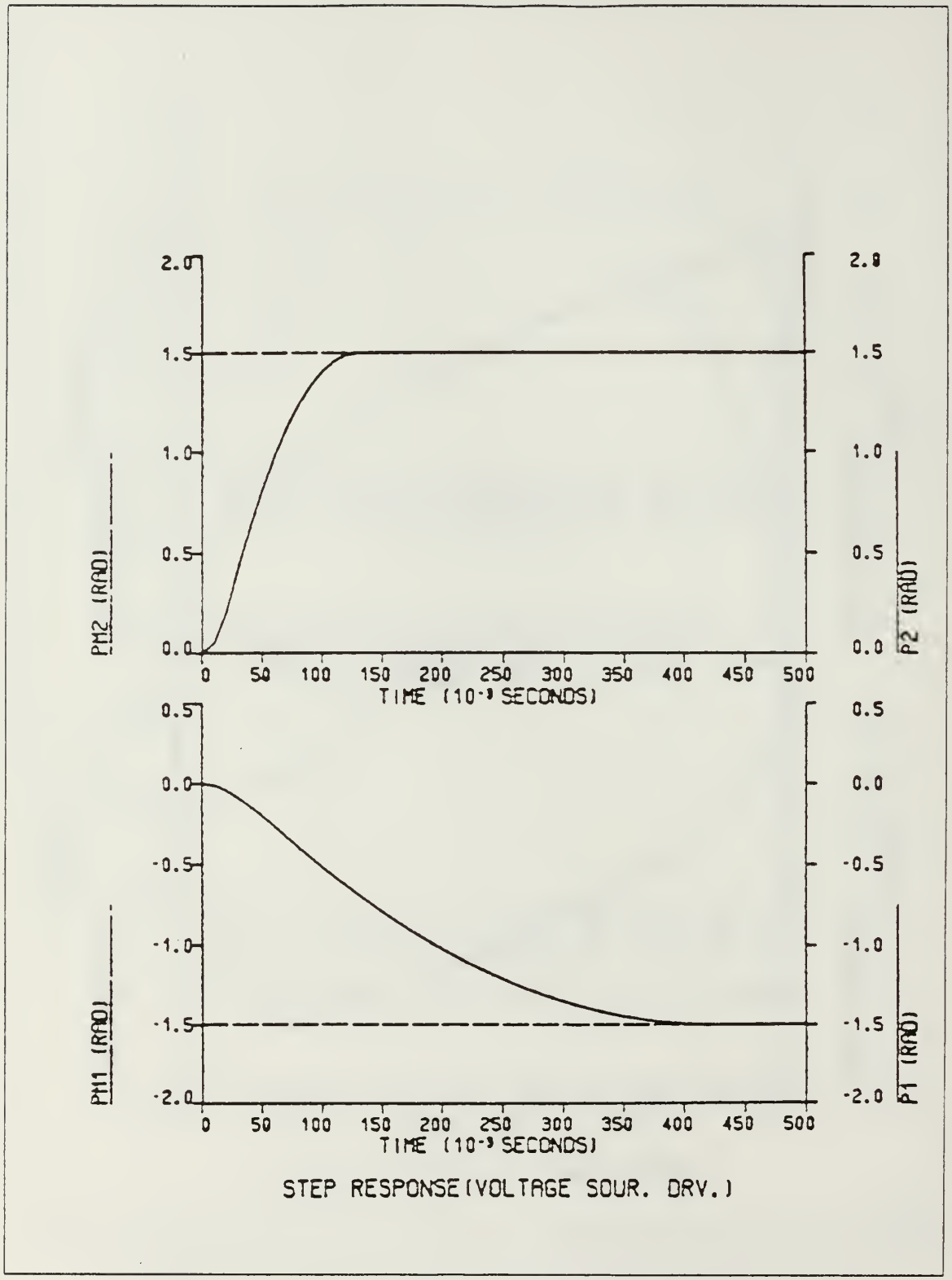

Figure 6.38 Step Response For Move #2 (With Gravity).

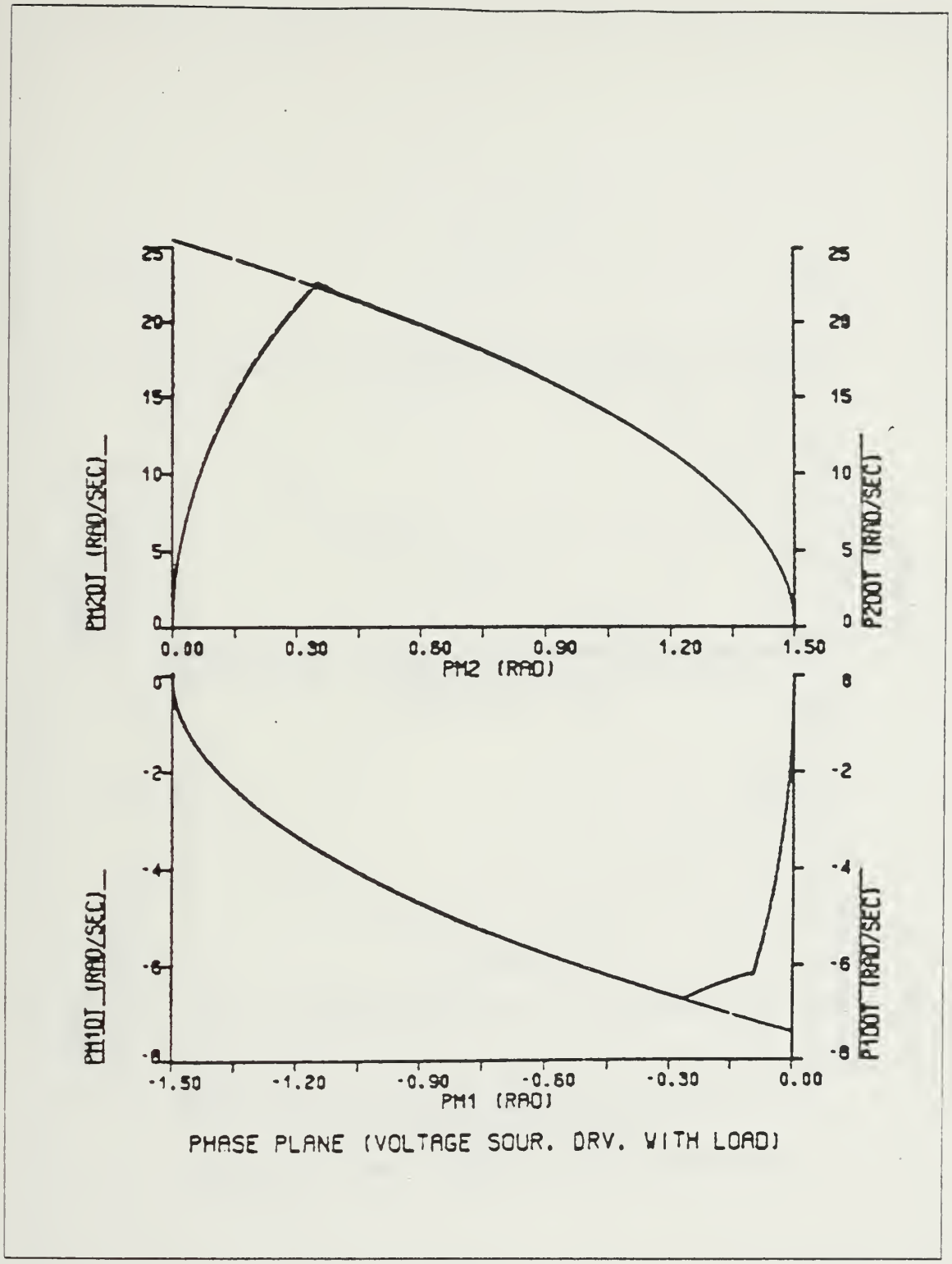

Figure 6.39 Phase Plane Trajectory For Move #2
(With Gravity - Loaded Arm).

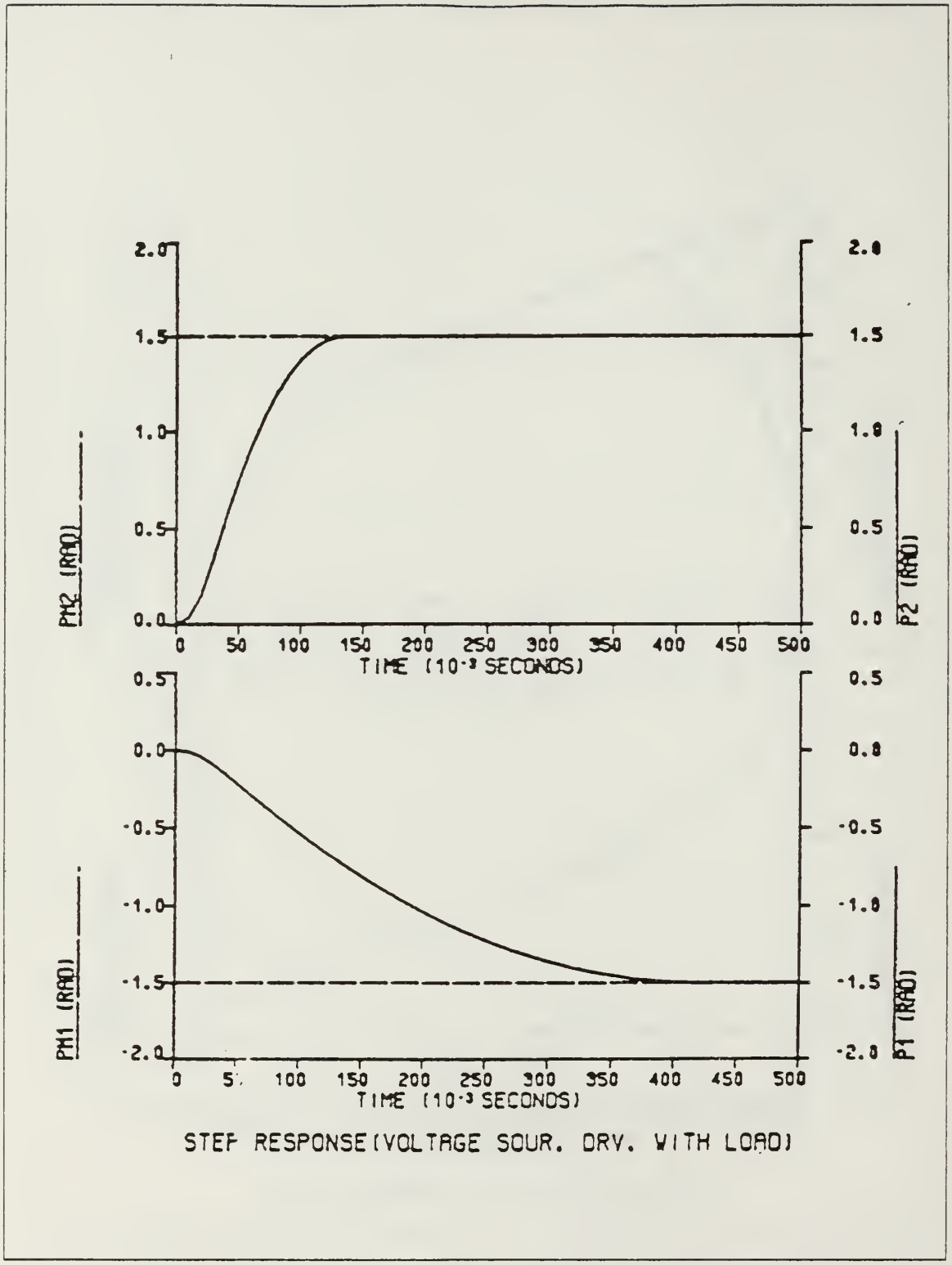

Figure 6.40 Step Response For Move #2
(With Gravity - Loaded Arm).

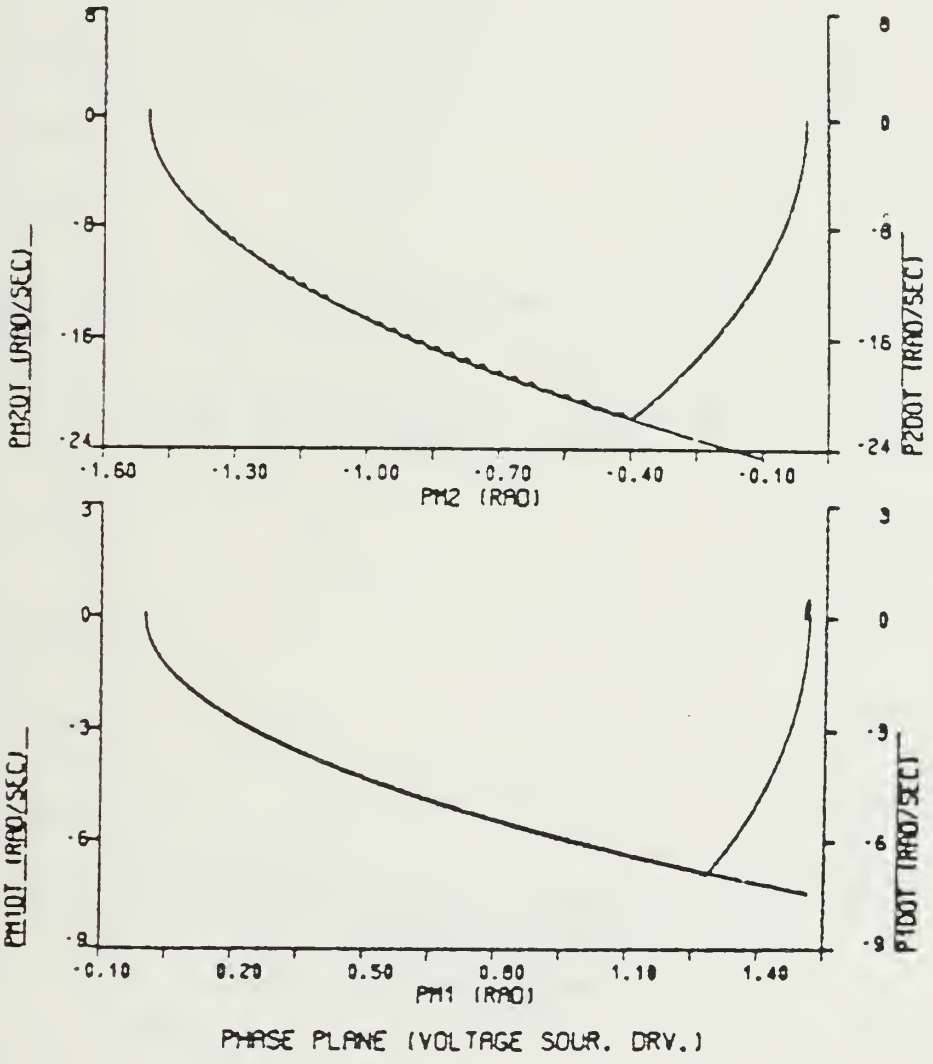

Figure 6.41 Phase Plane Trajectory For Move #3 (With Gravity).

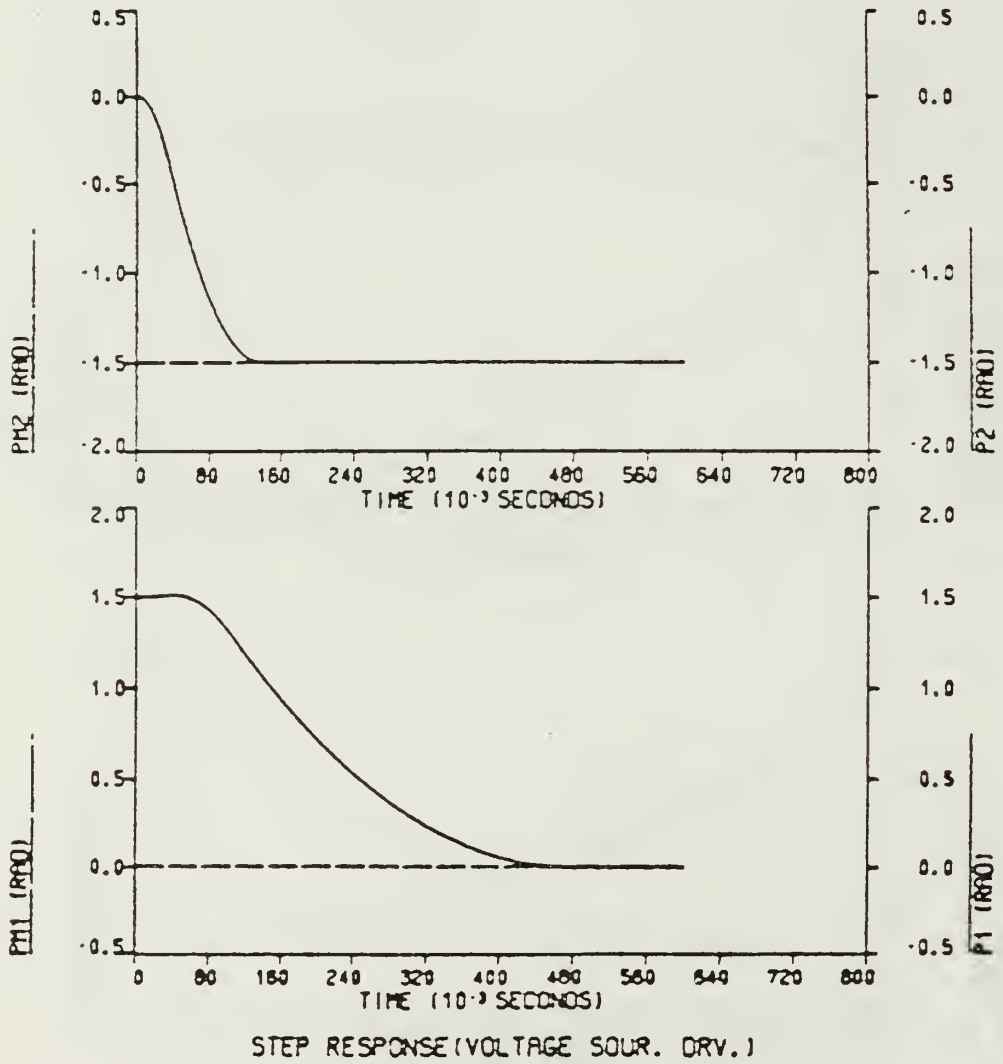

Figure 6.42 Step Response For Move #3 (With Gravity).

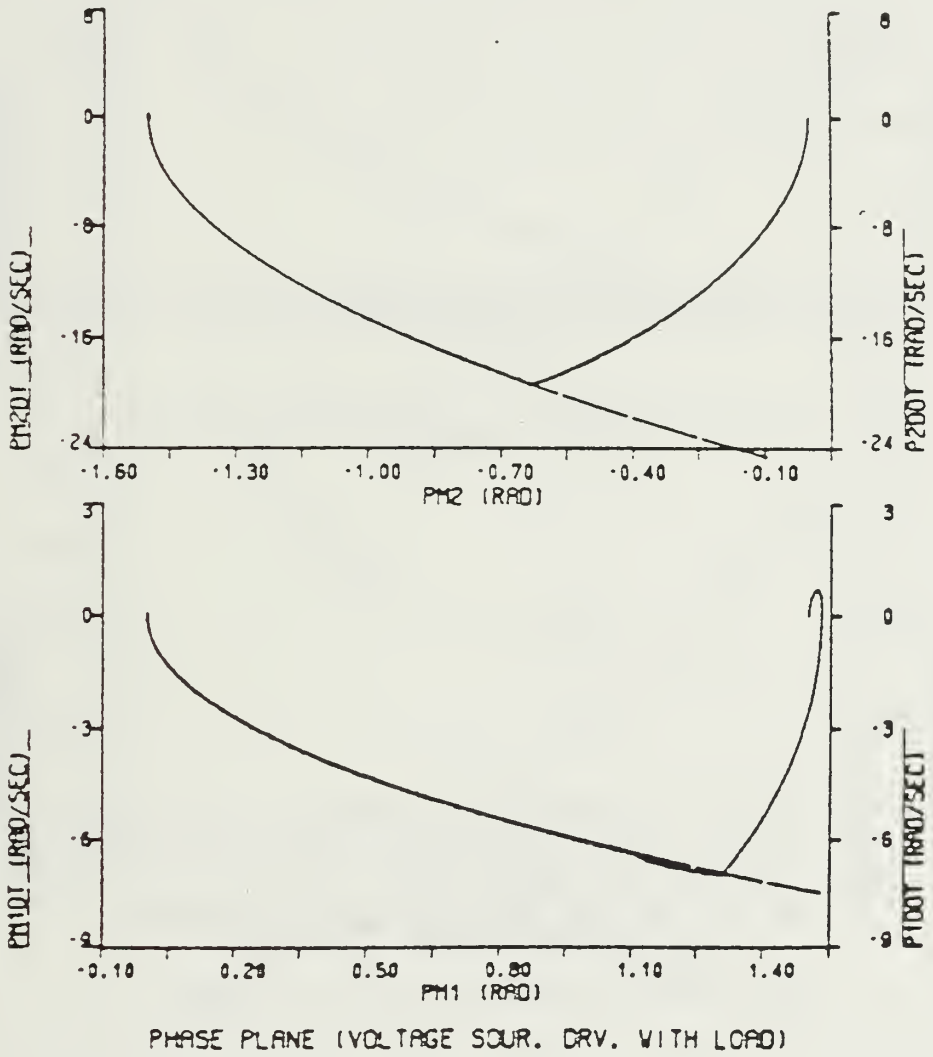

Figure 6.43 Phase Plane Trajectory For Move #3 (With Gravity).

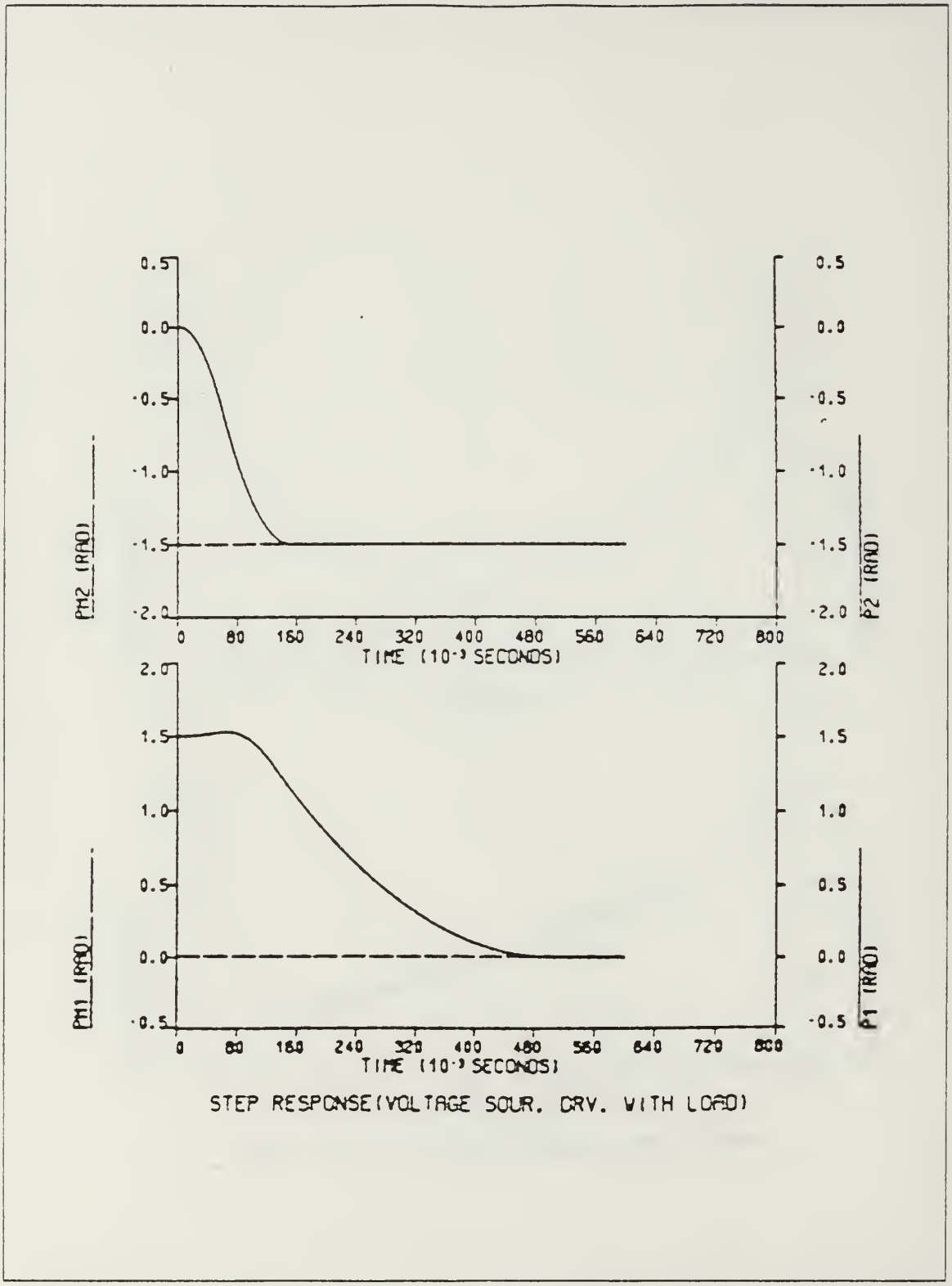

Figure 6.44 Step Response For Move #3 (With Gravity).

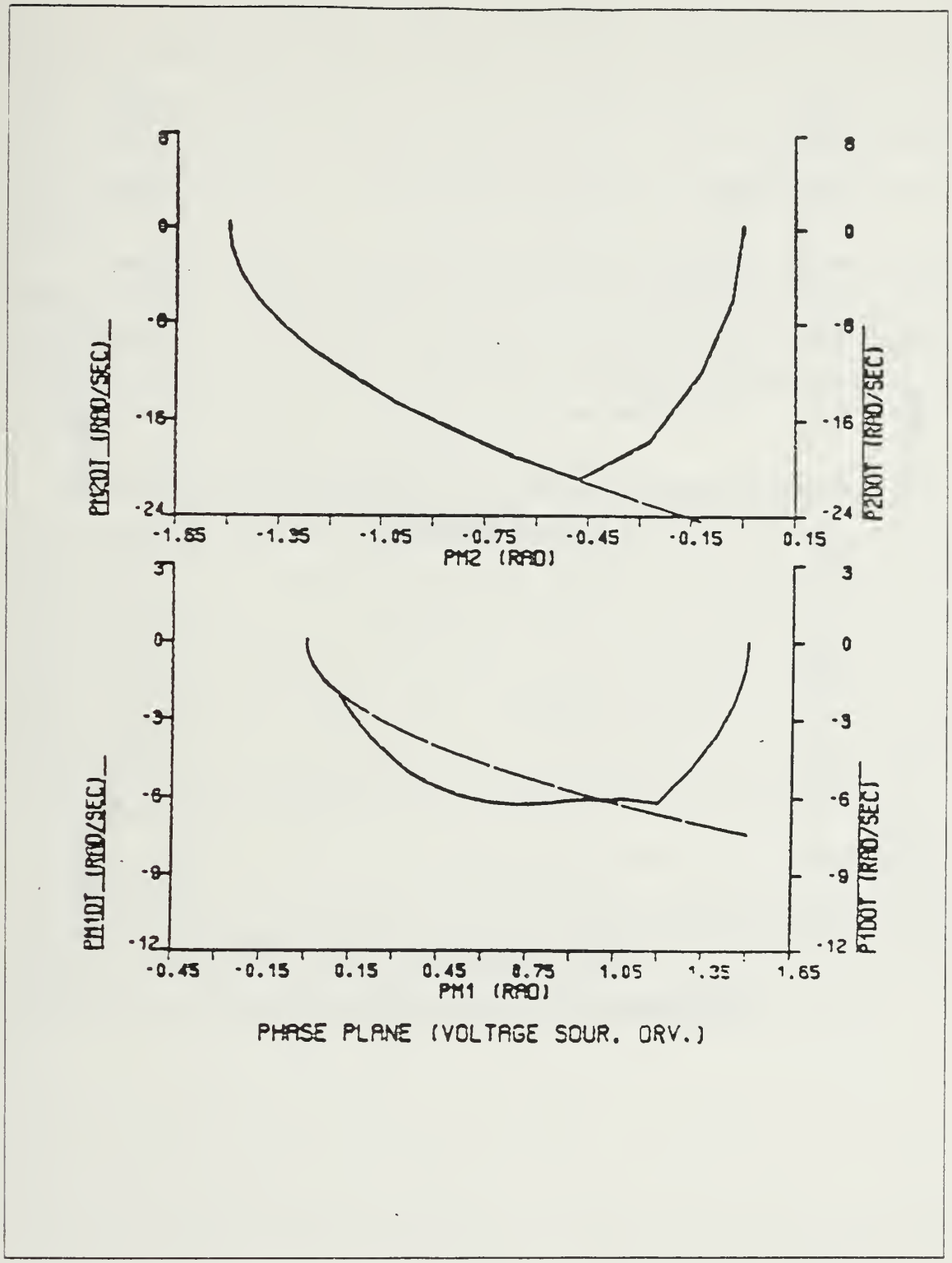

Figure 6.45 Phase Plane Trajectory For Move #3 (With Gravity)
JOINT2 Servo Motor Input Delayed 0.10 sec.

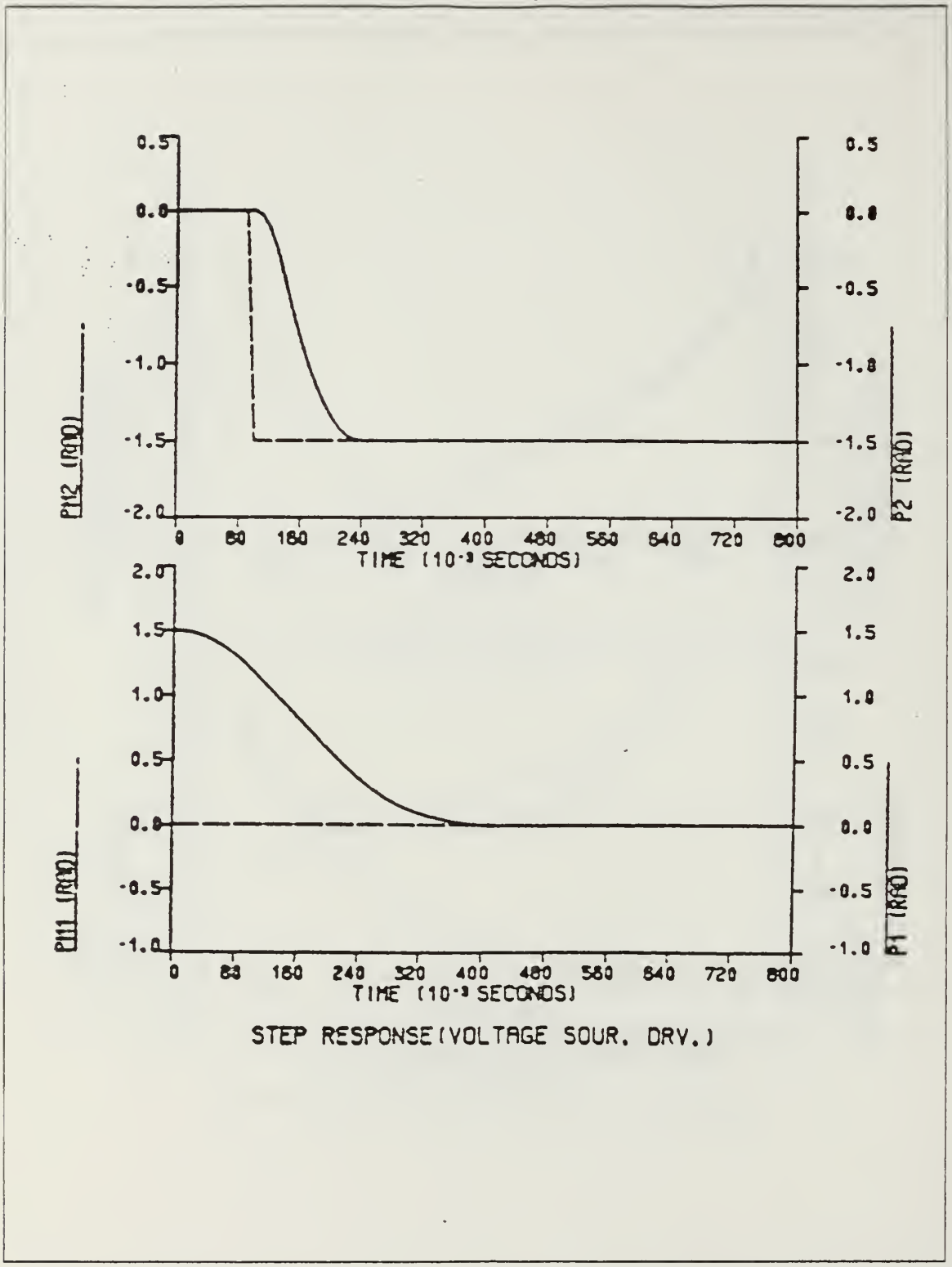

Figure 6.46 Step Response For Move #3 (With Gravity)
JOINT2 Servo Motor Input Delayed 0.10 sec.

It is also noticed that when JOINT2 servo motor starts accelerating, the reaction torque produced causes the JOINT1 servo motor velocity to go down for a while, resulting in passing over the curve and staying there for a certain amount of time before it catches up and follows the curve until the desired position is reached. From the step response curve (Figure 6.46), 60 milliseconds faster overall response is observed.

Phase plane plots and step response curves for Loaded arm with different input sequences are shown in Figures 6.47 and 6.48. Delayed (100 milliseconds) step position input for JOINT2 servo motor causes JOINT1 servo motor to overshoot. This result implies the importance of the effects of the inertial torques and interaction torques on the loaded arm.

b. Time Varying Position Command Input Used

Ramp input with tangent of 1 rad sec and a sinusoidal input were used to test the adaptive system under gravitational torques. Simulation results are shown in Figures 6.49 - 6.60. Phase plane trajectories of Figures 6.49 and 6.52 show second-order model and servo motor velocities are oscillating around the curve. From Figures 6.50 and 6.53, it is seen that JOINT2 servo motor follows the ramp input with very small errors, while JOINT1 servo motor is lagging behind the ramp input with larger errors. Figures 6.51 and 6.54 show errors between commanded position input and actual position of the servo motors. It can be observed, that the error tends to go to zero very slowly.

Simulation studies with sinusoidal input under gravitational torques are shown in Figures 6.55 - 6.60. Good curve following is observed from phase plane trajectories. Sine response curves in Figures 6.56 and 6.59, show the second-order models and servo motors follow the time varying position command with small errors. The error between desired and actual position is shown in Figures 6.57 and 6.60.

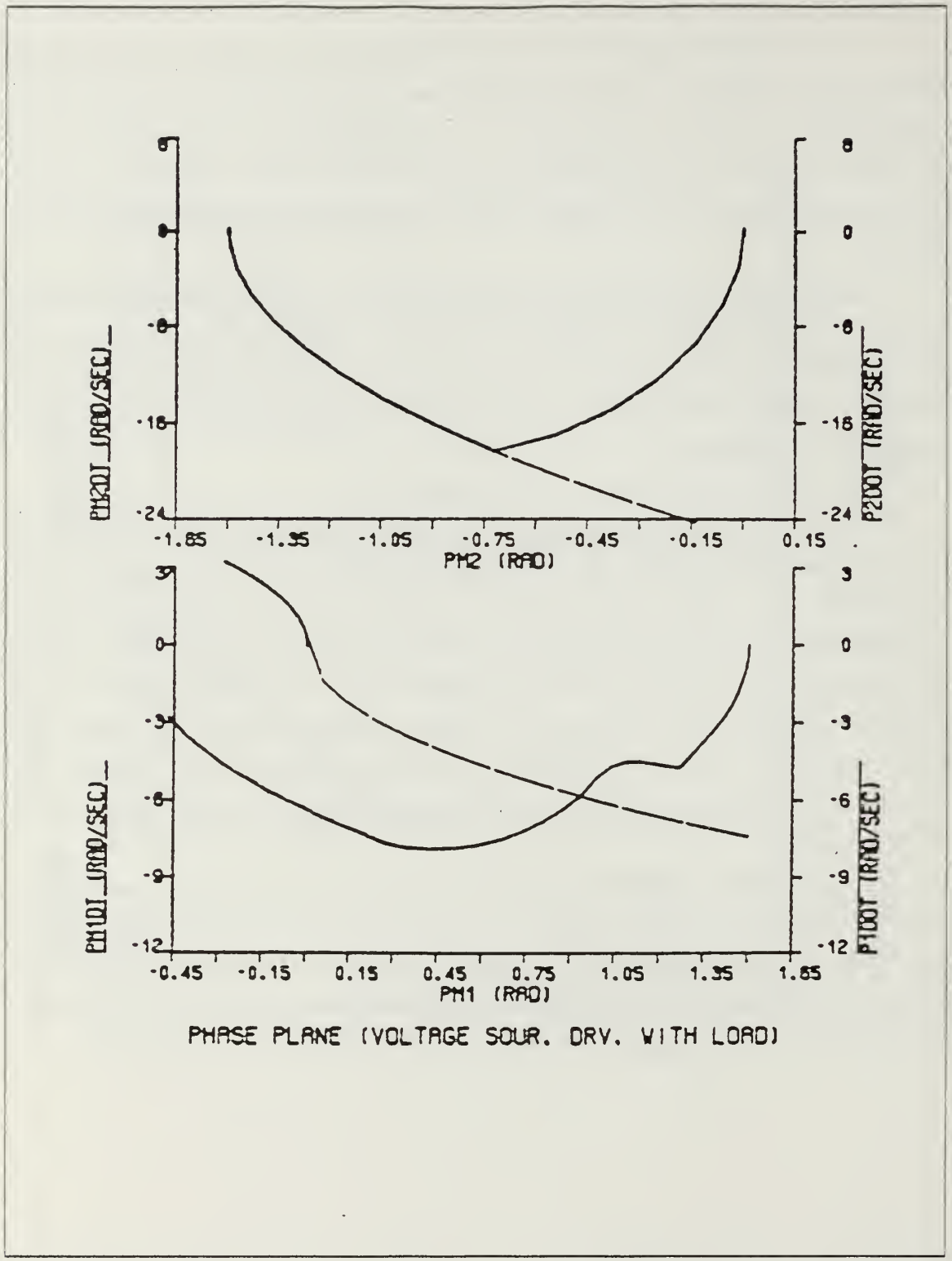

Figure 6.47 Phase Plane Trajectory For Move #3 (With Gravity)
JOINT2 Servo Motor Input Delayed 0.10 sec.

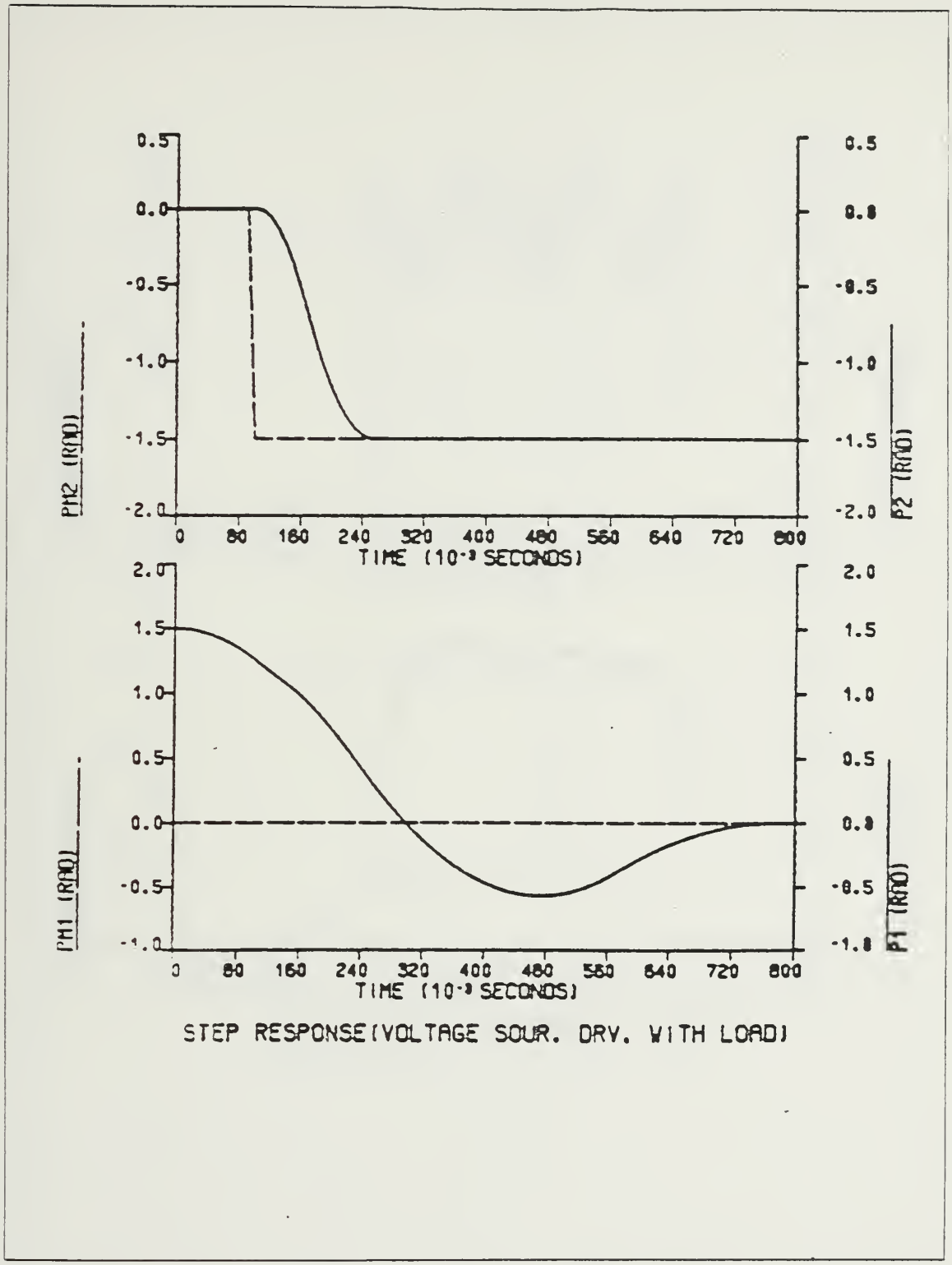

Figure 6.48 Step Response For Move #3 (With Gravity)
JOINT2 Servo Motor Input Delayed 0.10 sec.

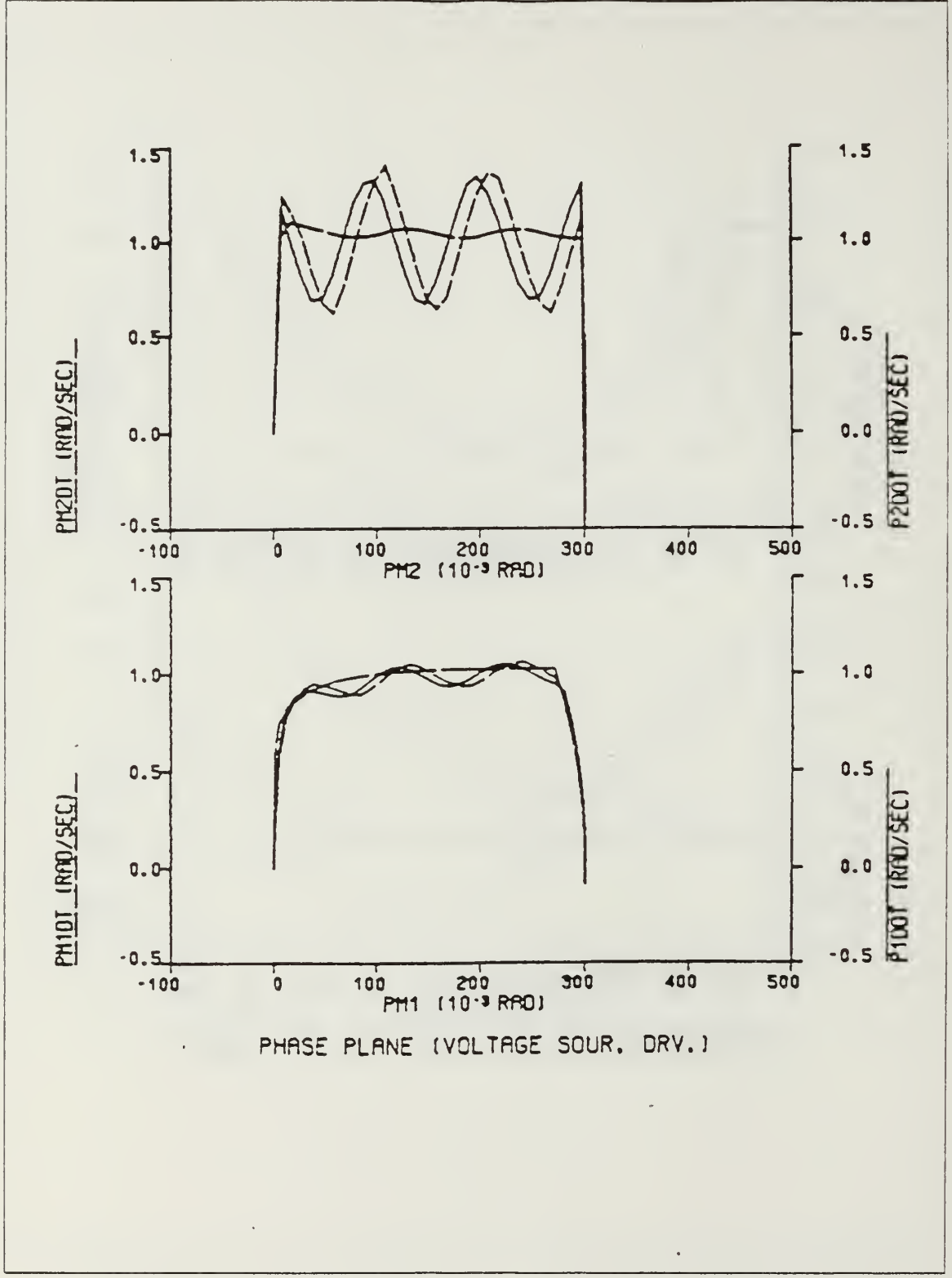

Figure 6.49 Phase Plane Trajectory For Ramp Input (With Gravity).

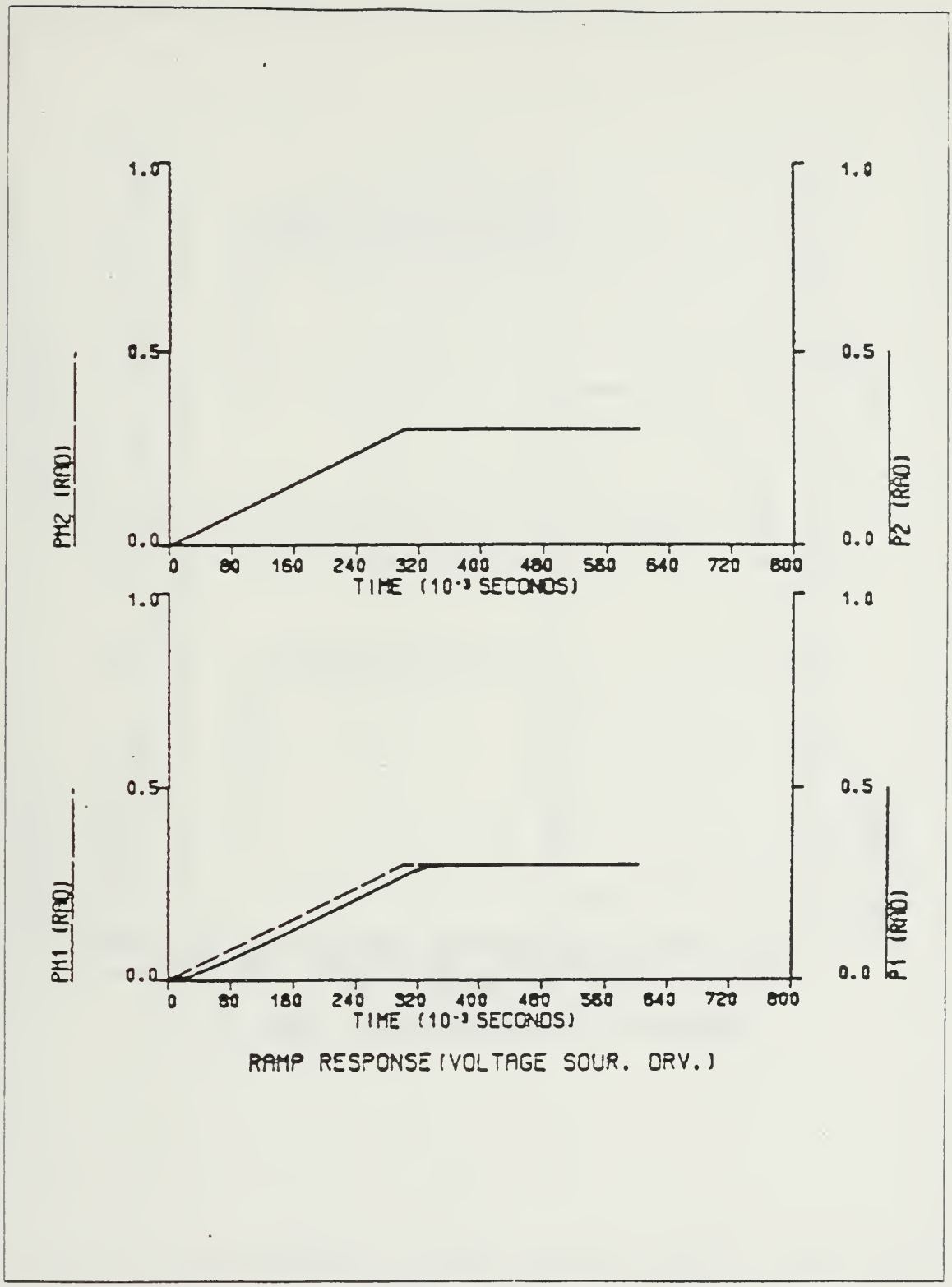

Figure 6.50 Ramp Response (With Gravity).

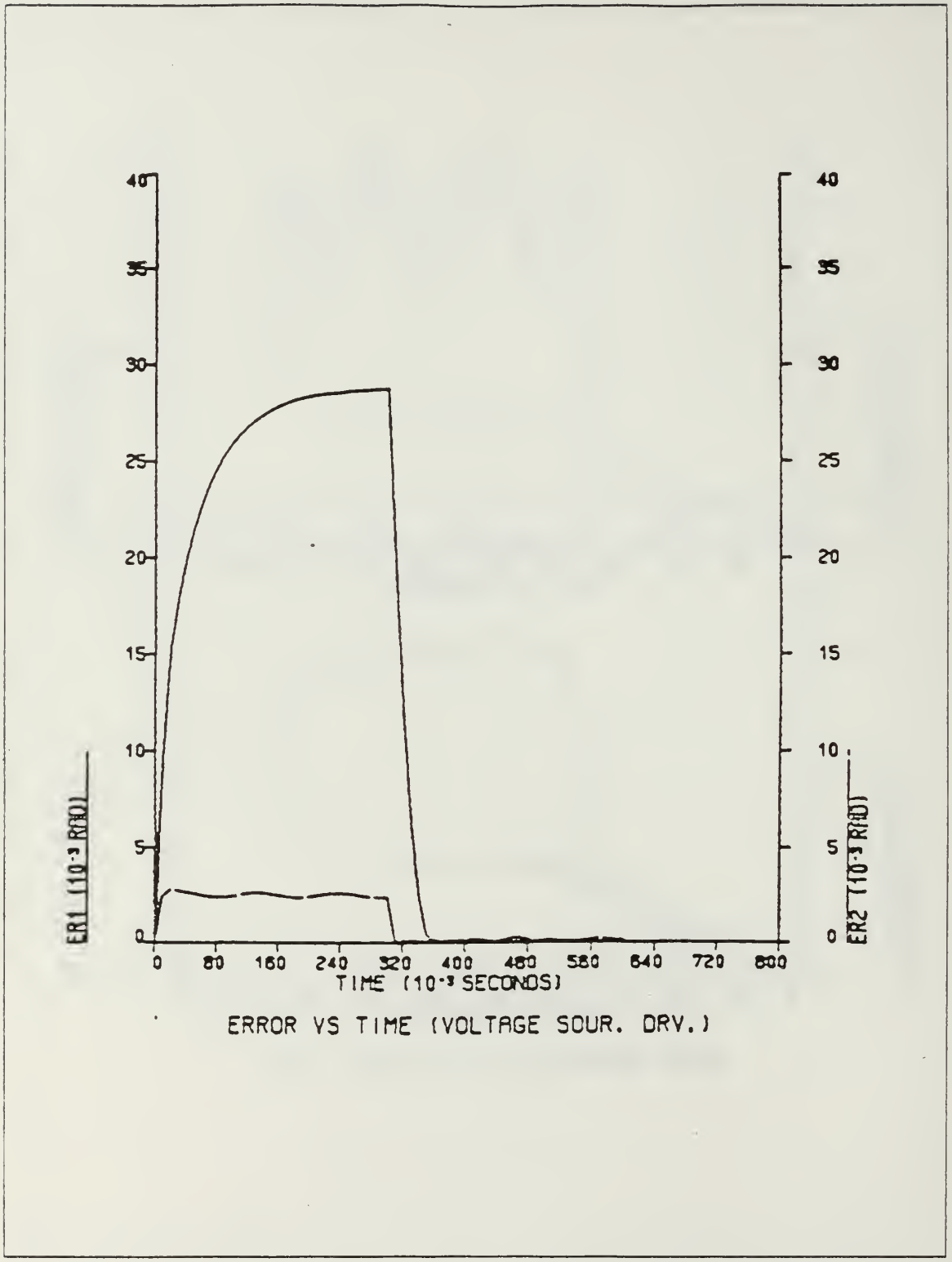

Figure 6.51 Error Between Commanded and Actual Position (With Gravity).

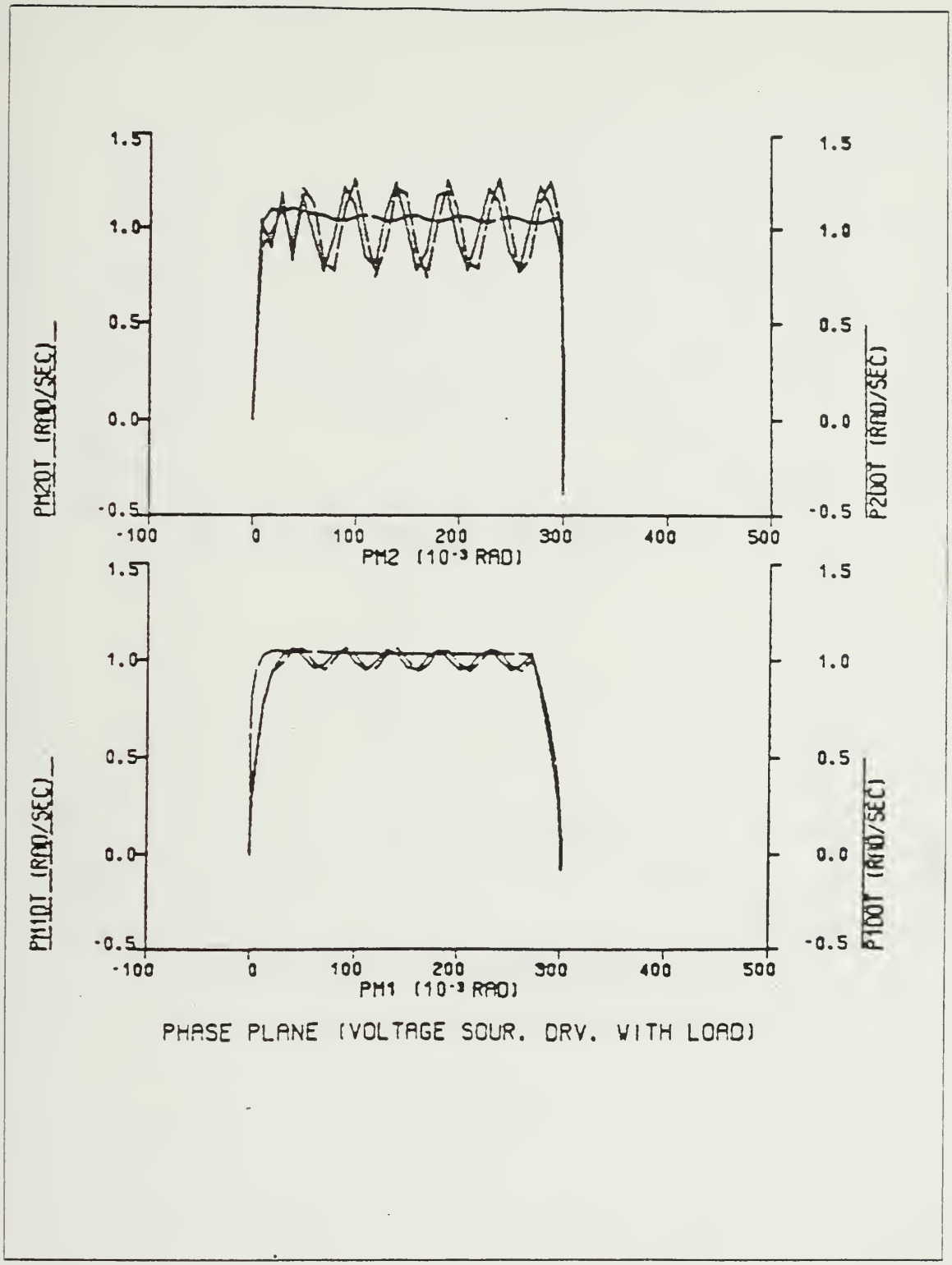

Figure 6.52 Phase Plane Trajectory For Ramp Input (With Gravity - Loaded Arm).

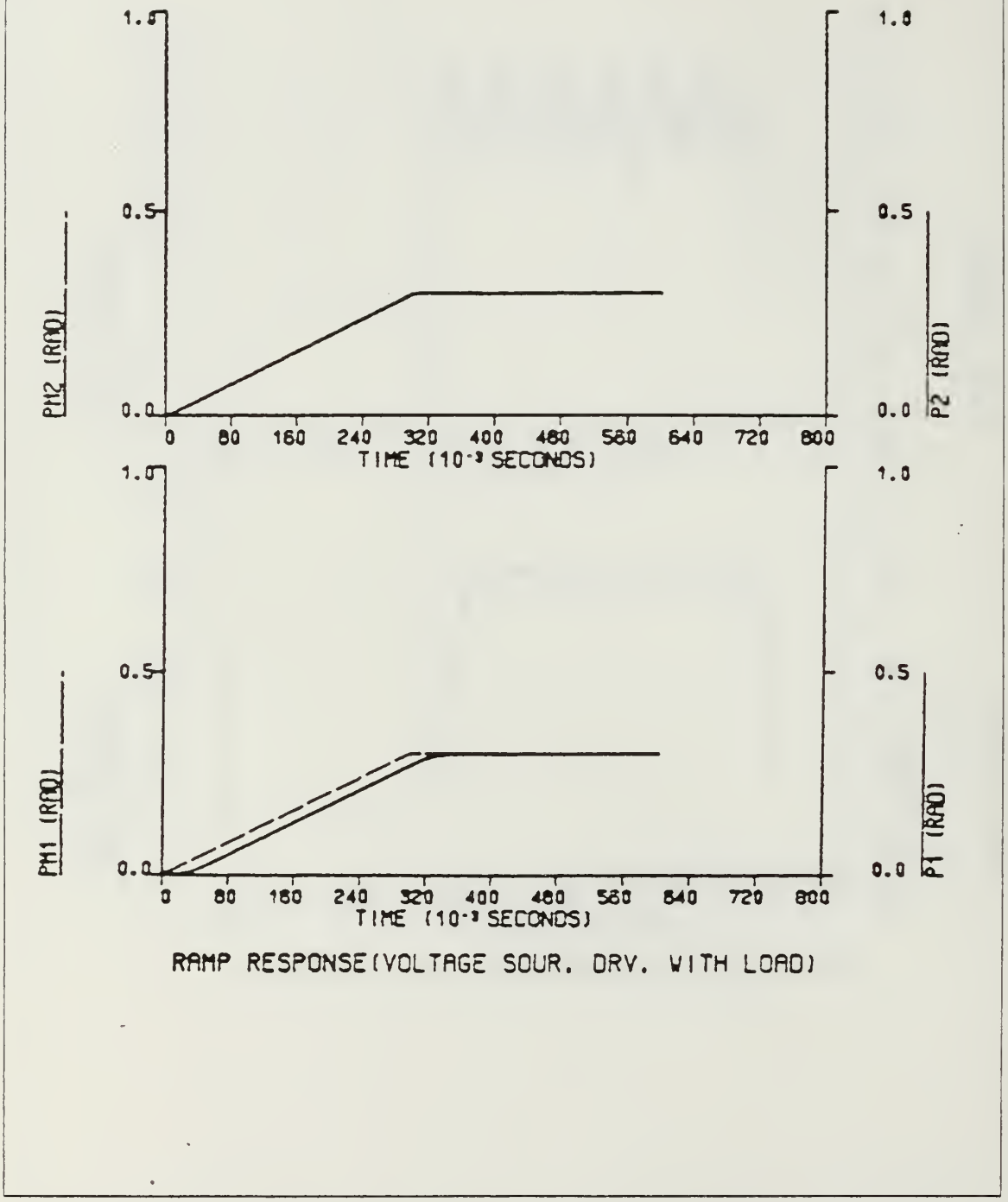

Figure 6.53 Ramp Response (With Gravity - Loaded Arm).

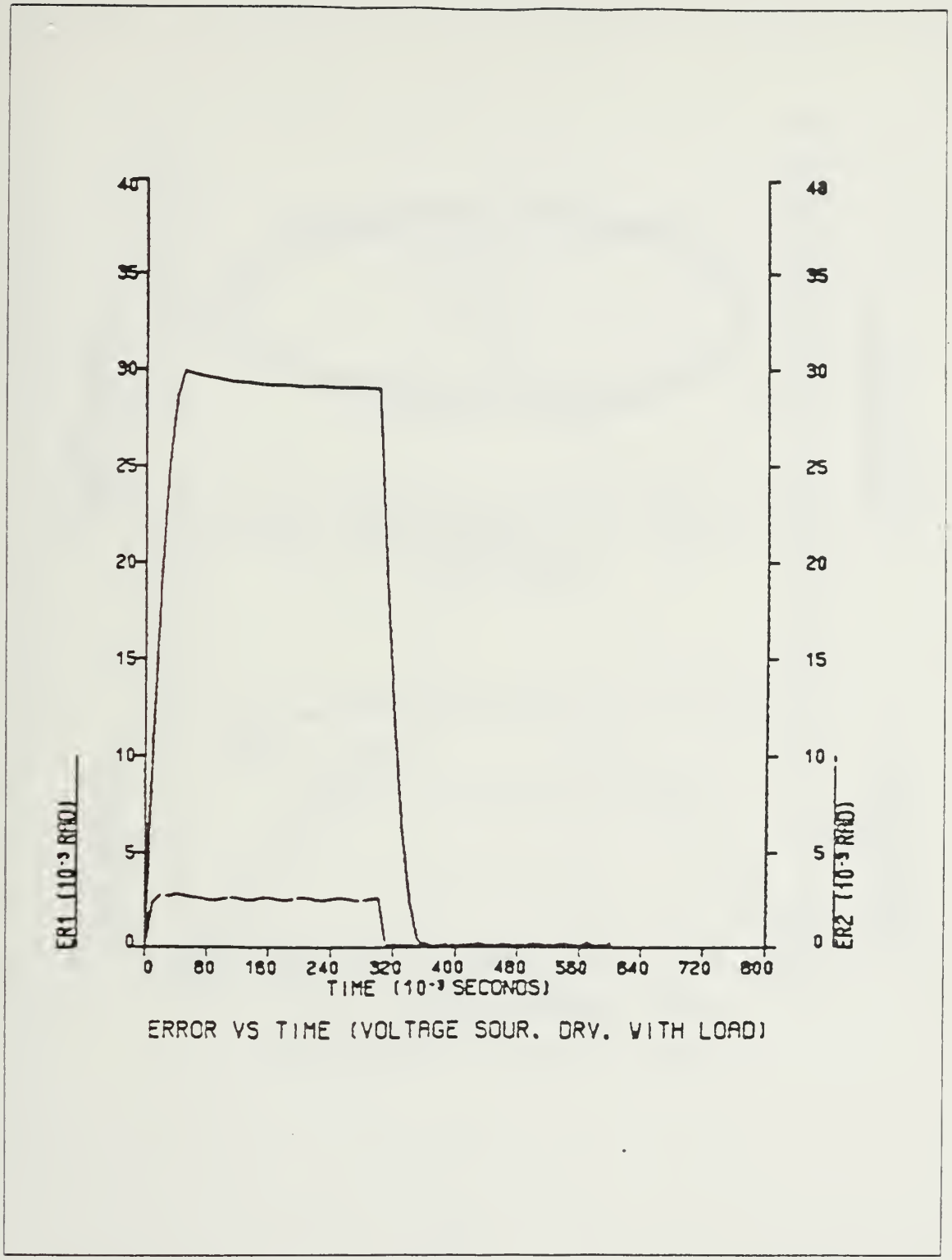

Figure 6.54 Error Between Commanded and Actual Position (With Gravity - Loaded Arm).

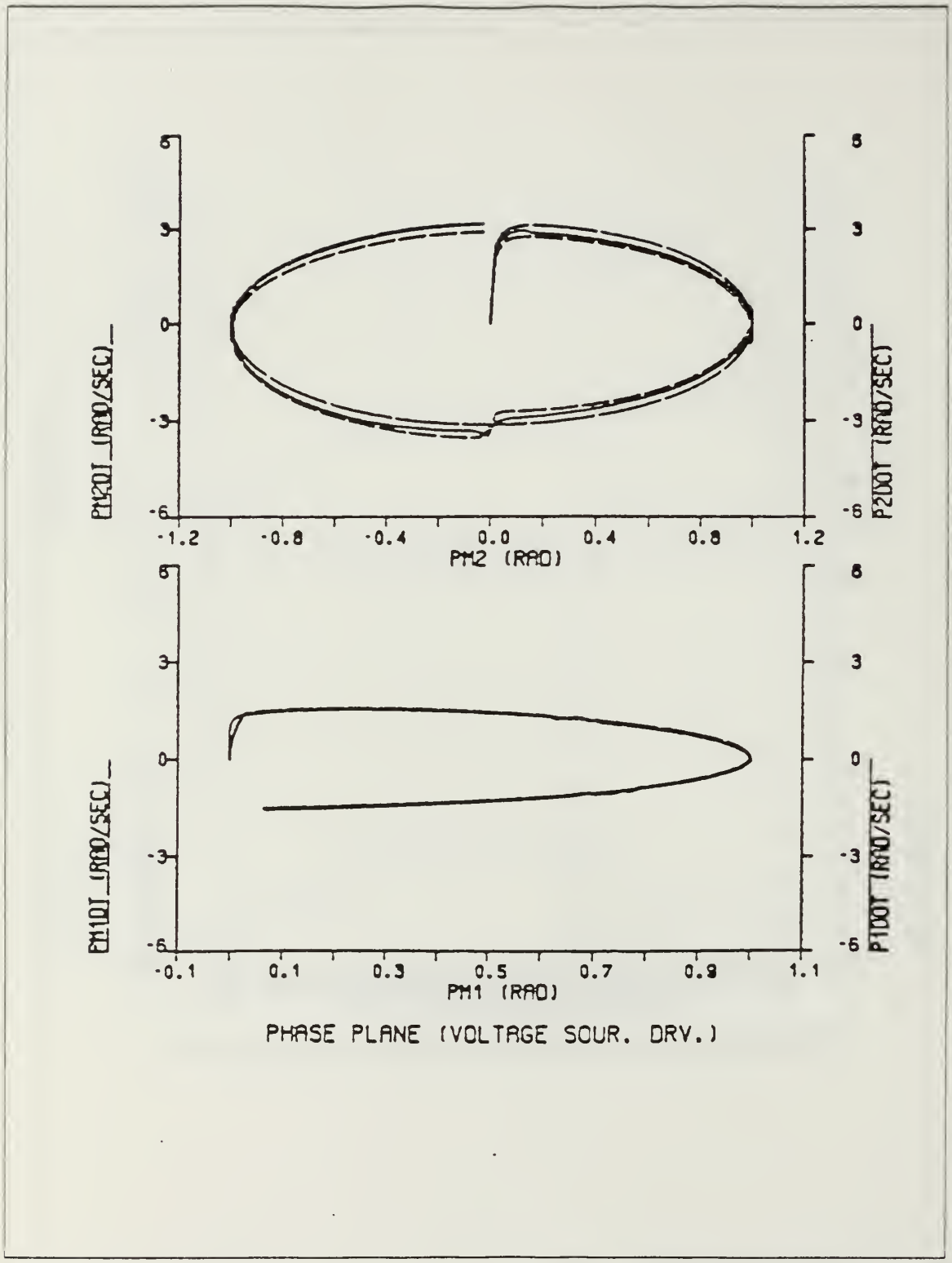

Figure 6.55 Phase Plane Trajectory For Sinusoidal Input (With Gravity).

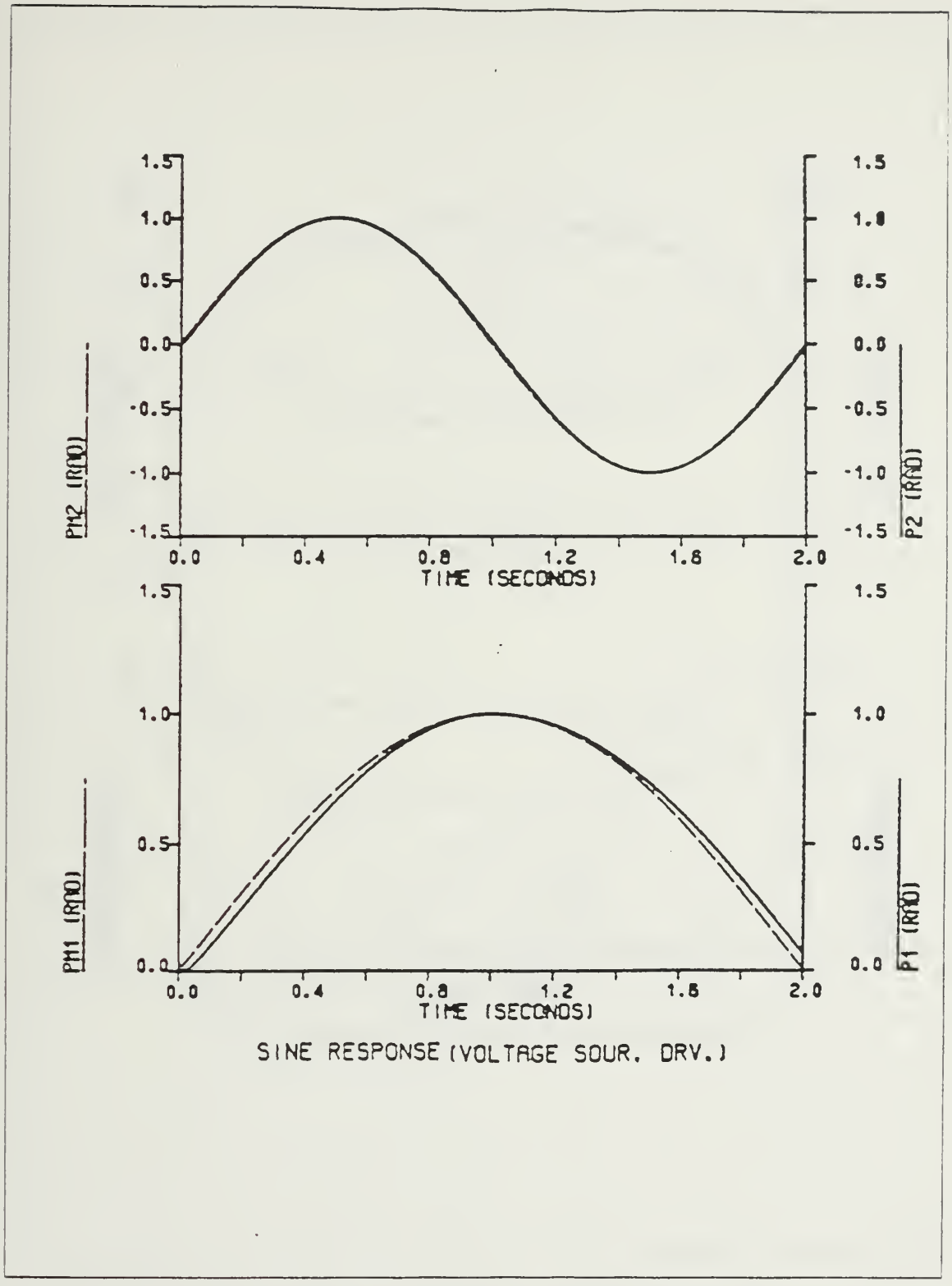

Figure 6.56 Sine Response (With Gravity).

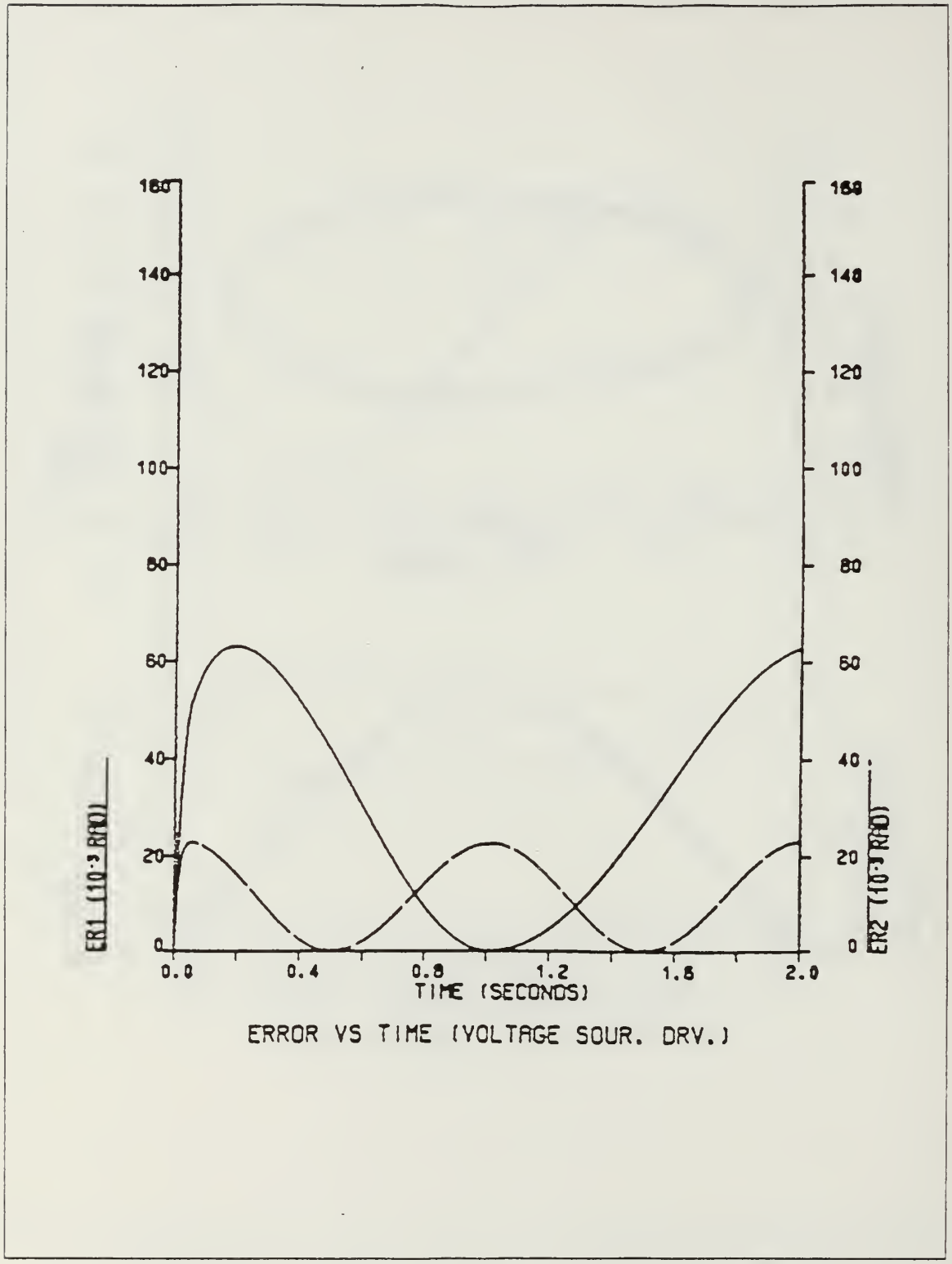

Figure 6.57 Error Between Commanded and Actual Position (With Gravity).

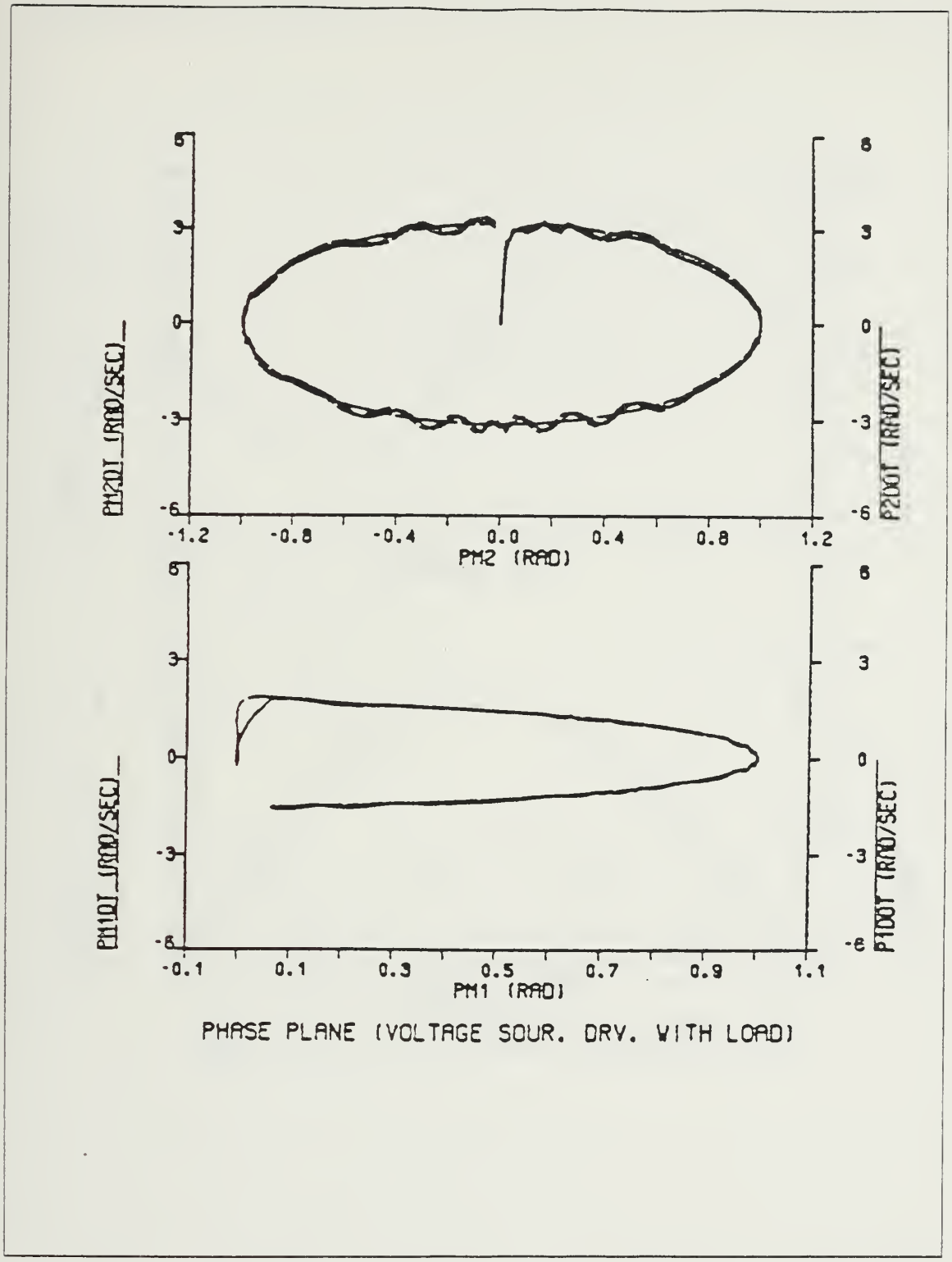

Figure 6.58 Phase Plane Trajectory For Sinusoidal Input (With Gravity - Loaded Arm).

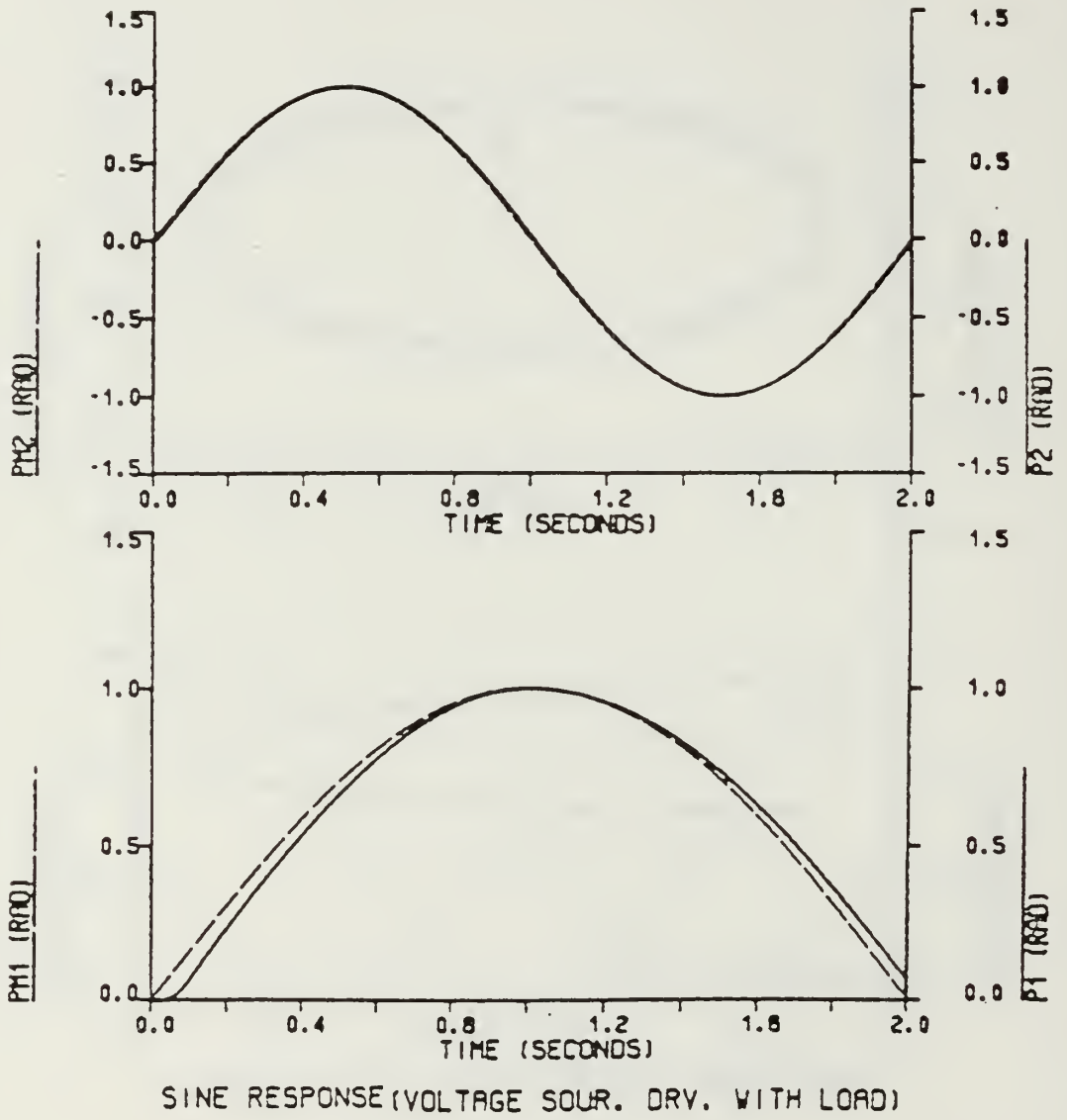

Figure 6.59 Sine Response (With Gravity - Loaded Arm).

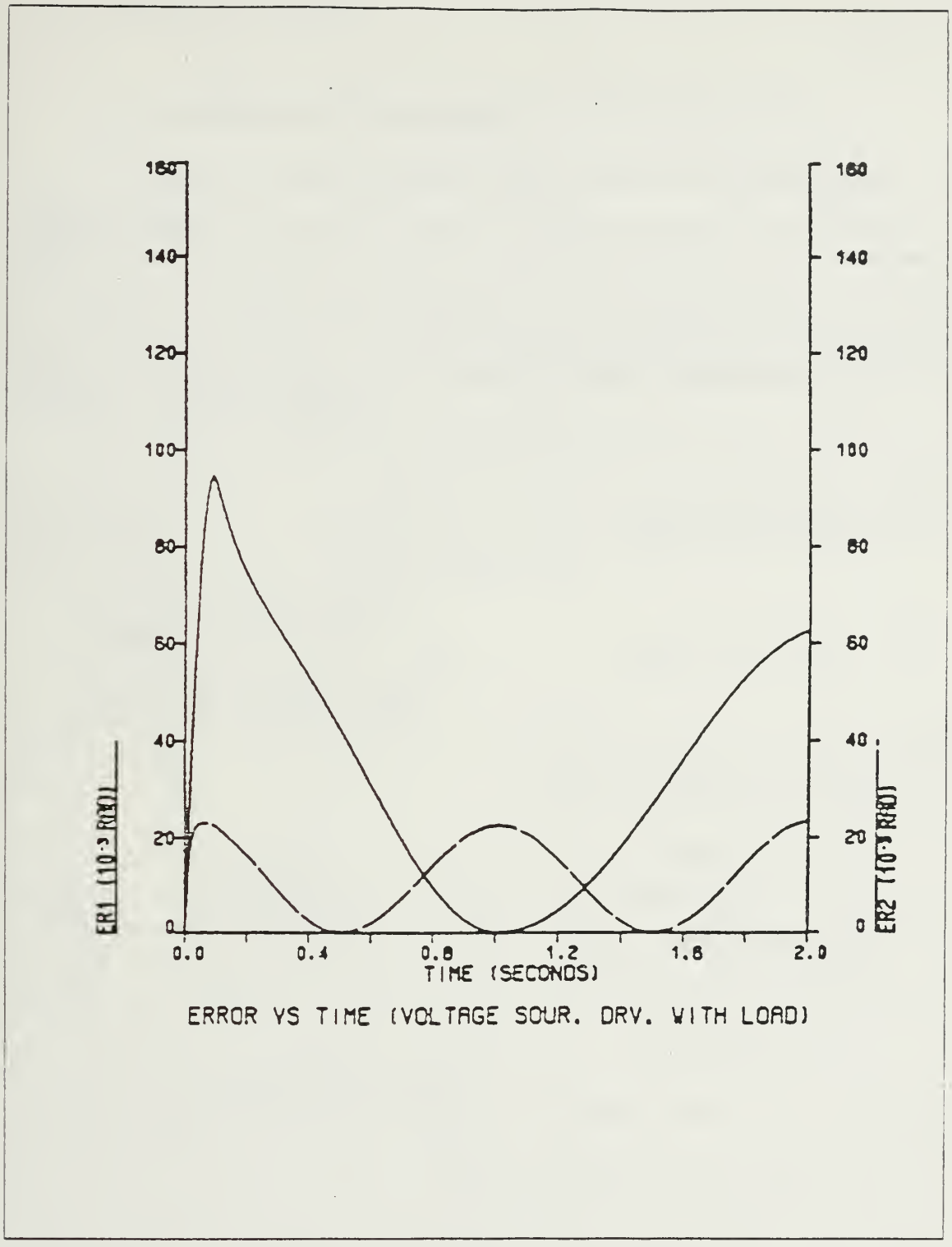

Figure 6.60 Error Between Commanded and Actual Position (With Gravity - Loaded Arm).

VII. THE CURRENT SOURCE DRIVE SYSTEM

A. DEVELOPMENT OF THE CURRENT SOURCE DRIVE SYSTEM

In a DC servo motor; to achieve constant acceleration, the armature circuit current must build up quickly to a constant value and provide constant torque. This is important for the second-order model to control the servo motor. A current source drive system can be used to accomplish this.

It can be shown [Ref. 2] that the transfer functions for a permanent magnet DC servo motor, when the viscous friction of the motor and load is small, are:

$$\frac{\theta(s)}{V(s)} = \frac{K_t}{s[(R+sL)Js + K_v K_t]} \qquad \text{(eqn 7.1)}$$

$$\frac{I(s)}{V(s)} = \frac{Js}{[(R+sL)Js + K_v K_t]} \qquad \text{(eqn 7.2)}$$

where

θ = Angular position of the shaft
V = Applied d-c voltage
I = Armature current
K_v = Back emf constant
K_t = Torque constant
J = Total inertia
R = Armature resistance
L = Armature inductance

The transfer function block diagram of a Current Source Drive is shown [Ref. 1] in Figure 7.1.

If the amplifier gain is chosen as such that

$$KA >> 1 \qquad \text{(eqn 7.3)}$$

then the equivalent transfer function of the amplifer can be written as;

$$\frac{V}{V_a} = \frac{[(R+sL)Js + K_v K_t]}{Js} \qquad \text{(eqn 7.4)}$$

The equivalent transfer function becomes:

$$\frac{\theta(s)}{V_a(s)} = \frac{K_t/J}{S^2} \qquad \text{(eqn 7.5)}$$

Thus if the amplifier gain is carefully chosen, the ideal motor of the second-order model will be approximated by the system and the effect of the back emf and armature inductance will become negligible.

Simulation block diagram of the current source drive system is shown in Figure 7.2. R_s was chosen to be 0.1 to minimize the influence on the electrical pole, inversely K_f was set at 10.0. The amplifier gain (KA) and saturation limit (VSATA) were chosen by trial and error. These values were found:

- Without gravitational torques
  KA1 = 150, VSATA1 = 100
  KA2 = 75, VSATA2 = 50
- Gravitational torques are included
  KA1 = 350, VSATA1 = 300
  KA2 = 175, VSATA2 = 150

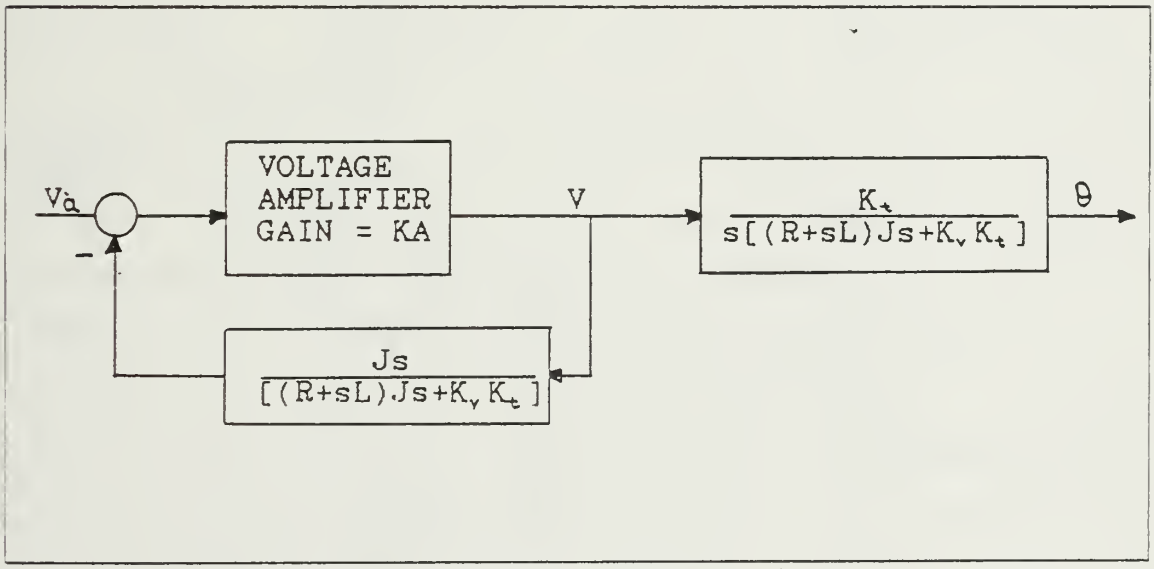

Figure 7.1 Transfer Function Block Diagram of the Current Source Drive.

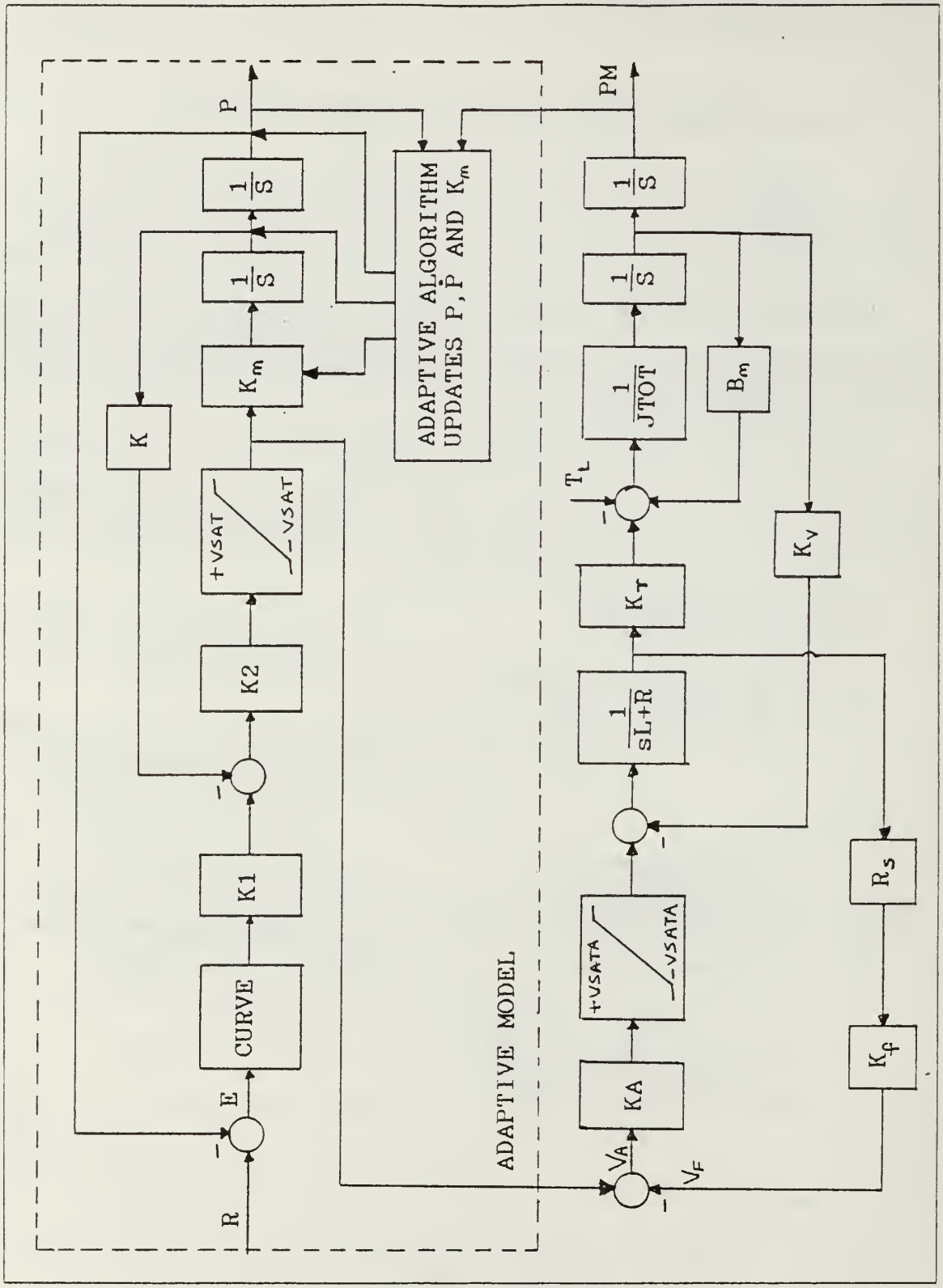

Figure 7.2 Block Diagram of the Current Source Drive System.

B. SIMULATION STUDIES OF THE ADAPTIVE SYSTEM.

DSL/VS simulation programs used in simulation of the adaptive system with Current Source Drive are listed in Appendix E and F. The simulation program listed in Appendix E is used for studies under a gravity-free environment. Appendix F lists the simulation program which includes gravitational torques. Again note that although PM cannot be observed in the actual system, it is available in the simulation and is used to check the validity of the algorithm.

1. Gravity-Free Environment

Step position command and time varying position command inputs are used to test the adaptive system under a gravity-free environment (No Gravitional Torques). Sample motions, Move #1 and Move #2 are used in the simulation studies of this part. Note that on all figures of Phase Plane Trajectories the angular velocity of the second-order model (P) and the angular velocity of the servo motor (PM) are both plotted as ordinates. The second-order model angular position (P) and the servo motor angular position (PM) are both plotted as ordinates in the time response plots. In general these curves fall on top of each other.

a. Step Position Command Input Used

Phase plane plot and step response curves for the unloaded arm under Move #1 are shown in Figures 7.3 and 7.4. In the phase plane plot PM and P are plotted versus PM. The step response curve shows P and PM are plotted versus time.

Good curve following characteristics are seen in Figure 7.3. Maximum angular velocity of 3.17 rad/sec and 12 rad/sec are observed for servo motors 1 and 2 respectively. The step response curves of Figure 7.4 show the second-order models and servo motors tracking together. Also much faster time response was observed for JOINT2 servo motor due to smaller inertia and supporting reaction torques in the direction of motion. Steady state accuracy of the order of 10E-4 is observed.

The simulation results for the loaded arm are shown in Figures 7.5 and 7.6. The effects of the reaction torques can be observed in these figures. At the beginning of the move, upward motion of the LINK2 produces an interaction torque on JOINT1 servo motor. This reaction torque opposes JOINT1 servo motor acceleration in the direction of motion. Therefore it takes some time to overcome the reaction torque, and LINK1 starts accelerating. To avoid this situation, JOINT2 servo motor position command input is delayed 150 milliseconds at the beginning of the Move #1. Simulation results are shown in Figures 7.7 - 7.10.

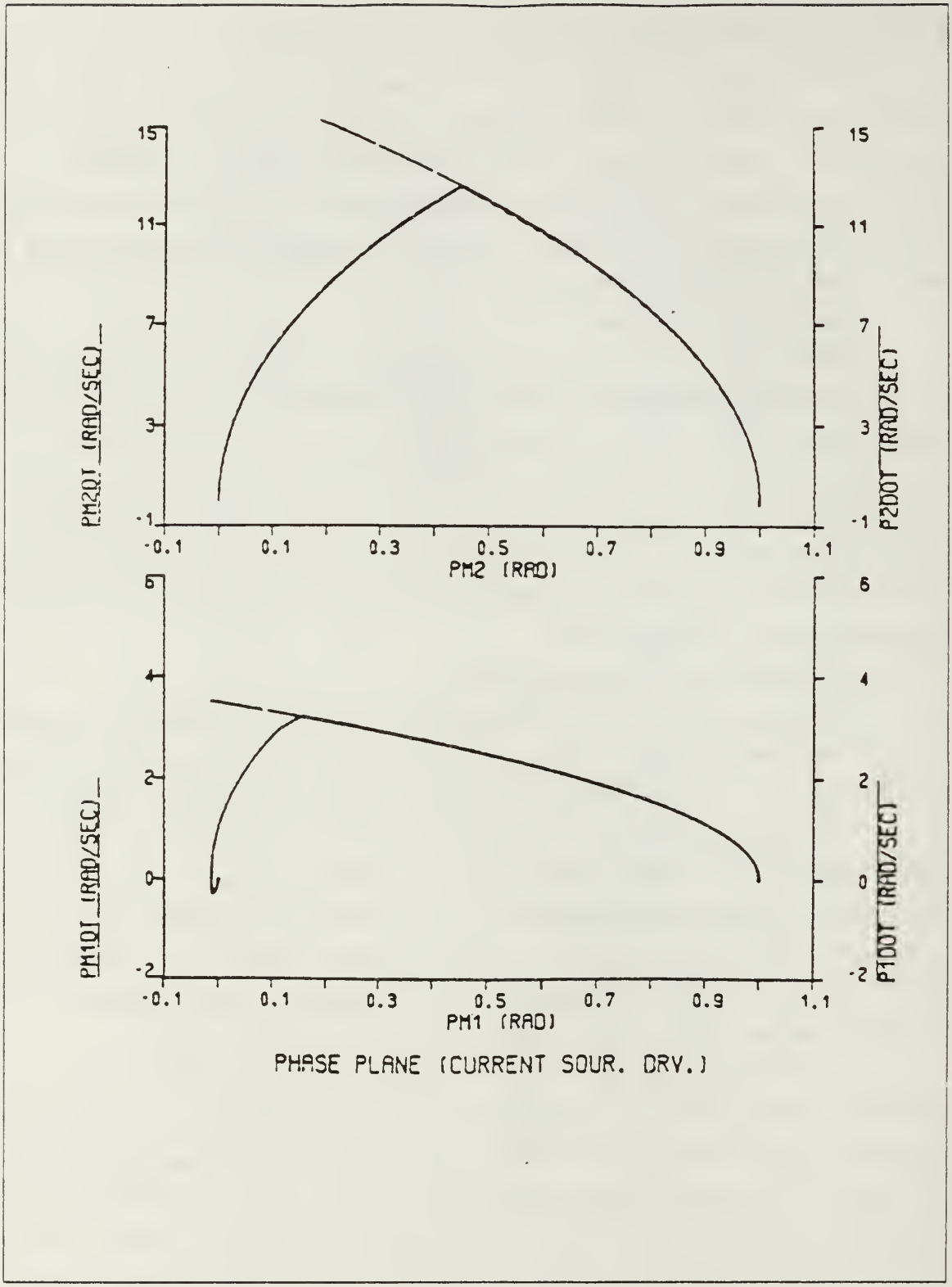

Figure 7.3 Phase Plane Trajectory For Move #1 (No Gravity).

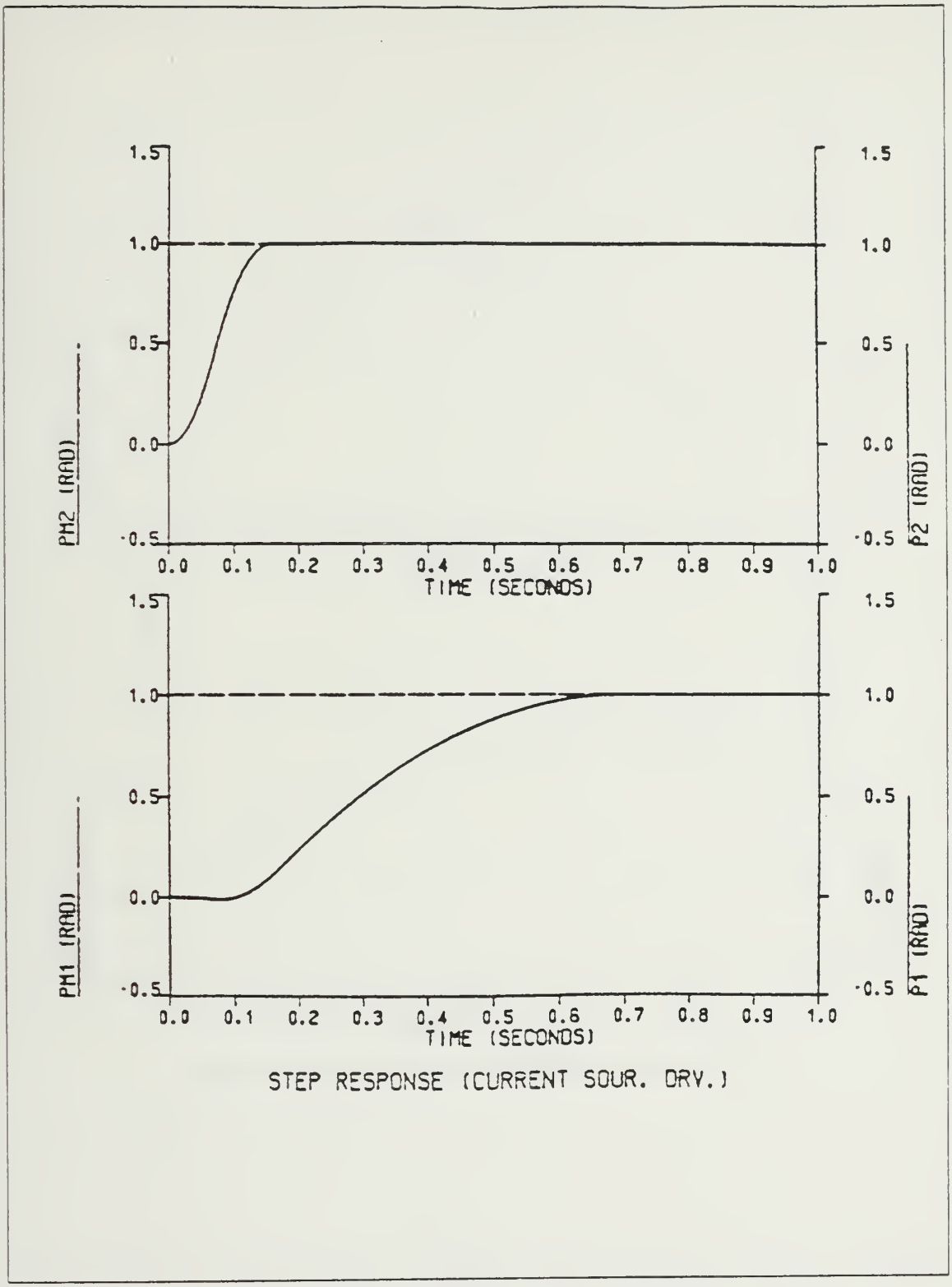

Figure 7.4 Step Response For Move #1 (No Gravity).

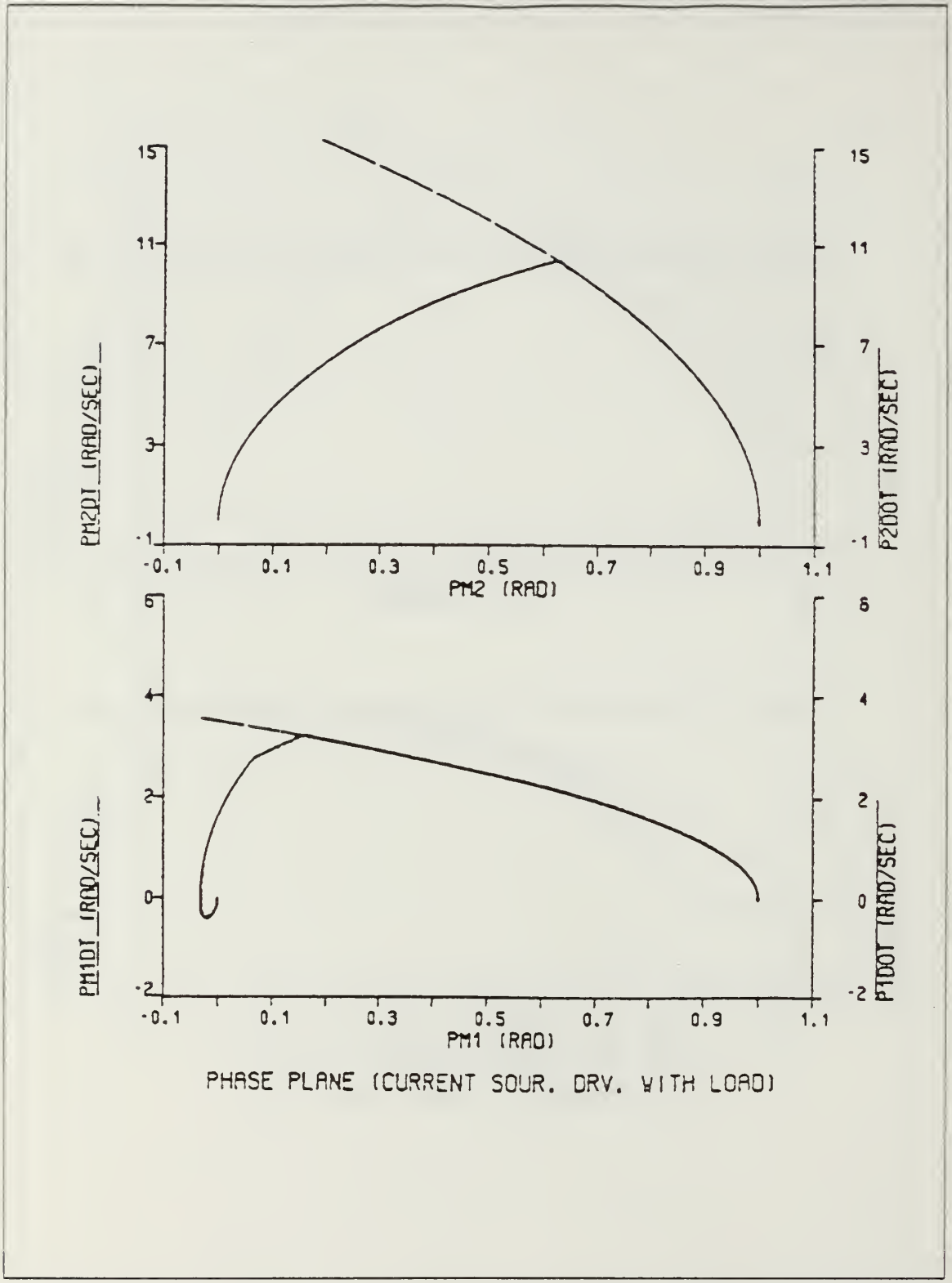

Figure 7.5 Phase Plane Trajectory For Move #1 (No Gravity).

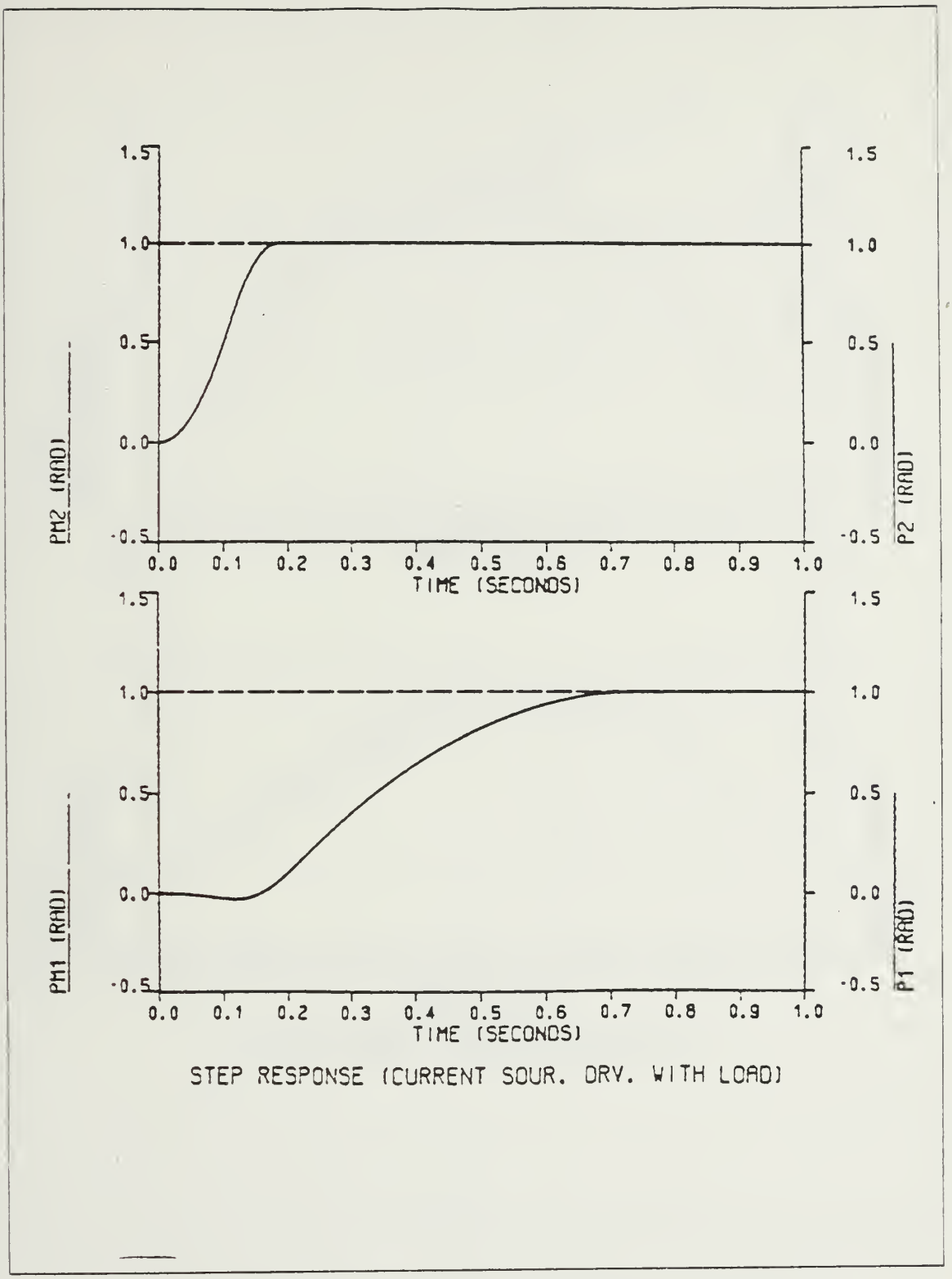

Figure 7.6 Step Response For Move #1 (No Gravity).

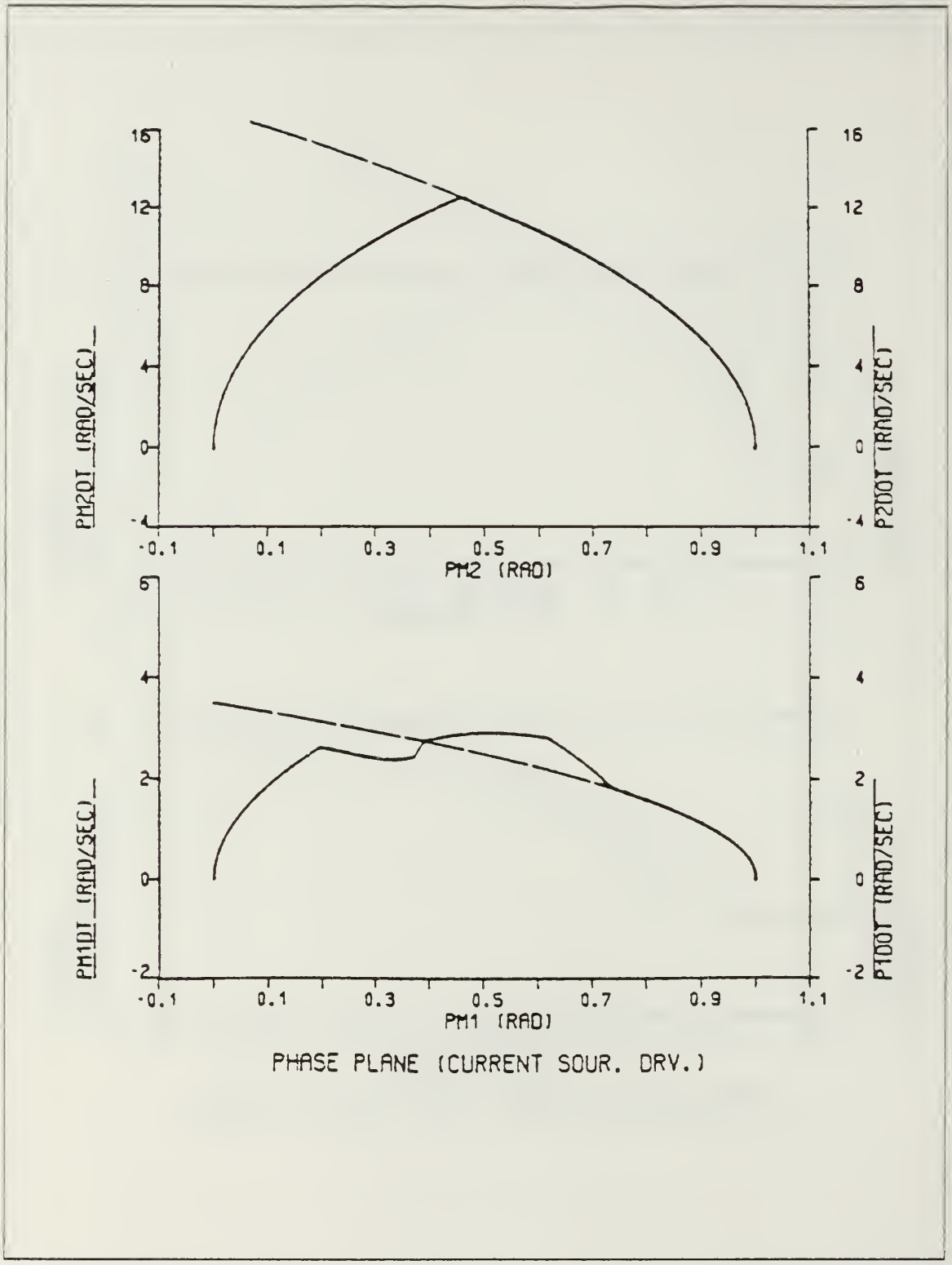

Figure 7.7 Phase Plane Trajectory For Move #1 (No Gravity) JOINT2 Servo Motor Input Delayed 0.15 sec..

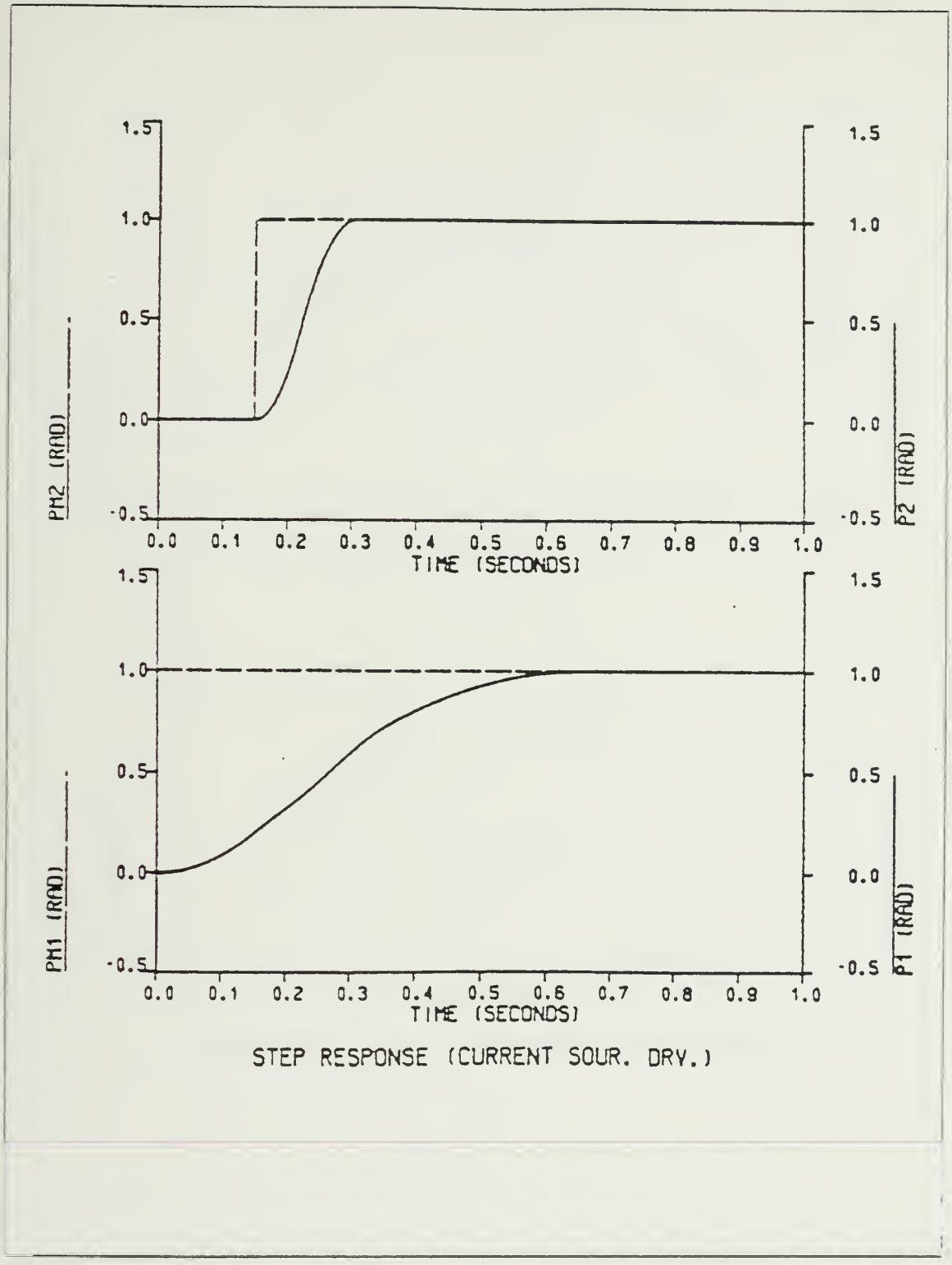

Figure 7.8 Step Response For Move #1 (No Gravity)
JOINT2 Servo Motor Input Delayed 0.15 sec..

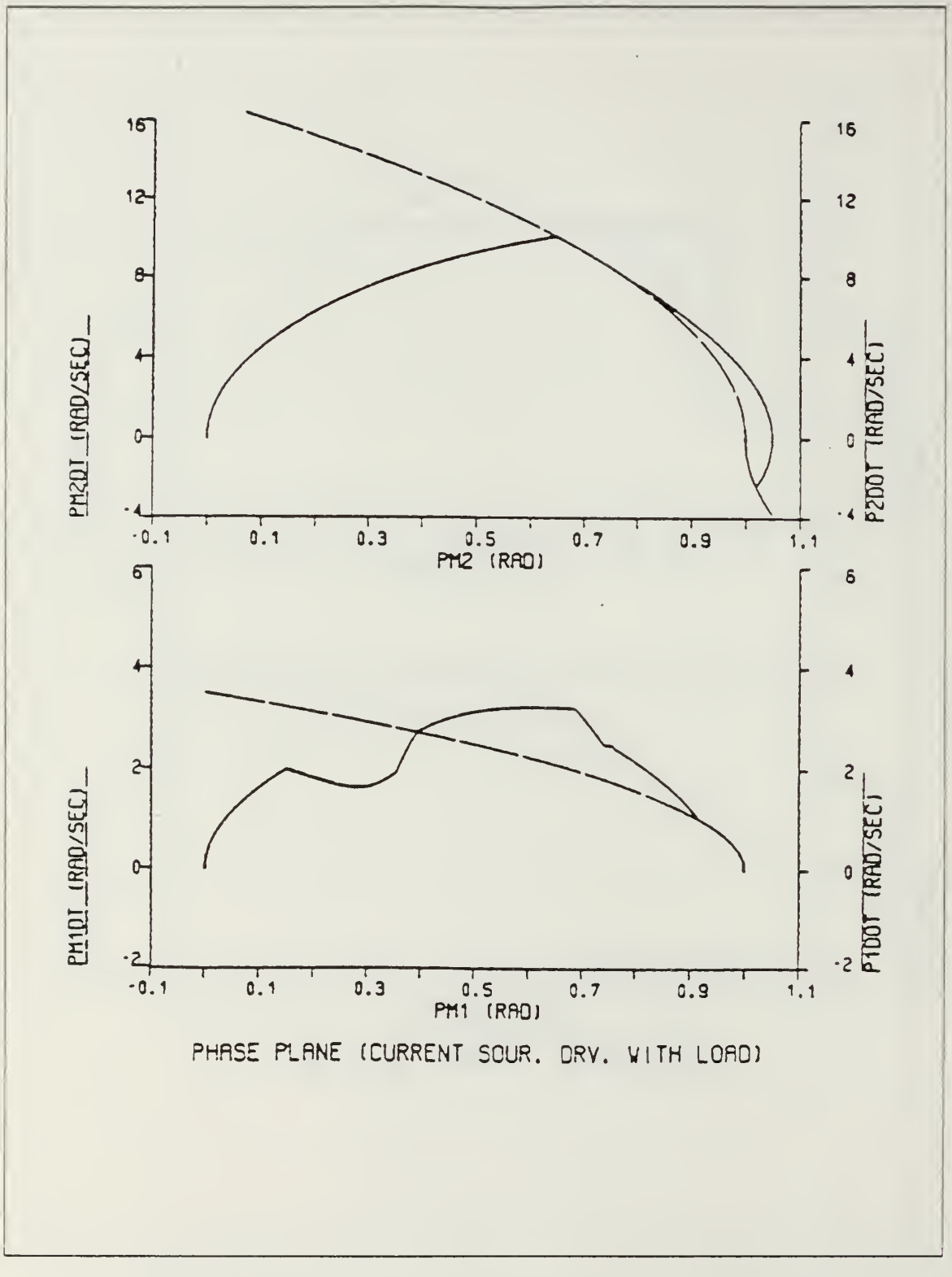

Figure 7.9 Phase Plane Trajectory For Move #1 (No Gravity)
JOINT2 Servo Motor Input Delayed 0.15 sec..

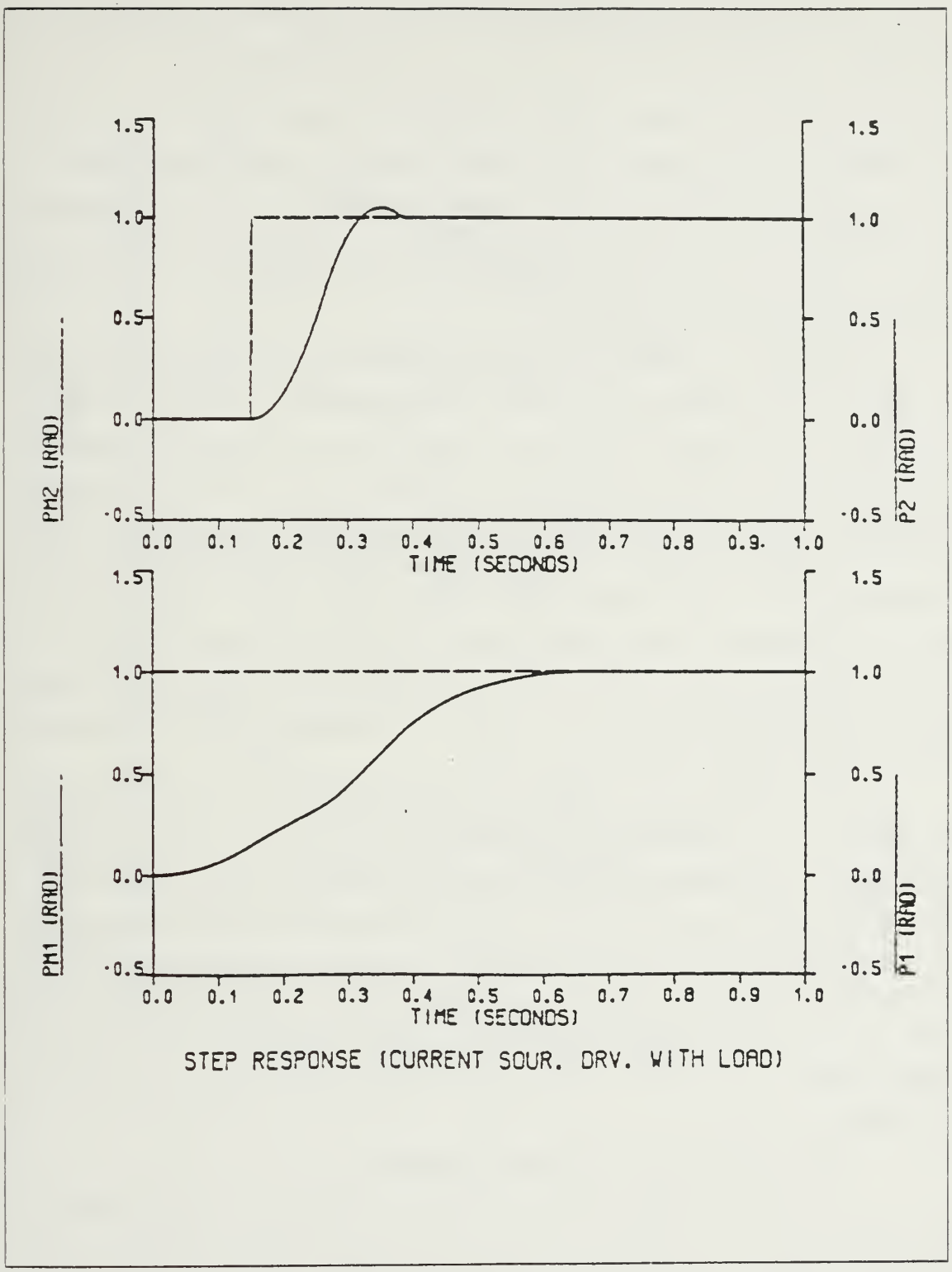

Figure 7.10 Step Response For Move #1 (No Gravity)
JOINT2 Servo Motor Input Delayed 0.15 sec..

The effects of the delayed JOINT2 servo motor can be observed in the phase plane trajectories of Figures 7.7 and 7.9. At the beginning, JOINT1 servo motor starts accelerating while JOINT2 servo motor stays still. When JOINT2 servo motor starts accelerating, the reaction torque produced by JOINT2 servo motor causes JOINT1 servo motor to decelerate for a while. Meanwhile, curve following seems lost, but after a while the adaptive system tracks and follows the curve until the final position. In the loaded arm case, 7% overshoot was observed for JOINT2 servo motor. This can be prevented by lowering the curve gain constant. Faster overall response was obtained with delayed input.

Figures 7.11 - 7.18 show simulation results for Move #2. Figures 7.11 and 7.13 are good examples to show the effects of the interaction torques on the servo motors. At the beginning of the move, the reaction torques produced by accelerations of the servo motors increase each other's acceleration in the direction of the move. Therefore, servo motors reach maximum angular velocities in a short time. When JOINT2 servo motor reaches the curve and starts braking, the interaction torque produced by JOINT2 servo motor opposes JOINT1 servo motor acceleration in the direction of the motion. Step response curves of Move #2 are shown in Figures 7.12 and 7.14. It can be observed, in the case of loaded arm, JOINT2 servo motor overshoots and undershoots before it reaches the steady-state. This is due to the reaction torque created by JOINT1 servo motor.

To take care of this deficiency, JOINT2 servo motor curve gain constant was lowered to 0.5. Simulation results are shown in Figures 7.15 - 7.18. Phase plane trajectories show that smaller, average velocities are obtained for JOINT2 servo motor with a lowered deceleration curve. Good curve following characteristics are observed. Step response curves show almost no overshoot but longer time response for JOINT2 servo motor. This can be thought of as a price to be paid to get no overshoot. But if we think over-all time response depends on JOINT1 servo motor, then this time increase response of JOINT2 servo motor doesn't bring on an additional time increase to the system.

b. Time Varying Position Command Input Used

The adaptive system under time varying command input was simulated by using a ramp input with tangent of 1 rad/sec and a sinusoidal input. Simulation results are shown in Figures 7.19 - 7.30. Phase plane trajectories of Figures 7.19 and 7.22 show; JOINT2 servo motor velocity builds up quickly and reaches the steady-state velocity in a short time.

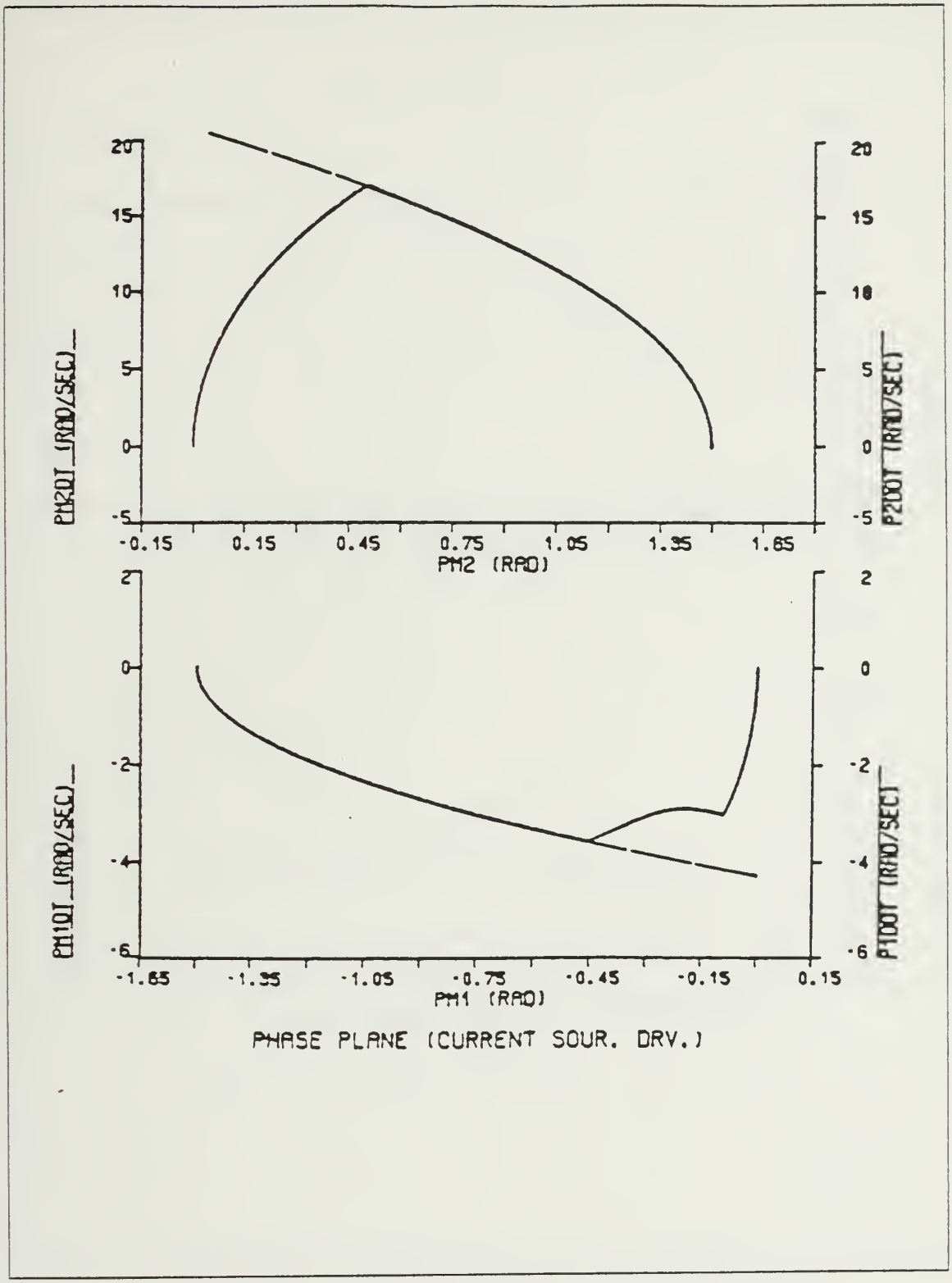

Figure 7.11 Phase Plane Trajectory For Move #2 (No Gravity).

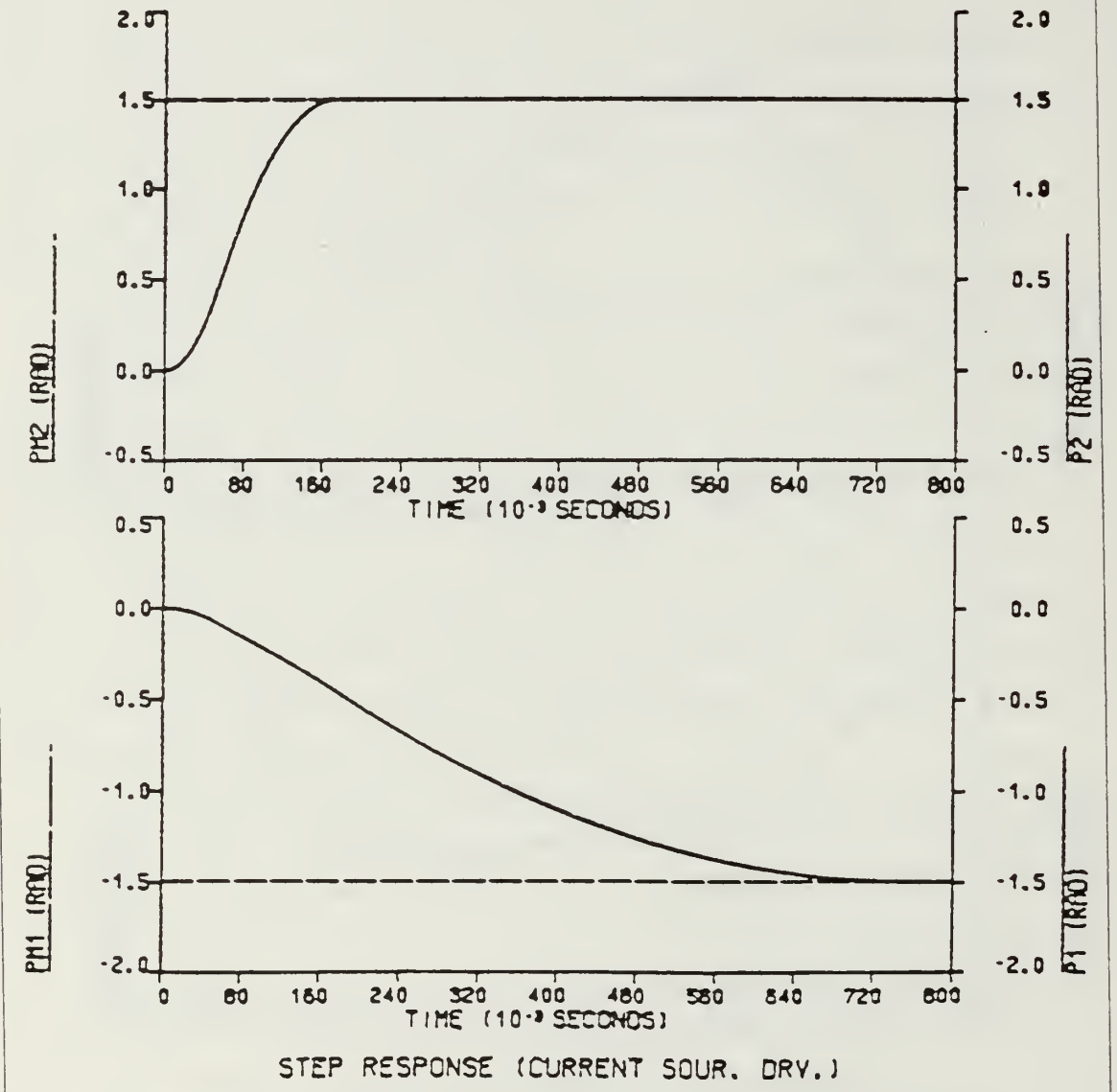

Figure 7.12 Step Response For Move #2 (No Gravity).

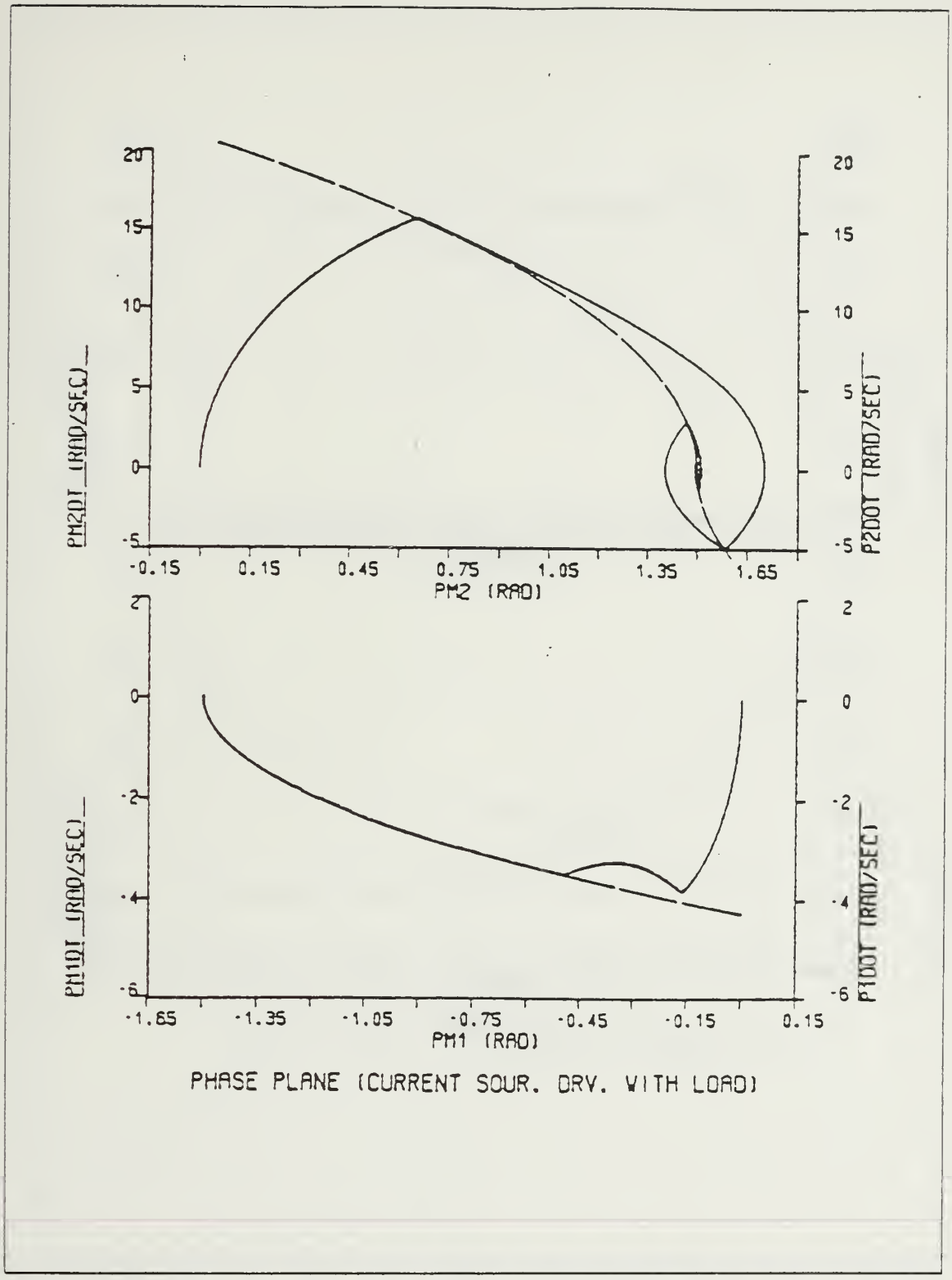

Figure 7.13 Phase Plane Trajectory For Move #2 (No Gravity).

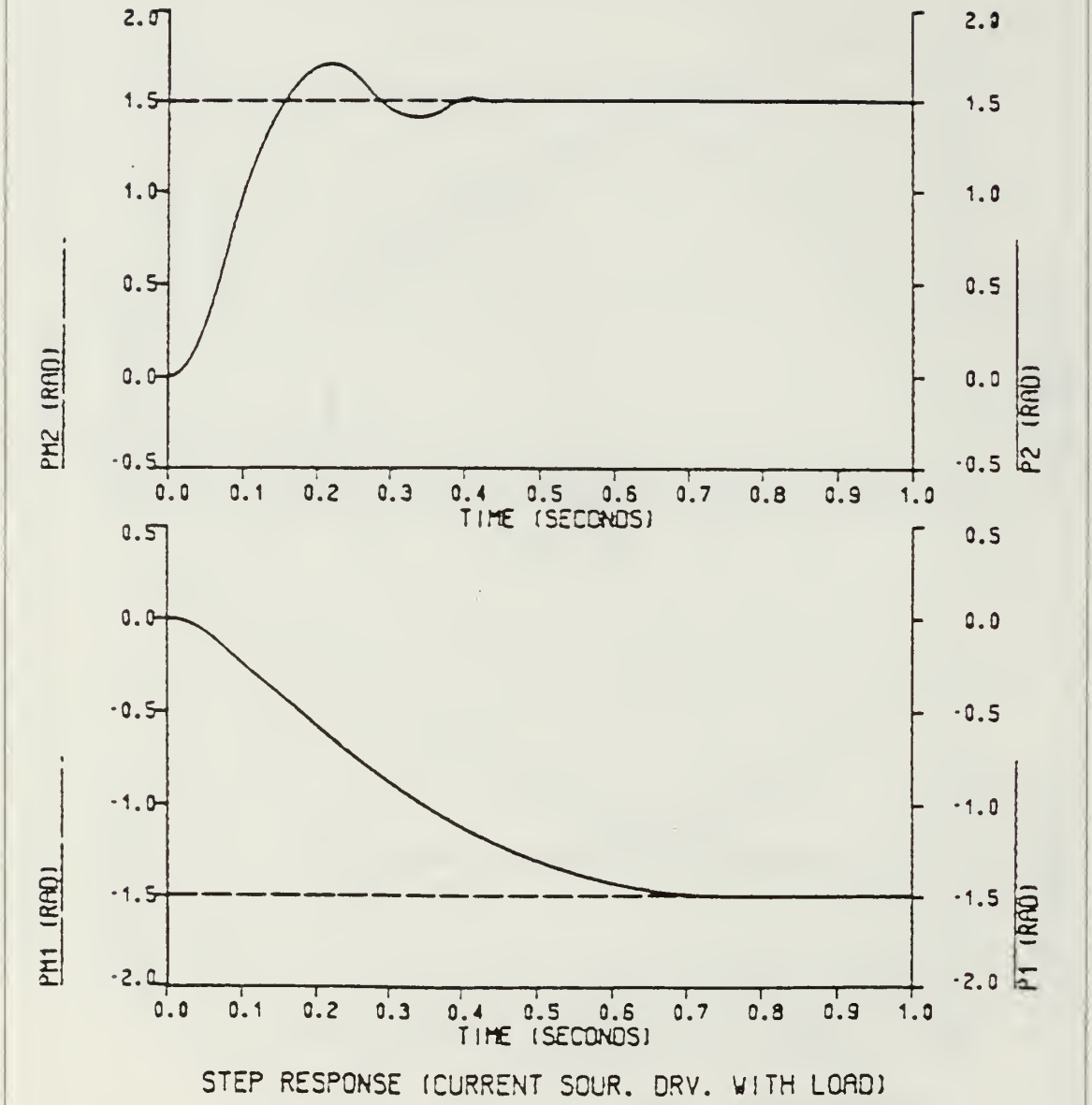

Figure 7.14 Step Response For Move #2 (No Gravity).

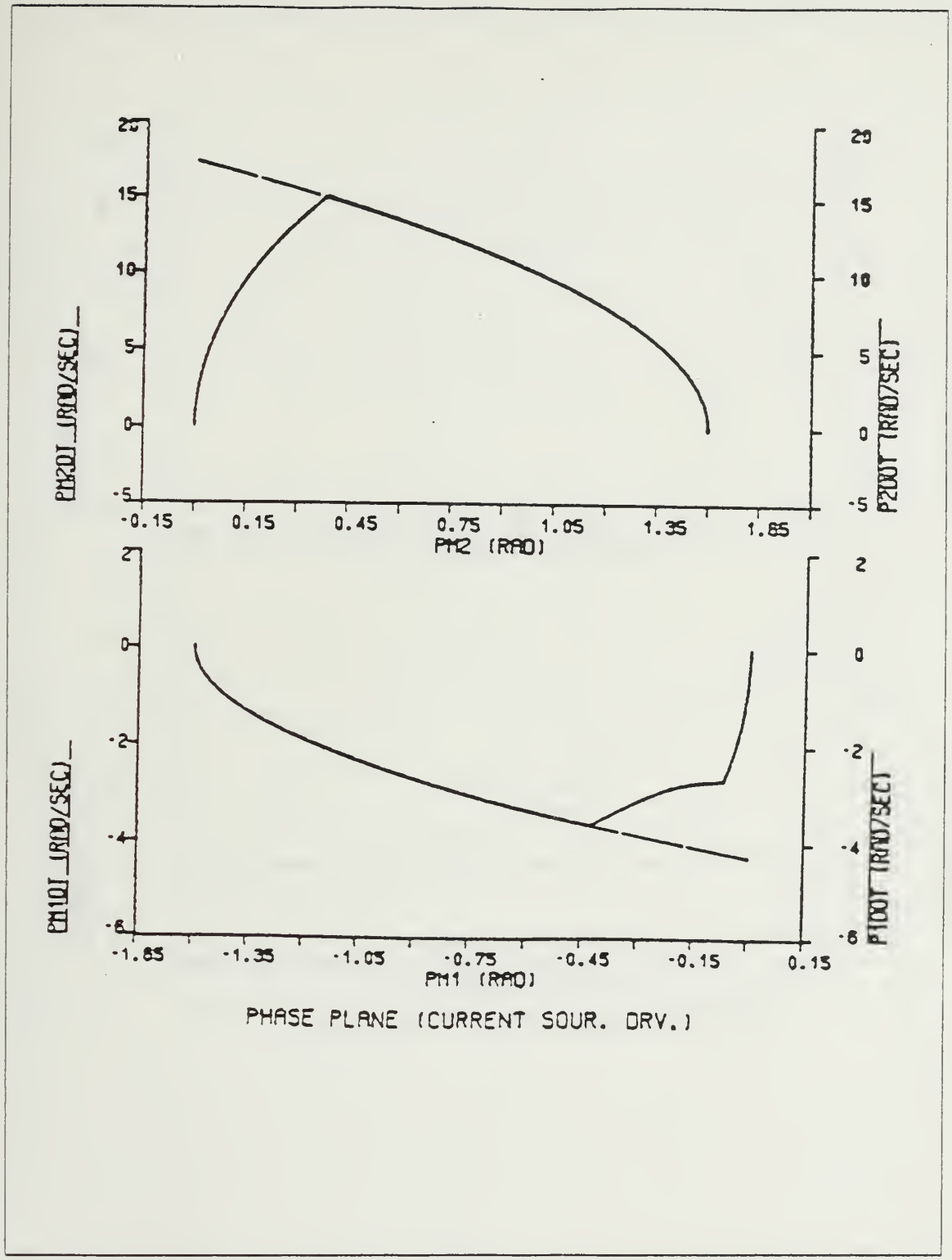

Figure 7.15 Phase Plane Trajectory For Move #2 (No Gravity)
JOINT2 Servo Motor Curve Gain Constant Lowered to 0.5.

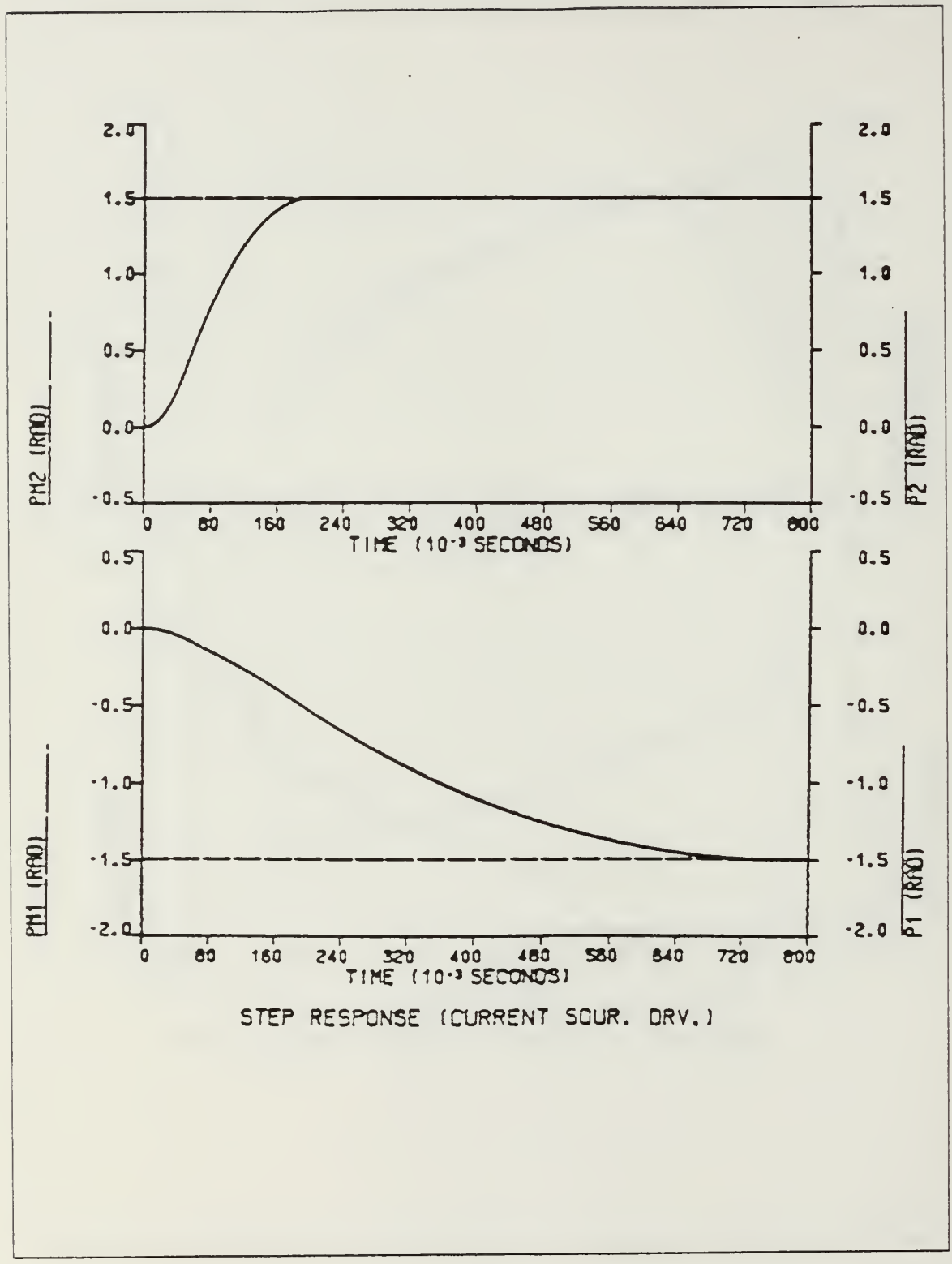

Figure 7.16 Step Response For Move #2 (No Gravity)
JOINT2 Servo Motor Curve Gain Constant Lowered to 0.5.

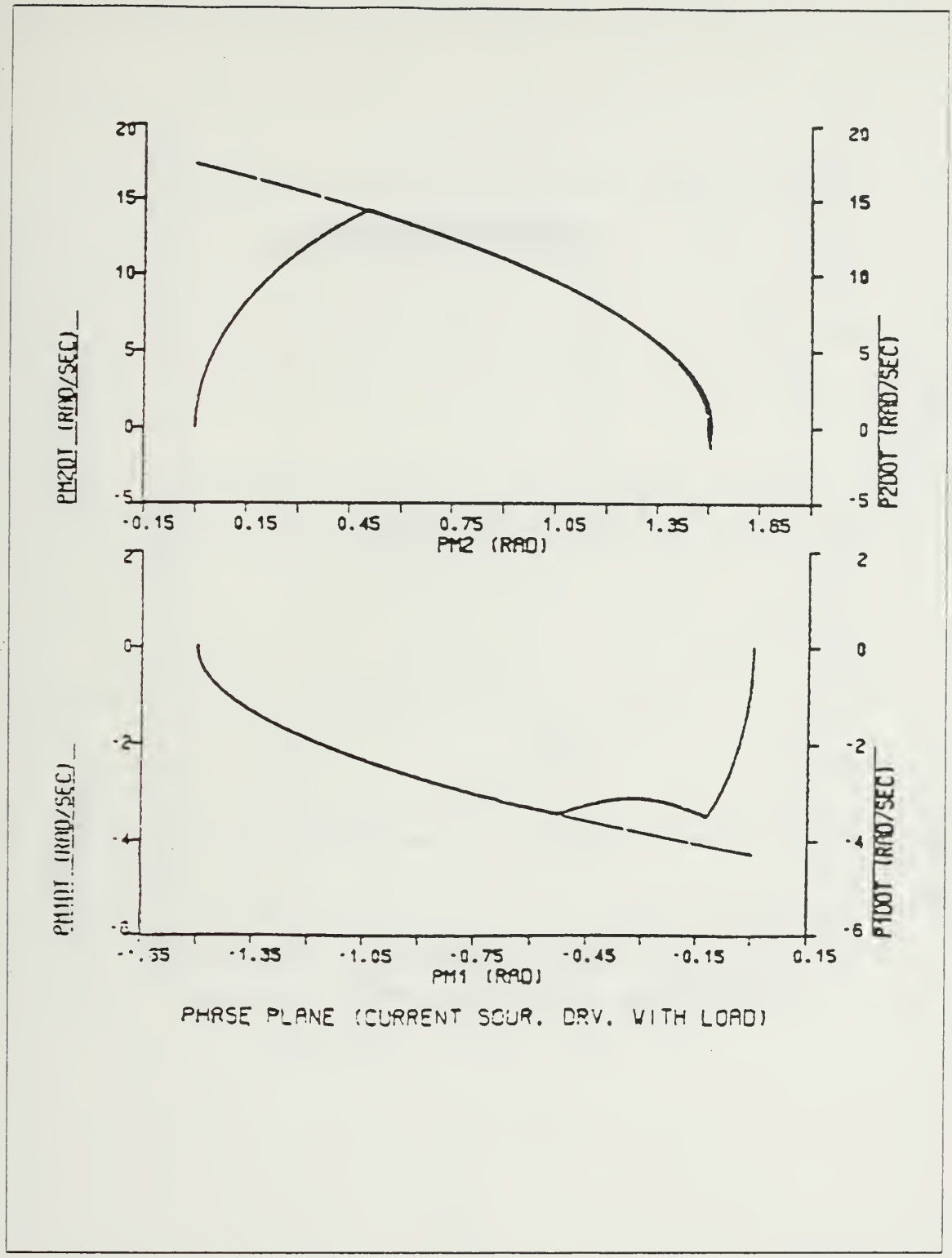

Figure 7.17. Phase Plane Trajectory For Move #2 (No Gravity)
JOINT2 Servo Motor Curve Gain Constant Lowered to 0.5.

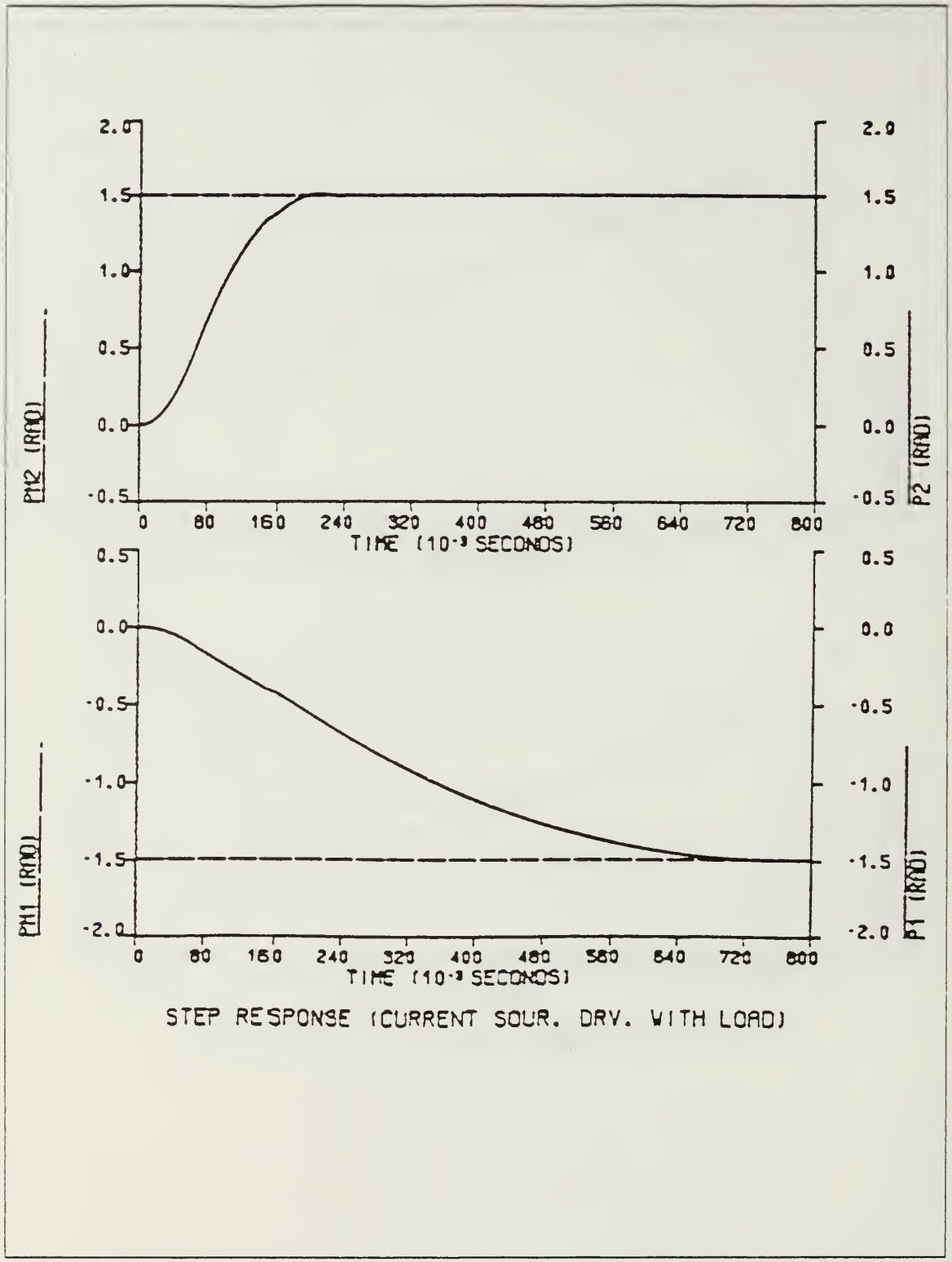

Figure 7.18 Step Response For Move #2 (No Gravity)
JOINT2 Servo Motor Curve Gain Constant Lowered to 0.5.

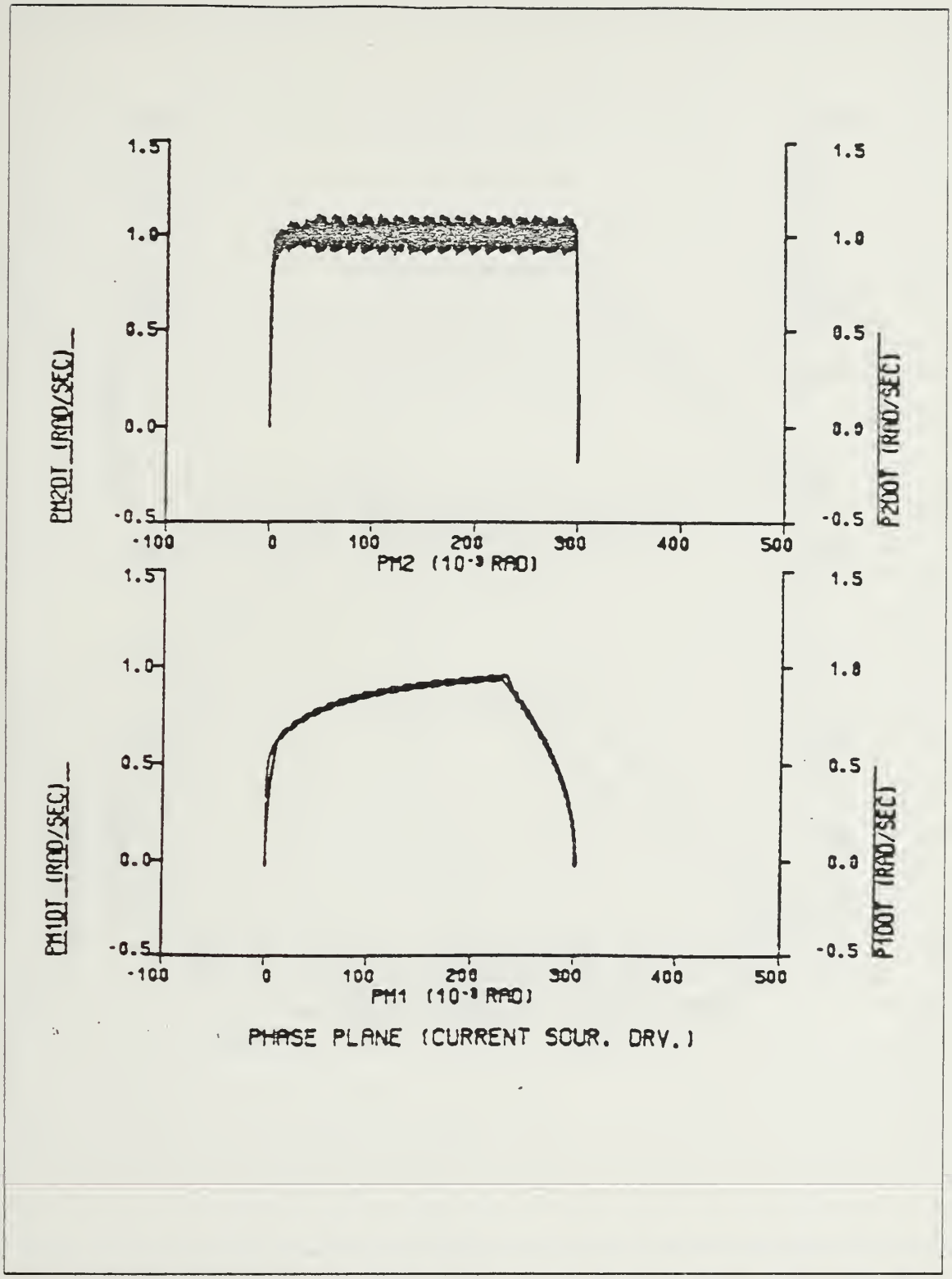

Figure 7.19 Phase Plane Trajectory For Ramp Input (No Gravity).

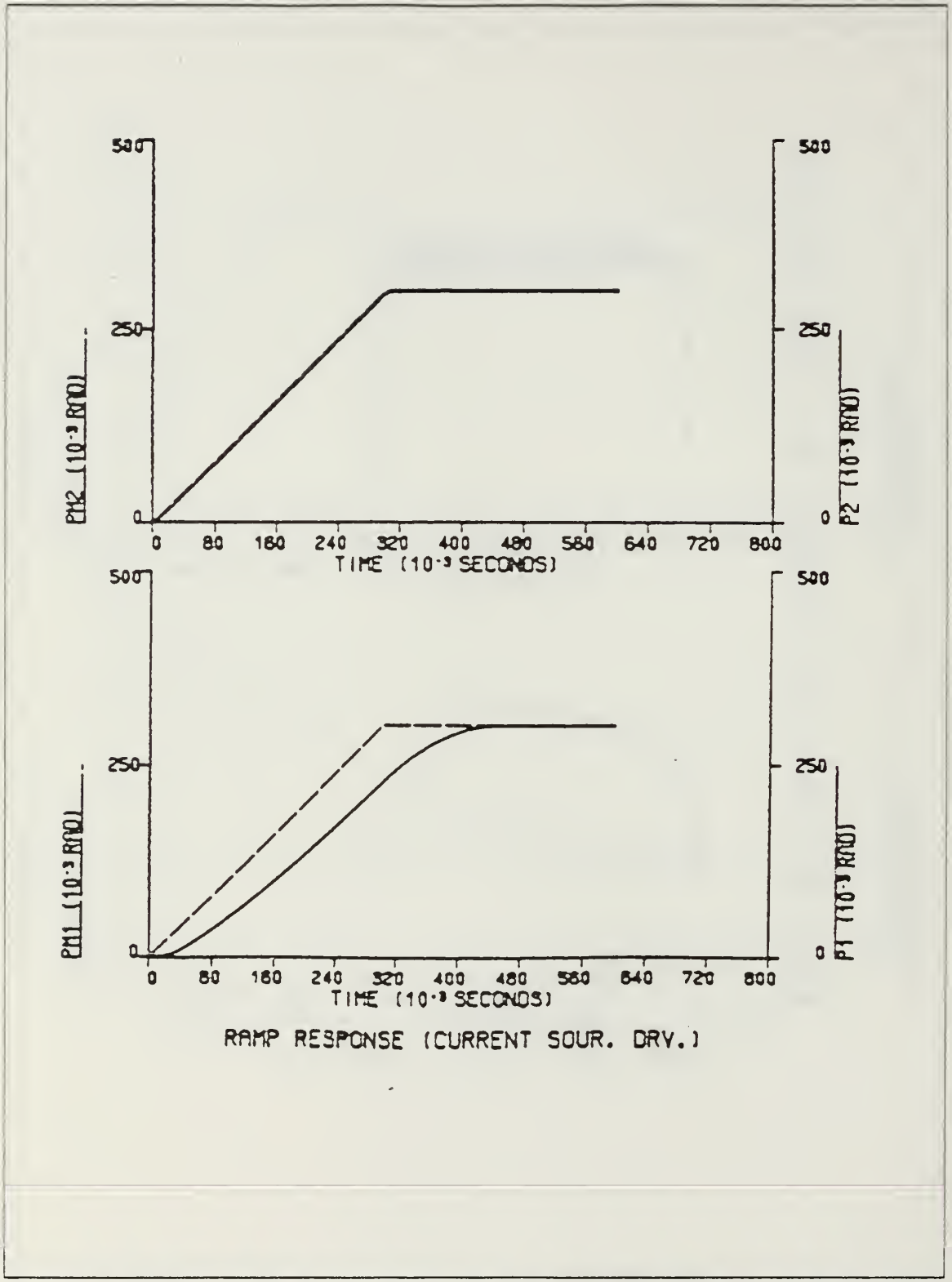

Figure 7.20 Ramp Response (No Gravity).

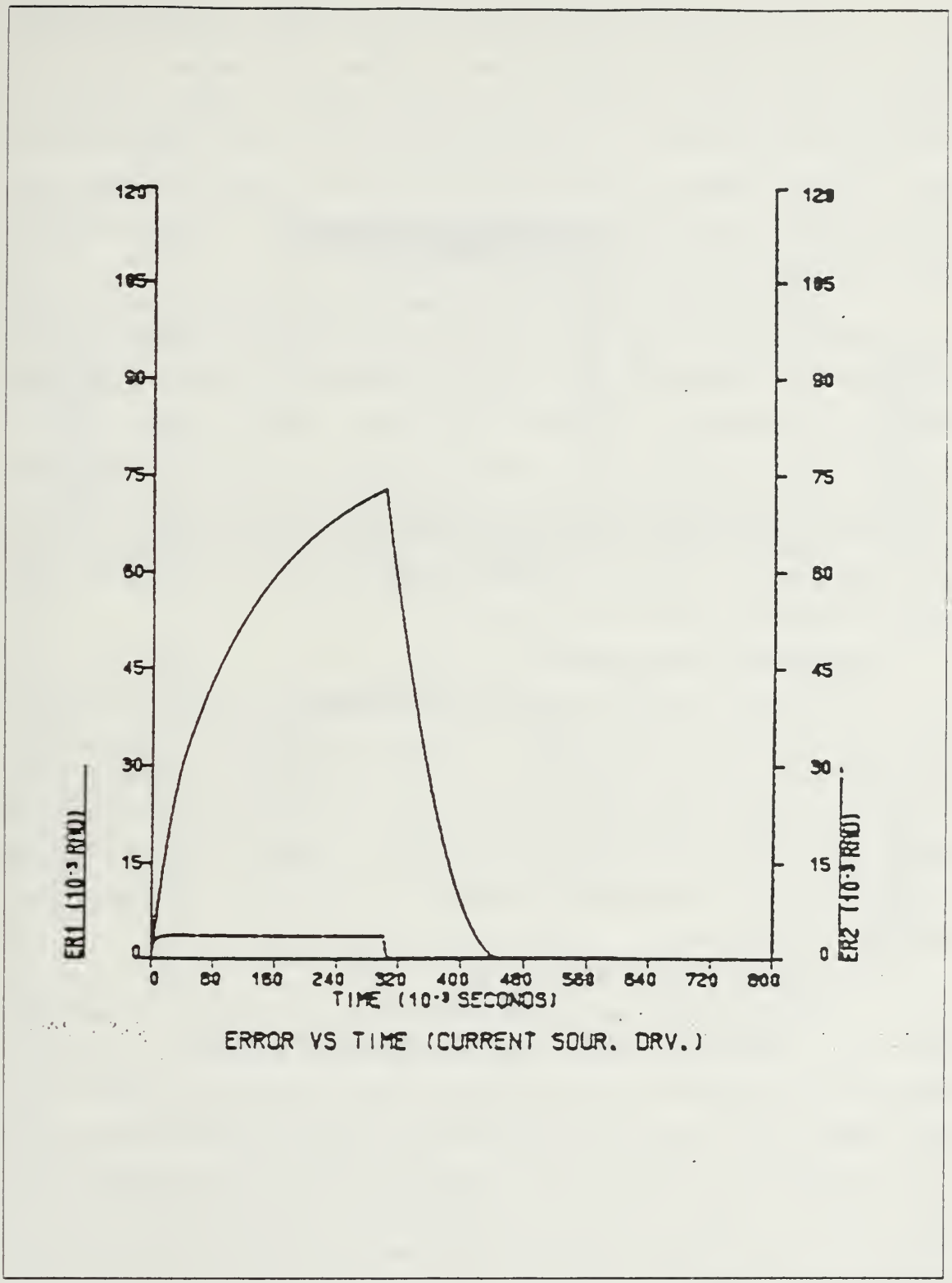

Figure 7.21 Error Between Commanded and Actual Position (No Gravity).

The second-order model and servo motor velocity of JOINT2 shudders around the curve until the desired position is reached. Large inertial torques and interaction torques prevent JOINT1 servo motor velocity to build up as fast as JOINT2 servo motor velotiey. It takes more time for JOINT1 servo motor velocity to reach steady-state velocity. Therefore, JOINT1 servo motor follows the ramp input with larger errors. Errors between commanded position input and actual position output of servo motor are shown in Figures 7.21 and 7.24.

Phase plane plots of simulation studies for sinusoidal input are shown in Figures 7.25 and 7.28. Good curve following capabilities are seen in phase plane trajectories. From Figures 7.26 and 7.29, it can be observed that JOINT2 servo motor follows the sinusoidal input easily while JOINT1 servo motor lags behind the sine input curve. The reasons for this we mentioned above in the case of a ramp input. Position errors for servo motors are shown in Figures 7.27 and 7.30. Again simulation studies show that the smaller the frequency of the sinusoidal position command input, the smaller the position error that is obtained. Also, for a fixed frequency, the smaller magnitude of input curve gives a smaller error.

2. **Gravitational Torques Included**

To simulate the adaptive system under gravitational torques, Moves #1, #2 and #3 were used. Again note that on all figures of phase plots, the second-order model velocity ($\dot{P}$) and servo motor velocity ($\dot{PM}$) are both plotted as ordinates versus servo motor angular position (PM). In time response curves, the second-order model angular position (PM) are both plotted as ordinates. In general, these curves fall on top of each other. In the simulation studies, both step and time varying position command input were used.

a. Step Position Command Input Used

Phase plane plots and step response curves for Move #1 are shown in Figures 7.31 - 7.34. In phase plane trajectories of Figures 7.31 and 7.33, it can be observed that gravitational torques and reaction torque produced by JOINT2 servo motor causes JOINT1 servo motor to move in the opposite direction of the move. Note that gravitational torques are at the maximum value at the beginning of the move. It takes a while to overcome the gravitational and reaction torques, after that the JOINT1 servo motor stars accelerating until it catches and follows the curve till the desired position is reached.

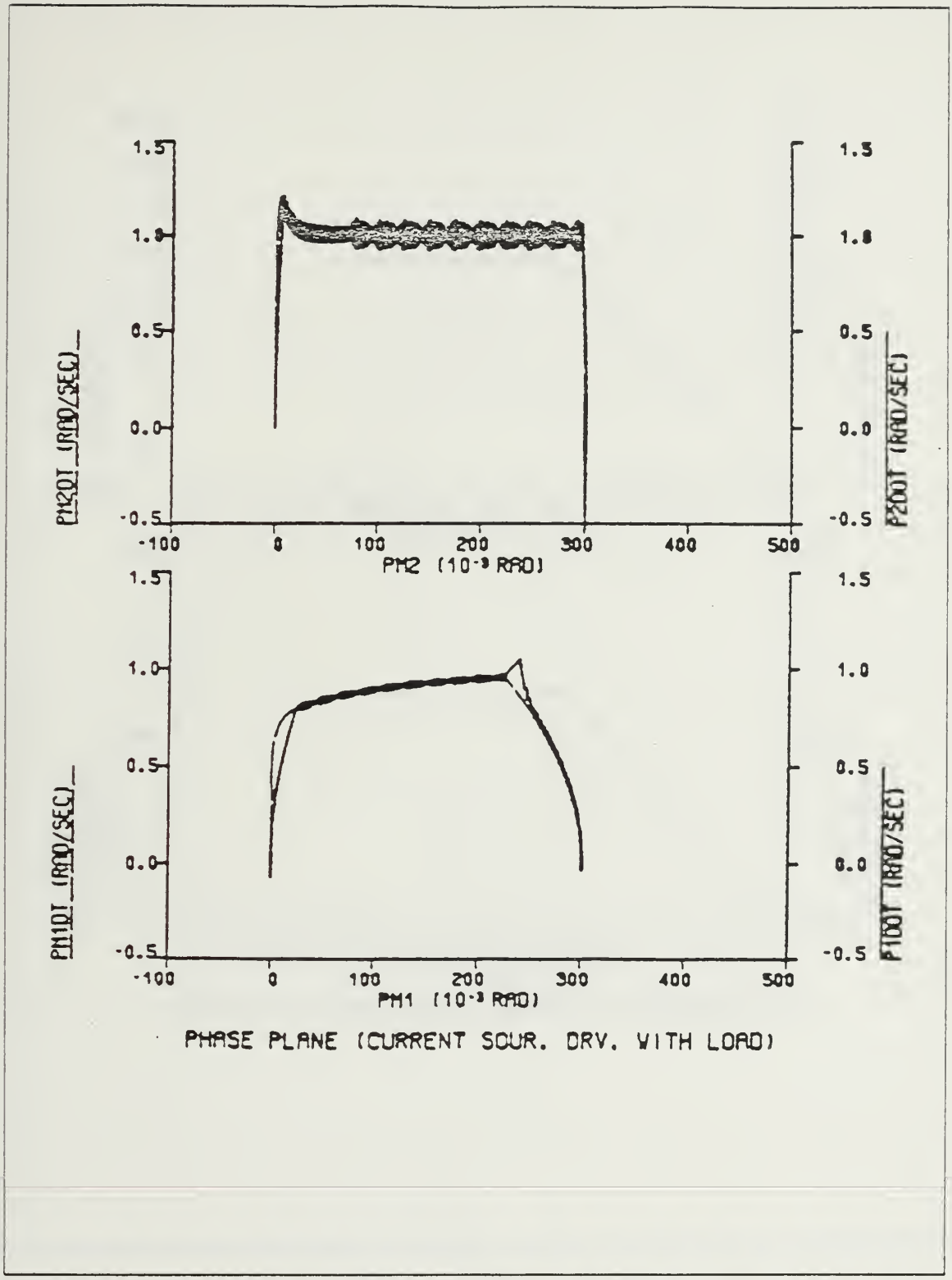

Figure 7.22 Phase Plane Trajectory For Ramp Input (No Gravity - Loaded Arm).

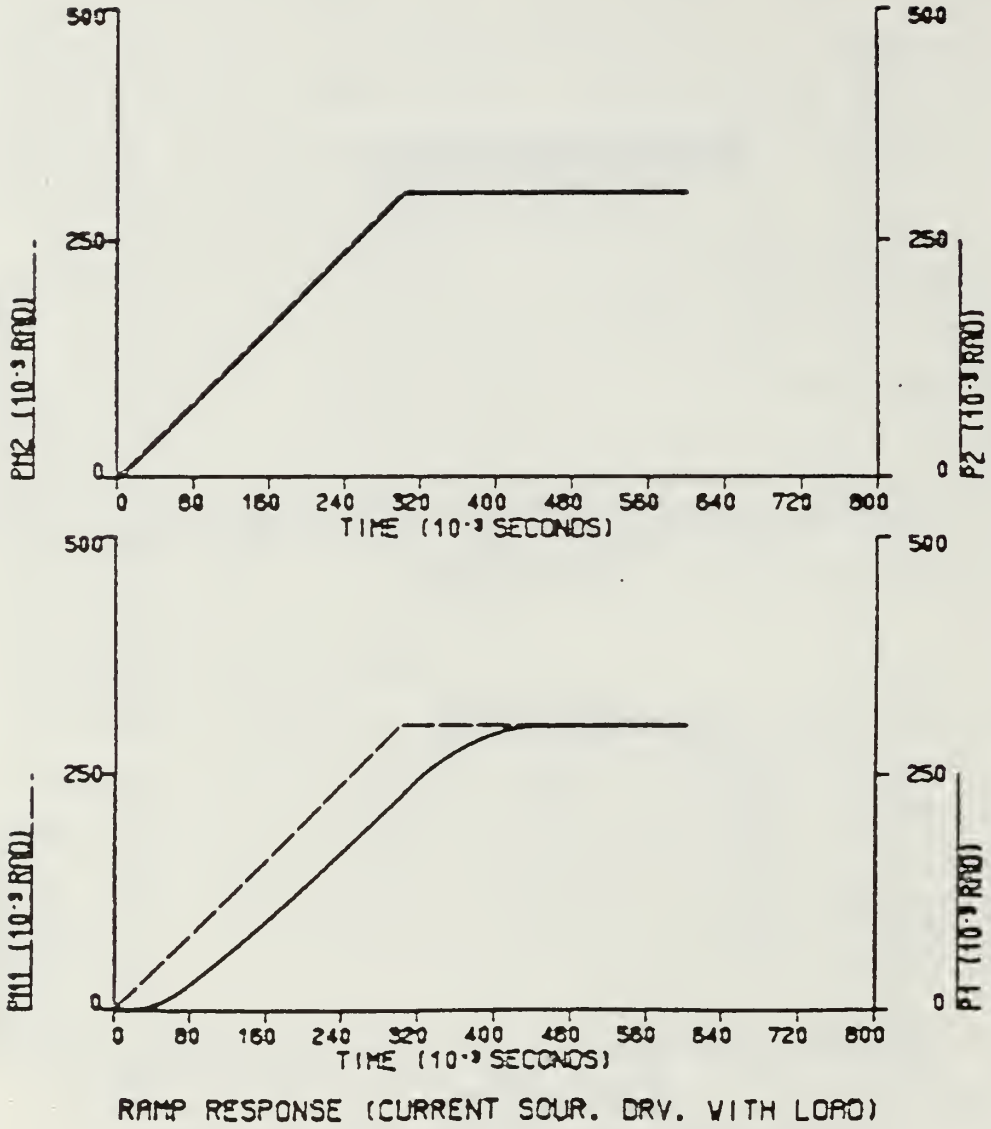

Figure 7.23 Ramp Response (No Gravity - Loaded Arm).

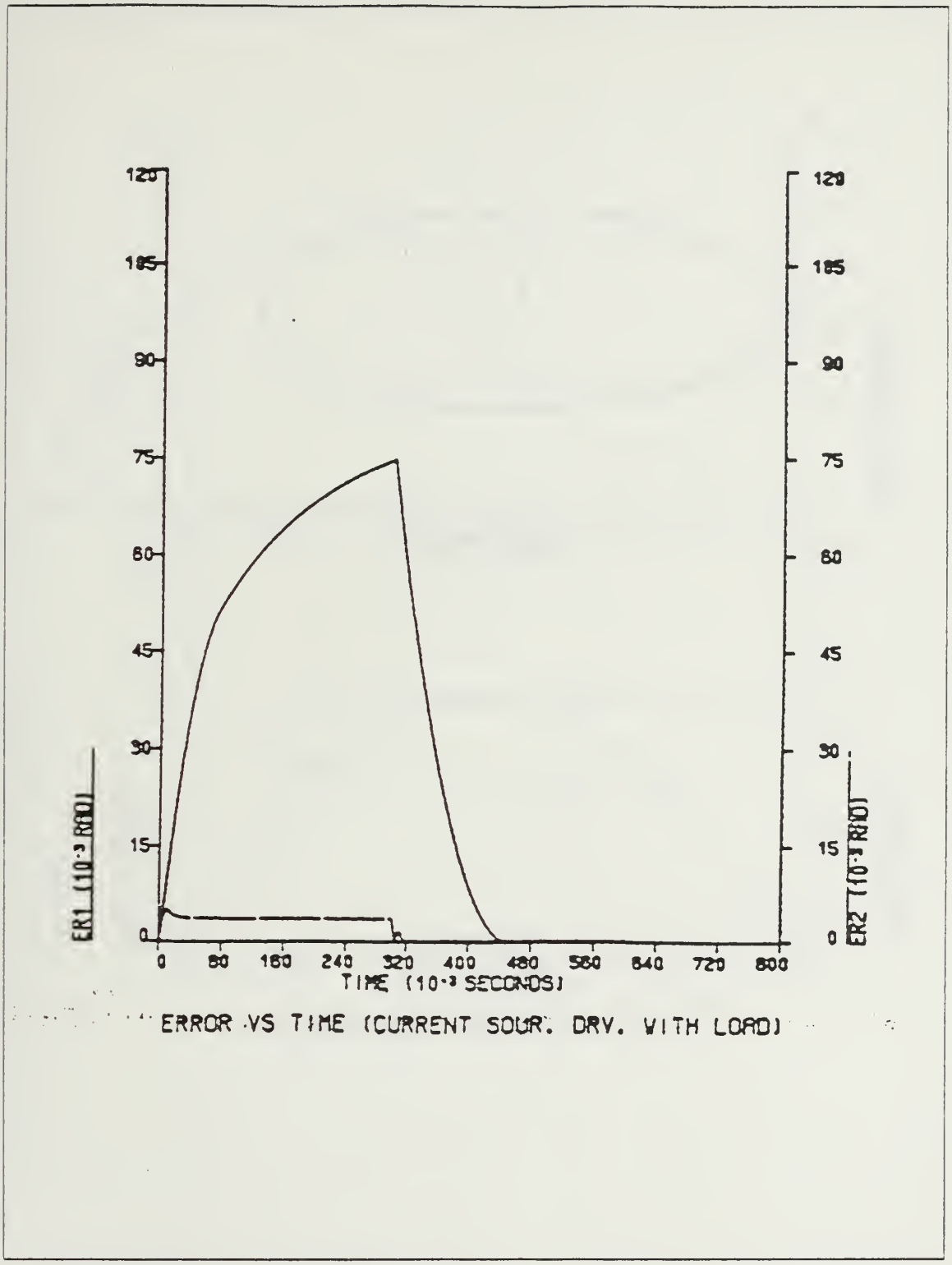

Figure 7.24 Error Between Commanded and Actual Position (No Gravity - Loaded Arm).

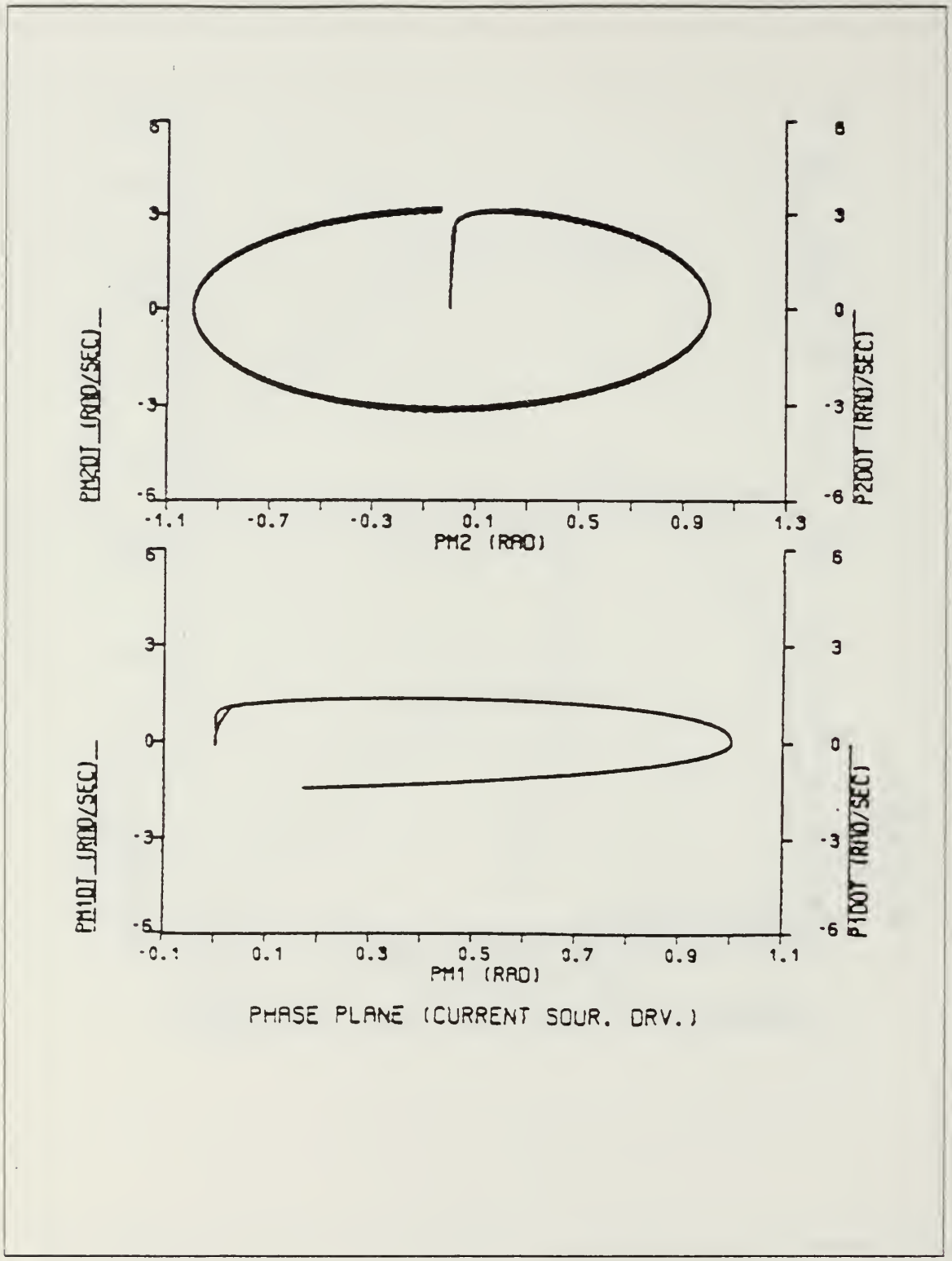

Figure 7.25 Phase Plane Trajectory For Sinusoidal Input (No Gravity).

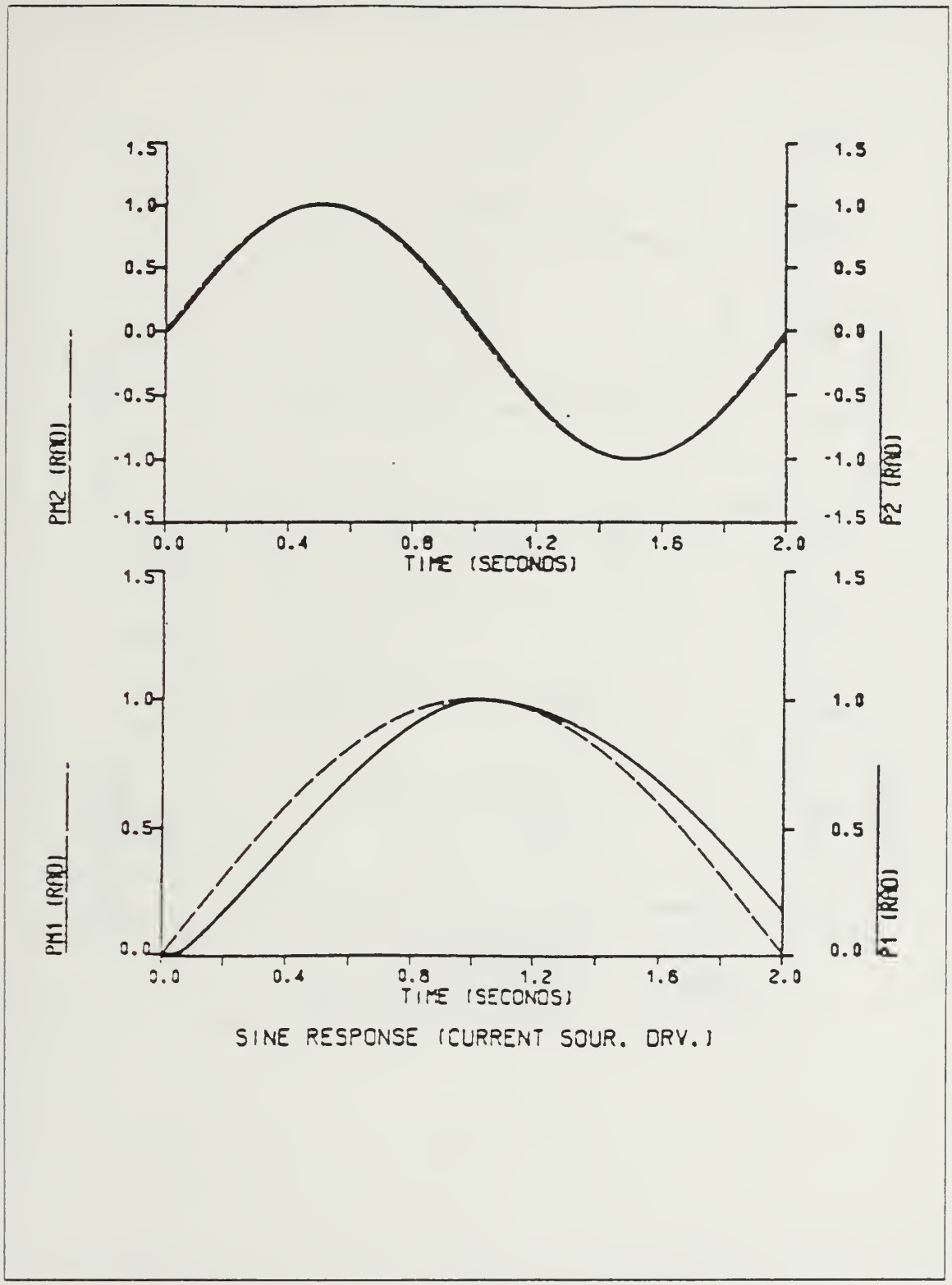

Figure 7.26 Sine Response (No Gravity).

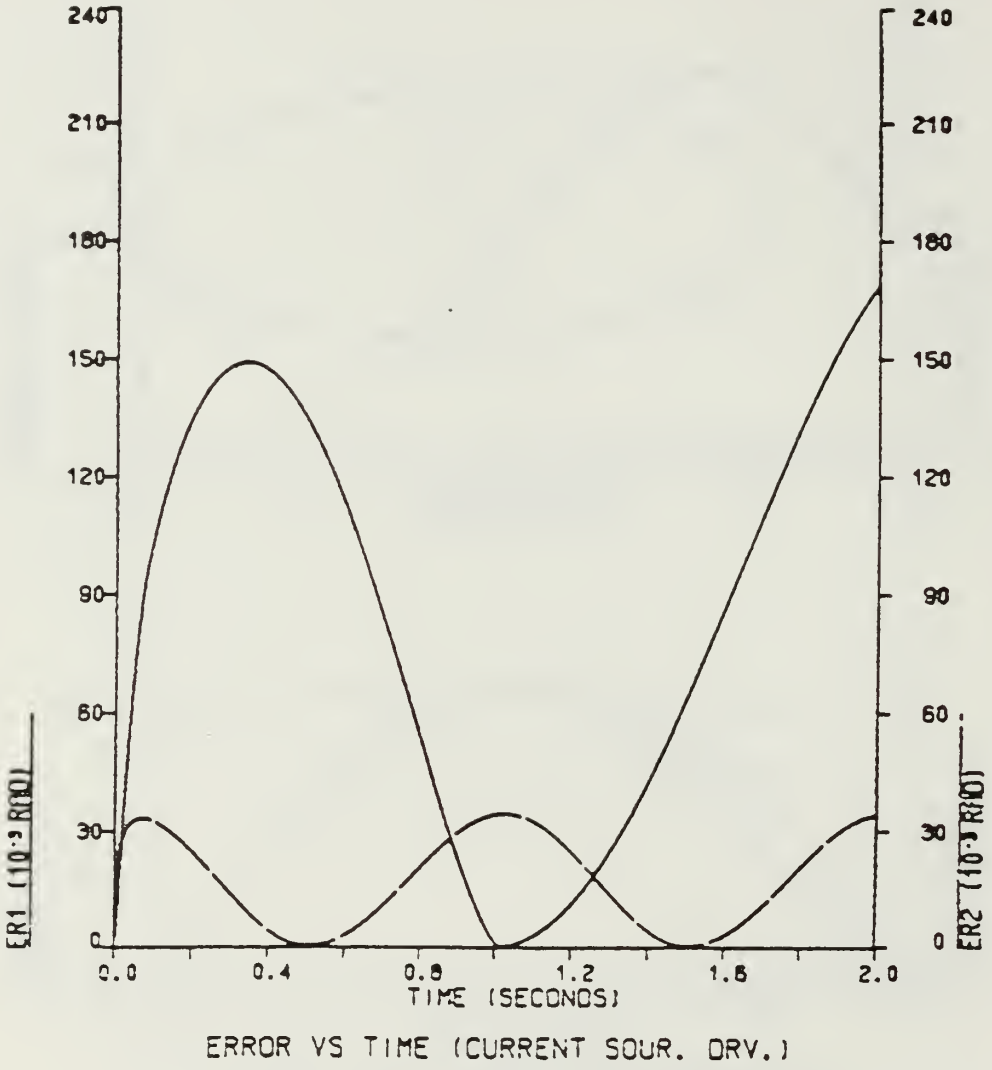

Figure 7.27 Error Between Commanded and Actual Position (No Gravity).

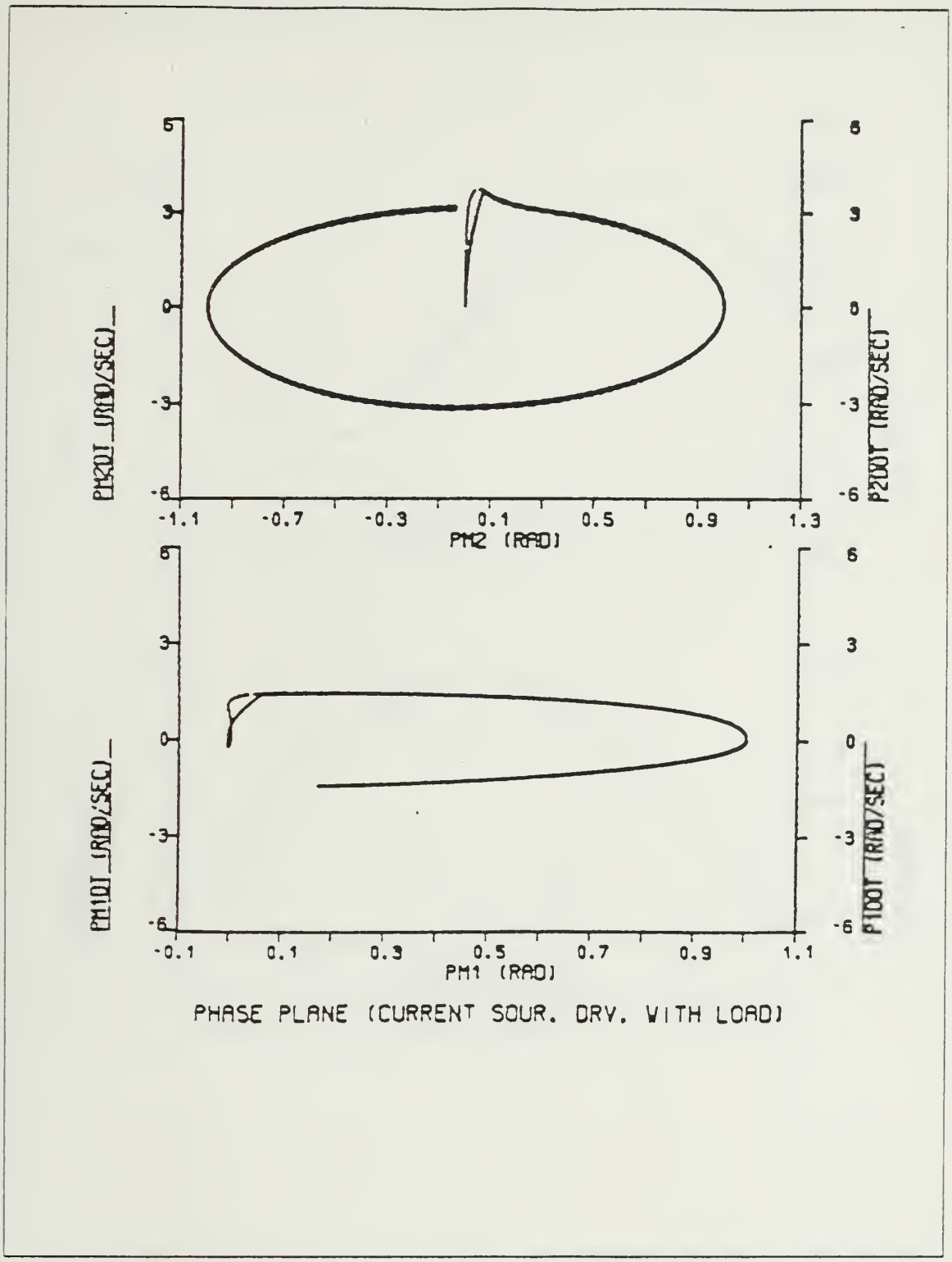

Figure 7.28 Phase Plane Trajectory For Sinusoidal Input (No Gravity - Loaded Arm).

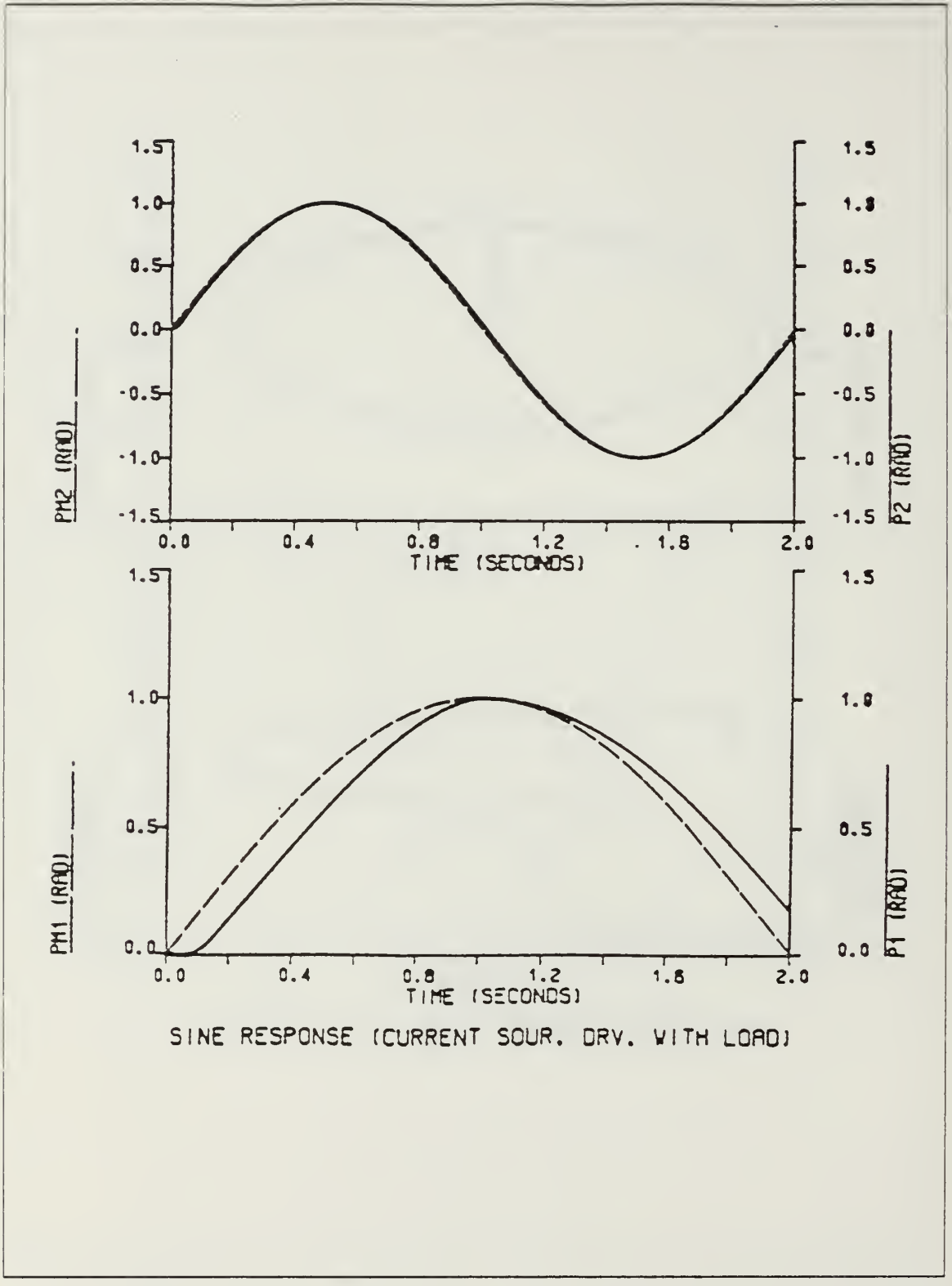

Figure 7.29 Sine Response (No Gravity - Loaded Arm).

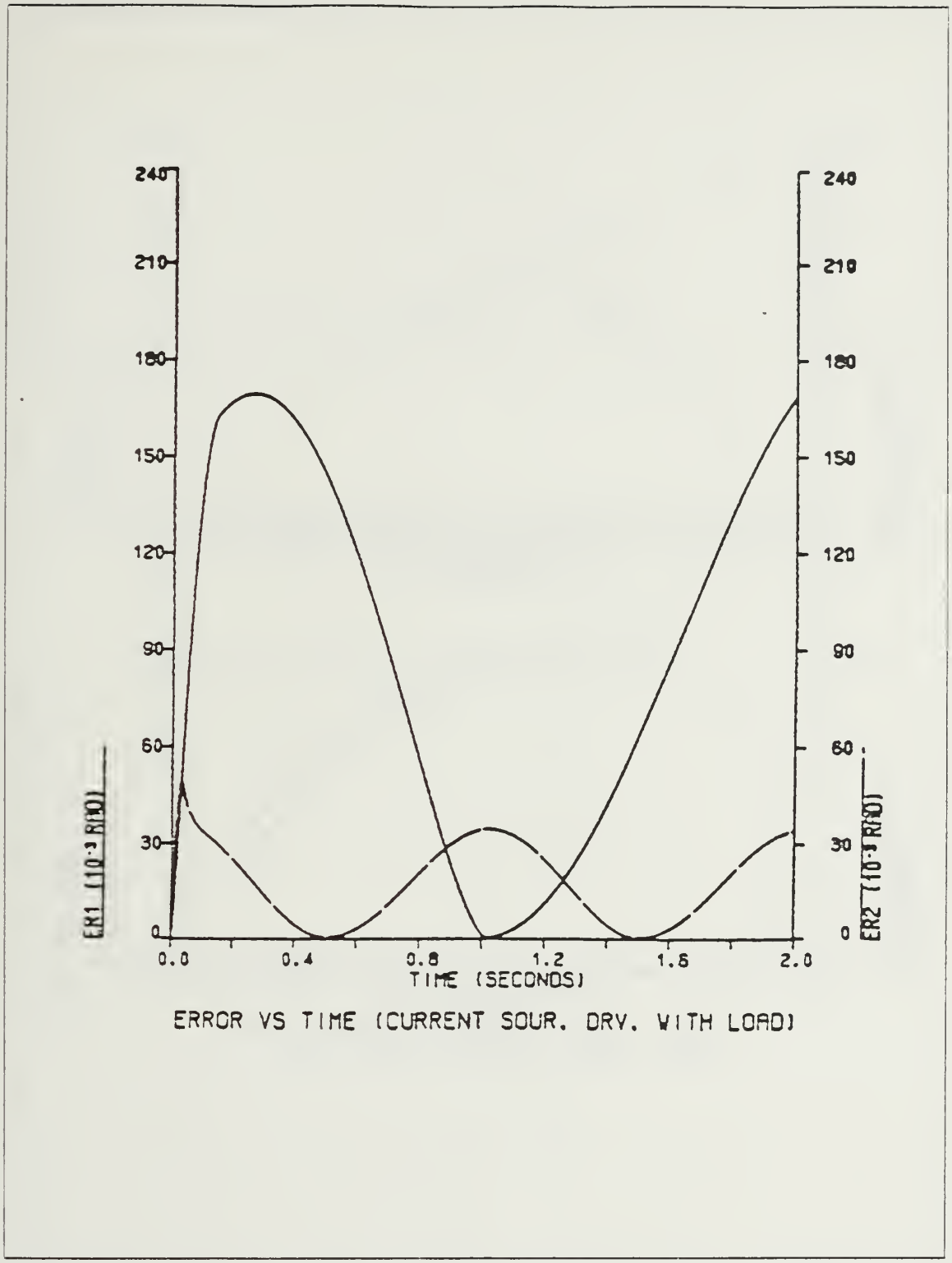

Figure 7.30 Error Between Commanded and Actual Position (No Gravity - Loaded Arm).

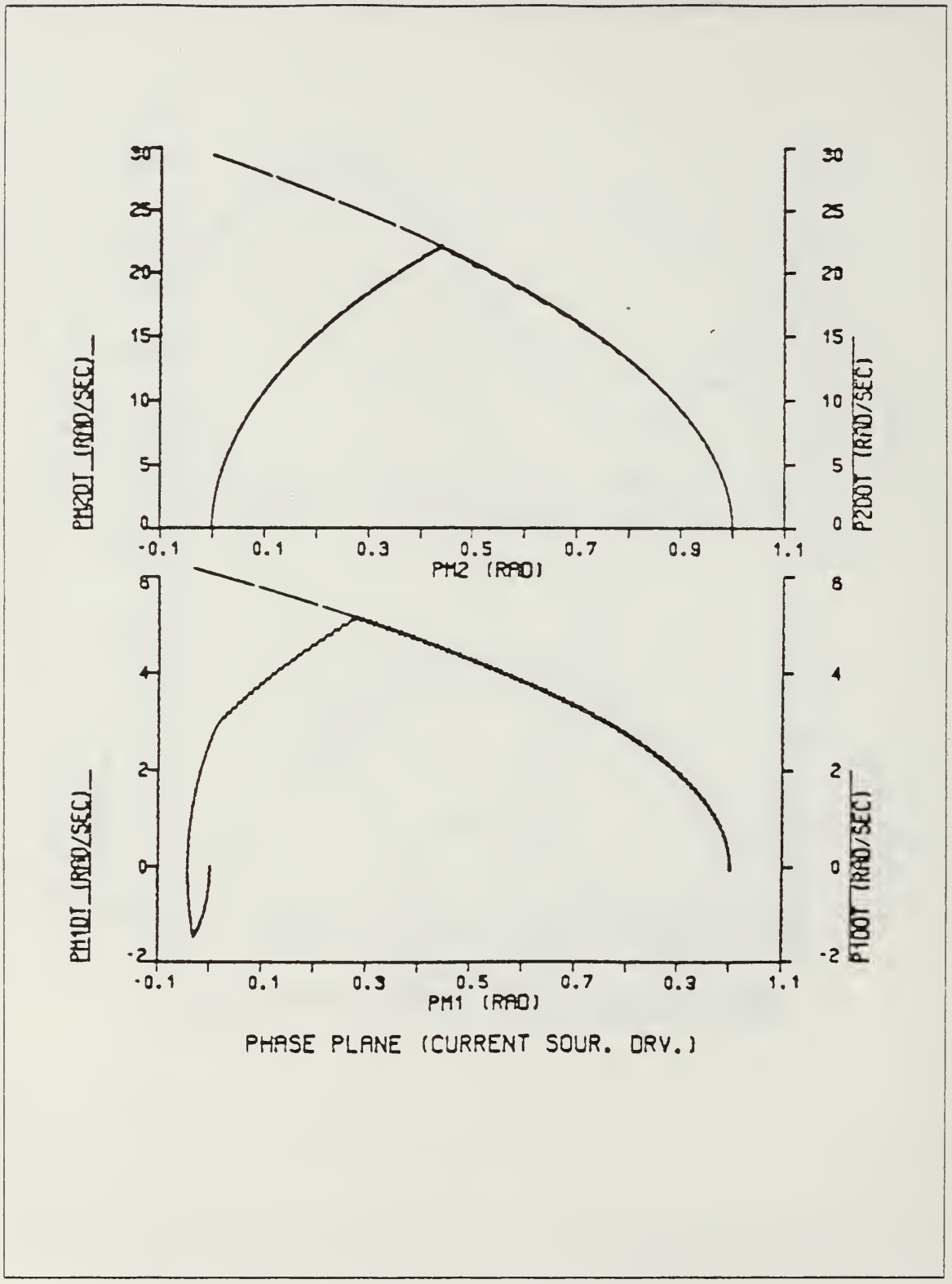

Figure 7.31 Phase Plane Trajectory For Move #1 (With Gravity).

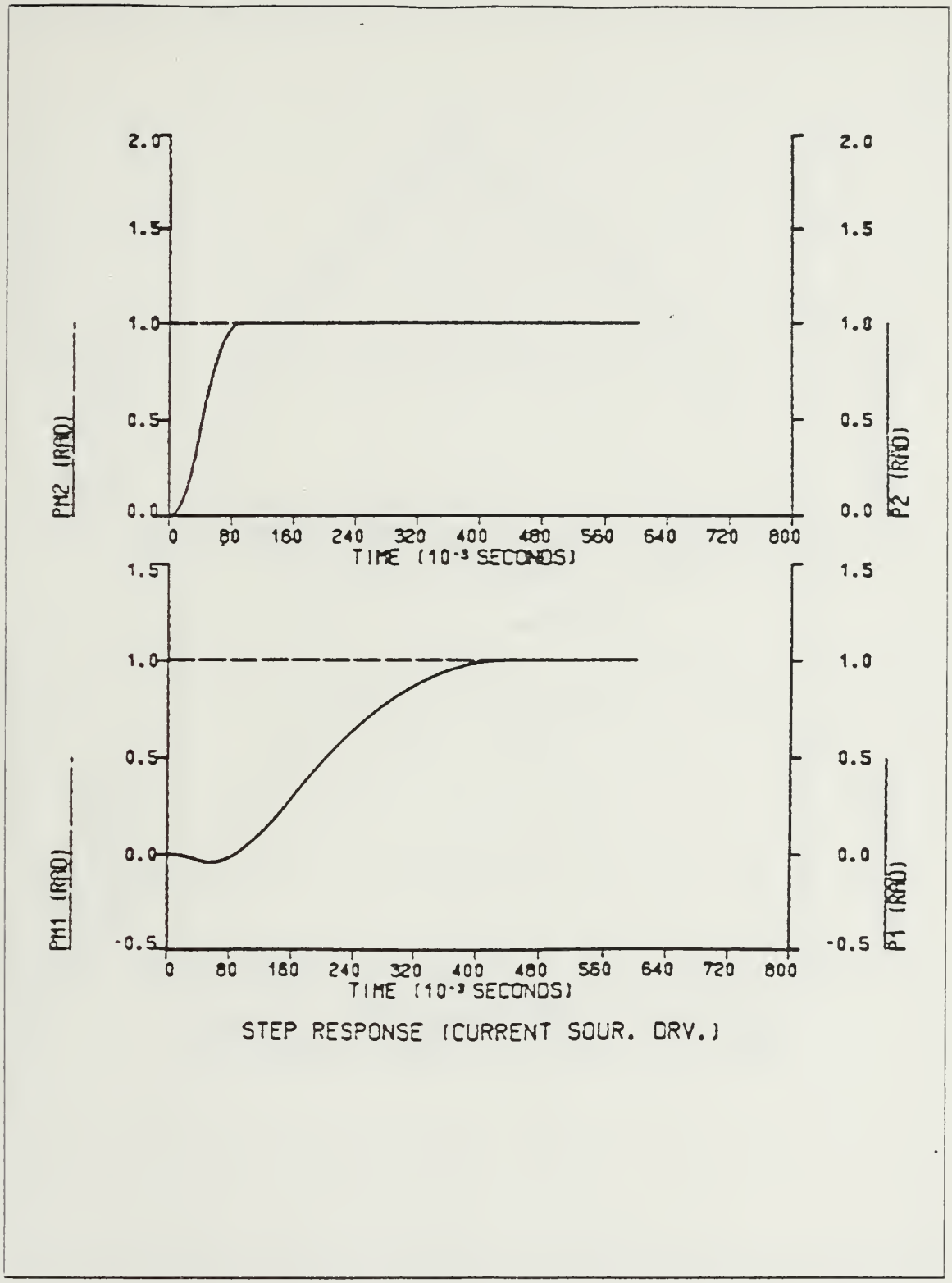

Figure 7.32 Step Response For Move #1 (With Gravity).

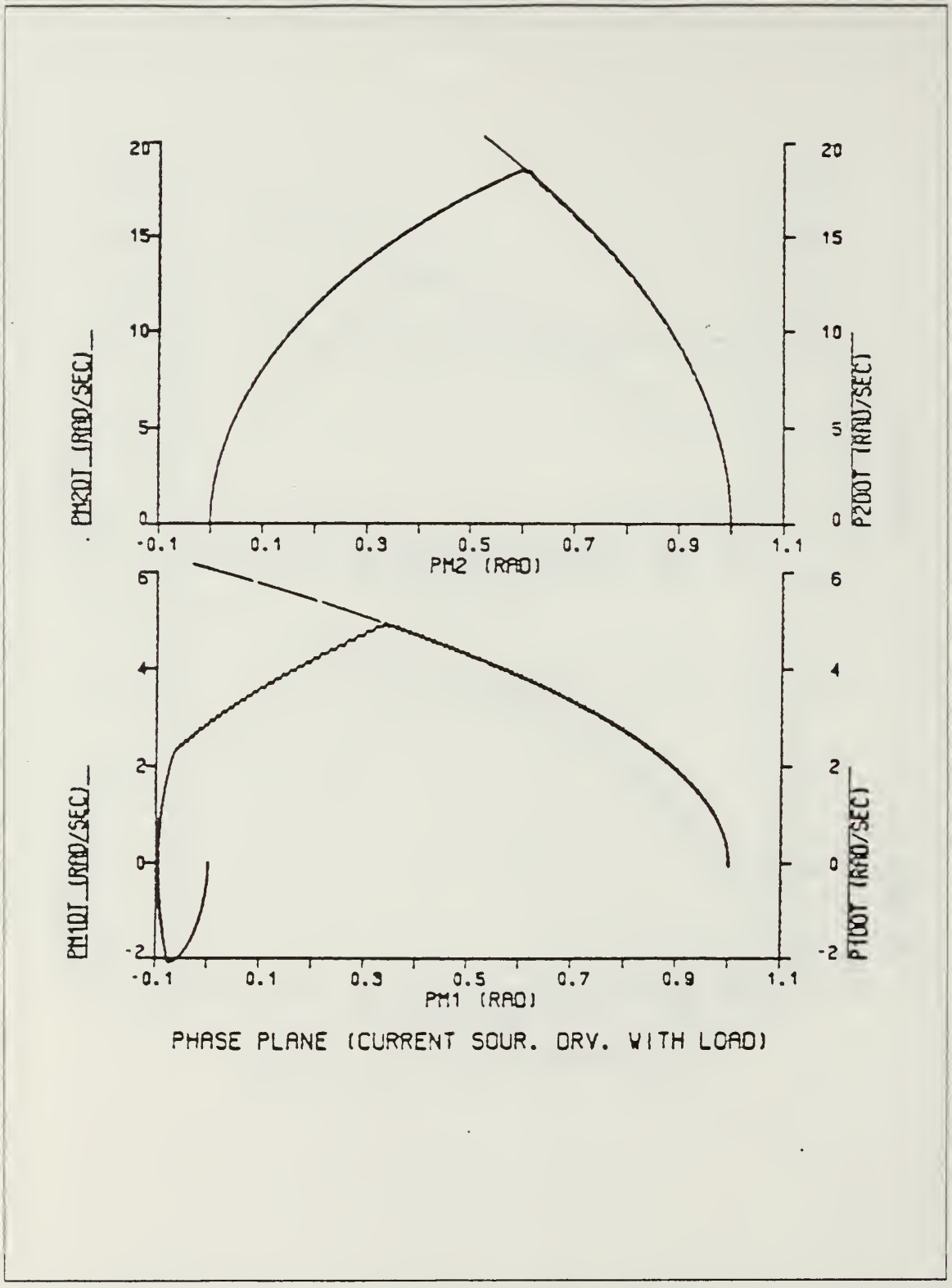

Figure 7.33 Phase Plane Trajectory For Move #1 (With Gravity).

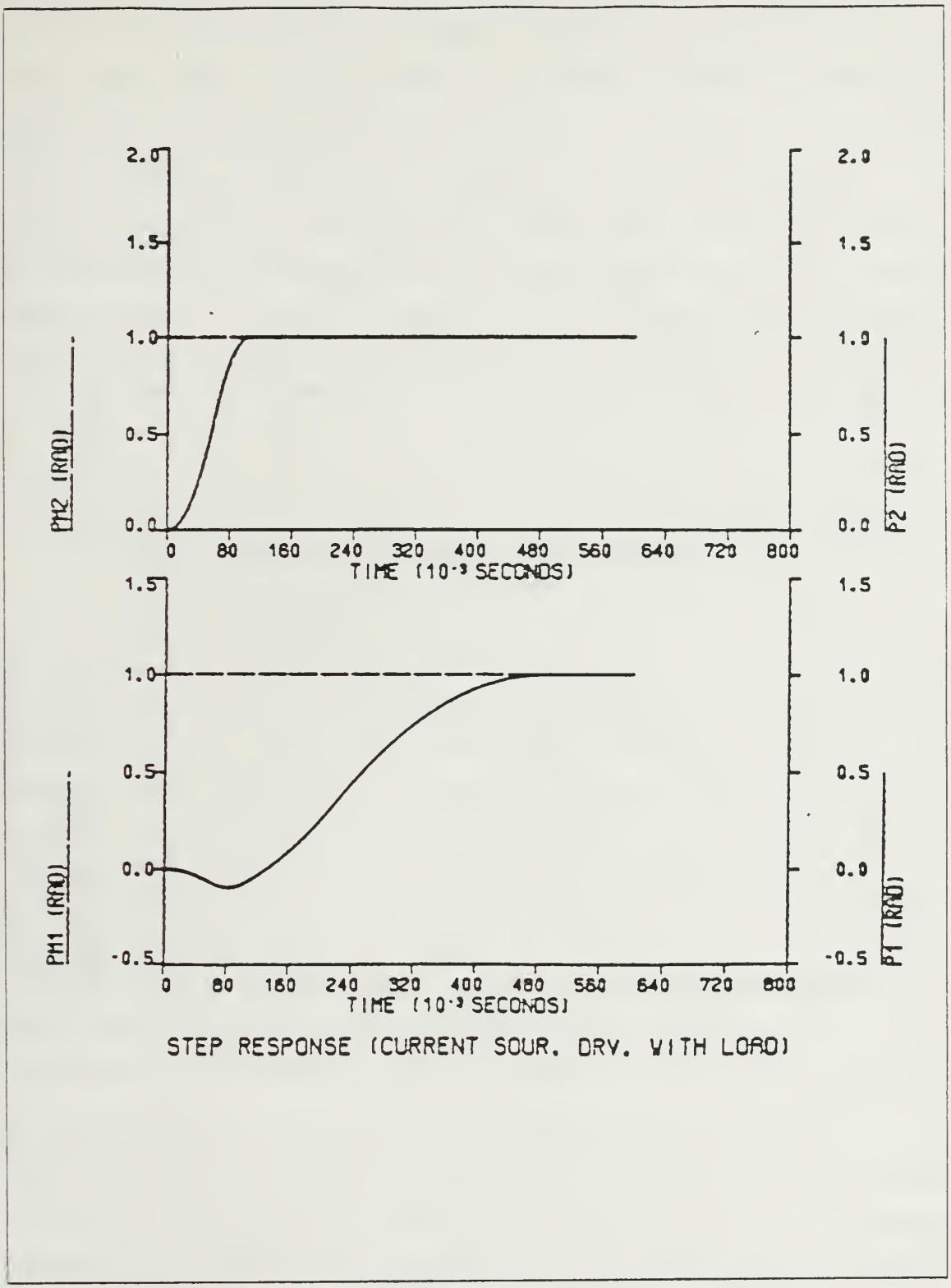

Figure 7.34 Step Response For Move #1 (With Gravity).

The phase plane plot for loaded arm (Figure 7.33) shows that the magnitude of the negative velocity was increased for JOINT1 servo motor. When JOINT2 servo motor catches, the curve starts deceleration, JOINT1 servo motor velocity starts increasing very rapidly until JOINT2 servo motor reaches the steady-state. If we think that the opposite movement of the JOINT1 servo motor has to be avoided, then a different input sequence may be used to accomplish this. For this purpose, JOINT2 servo position command input was delayed 200 milliseconds at the beginning. Simulation results are shown in Figures 7.35 and 7.36. From phase plane trajectories, it can be observed that JOINT1 servo motor can start accelerating without going in the wrong direction while JOINT2 servo motor stands still. A zig-zag shape is seen in JOINT1 servo motor trajectory due to the reaction torque produced by JOINT2 servo motor after it starts accelerating. Also, from step response (Figure 7.36), 10% overshoot is observed for JOINT2 servo motor due to the reaction torque produced by JOINT1 servo motor. The same overall time response was obtained.

Simulation results for Move #2 under simultaneous applied inputs, are shown in Figures 7.37 - 7.40. Phase plane trajectories (Figure 7.37) show that both second-order model and servo motor have good curve following capabilities with maximum velocities of 6.5 rad/sec and 27.6 rad/sec for the loaded arm. Figure 7.39 show that JOINT2 servo motor reaches steady-state after it overshoots twice and undershoots once. This is clearer in step response curves of Figures 7.40. A different input sequence was used to avoid the JOINT2 servo motor overshoot. Therefore, JOINT2 servo motor position command input was delayed 100 milliseconds. The purpose of this delay is to minimize the effect of the reaction torque produced by JOINT1 servo motor on JOINT2 servo motor. With delayed input JOINT2 servo motor reaches steady-state without overshoot, while JOINT1 servo motor decelerates. This deceleration provides additional braking torque on the JOINT2 servo motor. Simulation results are shown in Figures 7.41 - 7.44. The same overall time response was obtained.

Move #3 was used for additional testing of the system under different loading conditions. Simulation results are shown in Figures 7.45 - 7.48. Phase plane trajectories show that, at the beginning of the move, the reaction torque produced by acceleration of JOINT2 servo motor prevents JOINT1 servo motor from accelerating for a while. On the contrary the reaction torques do not work in favor of the servo motors for Move #3.

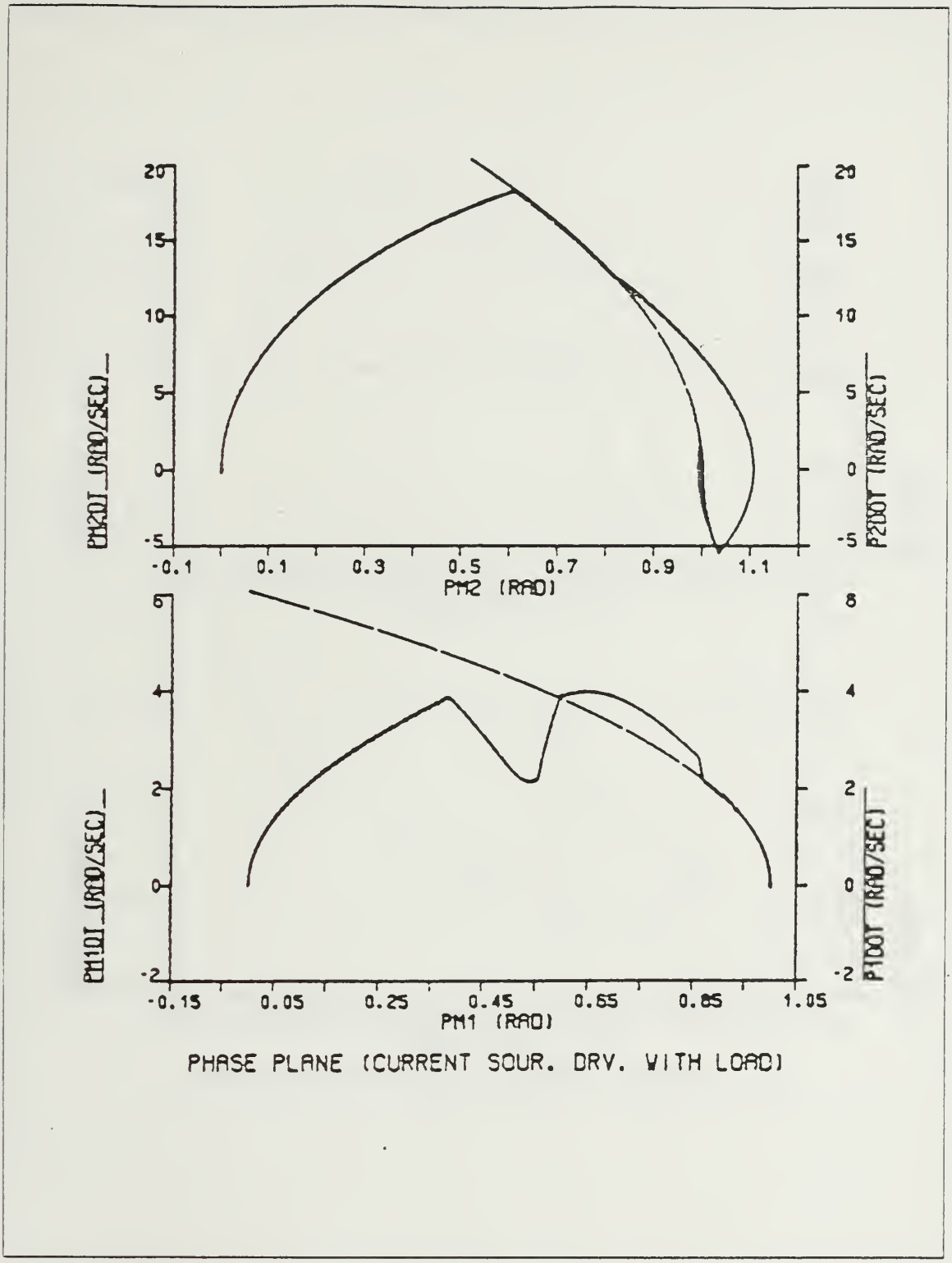

Figure 7.35 Phase Plane Trajectory For Move #1 (With Gravity)
JOINT2 Servo Motor Input Delayed 0.20 sec..

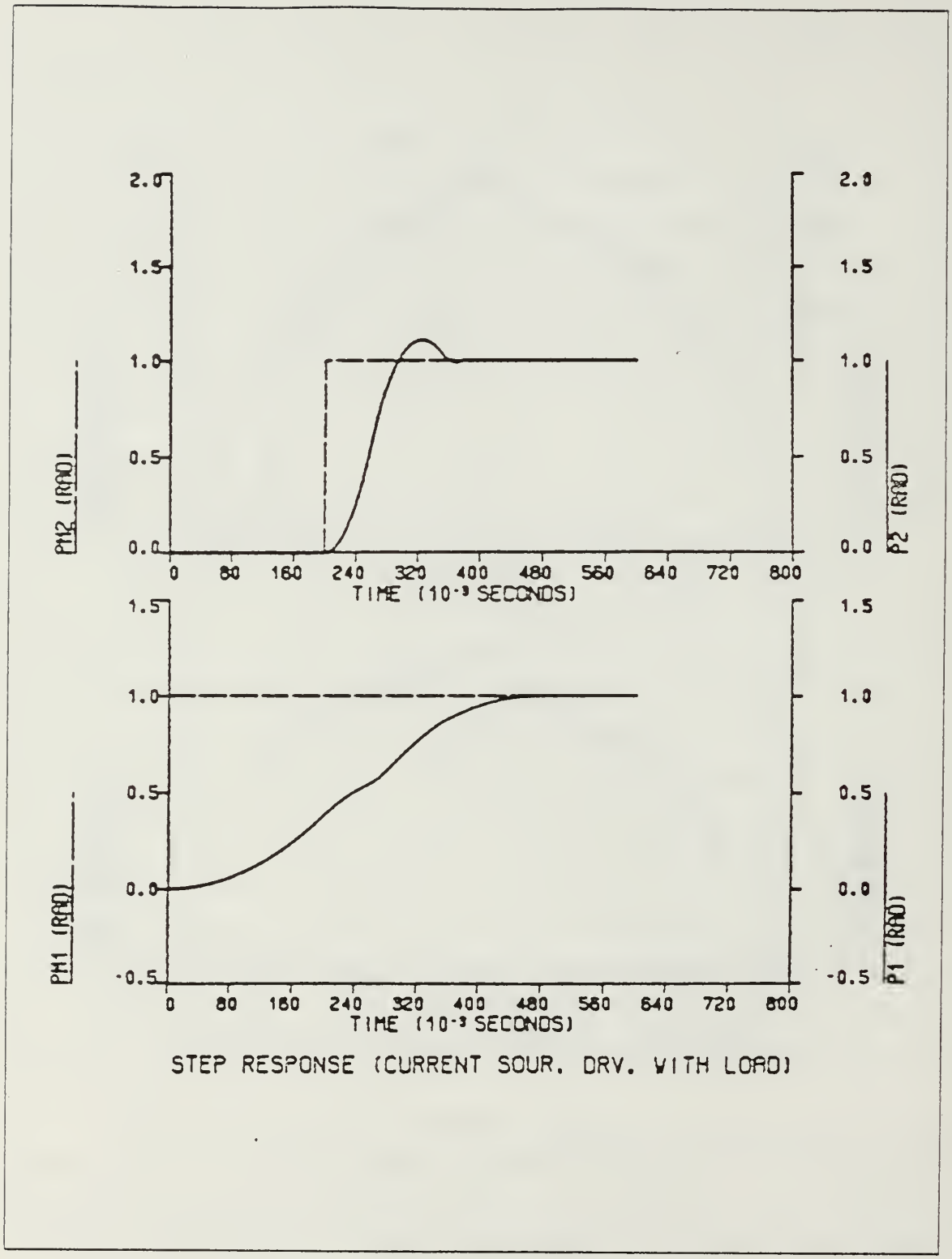

Figure 7.36 Step Response For Move #1 (With Gravity)
JOINT2 Servo Motor Input Delayed 0.20 sec..

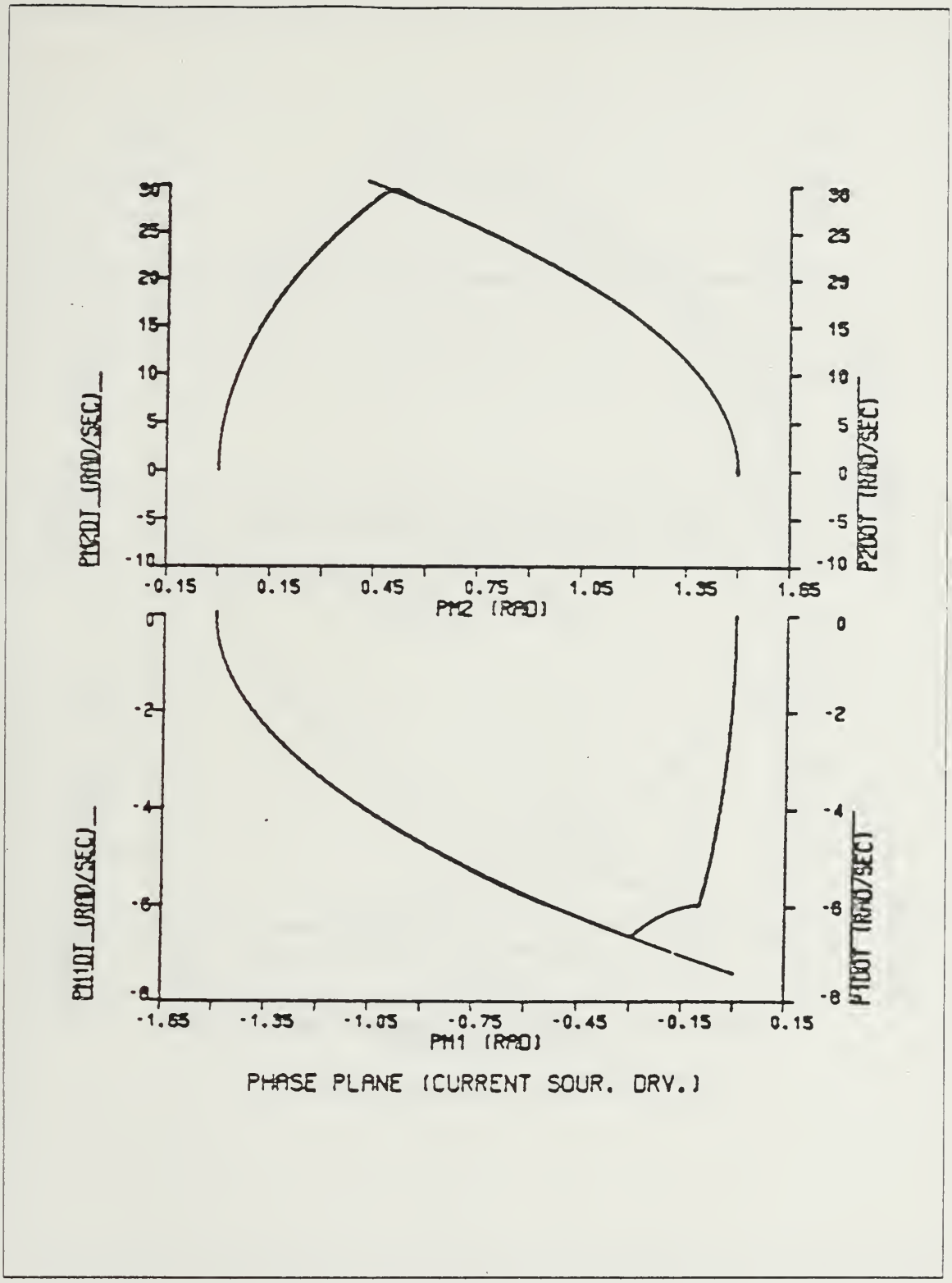

Figure 7.37 Phase Plane Trajectory For Move #2 (With Gravity).

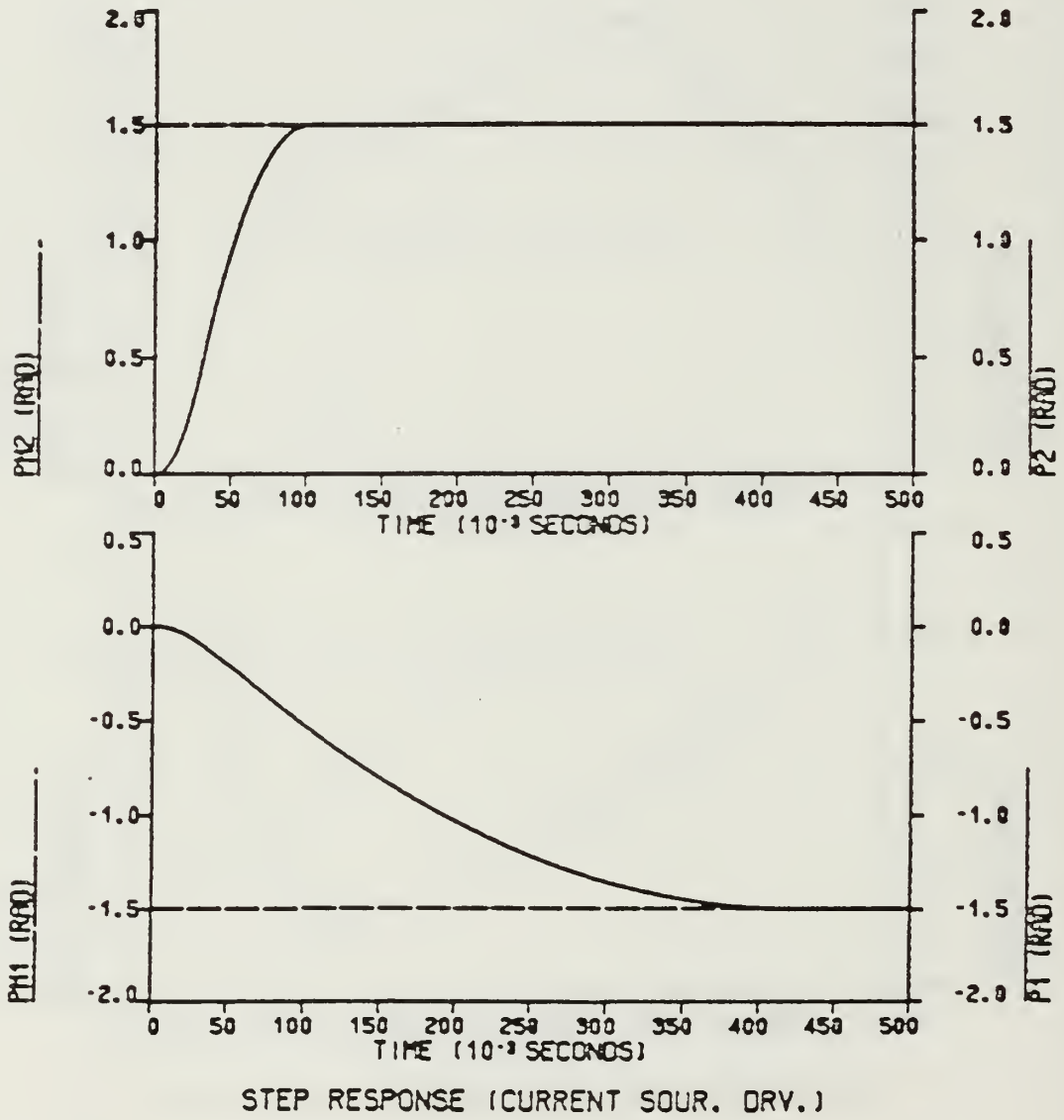

Figure 7.38 Step Response For Move #2 (With Gravity).

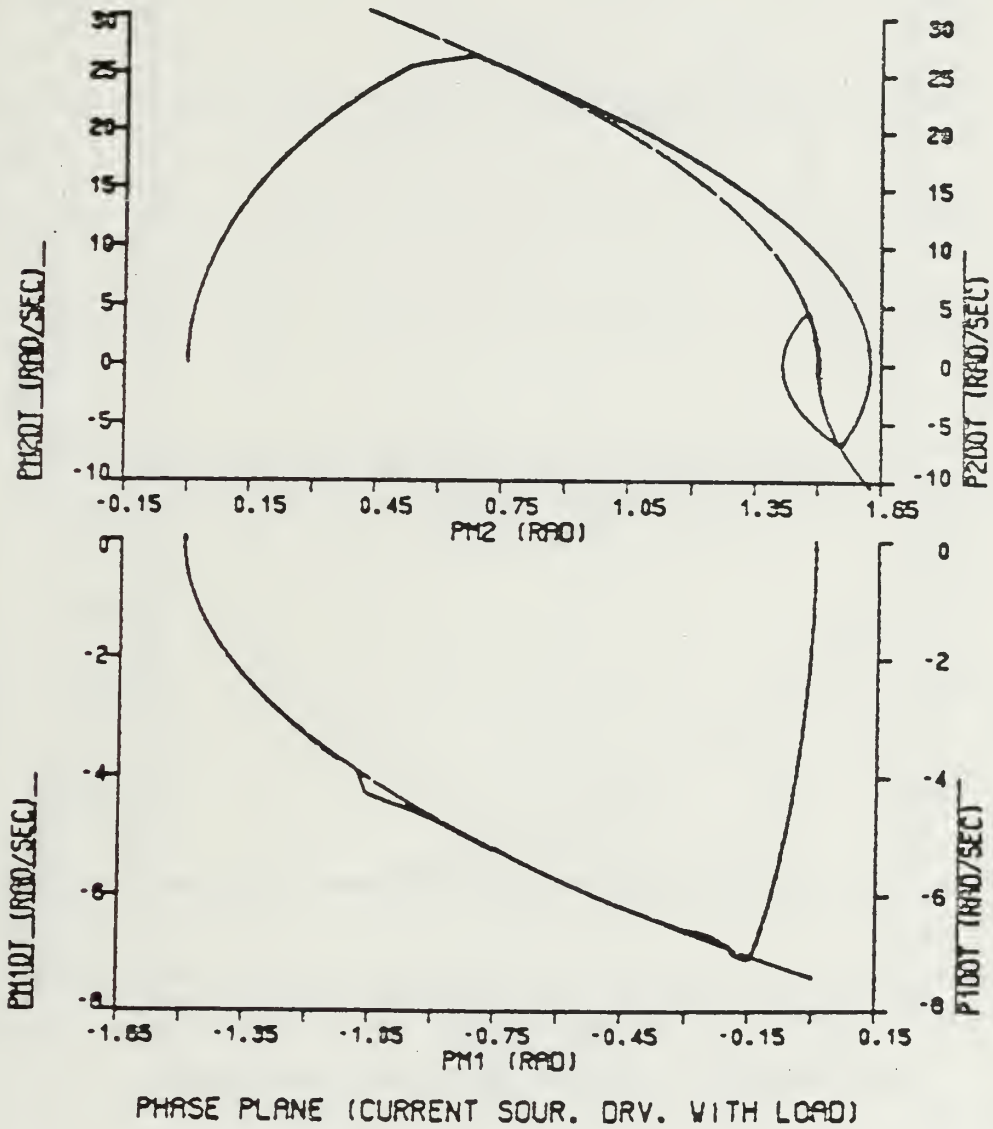

Figure 7.39 Phase Plane Trajectory For Move #2
(With Gravity - Loaded Arm).

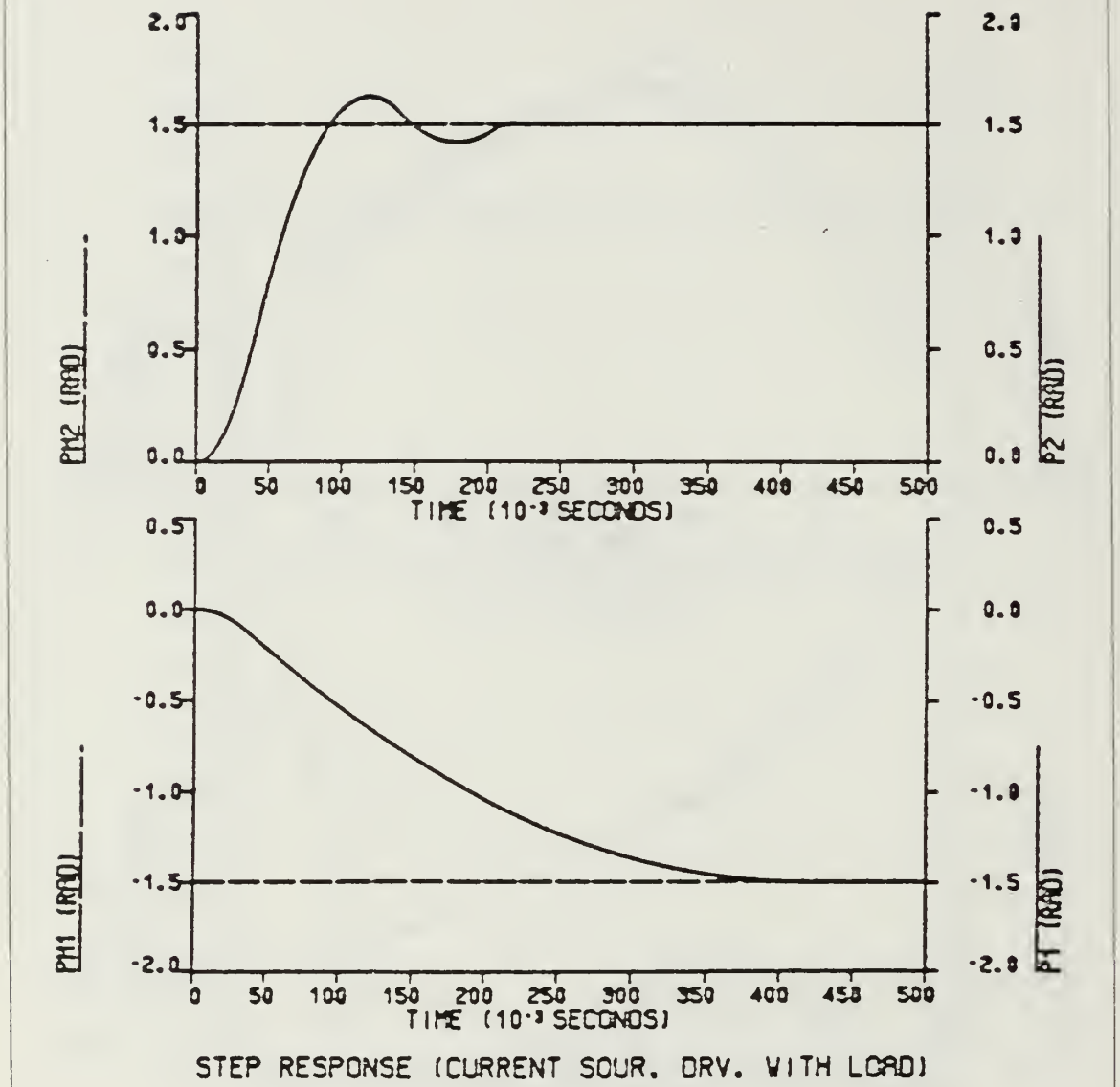

Figure 7.40 Step Response For Move #2
(With Gravity - Loaded Arm).

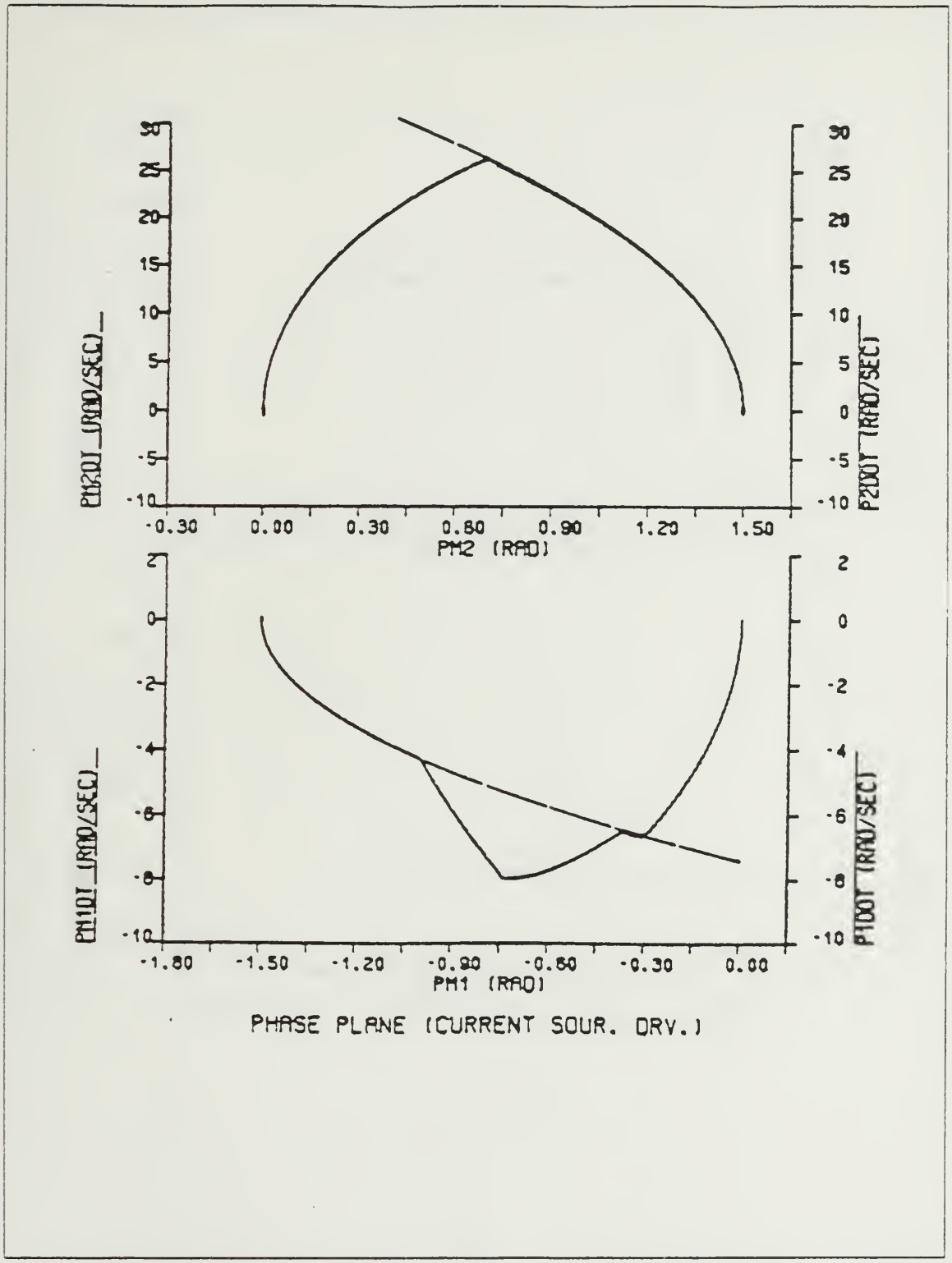

Figure 7.41 Phase Plane Trajectory For Move #2 (With Gravity) JOINT2 Servo Motor Input Delayed 0.10 sec..

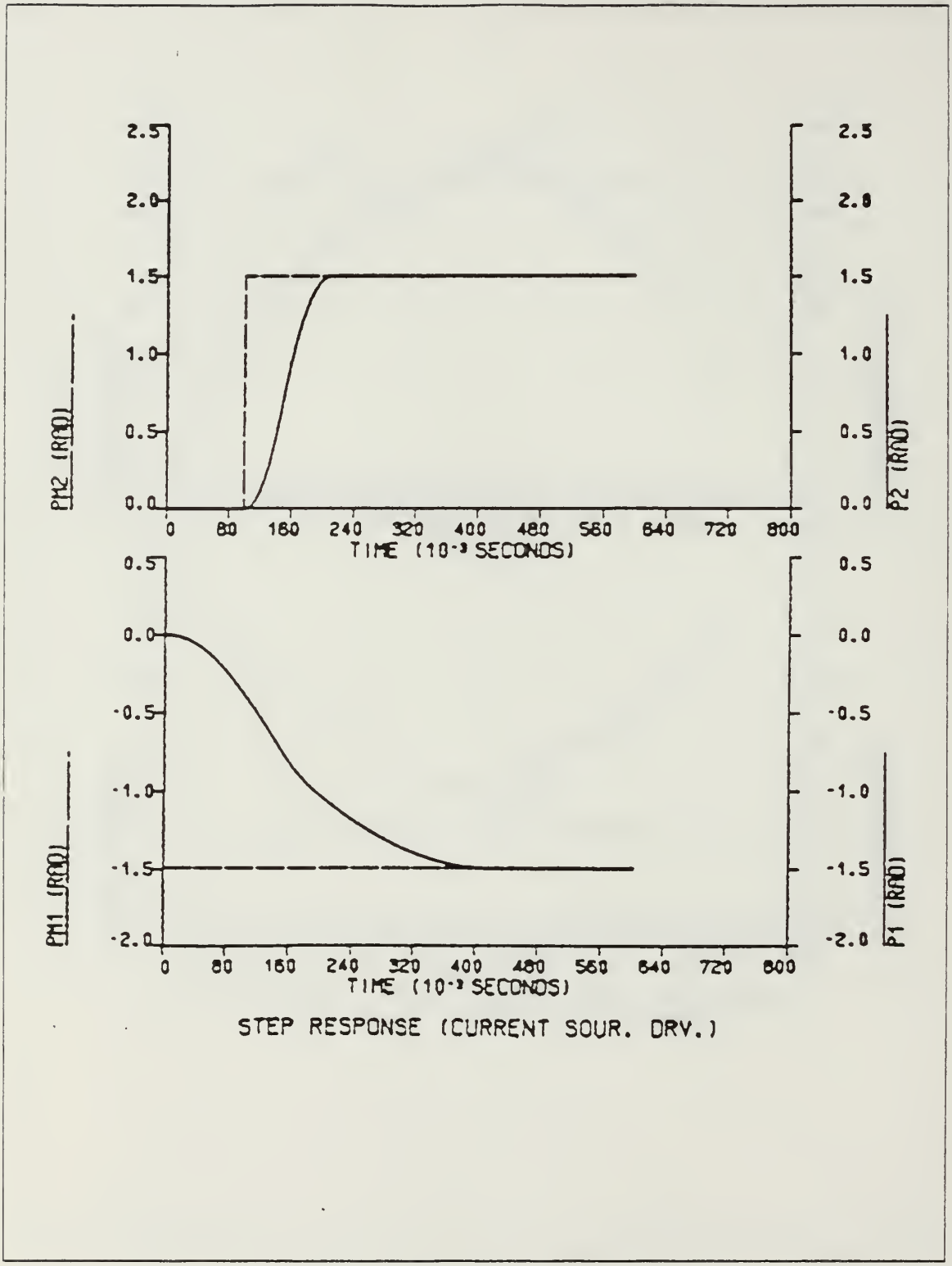

Figure 7.42 Step Response For Move #2 (With Gravity)
JOINT2 Servo Motor Input Delayed 0.10 sec..

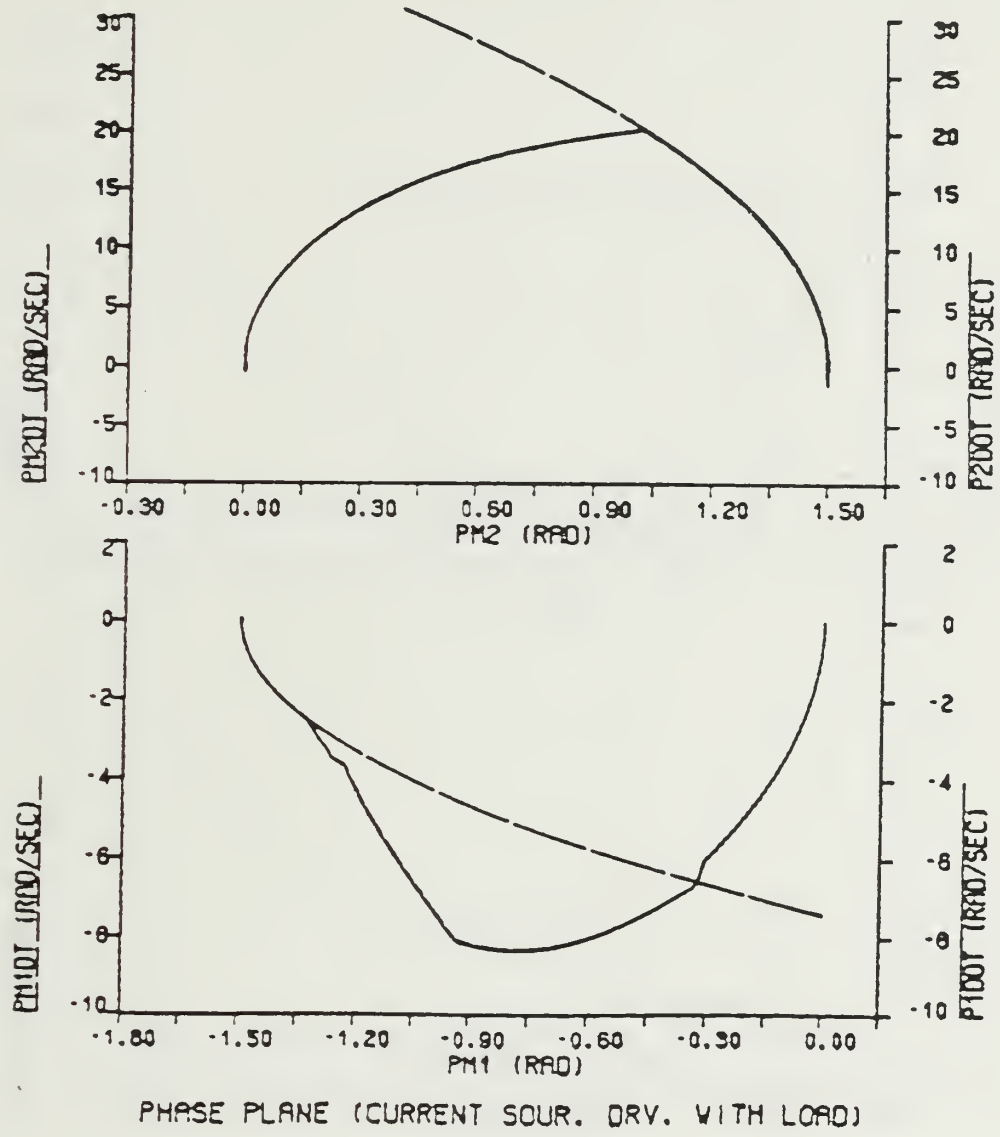

Figure 7.43 Phase Plane Trajectory For Move #2 (With Gravity)
JOINT2 Servo Motor Input Delayed 0.10 sec..

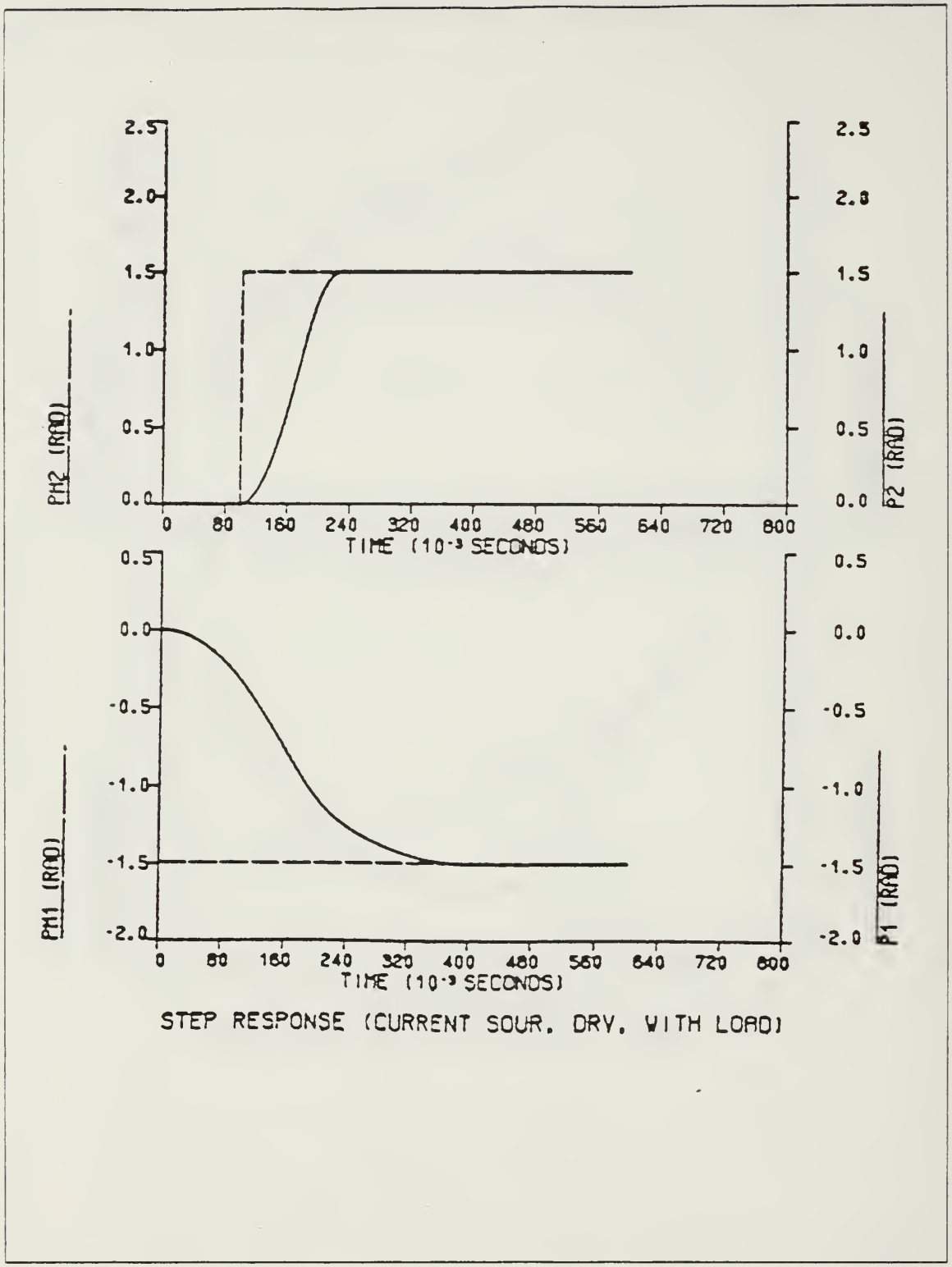

Figure 7.44 Step Response For Move #2 (With Gravity)
JOINT2 Servo Motor Input Delayed 0.10 sec..

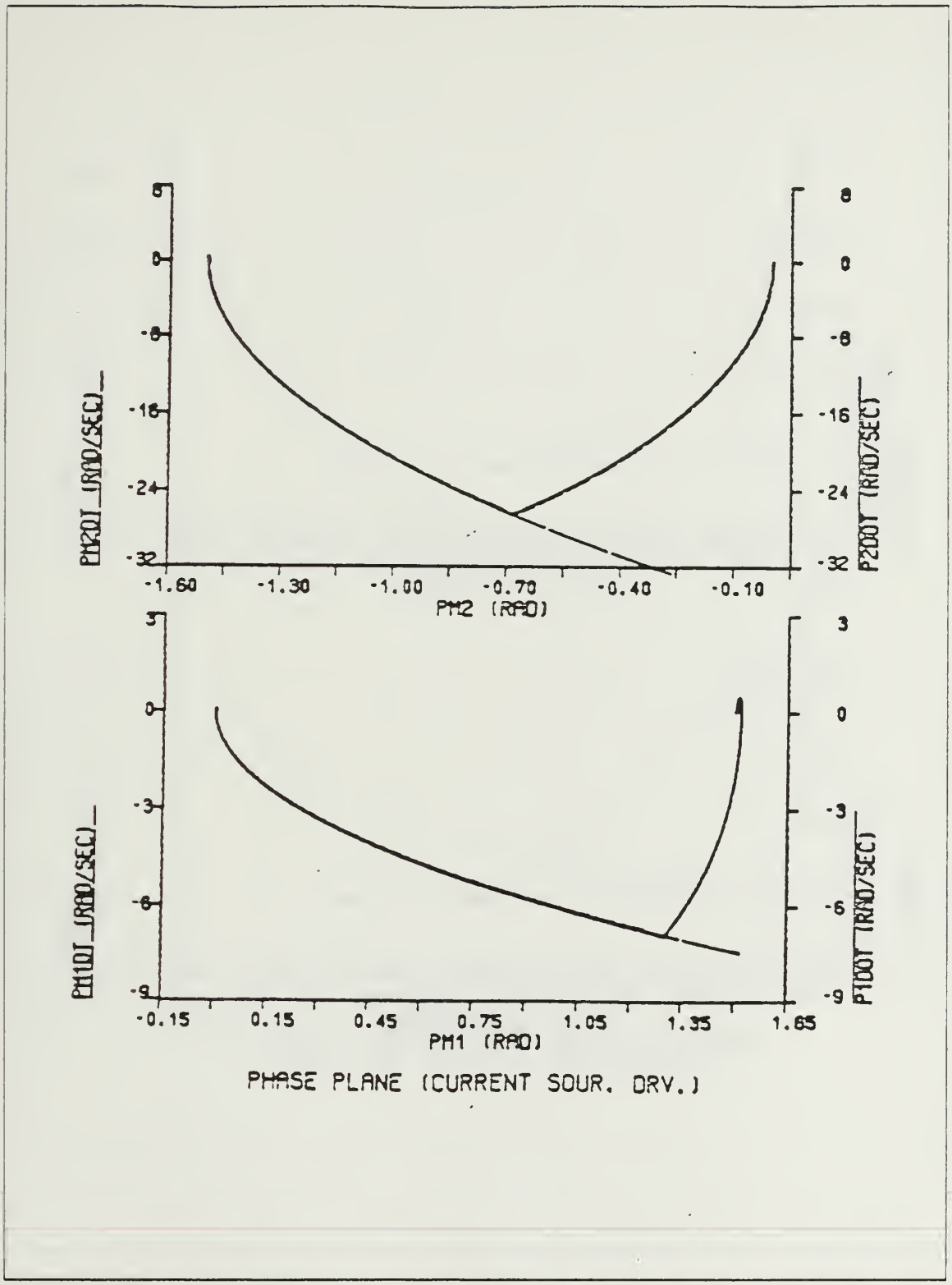

Figure 7.45 Phase Plane Trajectory For Move #3 (With Gravity).

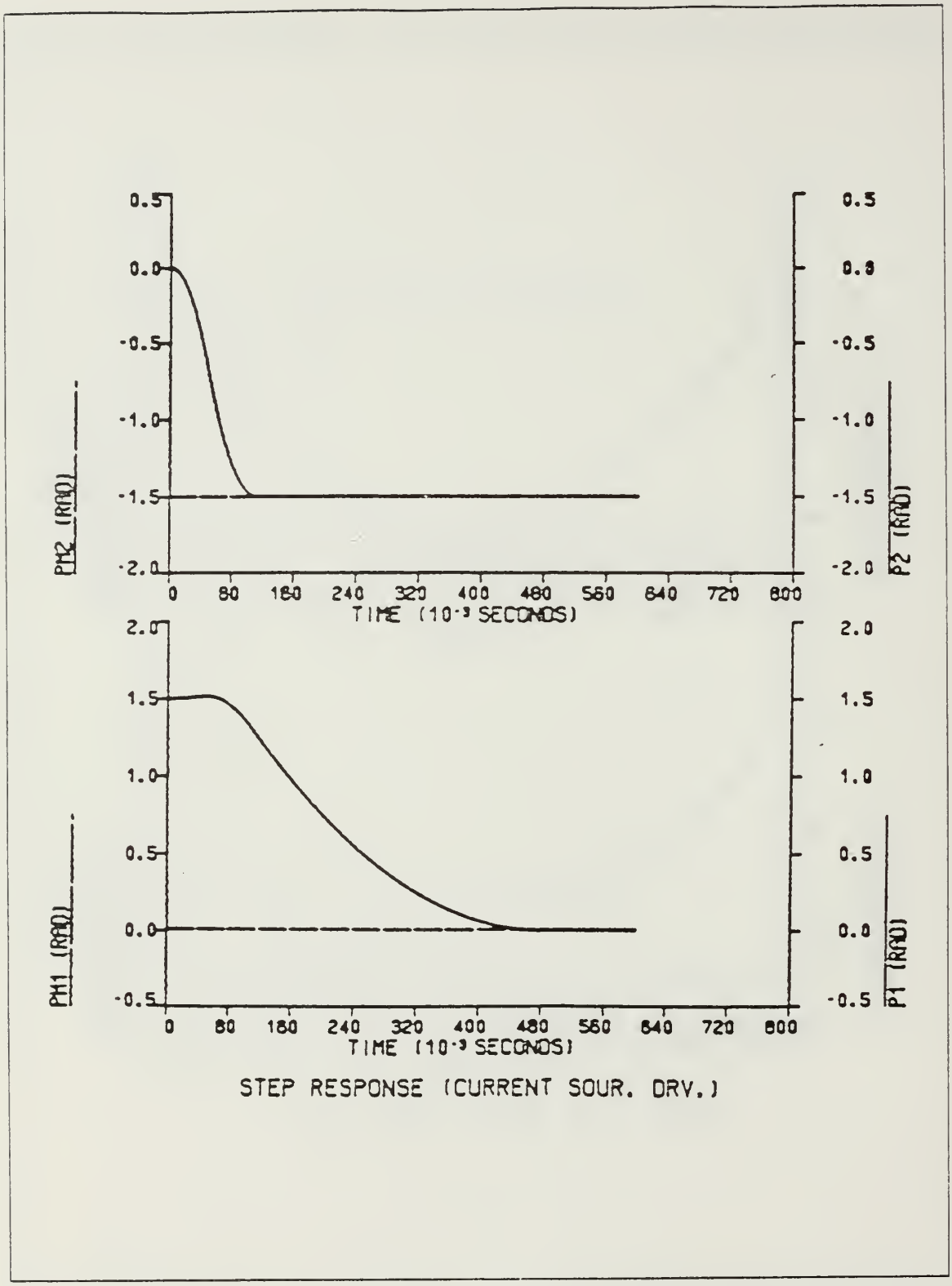

Figure 7.46 Step Response For Move #3 (With Gravity).

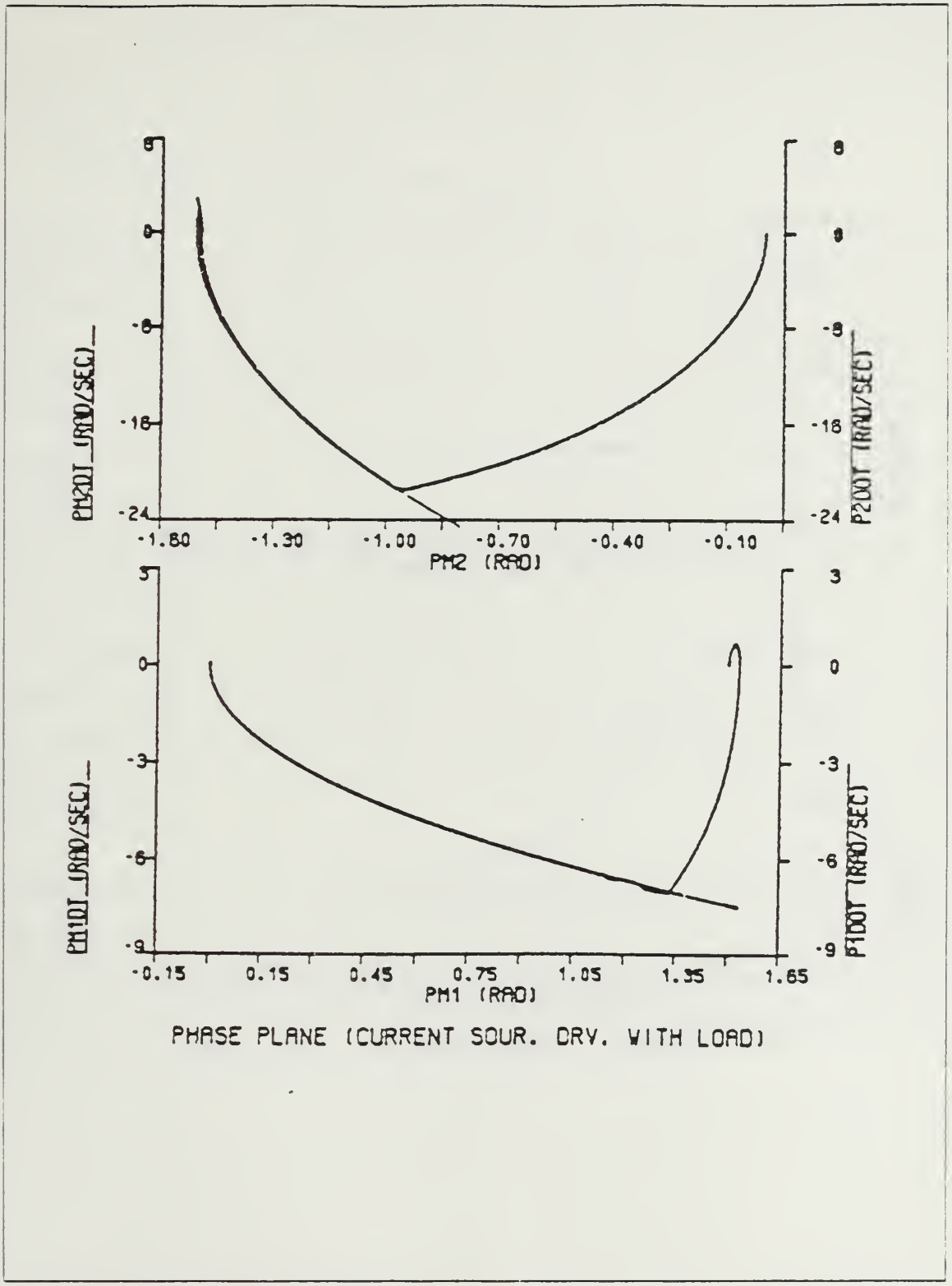

Figure 7.47 Phase Plane Trajectory For Move #3 (With Gravity).

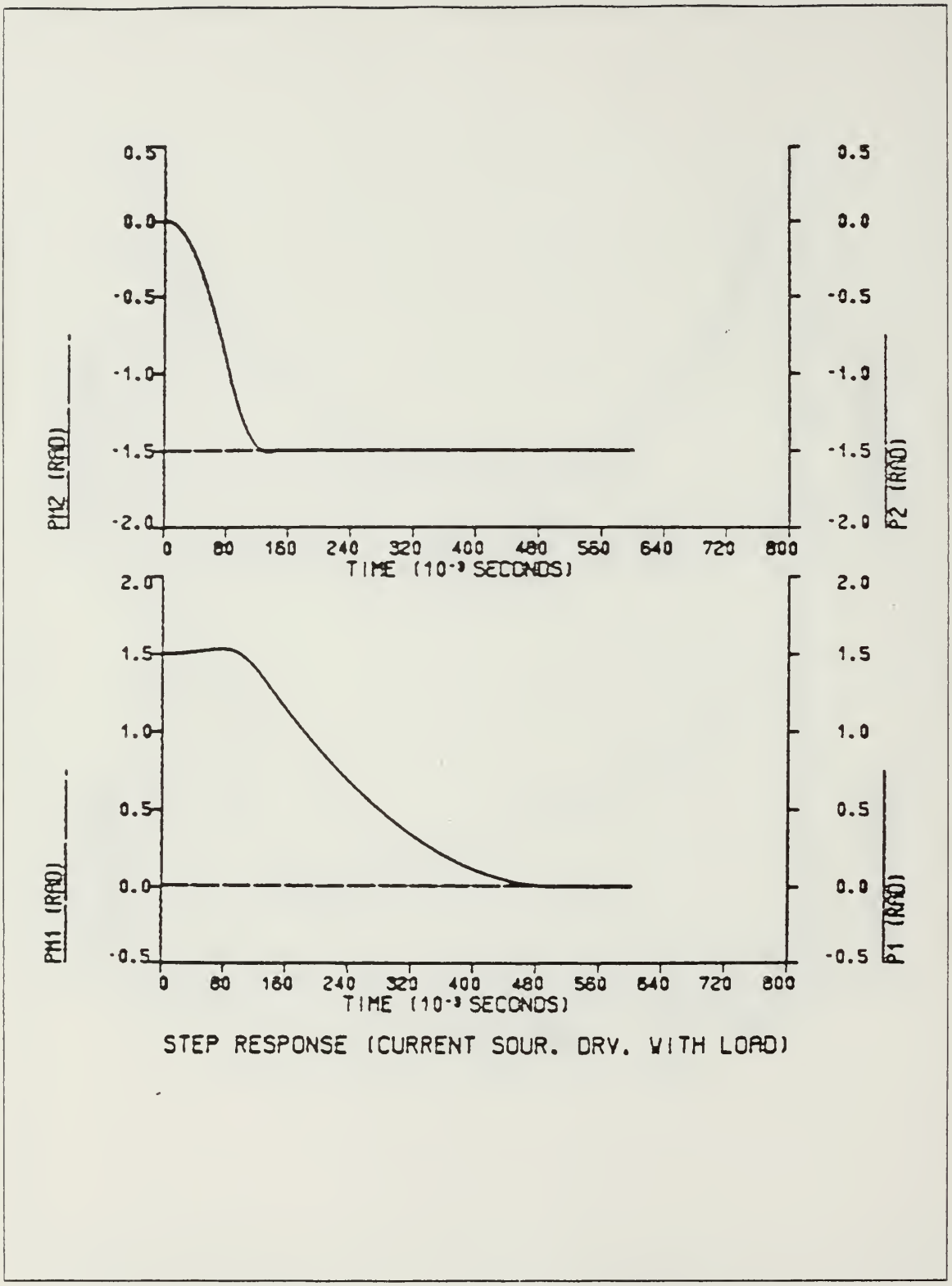

Figure 7.48 Step Response For Move #3 (With Gravity).

From phase plane trajectories 6.9 rad/sec and 21.3 rad/sec, maximum velocities are seen for servo motors 1 and 2 respectively. Good curve following capabilities for both the second-order model and servo motor are seen and they are on top of each other along the move.

b. Time Varying Position Command Input Used

To simulate the adaptive system under gravitational torques, a ramp input with a tangent of 1 rad/sec and a sinusoidal input were used. Simulation results are shown in Figures 7.49 - 7.60.

Phase plane trajectories of Figures 7.49 and 7.52 show that at the beginning of the move, the second-order model and servo motor velocities increase very rapidly to reach the steady-state value. It can be observed that this process takes a much shorter time for JOINT2 servo motor in comparison to JOINT1 servo motor. This can be thought to be the result of the reaction produced by JOINT2 servo motor. The second-order model and servo motor angular velocities shudder around the curve to follow it. Ramp response curves of Figures 7.50 and 7.53 show the JOINT2 servo motor is able to follow the ramp input easily with very small errors. Meanwhile, JOINT2 servo motor is lagging behind the ramp input because of the reasons mentioned above. Position error between commanded and actual angular position of the servo motors are shown in Figures 7.51 and 7.54. In the case of a loaded arm, the error reaches its maximum value at the beginning of the move, after that it decreases exponentially.

Figures 7.55 - 7.60 are the simulation results obtained with sinusoidal position input. Phase plane plots show that good curve following capabilities are observed. More shuddering around the curve is seen for JOINT2 servo motor. Sine response curves of Figures 7.56 and 7.59 show that both servo motors follow the commanded input. The position error between the desired angular position and actual servo motor angular position is shown in Figures 7.57 and 7.60.

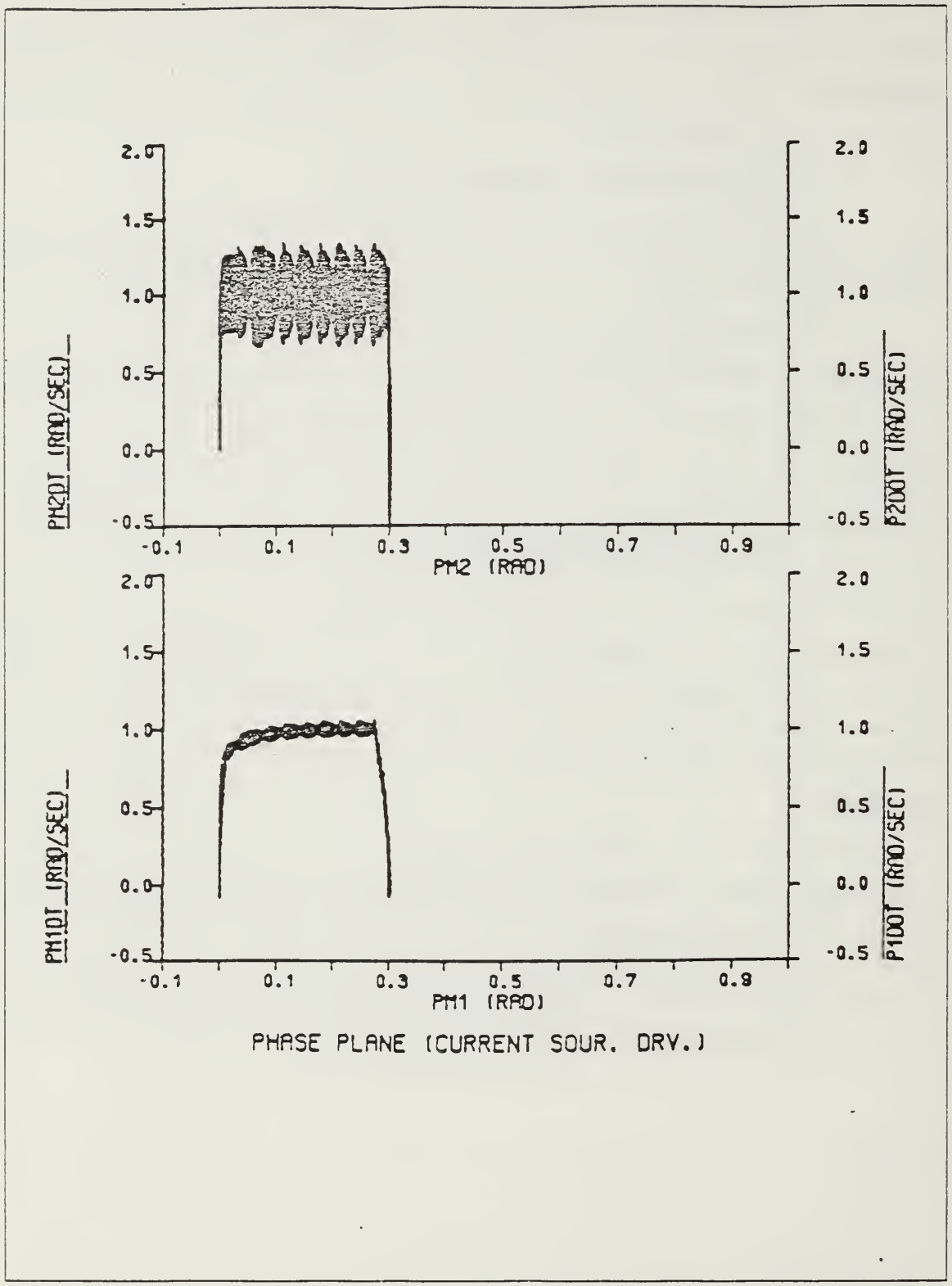

Figure 7.49 Phase Plane Trajectory For Ramp Input (With Gravity).

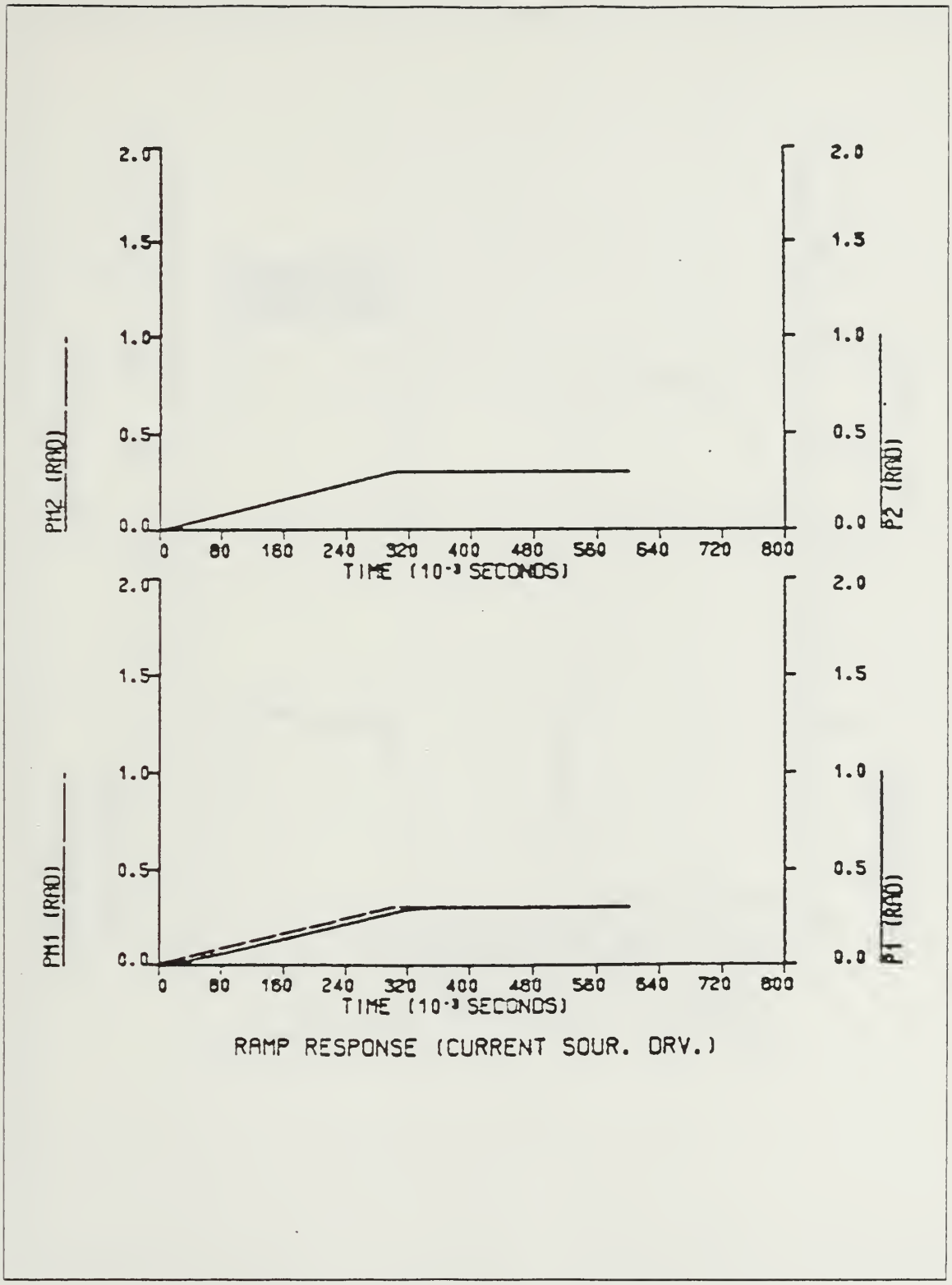

Figure 7.50 Ramp Response (With Gravity).

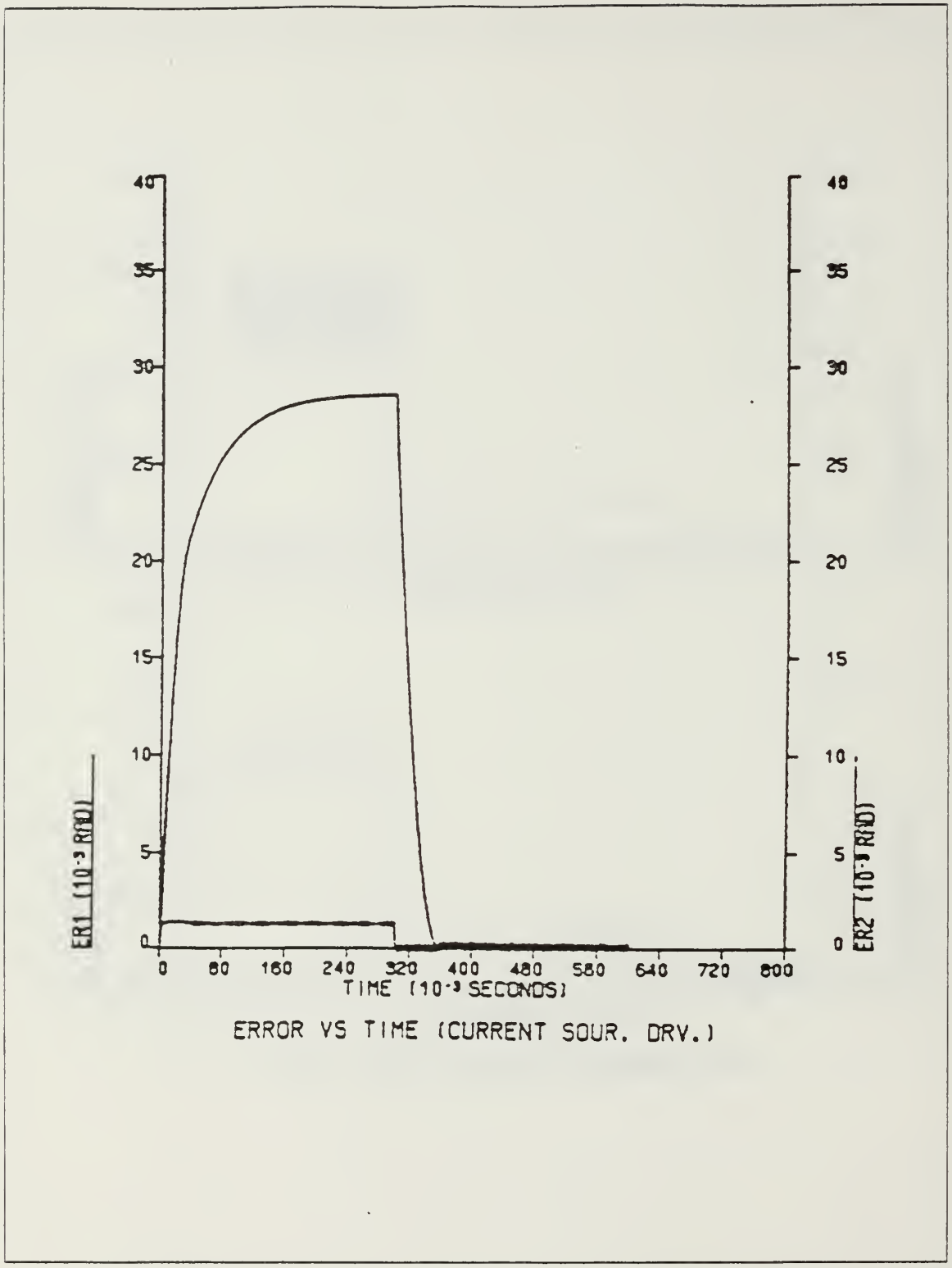

Figure 7.51 Error Between Commanded and Actual Position (With Gravity).

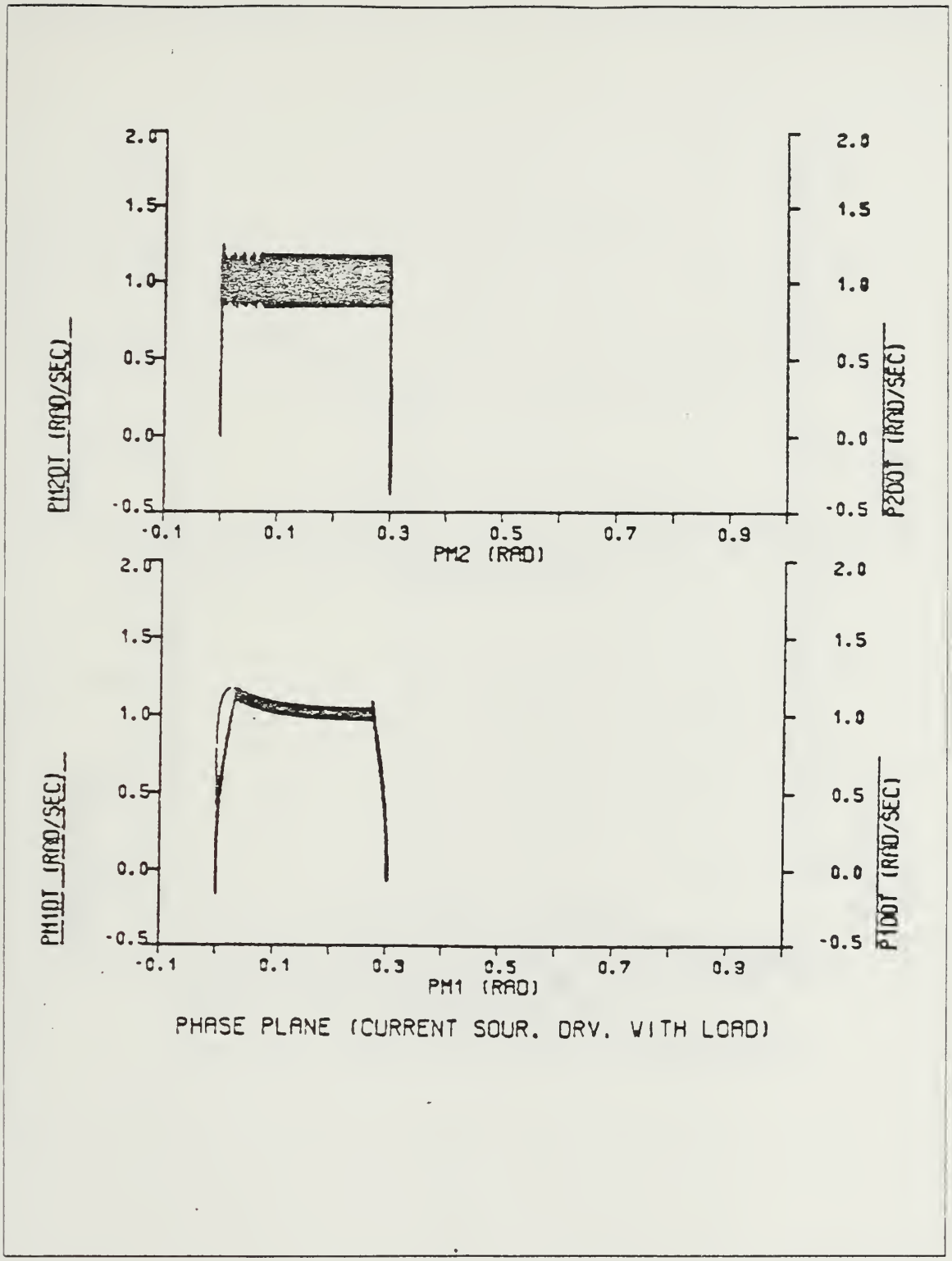

Figure 7.52 Phase Plane Trajectory For Ramp Input (With Gravity - Loaded Arm).

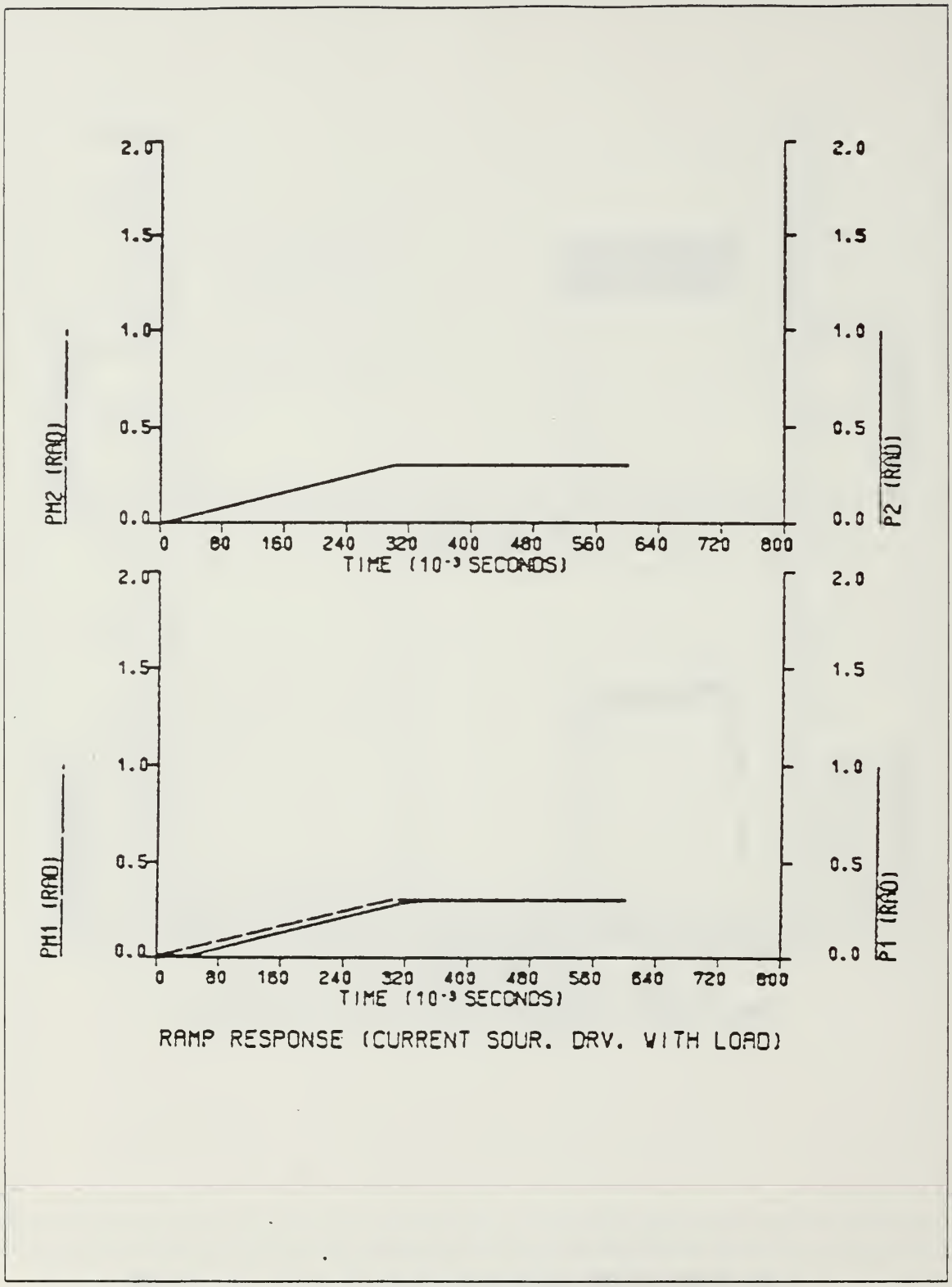

Figure 7.53 Ramp Response (With Gravity - Loaded Arm).

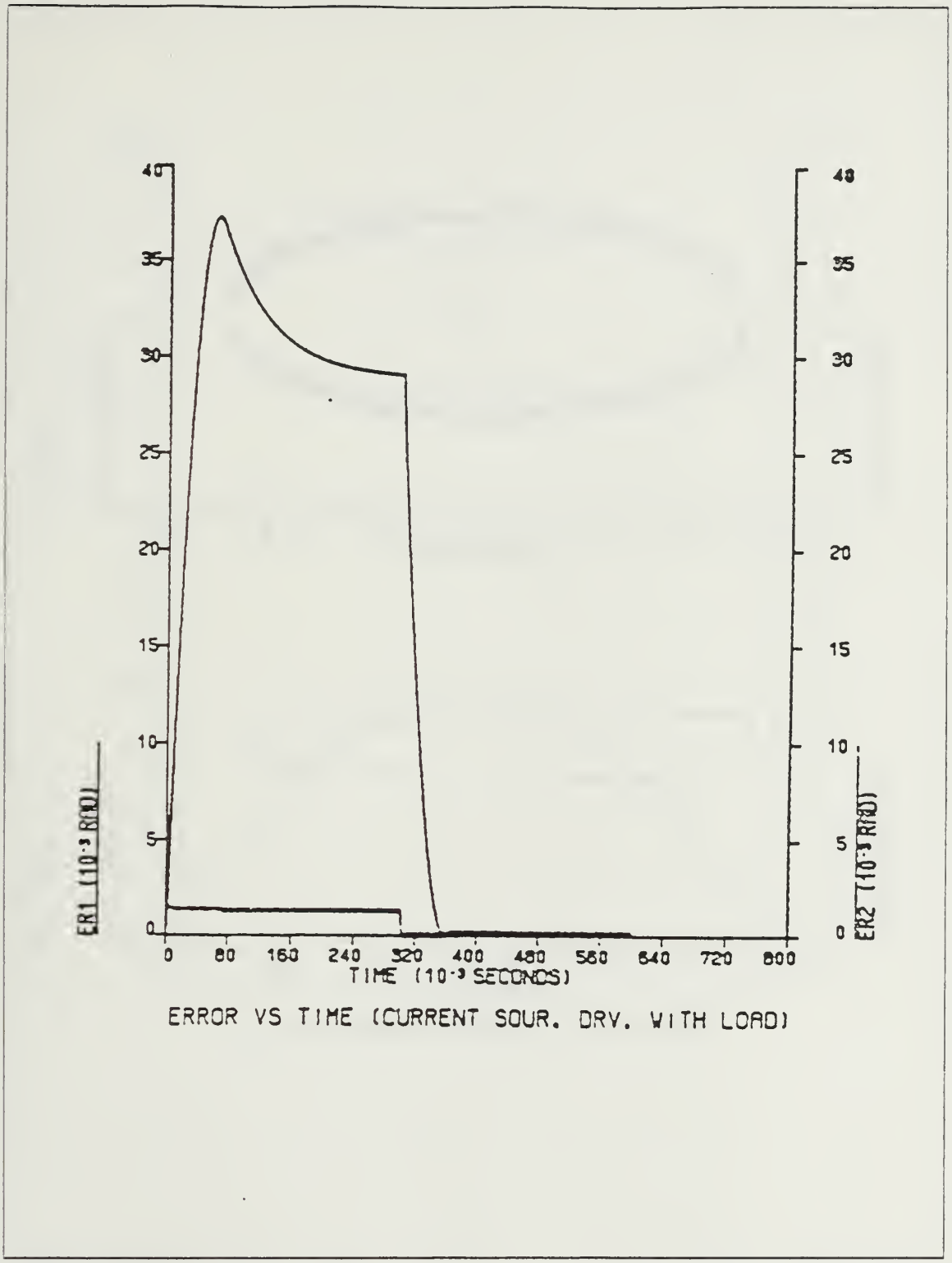

Figure 7.54 Error Between Commanded and Actual Position (With Gravity - Loaded Arm).

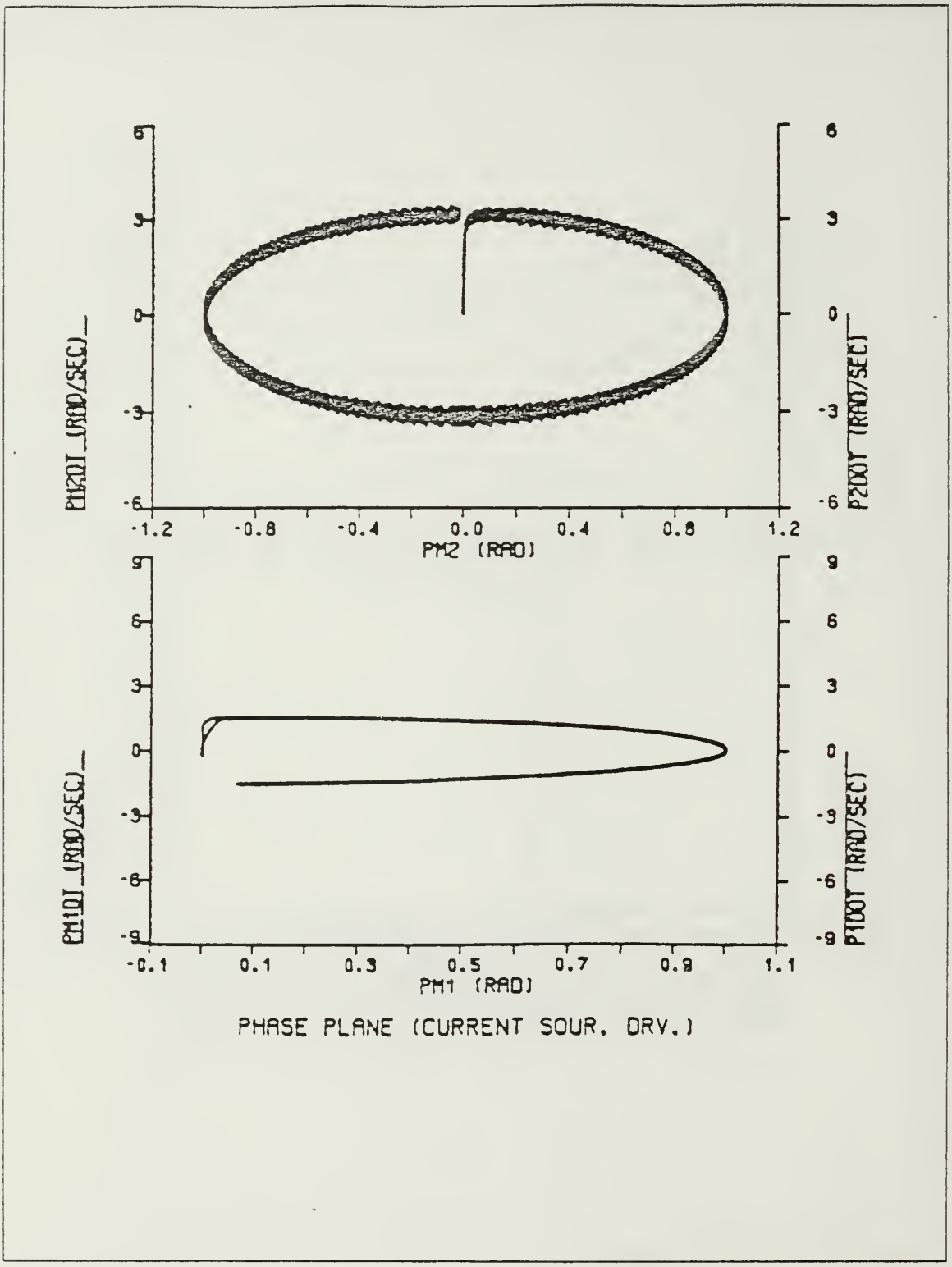

Figure 7.55 Phase Plane Trajectory For Sinusoidal Input (With Gravity).

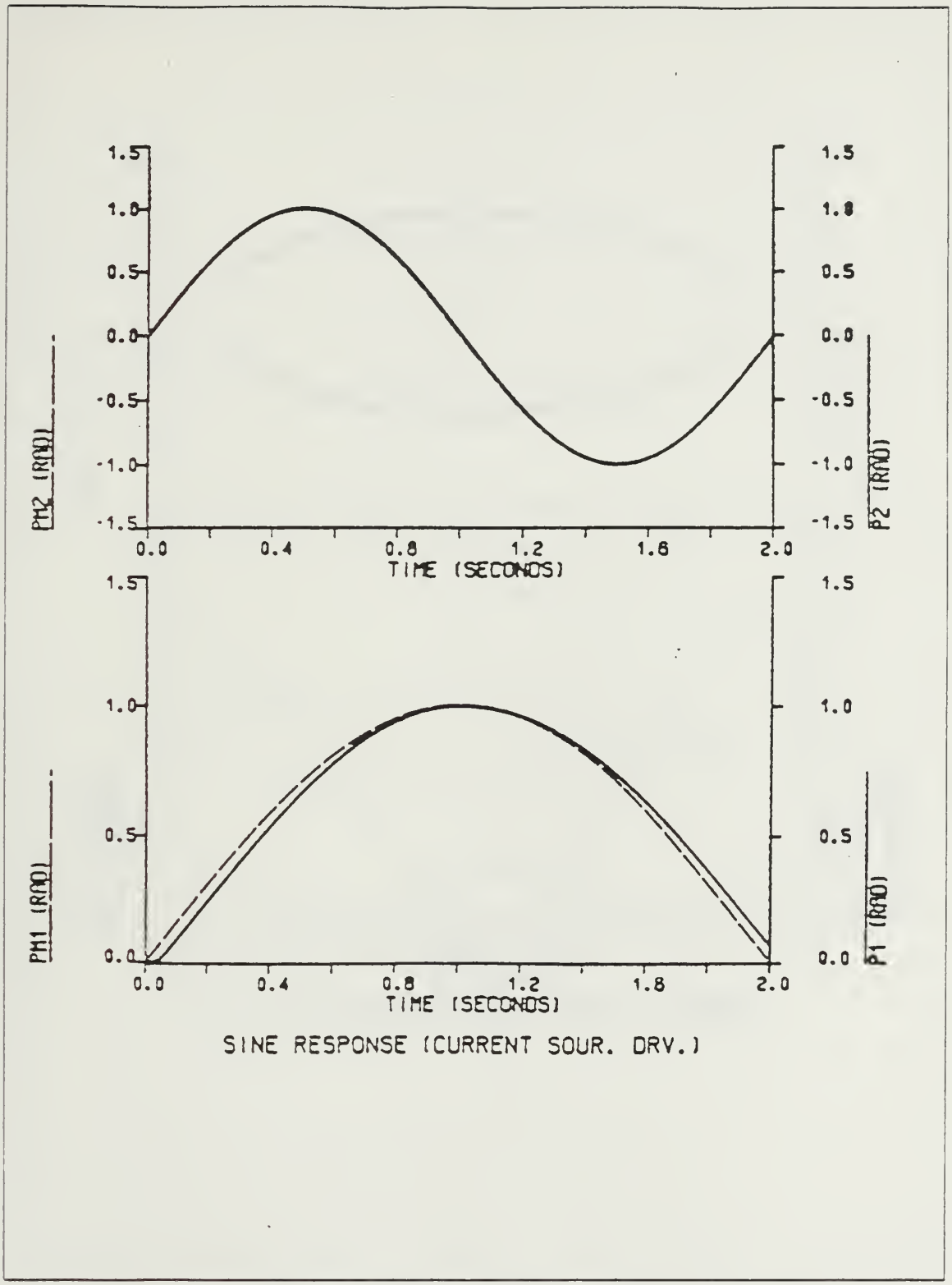

Figure 7.56 Sine Response (With Gravity).

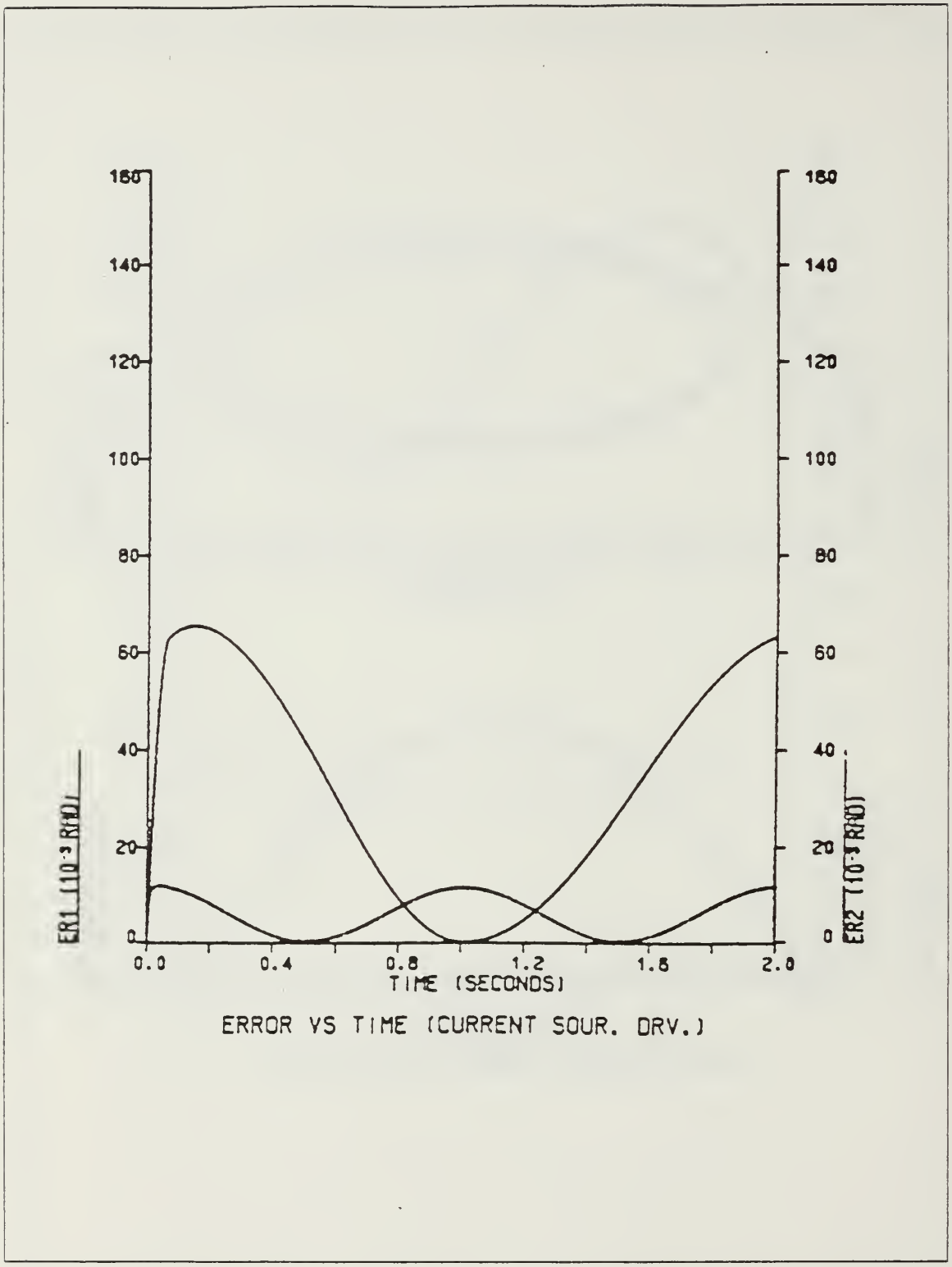

Figure 7.57 Error Between Commanded and Actual Position (With Gravity).

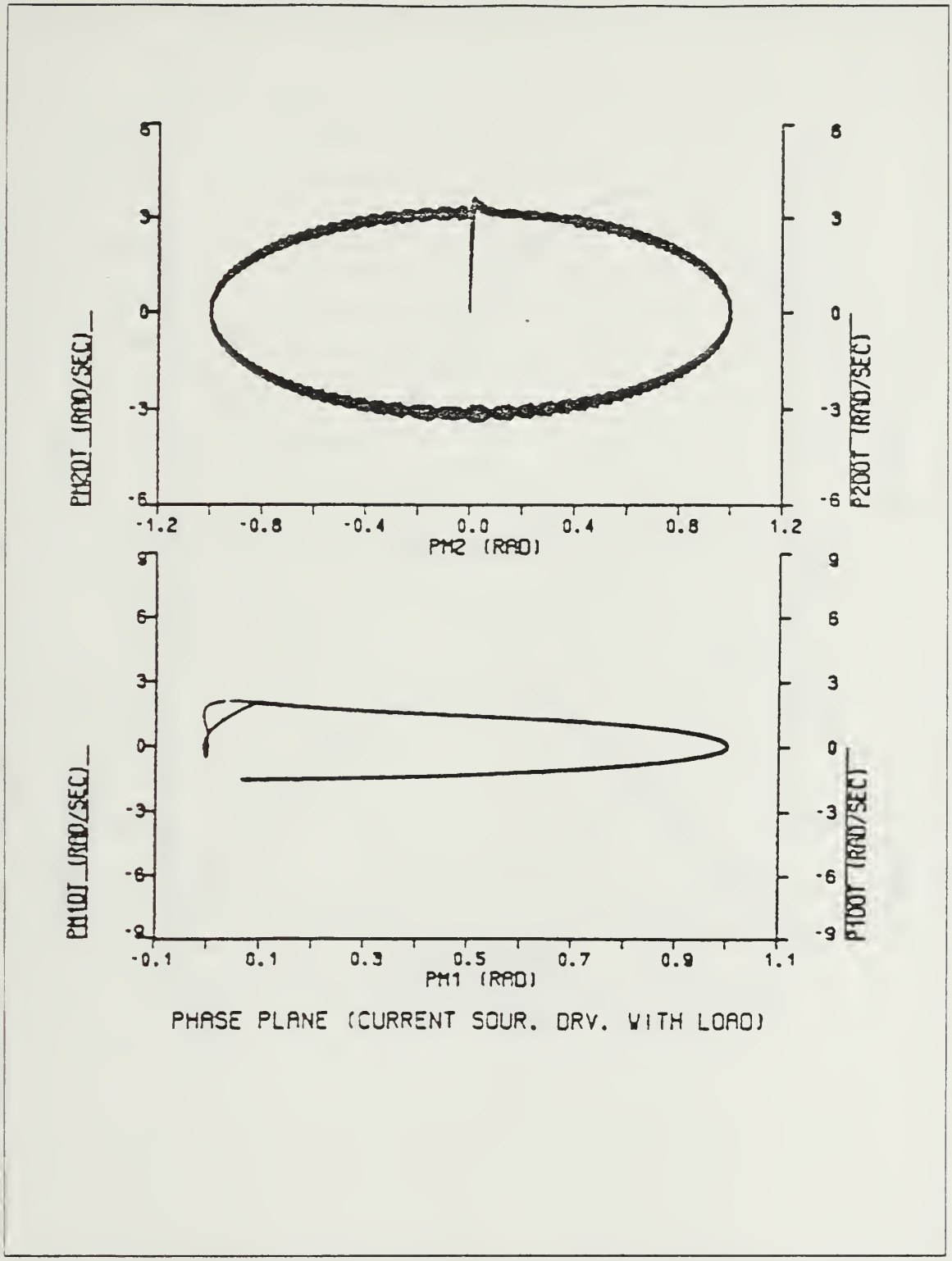

Figure 7.58 Phase Plane Trajectory For Sinusoidal Input (With Gravity - Loaded Arm).

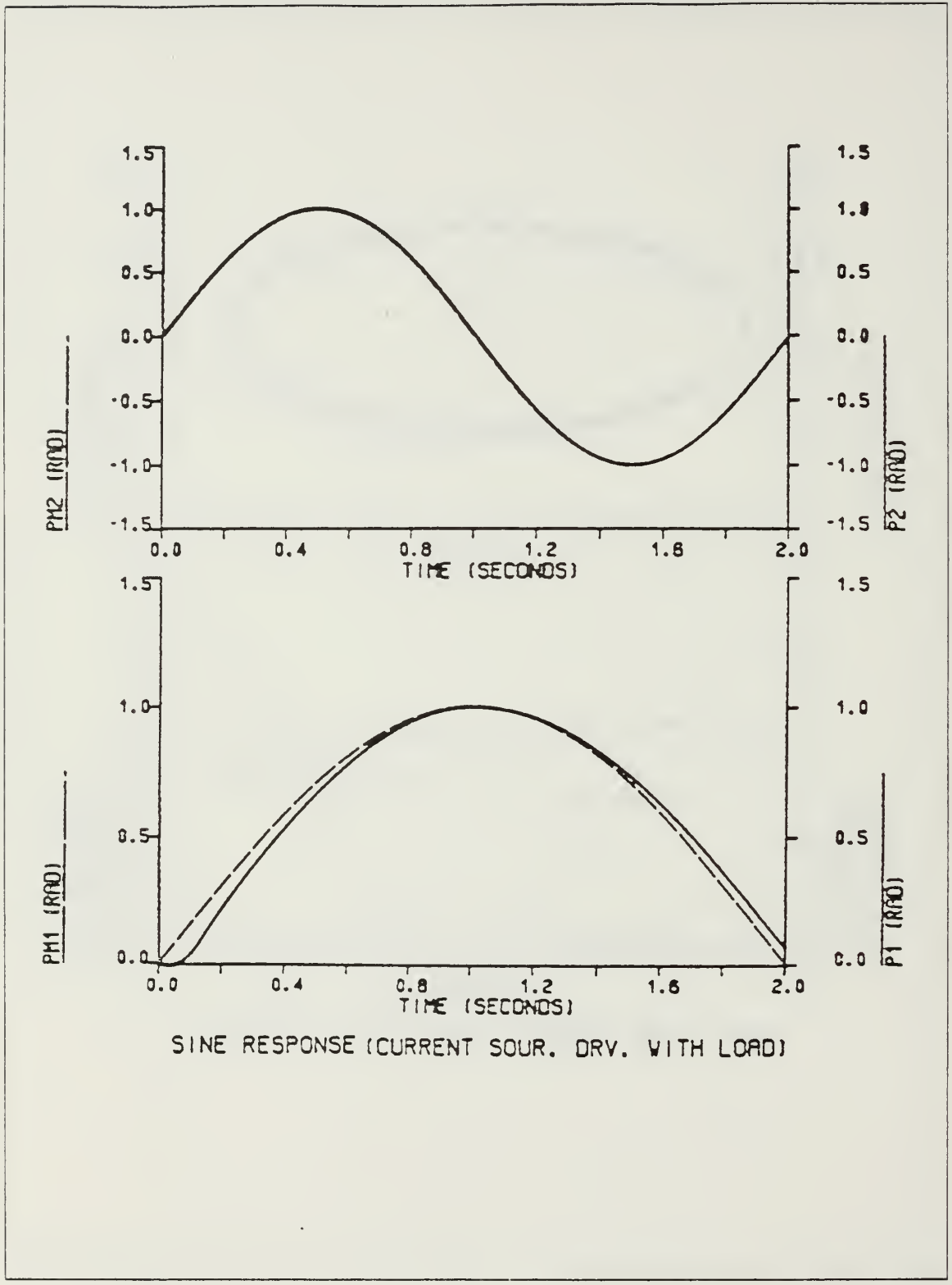

Figure 7.59 Sine Response (With Gravity - Loaded Arm).

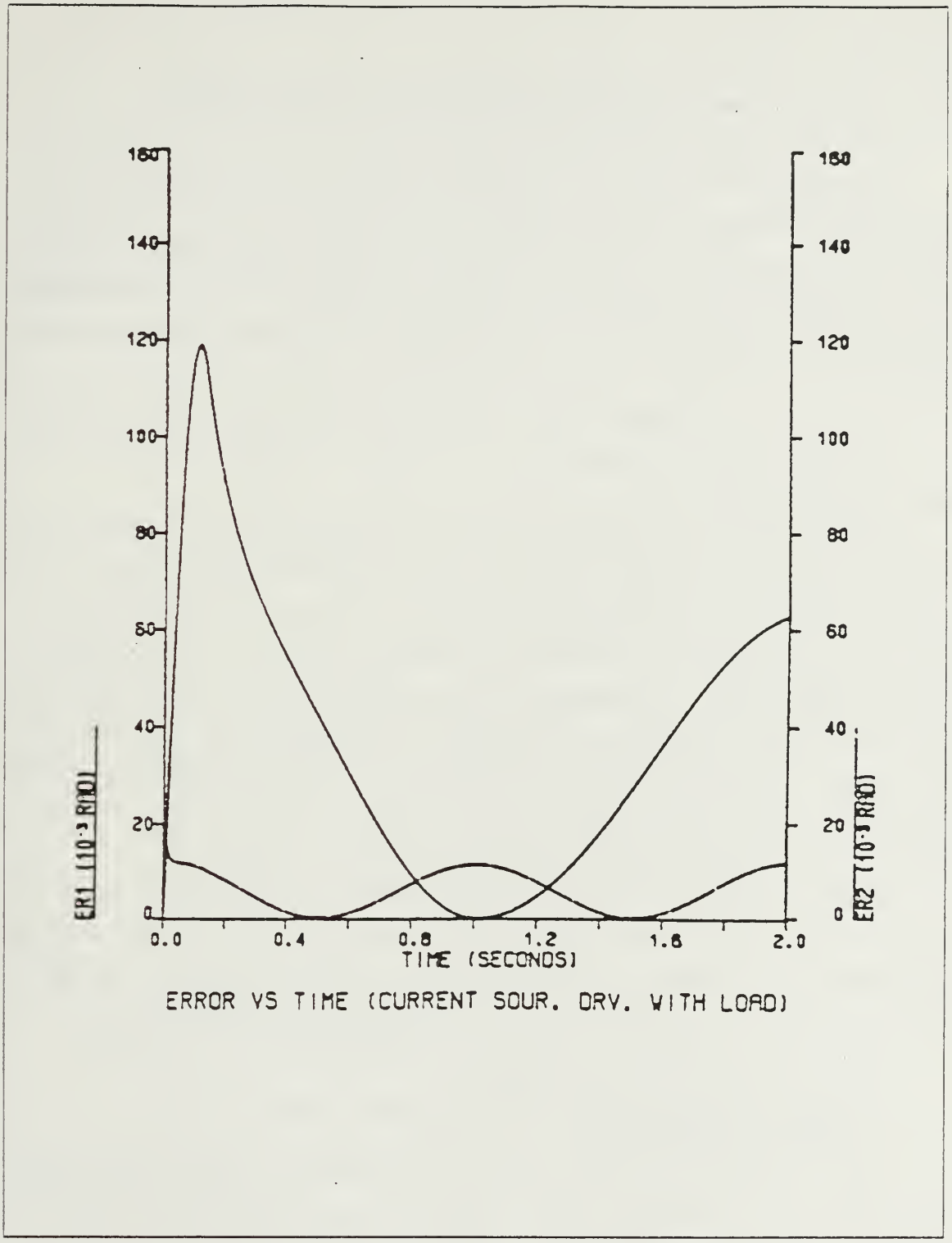

Figure 7.60 Error Between Commanded and Actual Position (With Gravity - Loaded Arm).

VIII. CONCLUSIONS/AREAS FOR FURTHER STUDY

As a result of the simulation studies done in this thesis, the near minimum time positioning of a two-link robot manipulator with an adaptive computer model seems feasible. Three sample moves were used to remove as many nonlinearities as necessary to test the adaptive system under large parameter variations. In these nonlinearities, coupling inertia, centripetal forces, actuator dynamics and gravitational torques were included.

As observed, servo motors overshoot for some of the moves. These conditions were overcome by offering alternatives such as lowering curve gain constant or using a different input sequence.

In this study, the direct-drive arm was used as a model. It was observed that in the case of the direct drive arm, the effects of the disturbance torques caused by the coupling inertia between links, and the centripetal, coriolis and gravitational forces on the robot arm, are larger. To overcome the disturbance torques, the servo motor has to apply larger torques. This requires a servo motor with high torque constant and high armature current capabilities. As an alternative solution to this, a gear train with a gear ratio of N may be used. Thus the effects of the disturbance torques were reduced by N. Of course, the price of this alternative is a slower system. It is up to the user to decide which is the best trade-off for a particular application.

Simulation results show that steady-state accuracy of the order of 10E-4 was observed for the step position command input. This accuracy may not be enough for some applications. Therefore a further study area arises here to position the LINK2 tip more accurately. Some alternative ways of doing this may be considered as;

1. Replace the curve with a linear compensator and remove the tachometer feedback within the adaptive model.
2. Replace the curve in the model with a gain block and modify the tachometer feedback gain.

In the modelling of the arm, a rigid body was assumed. Another area for further study arises when a lightweight, flexible structure is used to build the robot arm. The effects of the mechanical resonance is due to the flexible structure on the adaptive system to be studied.

In this thesis delayed steps were used to prevent undesired motions. To use this technique effectively in a robot, the magnitude of such step, and the required delay time must be predetermined by on-line calculation using some sort of algorithm which considers the initial oriantations of the arm, the commanded direction of the step, etc..

APPENDIX A

DSL PROGRAM FOR THE SECOND-ORDER MODEL SIMULATION

```
TITLE DSL PROGRAM OF THE SIMULATION MODEL
PARAM K1=0.60,K2=10000.,KM=4.0,VSAT=150.,K=1.0
PARAM REF=1.0
INITIAL
       A=SQRT(2.*KM*VSAT)
       XDOT=0.0
DYNAMIC
       R=REF*STEP(0.0)
       E=R-P
       IF(E.LT.0.0)XDOT=-A*K1*SQRT(ABS(E))
       IF(E.GE.0.0)XDOT=A*K1*SQRT(E)
DERIVATIVE
       XDOTE=XDOT-KPDOT
       KPDOT=PDOT*K
       V=LIMIT(-VSAT,VSAT,K2*XDOTE)
       PDDOT=KM*V
       PDOT=INTGRL(0.0,PDDOT)
       P=INTGRL(0.0,PDOT)
TERMINAL
METHOD RKSFX
CONTRL  FINTIM=0.15000,DELT=0.00005
PRINT  0.01,P,PDOT,XDOT,V,XDOTE
SAVE (G1)0.00005,P,XDOT,PDOT
SAVE (G3)0.00005,P,REF
GRAPH(G1/G1,DE=TEK618,PO=1,.5) P(LE=6.5,UN='RAD'),...
        XDOT(LE=8,NI=8,LO=0.,UN='RAD/SEC',SC=$AR),...
        PDOT(LE=8,NI=8,LO=0.0,UN='RAD/SEC',PO=6.5,SC=$AR)
GRAPH(G3/G3,DE=TEK618,PO=1,.5) TIME(LE=6.5,UN='SECONDS'),...
        P(LE=8,NI=8,LO=0,UN='RAD',SC=0.25),...
        REF(LE=8,NI=8,LO=0,SC=0.25,AX=OMIT)
LABEL (G1) PHASE PLANE
LABEL (G1) XDOT,PDOT VS P
LABEL (G3) STEP RESPONSE
LABEL (G3) P VS TIME
END
STOP
```

APPENDIX B

DERIVATION OF MATHEMATICAL MODEL FOR THE TWO-DEGREES-OF-FREEDOM PLANAR ROBOT ARM

The Lagrangian, $L = K - V$ of the system is:

$$\begin{aligned} L = {} & 1/2(m_1 d_1^2 + J_{m1})\dot{\theta}_1^2 + 1/2(m_2 d_2^2 + J_{m2})\dot{\theta}_2^2 \\ & + 1/2 m_2(d_1^2 + d_2^2 + 2d_1 d_2 \cos\theta_2)\dot{\theta}_1^2 \\ & + m_2(d_2^2 + d_1 d_2 \cos\theta_2)\dot{\theta}_1\dot{\theta}_2 \\ & - [(m_1 + m_2)d_1 \sin\theta_1 + m_2 d_2 \sin(\theta_1 + \theta_2)]g \end{aligned} \qquad \text{(eqn B.1)}$$

Taking partial derivatives of Equation B.1 with respect to θ_1 and θ_2 :

$$\frac{\partial L}{\partial \theta_1} = -(m_1 + m_2)g d_1 \cos\theta_1 - m_2 g d_2 \cos(\theta_1 + \theta_2) \qquad \text{(eqn B.2)}$$

$$\begin{aligned} \frac{\partial L}{\partial \theta_2} = {} & -(m_2 d_1 d_2 \sin\theta_2)\dot{\theta}_1^2 - (m_2 d_1 d_2 \sin\theta_2)\dot{\theta}_1\dot{\theta}_2 \\ & - m_2 g d_2 \cos(\theta_1 + \theta_2) \end{aligned} \qquad \text{(eqn B.3)}$$

Taking partial derivatives of Equation B.1 with respect to $\dot{\theta}_1$ and $\dot{\theta}_2$:

$$\begin{aligned} \frac{\partial L}{\partial \dot{\theta}_1} = {} & (m_1 d_1^2 + J_{m1})\dot{\theta}_1 \\ & + m_2(d_1^2 + d_2^2 + 2d_1 d_2 \cos\theta_2)\dot{\theta}_1 \\ & + m_2(d_2^2 + d_1 d_2 \cos\theta_2)\dot{\theta}_2 \end{aligned} \qquad \text{(eqn B.4)}$$

$$\frac{\partial L}{\partial \dot{\theta}_2} = (m_2 d_2^2 + J_{m2})\dot{\theta}_2 + m_2(d_2^2 + d_1 d_2 \cos\theta_2)\dot{\theta}_1 \qquad \text{(eqn B.5)}$$

Taking derivatives of Equations B.4 and B.5 with respect to time:

$$\begin{aligned} \frac{d}{dt}\left(\frac{\partial L}{\partial \dot{\theta}_1}\right) = {} & (m_1 d_1^2 + J_{m1} + m_2 d_1^2 + m_2 d_2^2 + 2m_2 d_1 d_2 \cos\theta_2)\ddot{\theta}_1 \\ & + (m_2 d_2^2 + m_2 d_1 d_2 \cos\theta_2)\ddot{\theta}_2 - (2m_2 d_1 d_2 \sin\theta_2)\dot{\theta}_1\dot{\theta}_2 \\ & - (m_2 d_1 d_2 \sin\theta_2)\dot{\theta}_2^2 \end{aligned} \qquad \text{(eqn B.6)}$$

$$\frac{d}{dt}\left(\frac{\partial L}{\partial \dot{\theta}_2}\right) = (m_2 d_2^2 + J_{m2})\ddot{\theta}_2 + m_2(d_2^2 + d_1 d_2 \cos\theta_2)\ddot{\theta}_1 - (m_2 d_1 d_2 \sin\theta_2)\dot{\theta}_1\dot{\theta}_2 \qquad \text{(eqn B.7)}$$

Substitude Equations B.2 - B.7 into Equation 3.1, obtain:

$$\begin{aligned} T_1 = {} & [(m_1 + m_2)d_1^2 + m_2 d_2^2 + J_{m1} + 2m_2 d_1 d_2 \cos\theta_2]\ddot{\theta}_1 \\ & + m_2(d_2^2 + d_1 d_2 \cos\theta_2)\ddot{\theta}_2 - (2m_2 d_1 d_2 \sin\theta_2)\dot{\theta}_1\dot{\theta}_2 \\ & - (m_2 d_1 d_2 \sin\theta_2)\dot{\theta}_2^2 + (m_1 + m_2)g d_1 \cos\theta_1 \\ & + m_2 g d_2 \cos(\theta_1 + \theta_2) \end{aligned} \qquad \text{(eqn B.8)}$$

$$\begin{aligned} T_2 = {} & (m_2 d_2^2 + J_{m2})\ddot{\theta}_2 + m_2(d_2^2 + d_1 d_2 \cos\theta_2)\ddot{\theta}_1 \\ & - (m_2 d_1 d_2 \sin\theta_2)\dot{\theta}_1\dot{\theta}_2 + (m_2 d_1 d_2 \sin\theta_2)\dot{\theta}_1\dot{\theta}_2 \\ & + (m_2 d_1 d_2 \sin\theta_2)\dot{\theta}_1^2 + m_2 g d_2 \cos(\theta_1 + \theta_2) \end{aligned} \qquad \text{(eqn B.9)}$$

When we arrange the terms in Equations B.8 and B.9, we obtain Equation 3.1.

APPENDIX C

DSL PROGRAM FOR VOLTAGE SOURCE DRIVE (NO GRAVITATIONAL TORQUES)

```
TITLE SIMULATION PROGRAM OF THE ADAPTIVE MODEL (VOLTAGE SOURCE DRIVE)
TITLE NO GRAVITATIONAL TORQUES
PARAM K1=0.60,K2=10000.,KM1=0.17,KM2=4.00,VSAT1=100.,K=1.0,T=0.00025
PARAM G=386.4,M1=0.248,M2=0.082,KT1=14.4,KT2=14.4,D1=15.,D2=10.
PARAM J1=0.033,J2=0.033,KV1=0.1012,KV2=0.1012,R1=0.91,R2=0.91,K3=0.6
PARAM REF1=1.0,REF2=1.0,L=0.0001,BM1=0.0429,BM2=0.0429,VSAT2=50.
INTGER N1,N2,FLAG1,FLAG2
INITIAL
        N1=0
        FLAG1=0
        N2=0
        FLAG2=0
        P1=0.0
        P2=0.0
        P1DOT=0.
        P2DOT=0.
        P1DDT=0.
        P2DDT=0.
        PM1=0.0
        PM2=0.0
        PM1DT=0.
        PM2DT=0.
        PM1DDT=0.
        PM2DDT=0.
        X1DOT=0.
        X2DOT=0.
        TL1=0.
        TL2=0.
        TL11=0.
        TL22=0.
        PP1=L/R1
        PP2=L/R2
        IM1=0.
        IM2=0.
        IM1=0.
        IM2=0.
        A1=SQRT(2.*KM1*VSAT1)
        A2=SQRT(2.*KM2*VSAT2)
DERIVATIVE
        RR1=REF1*STEP(0.0)
        RR2=REF2*STEP(0.0)
        RRD2=TRANSP(50,0.0,0.10,RR2)
        E1=RR1-P1
        E2=RRD2-P2
NOSORT
        D11=(M1+M2)*(D1**2)+M2*(D2**2)+2*M2*D1*D2*COS(PM2)
        D12=M2*(D2**2)+M2*D1*D2*COS(PM2)
        D22=M2*(D2**2)
        D122=-M2*D1*D2*SIN(PM2)
        D211=D122
        D112=D211
        D121=D112
        D212=D121
        D221=D212
        PMT=PM1+PM2
*     G1=(M1+M2)*G*D1*COS(PM1)+M2*G*D2*COS(PMT)
*     G2=M2*G*D2*COS(PMT)
        TL1=D12*PM2DDT+D122*PM2DT**2+2*D112*PM1DT*PM2DT
        TL2=D12*PM1DDT-D211*PM1DT**2
        JTOT1=J1+D11
```

```
        JTOT2=J2+D22
        IF(E1.LT.0.0)X1DOT=-A1*K1*SQRT(ABS(E1))
        IF(E1.GE.0.0)X1DOT=A1*K1*SQRT(E1)
        IF(E2.LT.0.0)X2DOT=-A2*K3*SQRT(ABS(E2))
        IF(E2.GE.0.0)X2DOT=A2*K3*SQRT(E2)
SORT
        X1DOTE=X1DOT-KP1DOT
        KP1DOT=P1DOT*K
        V1=LIMIT(-VSAT1,VSAT1,K2*X1DOTE)
NOSORT
        IF(FLAG1.EQ.1)GO TO 5
        IF(V1.LT.VSAT1.AND.TIME.GT.0.00005)FLAG1=1
        NSW1=N1
5      CONTINUE
SORT
        P1DDT=KM1*V1
        P1DOT=INTGRL(0.0,P1DDT)
        P1=INTGRL(0.0,P1DOT)
        VP1=V1-(KV1*PM1DT)
        IM1=REALPL(0.0,PP1,VP1/R1)
        TM1=KT1*IM1
        TNET1=TM1-PM1DT*BM1-TL1
        PM1DDT=(1./JTOT1)*TNET1
        PM1DT=INTGRL(0.0,PM1DDT)
        PM1=INTGRL(0.0,PM1DT)
        X2DOTE=X2DOT-KP2DOT
        KP2DOT=P2DOT*K
        V2=LIMIT(-VSAT2,VSAT2,K2*X2DOTE)
NOSORT
        IF(FLAG2.EQ.1)GO TO 6
        IF(V2.LT.VSAT2.AND.TIME.GT.0.00005)FLAG2=1
        NSW2=N2
6      CONTINUE
SORT
        P2DDT=KM2*V2
        P2DOT=INTGRL(0.0,P2DDT)
        P2=INTGRL(0.0,P2DOT)
        VP2=V2-(KV2*PM2DT)
        IM2=REALPL(0.0,PP2,VP2/R2)
        TM2=KT2*IM2
        TNET2=TM2-PM2DT*BM2-TL2
        PM2DDT=(1./JTOT2)*TNET2
        PM2DT=INTGRL(0.0,PM2DDT)
        PM2=INTGRL(0.0,PM2DT)
SAMPLE
NOSORT
        IF(N2.EQ.0)GO TO 21
        IF(N1.EQ.0)GO TO 20
        P2=PM2
        P1=PM1
        KS2=ABS(2.*PM2/(V2*((N2*T)**2)))
        KS1=ABS(2.*PM1/(V1*((N1*T)**2)))
        IF(FLAG2.EQ.0)KM2=KS2
        IF(FLAG1.EQ.0)KM1=KS1
        IF(N2.GE.2)PM2DTL=(PM2-PM22L)/(2.*T)
        IF(N1.GE.2)PM1DTL=(PM1-PM12L)/(2.*T)
        IF(FLAG2.EQ.0)P2DOT=(2.*((PM2-PM2LST)/T))-PM2DTL
        IF(FLAG1.EQ.0)P1DOT=(2.*((PM1-PM1LST)/T))-PM1DTL
        IF(N2.EQ.NSW2.AND.FLAG2.EQ.1)GO TO 21
        IF(N1.EQ.NSW1.AND.FLAG1.EQ.1)GO TO 20
        IF(FLAG2.EQ.1)P2DOT=(2.*((PM2-PM2LST)/T))-PM2DTL
        IF(FLAG1.EQ.1)P1DOT=(2.*((PM1-PM1LST)/T))-PM1DTL
21     N2=N2+1
20     N1=N1+1
        PM2DTL=P2DOT
        PM1DTL=P1DOT
        P2DOT=PM2DTL
        PM22L=PM2LST
        PM12L=PM1LST
```

```
       PM2LST=PM2
       PM1LST=PM1
*     ER1=ABS(RR1-PM1)
*     ER2=ABS(RR2-PM2)
SORT
TERMINAL
FINISH  PM1=1.00
METHOD RKSFX
CONTRL  FINTIM=0.70000,DELT=0.00005,DELS=.00025
PRINT 0.010,X1DOT,P1DOT,PM1DT,X2DOT,P2DOT,PM2DT,PM1,RR1,PM2,RR2,TM1,TM2
SAVE (S1) 0.01, X1DOT,P1DOT,PM1DT,X2DOT,P2DOT,PM2DT,PM1,PM2
SAVE (S3) 0.01, P1,PM1,REF1,P2,PM2,REF2,RR1,RRD2
GRAPH (L1/S1,DE=TEK618,PO=1,.5) PM1(LE=6.0,UN='RAD',LO=-0.10,SC=0.10,...
        NI=12),P1DOT(LE=4,NI=4,LO=-2.0,UN='RAD/SEC',SC=2.0,PO=6.0),...
        X1DOT(LE=4,NI=4,LO=-2.0,SC=2.0,UN='RAD/SEC',AX=OMIT),...
        PM1DT(LE=4,NI=4,LO=-2.0,UN='RAD/SEC',SC=2.0)
GRAPH (L2/S1,DE=TEK618,OV,PO=1,5) PM2(LE=6.0,UN='RAD',LO=-0.10,...
       SC=0.10,NI=12), P2DOT(LE=4,NI=4,LO=0.0,UN='RAD/SEC',SC=5.0,...
       PO=6.),X2DOT(LE=4,NI=4,LO=0.0,UN='RAD/SEC',SC=5.0,AX=OMIT),...
       PM2DT(LE=4,NI=4,LO=0.0,UN='RAD/SEC',SC=5.0)
GRAPH (L3/S3,DE=TEK618,PO=1,.5) TIME(LE=6.0,UN='SECONDS'),...
        P1(LE=4,NI=4,LO=-.5,UN='RAD',SC=0.50,PO=6.0),...
        PM1(LE=4,NI=4,LO=-.5,UN='RAD',SC=0.50),...
        RR1(LE=4,NI=4,LO=-.5,SC=0.50,AX=OMIT)
GRAPH (L4/S3,DE=TEK618,PO=1,5,OV) TIME(LE=6.0,UN='SECONDS'),...
         P2(LE=4,NI=4,LO=-.5,UN='RAD',SC=0.50,PO=6.0),...
         PM2(LE=4,NI=4,LO=-.5,UN='RAD',SC=0.50),...
         RRD2(LE=4,NI=4,LO=-.5,SC=0.50,AX=OMIT)
*RAPH(L5/S3,DE=TEK618,PO=1,.5) TIME(LE=6.0,UN='SECONDS'),...
*       ER1(LE=8,NI=8,LO=0.,UN='RAD',SC=0.005),...
*       ER2(LE=8,NI=8,LO=0.,UN='RAD',SC=0.005,PO=6.)
LABEL (L1) PHASE PLANE (VOLTAGE SOUR. DRV. WITH LOAD)
LABEL (L3) STEP RESPONSE(VOLTAGE SOUR. DRV. WITH LOAD)
LABEL (L5) ERROR VS TIME (VOLTAGE SOUR. DRV. WITH LOAD)
END
STOP
```

APPENDIX D

DSL PROGRAM FOR VOLTAGE SOURCE DRIVE (GRAVITATIONAL TORQUES INCLUDED)

```
TITLE SIMULATION PROGRAM OF THE ADAPTIVE MODEL (VOLTAGE SOURCE DRIVE)
TITLE GRAVITATIONAL TORQUES INCLUDED
PARAM K1=0.60,K2=10000.,KM1=0.17,KM2=4.00,VSAT1=300.,K=1.0,T=0.00025
PARAM G=386.4,M1=0.248,M2=0.082,KT1=14.4,KT2=14.4,D1=15.,D2=10.
PARAM J1=0.033,J2=0.033,KV1=0.1012,KV2=0.1012,R1=0.91,R2=0.91,K3=0.6
PARAM REF1=1.0,REF2=1.0;L=0.0001,BM1=0.0429,BM2=0.0429,VSAT2=150.
INTGER N1,N2,FLAG1,FLAG2
INITIAL
        N1=0
        FLAG1=0
        N2=0
        FLAG2=0
        P1=0.0
        P2=0.0
        P1DOT=0.
        P2DOT=0.
        P1DDT=0.
        P2DDT=0.
        PM1=0.0
        PM2=0.0
        PM1DT=0.
        PM2DT=0.
        PM1DDT=0.
        PM2DDT=0.
        X1DOT=0.
        X2DOT=0.
        TL1=0.
        TL2=0.
        TL11=0.
        TL22=0.
        PP1=L/R1
        PP2=L/R2
        TM1=0.
        TM2=0.
        IM1=0.
        IM2=0.
        A1=SQRT(2.*KM1*VSAT1)
        A2=SQRT(2.*KM2*VSAT2)
DERIVATIVE
        RR1=REF1*STEP(0.0)
        RR2=REF2*STEP(0.0)
        RRD2=TRANSP(50,0.0,0.10,RR2)
        E1=RR1-P1
        E2=RRD2-P2
NOSORT
        D11=(M1+M2)*(D1**2)+M2*(D2**2)+2*M2*D1*D2*COS(PM2)
        D12=M2*(D2**2)+M2*D1*D2*COS(PM2)
        D22=M2*(D2**2)
        D122=-M2*D1*D2*SIN(PM2)
        D211=D122
        D112=D211
        D121=D112
        D212=D121
        D221=D212
        PMT=PM1+PM2
        G1=(M1+M2)*G*D1*COS(PM1)+M2*G*D2*COS(PMT)
        G2=M2*G*D2*COS(PMT)
        TL1=D12*PM2DDT+D122*PM2DT**2+2*D112*PM1DT*PM2DT+G1
        TL2=D12*PM1DDT-D211*PM1DT**2+G2
        JTOT1=J1+D11
```

```
        JTOT2=J2+D22
        IF(E1.LT.0.0)X1DOT=-A1*K1*SQRT(ABS(E1))
        IF(E1.GE.0.0)X1DOT=A1*K1*SQRT(E1)
        IF(E2.LT.0.0)X2DOT=-A2*K3*SQRT(ABS(E2))
        IF(E2.GE.0.0)X2DOT=A2*K3*SQRT(E2)
SORT
        X1DOTE=X1DOT-KP1DOT
        KP1DOT=P1DOT*K
        V1=LIMIT(-VSAT1,VSAT1,K2*X1DOTE)
NOSORT
        IF(FLAG1.EQ.1)GO TO 5
        IF(V1.LT.VSAT1.AND.TIME.GT.0.00005)FLAG1=1
        NSW1=N1
5      CONTINUE
SORT
        P1DDT=KM1*V1
        P1DOT=INTGRL(0.0,P1DDT)
        P1=INTGRL(0.0,P1DOT)
        VP1=V1-(KV1*PM1DT)
        IM1=REALPL(0.0,PP1,VP1/R1)
        TM1=KT1*IM1
        TNET1=TM1-PM1DT*BM1-TL1
        PM1DDT=(1./JTOT1)*TNET1
        PM1DT=INTGRL(0.0,PM1DDT)
        PM1=INTGRL(0.0,PM1DT)
        X2DOTE=X2DOT-KP2DOT
        KP2DOT=P2DOT*K
        V2=LIMIT(-VSAT2,VSAT2,K2*X2DOTE)
NOSORT
        IF(FLAG2.EQ.1)GO TO 6
        IF(V2.LT.VSAT2.AND.TIME.GT.0.00005)FLAG2=1
        NSW2=N2
6      CONTINUE
SORT
        P2DDT=KM2*V2
        P2DOT=INTGRL(0.0,P2DDT)
        P2=INTGRL(0.0,P2DOT)
        VP2=V2-(KV2*PM2DT)
        IM2=REALPL(0.0,PP2,VP2/R2)
        TM2=KT2*IM2
        TNET2=TM2-PM2DT*BM2-TL2
        PM2DDT=(1./JTOT2)*TNET2
        PM2DT=INTGRL(0.0,PM2DDT)
        PM2=INTGRL(0.0,PM2DT)
SAMPLE
NOSORT
        IF(N2.EQ.0)GO TO 21
        IF(N1.EQ.0)GO TO 20
        P2=PM2
        P1=PM1
        KS2=ABS(2.*PM2/(V2*((N2*T)**2)))
        KS1=ABS(2.*PM1/(V1*((N1*T)**2)))
        IF(FLAG2.EQ.0)KM2=KS2
        IF(FLAG1.EQ.0)KM1=KS1
        IF(N2.GE.2)PM2DTL=(PM2-PM22L)/(2.*T)
        IF(N1.GE.2)PM1DTL=(PM1-PM12L)/(2.*T)
        IF(FLAG2.EQ.0)P2DOT=(2.*((PM2-PM2LST)/T))-PM2DTL
        IF(FLAG1.EQ.0)P1DOT=(2.*((PM1-PM1LST)/T))-PM1DTL
        IF(N2.EQ.NSW2.AND.FLAG2.EQ.1)GO TO 21
        IF(N1.EQ.NSW1.AND.FLAG1.EQ.1)GO TO 20
        IF(FLAG2.EQ.1)P2DOT=(2.*((PM2-PM2LST)/T))-PM2DTL
        IF(FLAG1.EQ.1)P1DOT=(2.*((PM1-PM1LST)/T))-PM1DTL
21     N2=N2+1
20     N1=N1+1
        PM2DTL=P2DOT
        PM1DTL=P1DOT
        P2DOT=PM2DTL
        PM22L=PM2LST
        PM12L=PM1LST
```

```
        PM2LST=PM2
        PM1LST=PM1
*      ER1=ABS(RR1-PM1)
*      ER2=ABS(RR2-PM2)
SORT
TERMINAL
FINISH  PM1=1.00
METHOD RKSFX
CONTRL  FINTIM=0.70000,DELT=0.00005,DELS=.00025
PRINT 0.010,X1DOT,P1DOT,PM1DT,X2DOT,P2DOT,PM2DT,PM1,RR1,PM2,RR2,TM1,TM2
SAVE (S1) 0.01, X1DOT,P1DOT,PM1DT,X2DOT,P2DOT,PM2DT,PM1,PM2
SAVE (S3) 0.01, P1,PM1,REF1,P2,PM2,REF2,RR1,RRD2
GRAPH (L1/S1,DE=TEK618,PO=1,.5) PM1(LE=6.0,UN='RAD',LO=-0.10,SC=0.10,...
         NI=12),P1DOT(LE=4,NI=4,LO=-2.0,UN='RAD/SEC',SC=2.0,PO=6.0),...
         X1DOT(LE=4,NI=4,LO=-2.0,SC=2.0,UN='RAD/SEC',AX=OMIT),...
         PM1DT(LE=4,NI=4,LO=-2.0,UN='RAD/SEC',SC=2.0)
GRAPH (L2/S1,DE=TEK618,OV,PO=1,5) PM2(LE=6.0,UN='RAD',LO=-0.10,...
        SC=0.10,NI=12), P2DOT(LE=4,NI=4,LO=0.0,UN='RAD/SEC',SC=5.0,...
        PO=6.),X2DOT(LE=4,NI=4,LO=0.0,UN='RAD/SEC',SC=5.0,AX=OMIT),...
        PM2DT(LE=4,NI=4,LO=0.0,UN='RAD/SEC',SC=5.0)
GRAPH (L3/S3,DE=TEK618,PO=1,.5) TIME(LE=6.0,UN='SECONDS'),...
         P1(LE=4,NI=4,LO=-.5,UN='RAD',SC=0.50,PO=6.0),...
         PM1(LE=4,NI=4,LO=-.5,UN='RAD',SC=0.50),...
         RR1(LE=4,NI=4,LO=-.5,SC=0.50,AX=OMIT)
GRAPH (L4/S3,DE=TEK618,PO=1,5,OV) TIME(LE=6.0,UN='SECONDS'),...
          P2(LE=4,NI=4,LO=-.5,UN='RAD',SC=0.50,PO=6.0),...
          PM2(LE=4,NI=4,LO=-.5,UN='RAD',SC=0.50),...
          RRD2(LE=4,NI=4,LO=-.5,SC=0.50,AX=OMIT)
*RAPH(L5/S3,DE=TEK618,PO=1,.5) TIME(LE=6.0,UN='SECONDS'),...
*       ER1(LE=8,NI=8,LO=0.,UN='RAD',SC=0.005),...
*       ER2(LE=8,NI=8,LO=0.,UN='RAD',SC=0.005,PO=6.)
LABEL (L1) PHASE PLANE (VOLTAGE SOUR. DRV. WITH LOAD)
LABEL (L3) STEP RESPONSE(VOLTAGE SOUR. DRV. WITH LOAD)
LABEL (L5) ERROR VS TIME (VOLTAGE SOUR. DRV. WITH LOAD)
END
STOP
```

APPENDIX E

DSL PROGRAM FOR CURRENT SOURCE DRIVE (NO GRAVITATIONAL TORQUES)

```
TITLE SIMULATION PROGRAM OF THE ADAPTIVE MODEL (CURRENT SOURCE DRIVE)
TITLE NO GRAVITATIONAL TORQUES
PARAM K1=0.60,K2=10000.,KM1=0.17,KM2=4.00,VSAT=100.,K=1.0,T=0.00025
PARAM G=386.4,M1=0.248,M2=0.082,KT1=14.4,KT2=14.4,D1=15.,D2=10.
PARAM J1=0.033,J2=0.033,KV1=0.1012,KV2=0.1012,R1=0.91,R2=0.91,K3=0.6
PARAM REF1=1.0,REF2=1.0,L=0.0001,BM1=0.0429,BM2=0.0429
PARAM RS=0.1,VSATA1=100,KA1=150,VSATA2=50,KA2=75
INTGER N1,N2,FLAG1,FLAG2
INITIAL
        N1=0
        FLAG1=0
        N2=0
        FLAG2=0
        P1=0.0
        P2=0.0
        P1DOT=0.
        P2DOT=0.
        P1DDT=0.
        P2DDT=0.
        PM1=0.0
        PM2=0.0
        PM1DT=0.
        PM2DT=0.
        PM1DDT=0.
        PM2DDT=0.
        X1DOT=0.
        X2DOT=0.
        TL1=0.
        TL2=0.
        TL11=0.
        TL22=0.
        KF=1./RS
        RTOT1=R1+RS
        RTOT2=R2+RS
        PP1=L/RTOT1
        PP2=L/RTOT2
        TM1=0.
        TM2=0.
        IM1=0.
        IM2=0.
        A1=SQRT(2.*KM1*VSAT)
        A2=SQRT(2.*KM2*VSAT)
DERIVATIVE
        RR1=REF1*SIN(3.14*TIME)
        RR2=REF2*SIN(3.14*TIME)
*     RRD1=TRANSP(50,0.0,0.15,RR1)
        E1=RR1-P1
        E2=RR2-P2
NOSORT
        D11=(M1+M2)*(D1**2)+M2*(D2**2)+2*M2*D1*D2*COS(PM2)
        D12=M2*(D2**2)+M2*D1*D2*COS(PM2)
        D22=M2*(D2**2)
        D122=-M2*D1*D2*SIN(PM2)
        D211=D122
        D112=D211
        D121=D112
        D212=D121
        D221=D212
        PMT=PM1+PM2
*     G1=(M1+M2)*G*D1*COS(PM1)+M2*G*D2*COS(PMT)
```

```
*     G2=M2*G*D2*COS(PMT)
       TL1=D12*PM2DDT+D122*PM2DT**2+2*D112*PM1DT*PM2DT
       TL2=D12*PM1DDT-D211*PM1DT**2
       JTOT1=J1+D11
       JTOT2=J2+D22
       IF(E1.LT.0.0)X1DOT=-A1*K1*SQRT(ABS(E1))
       IF(E1.GE.0.0)X1DOT=A1*K1*SQRT(E1)
       IF(E2.LT.0.0)X2DOT=-A2*K3*SQRT(ABS(E2))
       IF(E2.GE.0.0)X2DOT=A2*K3*SQRT(E2)
SORT
       X1DOTE=X1DOT-KP1DOT
       KP1DOT=P1DOT*K
       V1=LIMIT(-VSAT,VSAT,K2*X1DOTE)
NOSORT
       IF(FLAG1.EQ.1)GO TO 5
       IF(V1.LT.VSAT.AND.TIME.GT.0.00005)FLAG1=1
       NSW1=N1
5     CONTINUE
SORT
       P1DDT=KM1*V1
       P1DOT=INTGRL(0.0,P1DDT)
       P1=INTGRL(0.0,P1DOT)
       VF1=KF*IM1*RS
       VA1=V1-VF1
       VM1=LIMIT(-VSATA1,VSATA1,VA1*KA1)
       VD1=VM1-KV1*PM1DT
       IM1=REALPL(0.0,PP1,VD1/RTOT1)
       TM1=KT1*IM1
       TNET1=TM1-PM1DT*BM1-TL1
       PM1DDT=(1./JTOT1)*TNET1
       PM1DT=INTGRL(0.0,PM1DDT)
       PM1=INTGRL(0.0,PM1DT)
       X2DOTE=X2DOT-KP2DOT
       KP2DOT=P2DOT*K
       V2=LIMIT(-VSAT,VSAT,K2*X2DOTE)
NOSORT
       IF(FLAG2.EQ.1)GO TO 6
       IF(V2.LT.VSAT.AND.TIME.GT.0.00005)FLAG2=1
       NSW2=N2
6     CONTINUE
SORT
       P2DDT=KM2*V2
       P2DOT=INTGRL(0.0,P2DDT)
       P2=INTGRL(0.0,P2DOT)
       VF2=KF*IM2*RS
       VA2=V2-VF2
       VM2=LIMIT(-VSATA2,VSATA2,VA2*KA2)
       VD2=VM2-KV2*PM2DT
       IM2=REALPL(0.0,PP2,VD2/RTOT2)
       TM2=KT2*IM2
       TNET2=TM2-PM2DT*BM2-TL2
       PM2DDT=(1./JTOT2)*TNET2
       PM2DT=INTGRL(0.0,PM2DDT)
       PM2=INTGRL(0.0,PM2DT)
SAMPLE
NOSORT
       IF(N2.EQ.0)GO TO 21
       IF(N1.EQ.0)GO TO 20
       P2=PM2
       P1=PM1
       KS2=ABS(2.*PM2/(V2*((N2*T)**2)))
       KS1=ABS(2.*PM1/(V1*((N1*T)**2)))
       IF(FLAG2.EQ.0)KM2=KS2
       IF(FLAG1.EQ.0)KM1=KS1
       IF(N2.GE.2)PM2DTL=(PM2-PM22L)/(2.*T)
       IF(N1.GE.2)PM1DTL=(PM1-PM12L)/(2.*T)
       IF(FLAG2.EQ.0)P2DOT=(2.*((PM2-PM2LST)/T))-PM2DTL
       IF(FLAG1.EQ.0)P1DOT=(2.*((PM1-PM1LST)/T))-PM1DTL
       IF(N2.EQ.NSW2.AND.FLAG2.EQ.1)GO TO 21
```

```
        IF(N1.EQ.NSW1.AND.FLAG1.EQ.1)GO TO 20
        IF(FLAG2.EQ.1)P2DOT=(2.*((PM2-PM2LST)/T))-PM2DTL
        IF(FLAG1.EQ.1)P1DOT=(2.*((PM1-PM1LST)/T))-PM1DTL
21     N2=N2+1
20     N1=N1+1
         PM2DTL=P2DOT
         PM1DTL=P1DOT
         PM22L=PM2LST
         PM12L=PM1LST
         PM2LST=PM2
         PM1LST=PM1
         ER1=ABS(RR1-PM1)
         ER2=ABS(RR2-PM2)
SORT
TERMINAL
*INISH  PM1=1.0
METHOD RKSFX
CONTRL  FINTIM=1.00000,DELT=0.00005,DELS=0.00025
PRINT 0.020,X1DOT,PM1DT,P1DOT,X2DOT,P2DOT,PM2DT,PM1,RR1,TL1,PM2,RR2,TL2
SAVE (S1) 0.001, X1DOT,P1DOT,PM1DT,X2DOT,P2DOT,PM2DT,PM1,PM2
SAVE (S3) 0.001, P1,PM1,REF1,P2,PM2,REF2,ER1,ER2,RR1,RR2
GRAPH (L1/S1,DE=TEK618,PO=1,.5) PM1(LE=6.0,UN='RAD',LO=-0.10,SC=0.1,...
         NI=12),P1DOT(LE=4,NI=6,LO=-6.,UN='RAD/SEC',SC=3.0,PO=6.0),...
         X1DOT(LE=4,NI=6,SC=3.0,LO=-6.,UN='RAD/SEC',AX=OMIT),...
         PM1DT(LE=4,NI=6,LO=-6.,UN='RAD/SEC',SC=3.0)
GRAPH (L2/S1,DE=TEK618,PO=1,5,OV) PM2(LE=6.0,UN='RAD',LO=-0.1,...
       SC=0.10,NI=12), P2DOT(LE=4,NI=4,LO=-6.0,UN='RAD/SEC',SC=3.0,...
       PO=6.0), X2DOT(LE=4,NI=4,LO=-6.0,UN='RAD/SEC',SC=3.0,AX=OMIT),...
       PM2DT(LE=4,NI=4,LO=-6.0,UN='RAD/SEC',SC=3.0)
GRAPH (L3/S3,DE=TEK618,PO=1,.5) TIME(LE=6.0,UN='SECONDS'),...
         P1(LE=4,NI=3,LO=0.0,UN='RAD',SC=0.50,PO=6.0),...
         PM1(LE=4,NI=3,LO=0.0,UN='RAD',SC=0.50),...
         RR1(LE=4,NI=3,LO=0.0,SC=0.50,AX=OMIT)
GRAPH (L4/S3,DE=TEK618,PO=1,5,OV) TIME(LE=6.0,UN='SECONDS'),...
          P2(LE=4,NI=3,LO=0.0,UN='RAD',SC=0.5,PO=6.0),...
          PM2(LE=4,NI=3,LO=0.0,UN='RAD',SC=0.5),...
          RR2(LE=4,NI=3,LO=0.0,SC=0.5,AX=OMIT)
GRAPH (L5/S3,DE=TEK618,PO=1,.5) TIME(LE=6.0,UN='SECONDS'),...
          ER1(LE=8,NI=8,LO=0.,UN='RAD',SC=0.05),...
          ER2(LE=8,NI=8,LO=0.,UN='RAD',SC=0.05,PO=6.)
LABEL (L1) PHASE PLANE (CURRENT SOUR. DRV. WITH LOAD)
LABEL (L3) SINE RESPONSE (CURRENT SOUR. DRV. WITH LOAD)
LABEL (L5) ERROR VS TIME (CURRENT SOUR. DRV. WITH LOAD)
END
STOP
```

APPENDIX F

DSL PROGRAM FOR CURRENT SOURCE DRIVE (GRAVITATIONAL TORQUES INCLUDED)

```
TITLE SIMULATION PROGRAM OF THE ADAPTIVE MODEL (CURRENT SOURCE DRIVE)
TITLE GRAVITATIONAL TORQUES INCLUDED
PARAM K1=0.60,K2=10000.,KM1=0.17,KM2=4.00,VSAT=300.,K=1.0,T=0.00025
PARAM G=386.4,M1=0.248,M2=0.082,KT1=14.4,KT2=14.4,D1=15.,D2=10.
PARAM J1=0.033,J2=0.033,KV1=0.1012,KV2=0.1012,R1=0.91,R2=0.91,K3=0.6
PARAM REF1=1.0,REF2=1.0,L=0.0001,BM1=0.0429,BM2=0.0429
PARAM RS=0.1,VSATA1=300,KA1=350,VSATA2=150,KA2=175
INTGER N1,N2,FLAG1,FLAG2
INITIAL
        N1=0
        FLAG1=0
        N2=0
        FLAG2=0
        P1=0.0
        P2=0.0
        P1DOT=0.
        P2DOT=0.
        P1DDT=0.
        P2DDT=0.
        PM1=0.0
        PM2=0.0
        PM1DT=0.
        PM2DT=0.
        PM1DDT=0.
        PM2DDT=0.
        X1DOT=0.
        X2DOT=0.
        TL1=0.
        TL2=0.
        TL11=0.
        TL22=0.
        KF=1./RS
        RTOT1=R1+RS
        RTOT2=R2+RS
        PP1=L/RTOT1
        PP2=L/RTOT2
        TM1=0.
        TM2=0.
        IM1=0.
        IM2=0.
        A1=SQRT(2.*KM1*VSAT)
        A2=SQRT(2.*KM2*VSAT)
DERIVATIVE
        RR1=REF1*SIN(3.14*TIME)
        RR2=REF2*SIN(3.14*TIME)
*     RRD1=TRANSP(50,0.0,0.15,RR1)
        E1=RR1-P1
        E2=RR2-P2
NOSORT
        D11=(M1+M2)*(D1**2)+M2*(D2**2)+2*M2*D1*D2*COS(PM2)
        D12=M2*(D2**2)+M2*D1*D2*COS(PM2)
        D22=M2*(D2**2)
        D122=-M2*D1*D2*SIN(PM2)
        D211=D122
        D112=D211
        D121=D112
        D212=D121
        D221=D212
        PMT=PM1+PM2
        G1=(M1+M2)*G*D1*COS(PM1)+M2*G*D2*COS(PMT)
```

```
        G2=M2*G*D2*COS(PMT)
        TL1=D12*PM2DDT+D122*PM2DT**2+2*D112*PM1DT*PM2DT+G1
        TL2=D12*PM1DDT-D211*PM1DT**2+G2
        JTOT1=J1+D11
        JTOT2=J2+D22
        IF(E1.LT.0.0)X1DOT=-A1*K1*SQRT(ABS(E1))
        IF(E1.GE.0.0)X1DOT=A1*K1*SQRT(E1)
        IF(E2.LT.0.0)X2DOT=-A2*K3*SQRT(ABS(E2))
        IF(E2.GE.0.0)X2DOT=A2*K3*SQRT(E2)
SORT
        X1DOTE=X1DOT-KP1DOT
        KP1DOT=P1DOT*K
        V1=LIMIT(-VSAT,VSAT,K2*X1DOTE)
NOSORT
        IF(FLAG1.EQ.1)GO TO 5
        IF(V1.LT.VSAT.AND.TIME.GT.0.00005)FLAG1=1
        NSW1=N1
5      CONTINUE
SORT
        P1DDT=KM1*V1
        P1DOT=INTGRL(0.0,P1DDT)
        P1=INTGRL(0.0,P1DOT)
        VF1=KF*IM1*RS
        VA1=V1-VF1
        VM1=LIMIT(-VSATA1,VSATA1,VA1*KA1)
        VD1=VM1-KV1*PM1DT
        IM1=REALPL(0.0,PP1,VD1/RTOT1)
        TM1=KT1*IM1
        TNET1=TM1-PM1DT*BM1-TL1
        PM1DDT=(1./JTOT1)*TNET1
        PM1DT=INTGRL(0.0,PM1DDT)
        PM1=INTGRL(0.0,PM1DT)
        X2DOTE=X2DOT-KP2DOT
        KP2DOT=P2DOT*K
        V2=LIMIT(-VSAT,VSAT,K2*X2DOTE)
NOSORT
        IF(FLAG2.EQ.1)GO TO 6
        IF(V2.LT.VSAT.AND.TIME.GT.0.00005)FLAG2=1
        NSW2=N2
6      CONTINUE
SORT
        P2DDT=KM2*V2
        P2DOT=INTGRL(0.0,P2DDT)
        P2=INTGRL(0.0,P2DOT)
        VF2=KF*IM2*RS
        VA2=V2-VF2
        VM2=LIMIT(-VSATA2,VSATA2,VA2*KA2)
        VD2=VM2-KV2*PM2DT
        IM2=REALPL(0.0,PP2,VD2/RTOT2)
        TM2=KT2*IM2
        TNET2=TM2-PM2DT*BM2-TL2
        PM2DDT=(1./JTOT2)*TNET2
        PM2DT=INTGRL(0.0,PM2DDT)
        PM2=INTGRL(0.0,PM2DT)
SAMPLE
NOSORT
        IF(N2.EQ.0)GO TO 21
        IF(N1.EQ.0)GO TO 20
        P2=PM2
        P1=PM1
        KS2=ABS(2.*PM2/(V2*((N2*T)**2)))
        KS1=ABS(2.*PM1/(V1*((N1*T)**2)))
        IF(FLAG2.EQ.0)KM2=KS2
        IF(FLAG1.EQ.0)KM1=KS1
        IF(N2.GE.2)PM2DTL=(PM2-PM22L)/(2.*T)
        IF(N1.GE.2)PM1DTL=(PM1-PM12L)/(2.*T)
        IF(FLAG2.EQ.0)P2DOT=(2.*((PM2-PM2LST)/T))-PM2DTL
        IF(FLAG1.EQ.0)P1DOT=(2.*((PM1-PM1LST)/T))-PM1DTL
        IF(N2.EQ.NSW2.AND.FLAG2.EQ.1)GO TO 21
```

```
        IF(N1.EQ.NSW1.AND.FLAG1.EQ.1)GO TO 20
        IF(FLAG2.EQ.1)P2DOT=(2.*((PM2-PM2LST)/T))-PM2DTL
        IF(FLAG1.EQ.1)P1DOT=(2.*((PM1-PM1LST)/T))-PM1DTL
21     N2=N2+1
20     N1=N1+1
        PM2DTL=P2DOT
        PM1DTL=P1DOT
        PM22L=PM2LST
        PM12L=PM1LST
        PM2LST=PM2
        PM1LST=PM1
        ER1=ABS(RR1-PM1)
        ER2=ABS(RR2-PM2)
SORT
TERMINAL
*INISH  PM1=1.0
METHOD RKSFX
CONTRL  FINTIM=1.00000,DELT=0.00005,DELS=0.00025
PRINT 0.020,X1DOT,PM1DT,P1DOT,X2DOT,P2DOT,PM2DT,PM1,RR1,TL1,PM2,RR2,TL2
SAVE (S1) 0.001, X1DOT,P1DOT,PM1DT,X2DOT,P2DOT,PM2DT,PM1,PM2
SAVE (S3) 0.001, P1,PM1,REF1,P2,PM2,REF2,ER1,ER2,RR1,RR2
GRAPH (L1/S1,DE=TEK618,PO=1,.5) PM1(LE=6.0,UN='RAD',LO=-0.1,SC=0.1,...
        NI=12),P1DOT(LE=4,NI=6,LO=-6.,UN='RAD/SEC',SC=3.0,PO=6.0),...
        X1DOT(LE=4,NI=6,SC=3.0,LO=-6.,UN='RAD/SEC',AX=OMIT),...
        PM1DT(LE=4,NI=6,LO=-6.,UN='RAD/SEC',SC=3.0)
GRAPH (L2/S1,DE=TEK618,PO=1,5,OV) PM2(LE=6.0,UN='RAD',LO=-0.1,...
       SC=0.10,NI=12), P2DOT(LE=4,NI=4,LO=-6.0,UN='RAD/SEC',SC=3.0,...
       PO=6.0), X2DOT(LE=4,NI=4,LO=-6.0,UN='RAD/SEC',SC=3.,AX=OMIT),...
       PM2DT(LE=4,NI=4,LO=-6.0,UN='RAD/SEC',SC=3.0)
GRAPH (L3/S3,DE=TEK618,PO=1,.5) TIME(LE=6.0,UN='SECONDS'),...
        P1(LE=4,NI=3,LO=0.0,UN='RAD',SC=0.50,PO=6.0),...
        PM1(LE=4,NI=3,LO=0.0,UN='RAD',SC=0.50),...
        RR1(LE=4,NI=3,LO=0.0,SC=0.50,AX=OMIT)
GRAPH (L4/S3,DE=TEK618,PO=1,5,OV) TIME(LE=6.0,UN='SECONDS'),...
          P2(LE=4,NI=3,LO=0.0,UN='RAD',SC=0.5,PO=6.0),...
          PM2(LE=4,NI=3,LO=0.0,UN='RAD',SC=0.5),...
          RR2(LE=4,NI=3,LO=0.0,SC=0.5,AX=OMIT)
GRAPH (L5/S3,DE=TEK618,PO=1,.5) TIME(LE=6.0,UN='SECONDS'),...
          ER1(LE=8,NI=8,LO=0.,UN='RAD',SC=0.05),...
          ER2(LE=8,NI=8,LO=0.,UN='RAD',SC=0.05,PO=6.)
LABEL (L1) PHASE PLANE (CURRENT SOUR. DRV. WITH LOAD)
LABEL (L3) SINE RESPONSE (CURRENT SOUR. DRV. WITH LOAD)
LABEL (L5) ERROR VS TIME (CURRENT SOUR. DRV. WITH LOAD)
END
STOP
```

LIST OF REFERENCES

1. Wikstrom, R. K., *An Adaptive Model Based Disk File Head Positioning Servo System*, Master's Thesis, Naval Postgraduate School, Monterey, California, September 1985.

2. Thaler, G. J. and Stein, W. A., "Transfer Function and Parameter Evaluation for D-C Servomotors," *Applications and Industry*, pp. 410-417, January 1956.

3. Thaler, G. J., *Nonlinear Feedback Controls Theory, and Methods for Analysis and Design*, unpublished notes for ECE 4350, Nonlinear Controls, Naval Postgraduate School, Monterey, California, October 1986.

4. Paul, R. P., *Robot Manipulators: Mathematics, Programming, and Control*, The MIT Press, 1981.

5. Luh, J. Y., Fisher, W. D., and Paul, R. C., "Joint Torque Control by a Direct Feedback for Industrial Robots," *IEEE Transactions on Automatic Control*, V. AC-28, No. 2, pp. 153-161, February 1983.

INITIAL DISTRIBUTION LIST

		No. Copies
1.	Defense Technical Information Center Cameron Station Alexandria, Virginia 22304-6145	2
2.	Library, Code 0142 Naval Postgraduate School Monterey, California 93943-5002	2
3.	Professor G. J. Thaler, Code 62Tr Department of Electrical & Computer Engineering Naval Postgraduate School Monterey, California 93943	5
4.	Professor H. A. Titus, Code 62Ti Department of Electrical & Computer Engineering Naval Postgraduate School Monterey, California 93943	1
5.	Kemal Ozaslan Celebidere Sokak No = 23/4 Yenikoy Istanbul - TURKEY	5
6.	Professor L. W. Chang, Code 69Ck Department of Mechanical Engineering Naval Postgraduate School Monterey, California 93943	1
7.	Professor D. L. Smith, Code 69Sm Department of Mechanical Engineering Naval Postgraduate School Monterey, California 93943	1
8.	Professor R. Werneth, Code 69Wh Department of Mechanical Engineering Naval Postgraduate School Monterey, California 93943	1
9.	Cpt. Paulo Roberto de Souza Centro Tecnico Aeroespacial - IAE - ESB 12225 - S. Jose dos Campos - SP - Brasil	1
10.	Nusret Yurutucu 7220 Trenton Place Gilroy, California 95020	1
11.	Mr. James Toreson XEBEC 2221 Old Okland Road San Jose, California 95131	1
12.	Mr. Tom Hickok XEBEC 2221 Old Okland Road San Jose, California 95131	1

13. Mr. Ron Lesti 1
XEBEC
2221 Old Okland Road
San Jose, California 95131

14. Deniz Harb Okulu 1
Komutanligi Kutuphanesi
Tuzla ISTANBUL - TURKEY

15. Taskizak Tersane Komutanligi 1
ARGE Bolumu Kutuphanesi
Kasimpasa, ISTANBUL - TURKEY